1P

NIMBUS-D SOLAR-CONVERSION POWER SUPPLY SUBSYSTEM

QUARTERLY TECHNICAL REPORT NO. 5
15 DECEMBER 1968 THROUGH 15 MARCH 1969

Contract No. NAS5-10470

Prepared by

RCA Astro-Electronics Division
Defense Electronic Products

for

Goddard Space Flight Center
National Aeronautics and Space Administration
Greenbelt, Maryland

AED R-3443

Issued: June 18, 1969

NIMBUS-D SOLAR-CONVERSION POWER SUPPLY SUBSYSTEM

QUARTERLY TECHNICAL REPORT NO. 5
15 DECEMBER 1968 THROUGH 15 MARCH 1969

Contract No. NAS5-10470

Prepared by

RCA Astro-Electronics Division
Defense Electronic Products

for

Goddard Space Flight Center
National Aeronautics and Space Administration
Greenbelt, Maryland

AED R-3443

Issued: June 18, 1969

PREFACE

This is the fifth in a series of quarterly technical reports on the development of the Solar-Conversion Power Supply Subsystem for the Nimbus-D Meteorological Satellite. This project is being conducted by the Astro-Electronics Division (AED) of the RCA Corp. for the National Aeronautics and Space Administration (NASA) under Contract No. NAS5-10470. This report contains data on RCA activities and plans that relate to the technical and schedule pursuance of the contract objectives, and covers the period from December 15, 1968 through March 15, 1969.

TABLE OF CONTENTS

Section		Page
1	INTRODUCTION	1
	A. CONTRACT OBJECTIVES	1
	B. SUBSYSTEM DESCRIPTION	1
	C. CONTRACT DATA	2
	D. SYSTEM ACTIVITIES	2
2	SOLAR ARRAY	7
	A. GENERAL	7
	B. NIMBUS-B2 ARRAY	7
	C. NIMBUS-D ARRAY	7
	1. Solar Cell Humidity Tests	7
	2. Substrate Procurement	8
	3. Solar-Cell Module Fabrication	8
	4. Plans for Next Report Period	8
3	STORAGE MODULE	9
	A. GENERAL	9
	B. NIMBUS-B2 STORAGE MODULES	9
	C. NIMBUS-D STORAGE MODULES	9
	1. Procurement	9
	2. Manufacturing	10
	3. Plans for Next Report Period	12
4	CONTROL MODULE	13
	A. GENERAL	13
	B. NIMBUS-D CONTROL MODULE	13
	1. Unit Tests	13
	2. Predicted Control Module Input Characteristics	13
	3. Plans for Next Report Period	13
5	ENGINEERING RELIABILITY	15
APPENDIX		
I	NIMBUS-B2 SOLAR ARRAY TEST REPORT	I-1
	A. INTRODUCTION	I-1
	B. SUMMARY	I-1
	C. GENERAL DESCRIPTION	I-3

TABLE OF CONTENTS (Continued)

Section		Page
APPENDIX		
I (Continued)		
	D. TEST PROCEDURES	I-8
	1. Module Tests	I-8
	2. Weight and Balance Test	I-9
	3. Electrical Acceptance Test	I-9
	4. Deployment Drive Motor	I-9
	5. Illumination Test	I-9
	6. Thermal Vacuum Tests	I-10
	E. TEST RESULTS	I-10
	1. Temperature Telemetry Calibration Data	I-10
	2. Voltage Telemetry Performance Test Data	I-13
	3. Voltage Telemetry Overprotection Test Data	I-15
	4. Weight and Balance Test Data	I-16
	5. Electrical Acceptance Test Data	I-25
	6. Deployment Drive Motor Acceptance Test Data	I-28
	7. Illumination Test Data	I-38
	8. Thermal Vacuum Test Data	I-49
	F. POWER SUMMARY	I-50
II	HUMIDITY TEST REPORT	II-1
	A. GENERAL	II-1
	B. ELECTRICAL, VISUAL, AND HUMIDITY TESTS	II-1
	C. TEST RESULTS AND CONCLUSIONS	II-1
	1. Test No. 1 Results	II-1
	2. Test No. 3 Results	II-2
	3. Test Anomaly Summary	II-2
III	NIMBUS-D SOLAR ARRAY SUBSTRATE FABRICATION REPORT	III-1
	A. INTRODUCTION	III-1
	B. SUBSTRATE MATERIALS	III-3
	C. PROCESS DEVELOPMENT	III-3
	D. MOLD DESIGN AND FABRICATION	III-4
	E. FABRICATION OF DESTRUCT UNITS	III-9
	1. Transition	III-9
	2. Platform	III-9
	3. Detailed Parts	III-12
	F. DEVELOPMENT OF MEASUREMENT TECHNIQUES	III-17
	1. General	III-17
	2. Documentation	III-17

TABLE OF CONTENTS (Continued)

Section		Page
APPENDIX III (Continued)		
	G. EVALUATION OF DESTRUCT UNIT	III-21
	1. Flexural Strength Test	III-21
	2. Lap Shear Strength Test	III-21
	3. Peel Strength Test	III-21
	4. Dimensional Test Data	III-26
	5. Torque Measurement Data	III-27
	6. Weight Data	III-32
	H. RECOMMENDATIONS AND CONCLUSIONS	III-32
	1. Introduction	III-32
	2. Recommendations	III-33
	3. Conclusions	III-33
IV	NIMBUS-B2 STORAGE MODULE REWORK, TEST, AND ALIGNMENT DATA REPORT	IV-1
	A. REPAIR CYCLE	IV-1
	B. TEST SEQUENCE	IV-1
	C. TEST RESULTS	IV-2
V	NIMBUS-D STORAGE MODULE TEST AND CALIBRATION REPORT	V-1
	A. STORAGE CELL DATA	V-1
	B. HEAT SINK TRANSISTOR REPLACEMENT AND TEST RESULTS	V-1
	1. Replacement Part Selection	V-1
	2. Special Thermal Tests	V-7
	C. STORAGE MODULE TEST DATA	V-11
	1. General	V-11
	2. Test Results and Conclusion	V-12
VI	CONTROL MODULE TEST REPORT	VI-1
	A. General	VI-1
	B. TEST RESULTS	VI-1
VII	NIMBUS-B2 SOLAR ARRAY THERMAL VACUUM TEST REPORT	VII-1
	A. INTRODUCTION	VII-1
	1. Purpose	VII-1
	2. Scope	VII-1
	3. Summary	VII-1

TABLE OF CONTENTS (Continued)

Section		Page
APPENDIX		
VII (Continued)		
B.	CALIBRATION TEST	VII-1
C.	THERMAL VACUUM TEST	VII-2
1.	Test Setup	VII-2
2.	Test Chronology and Results	VII-2

LIST OF ILLUSTRATIONS

Figure		Page
1	Predicted Beginning-of-Life I-V Characteristics Control Module Input	14
I-1	Nimbus-B2 I-V Characteristics vs Temperature at Output Side of Blocking Diodes	I-2
I-2	Temperature Telemetry Calibration, Serial No. 5, 3.2°C Gradient Shifted	I-4
I-3	Temperature Telemetry Calibration, Serial No. 6, 3.2°C Gradient Shifted	I-5
I-4	Typical Voltage Telemetry Curve, Module Boards A, F, G, and J	I-6
I-5	Temperature Telemetry Calibration Curve, Serial No. 4	I-11
I-6	Temperature Telemetry Calibration Curve, Serial No. 5	I-11
I-7	Temperature Telemetry Calibration Curve, Serial No. 6	I-12
I-8	Temperature Telemetry Schematic	I-12
I-9	Temperature Telemetry Calibration Curve Serial No. 4, Post Repair	I-14
I-10	Overvoltage Protection Schematic	I-14
I-11	Solar Platform Balance Test Setup	I-17
I-12	Solar Array Balance, Clock was Rotation	I-18
I-13	Solar Array Balance Counter Clock was Rotation	I-19
I-14	Solar Array Eccentricity	I-21
I-15	Solar Array Center of Rotation vs Center of Gravity	I-23
I-16	DC Isolation and Continuity Test Setup	I-26
I-17	Illumination Test Setup	I-27
I-18	Post-Fabrication I-V Characteristic, Board A	I-29
I-19	Post-Fabrication I-V Characteristic, Board B	I-29
I-20	Post-Fabrication I-V Characteristic, Board C	I-30
I-21	Post-Fabrication I-V Characteristic, Board D	I-30
I-22	Post-Fabrication I-V Characteristic, Board E	I-31
I-23	Post-Fabrication I-V Characteristic, Board G	I-31
I-24	Post-Fabrication I-V Characteristic, Board H	I-32
I-25	Post-Fabrication I-V Characteristic, Board J	I-32
I-26	Post-Fabrication I-V Characteristic, Board K	I-33
I-27	Module 52, Board H I-V Characteristics, Cells No. 6, 7, and 8	I-33
I-28	Deployment Motor-Drive Assembly Test Flow Diagram	I-35
I-29	Deployment Motor-Drive Assembly Torque-Speed Characteristics at 24.0 Volts dc	I-36
I-30	Pre-Thermal Indoor I-V Characteristics, Board A	I-42

LIST OF ILLUSTRATIONS (Continued)

Figure		Page
I-31	Pre-Thermal Indoor I-V Characteristics, Board B	I-42
I-32	Pre-Thermal Indoor I-V Characteristics, Board C	I-43
I-33	Pre-Thermal Indoor I-V Characteristics, Board D	I-43
I-34	Pre-Thermal Indoor I-V Characteristics, Board E	I-44
I-35	Pre-Thermal Indoor I-V Characteristics, Board G	I-44
I-36	Pre-Thermal Indoor I-V Characteristics, Board H	I-45
I-37	Pre-Thermal Indoor I-V Characteristics, Board J	I-45
I-38	Pre-Thermal Indoor I-V Characteristics, Board K	I-46
I-39	Pre-Thermal Indoor I-V Characteristics, Board L	I-46
I-40	Module No. 2 Board E I-V Characteristics	I-52
I-41	Pre-Thermal Indoor I-V Characteristics, Board E After Rework	I-52
I-42	Pre-Thermal Indoor I-V Characteristics, Board L After Rework	I-53
I-43	Post-Thermal Indoor I-V Characteristics, Board A	I-53
I-44	Post-Thermal Indoor I-V Characteristics, Board B	I-54
I-45	Post-Thermal Indoor I-V Characteristics, Board C	I-54
I-46	Post-Thermal Indoor I-V Characteristics, Board D	I-55
I-47	Post-Thermal Indoor I-V Characteristics, Board E	I-55
I-48	Post-Thermal Indoor I-V Characteristics, Board G	I-56
I-49	Post-Thermal Indoor I-V Characteristics, Board H	I-56
I-50	Post-Thermal Indoor I-V Characteristics, Board J	I-57
I-51	Post-Thermal Indoor I-V Characteristics, Board K	I-57
I-52	Post-Thermal Indoor I-V Characteristics, Board L	I-58
I-53	Post-Thermal Indoor I-V Characteristics, Board H After Rework	I-58
I-54	Post-Thermal Indoor I-V Characteristics, Board K After Rework	I-59
I-55	Post-Thermal Indoor I-V Characteristics, Board L After Rework	I-59
I-56	Predicted Solar Array I-V Characteristics, Pre-Thermal Vacuum	I-60
I-57	Predicted Solar Array I-V Characteristics, Post-Thermal Vacuum	I-60
I-58	Outdoor I-V Characteristics, Board A	I-61
I-59	Outdoor I-V Characteristics, Board B	I-61
I-60	Outdoor I-V Characteristics, Board C	I-62
I-61	Outdoor I-V Characteristics, Board D	I-62
I-62	Outdoor I-V Characteristics, Board E	I-63
I-63	Outdoor I-V Characteristics, Board F	I-63

LIST OF ILLUSTRATIONS (Continued)

Figure		Page
I-64	Outdoor I-V Characteristics, Board G	I-64
I-65	Outdoor I-V Characteristics, Board H	I-64
I-66	Outdoor I-V Characteristics, Board J	I-65
I-67	Outdoor I-V Characteristics, Board K	I-65
I-68	Outdoor I-V Characteristics, Board L	I-66
I-69	Outdoor I-V Characteristics, Board M	I-66
I-70	Solar Array I-V Characteristics, Corrected to Air Mass Zero	I-67
III-1	Peel Test Data Process Verification, Lot No. 1 (2 sheets)	III-5
III-2	Peel Test Data, Process Verification, Lot No. 2	III-7
III-3	Peel Test Data, Process Verification at the RCA Corp.	III-8
III-4	Transition Mold	III-10
III-5	Platform Mold	III-11
III-6	Recommended Cure Cycle for FM-1000 Adhesive	III-13
III-7	Recommended and Preferred Heat-Up Rates for FM-1000 Adhesive	III-14
III-8	Destruct Unit Heat-Up Rate, First Cure	III-15
III-9	Destruct Unit Heat-Up Rate, Second Cure	III-16
III-10	Holding Fixture for Dimensional Check, Earth Side Shown	III-18
III-11	Holding Fixture and Optical Instrumentation for Dimensional Check, Sun Side Shown	III-19
III-12	Holding Fixture and Electronic Instrumentation for Dimensional Check, Sun Side Shown	III-20
III-13	Destruct Panel, Sample Test Pattern	III-22
III-14	Flexure Test Set-Up	III-23
III-15	Peel Test Requirements	III-25
III-16	Destruct Unit Dimensional Test Data (3 sheets)	III-28
III-17	Deployment Test Positions	III-31
IV-1	Storage Module 003 Charge-Current Telemetry at 25°C	IV-3
IV-2	Storage Module 003 Charge-Current Telemetry at 0°C and 45°C	IV-4
IV-3	Storage Module 003 Discharge-Current Telemetry at 25°C	IV-5
IV-4	Storage Module 003 Discharge-Current Telemetry at 0°C and 45°C	IV-6
IV-5	Storage Module 003 Voltage Telemetry	IV-7
IV-6	Storage Module 003 Temperature Telemetry	IV-8
IV-7	Storage Module 008 Charge Current Telemetry at 25°C	IV-9
IV-8	Storage Module 008 Charge Current Telemetry at 0°C and 45°C	IV-10
IV-9	Storage Module 008 Discharge Current Telemetry at 25°C	IV-11
IV-10	Storage Module 008 Discharge Current Telemetry at 0°C and 45°C	IV-12

LIST OF ILLUSTRATIONS (Continued)

Figure		Page
IV-11	Storage Module 008 Voltage Telemetry	IV-13
IV-12	Storage Module 008 Temperature Telemetry	IV-14
V-1	Cycling Test, Maximum Voltage at End-of-Charge	V-2
V-2	Cycling Test, Maximum Charge Voltage	V-2
V-3	Cycling Test, Minimum Discharge Voltage	V-2
V-4	Cycling Test, Residual Capacity	V-3
V-5	Capacity Test at 40°C — RCA	V-3
V-6	Capacity Test at 25°C — RCA	V-3
V-7	Capacity Test at 0°C — RCA	V-4
V-8	Maximum Overcharge Voltage at 25°C	V-4
V-9	Maximum Overcharge Pressure at 25°C	V-4
V-10	Capacity Test at 0°C — GE	V-5
V-11	Capacity Test at 25°C — GE	V-5
V-12	Capacity Test at 50°C — GE	V-5
V-13	Internal Resistance Test	V-6
V-14	Storage Cell Weight	V-6
V-15	Power Dissipation Test Circuit	V-8
V-16	Power Dissipation Characteristics	V-8
V-17	Junction Temperature Calibration Test Circuit	V-9
V-18	Junction Temperature Calibration Curve	V-9
V-19	Junction Temperature Test Circuit	V-10
V-20	Junction Temperature Characteristics	V-10
VI-1	Main Regulator Efficiency	VI-4
VI-2	Main Regulator Current Limiting	VI-4
VI-3	Typical Regulator Output Impedance	VI-5
VI-4	Temperature Telemetry Test Current and Characteristics	VI-11
VII-1	Solar Platform Thermocouple Locations	VII-3
VII-2	Shroud Thermocouple Locations	VII-4
VII-3	Solar Platform Installation	VII-5
VII-4	Typical Day-Time Orbit Temperature Map	VII-6
VII-5	Typical Nighttime Orbit Temperature Map	VII-7

LIST OF TABLES

Table		Page
1	Solar Platform Test Data, Nimbus-B and B-2	5
2	Telemetry Circuit Test Voltages	10
3	Shunt Dissipator Transistor Screening Test Results	11
4	Beginning-of-Life Solar Cell Degradation	13
I-1	Voltage Telemetry Overvoltage Protection Test Data	I-15
I-2	DC Isolation Test Data	I-26
I-3	Continuity Test Data	I-27
I-4	Illumination Test Data	I-28
I-5	Deployment Motor-Drive Assembly Identification	I-28
I-6	Initial Speed-Torque Test Data	I-36
I-7	Final Speed-Torque Test Data	I-37
I-8	Cold Temperature Test Data	I-37
I-9	Sinusoidal Vibration Levels	I-38
I-10	Random Vibration Levels	I-38
I-11	Nimbus-B Deployment Motor-Drive Test Data	I-39
I-12	Nimbus-B2 Deployment Motor-Drove Test Data, Original Test	I-40
I-13	Nimbus-B2 Deployment Motor-Drive Test Data, Post Thermal Vacuum	I-41
I-14	Indoor/Outdoor I-V Characteristic Summary	I-48
I-15	Chronological Summary of Events	I-68
II-1	I-V Characteristics, Test No. 1 Sample Cells	II-3
II-2	I-V Characteristics, Test No. 2 Sample Cells	II-6
II-3	Test Anomoly Summary	II-7
III-1	Destruct Unit Lap Shear Test Data	III-21
III-2	Destruct Unit Peal Test Data	III-24
III-3	Interface Dimensions Test Results	III-26
III-4	Deployment Test Results	III-31
III-5	Angular Displacement Test Results	III-32
IV-1	Test Parameters and Results for Storage Modules 003 and 008	IV-2
V-1	Storage Module Test Sequence and Completion Date	V-12
V-2	Circuit Alignment and Electrical Test Data	V-13
V-3	Storage Module Capacity Test Data at 25°C	V-14
V-4	Twenty-Hour Open Circuit Cell Voltages (Volts dc) — SHORT TEST	V-14

LIST OF TABLES (Continued)

Table		Page
V-5	End-of-Charge Cell Voltages (Volts dc) — Capacity Test	V-15
V-6	End-of-Discharge Cell Voltages (Volts dc) — Capacity Test . .	V-16
VI-1	Nimbus-D Control Module Test Sequence and Completion Date .	VI-1
VI-2	Worst Case Test Measurements	VI-3
VI-3	Control Module Current Telemetry	VI-6
VI-4	Control Module Regulated Bus Current Telemetry (0.4 to 15 Volts)	VI-7
VI-5	Control Module Regulated Bus Current Telemetry (2.0 to 20.5 Volts)	VI-8
VI-6	Control Module Unregulated Bus Voltage Telemetry	VI-9
VI-7	Control Module Regulated and Auxiliary Bus Voltage Telemetry	VI-10
VI-8	Worst Case Telemetry Parameters	VI-11

SECTION 1

INTRODUCTION

A. CONTRACT OBJECTIVES

The objective of Contract No. NAS5-10470 is to furnish a Solar Conversion Power Supply Subsystem for use with the Nimbus-D Meteorological Satellite. This configuration will be identified as the Nimbus-D Solar Conversion Power Supply Subsystem.

The contract provides for the manufacture of one flight model and a set of three spare storage modules. The solar conversion power supply subsystem, consisting of one control module, eight storage modules, and solar array (2 solar platforms), will be nearly identical to the equipment supplied under Contract NAS5-9668. Assembly numbers are as follows:

Control Module	RCA-1759712-502
Storage Module	RCA-1759580-503
Solar Array (Nimbus-B2)	RCA-1975606-501 and -502
Solar Array (Nimbus-D)	RCA-1976429-501 and -502

All special test equipment required for the manufacture and test of the flight model equipment was manufactured and assembled under previous contracts.

B. SUBSYSTEM DESCRIPTION

The Solar Conversion Power-Supply Subsystem consists of eight identical storage modules, one control module, and one solar array. Each storage module contains a battery consisting of 23 series-connected, nickel cadmium cells and a group of electronic circuits designed to provide control and protection for the battery and other power subsystem components. These circuits and the battery are housed in cast-magnesium containers with sheet-magnesium covers. The control module consists of additional power subsystem electronic circuits housed in a machined-aluminum container. The solar array consists of two solar-cell platforms containing N-on-P silicon solar cells which are mounted on one side of the sun-oriented platforms. The purpose of the subsystem is to provide the spacecraft with electrical power; during satellite day, the solar array converts solar radiation to electrical energy that is supplied to the spacecraft subsystems and the batteries (charge cycle). During satellite night and peak daytime-load periods, the batteries supply the power to operate the spacecraft subsystems.

C. CONTRACT DATA

Failure of the Nimbus-B spacecraft to achieve orbit resulted in a planning effort for a Nimbus-B2 mission. The final plan provided for the qualification of one flight system (two solar platforms, one control module, and eight storage modules) and the following back-up equipment, one control module and three storage modules. Specific tasks defined by the Nimbus-B2 program plan are as follows:

- Manufacture and electrically qualify one solar array from equipment diverted from the Nimbus-D program.
- Evaluate, refurbish, and rework 11 storage modules (serial numbers 01 thru 09, 16, and 20) and two control modules (serial numbers 03 and 05) supplied as GFE from the General Electric Co.

Delivery of the Nimbus-B2 solar array and the issuance of the final test report, Appendix I of this document, completes the requirement for periodic reports (quarterly) pertaining to the Nimbus-B2 Solar Conversion Power Supply Subsystem. Subsequent quarterlies will contain data pertinent to RCA support of Spacecraft Integration and pre-launch activities requested by the customer.

D. SYSTEM ACTIVITIES

1. Introduction

A Nimbus-D power supply subsystem review was conducted at the GSFC facilities on January 21, 1969. The meeting was attended by personnel from the RCA Corporation, the General Electric Company, and the Goddard Space Flight Center. As a result of this meeting, there were 10 action items that required action by either the RCA Corporation or the General Electric Company. The action items specified as applicable to the RCA Corporation and solution to the action item are described separately.

2. Action Item No. 2

a. Problem: Store the Q-board in a controlled atmosphere for approximately 6-months. Then conduct an illumination test, generate a set of I-V characteristics, and compare the results to the data obtained from similar tests conducted during the initial Q-board tests.

b. Action Taken: The Q-board is secured in a dessicant bag and stored in the AED Space Power Laboratory. Further tests of the Q-board will be performed after six months in storage and with authorization from General Electric.

3. Action Item No. 3

a. Problem: Incorporate the following data into the Nimbus-D Subsystem Quarterly Report.

- Solar Cell Incoming Inspection Data
- Q-Board Test Report
- Solar Cell Humidity Test Results

b. Action Taken: The solar cell incoming inspection data and the Q-Board test report were incorporated into "Quarterly Technical Report No. 4" (AED-R 3394) issued February 29, 1969. The results of the solar cell humidity tests are contained in this report as the tests were still in process when Quarterly Technical Report No. 4 was issued.

4. Action Item No. 4

a. Problem: Provide the characteristics of new bonding material for wire bonding on Nimbus-B2 and -D, and of the old bonding material for wire bonding on Nimbus B. In addition to the bonding characteristics, provide a technical reason for using the new material.

b. Action Taken: The material originally specified and used to bond earth-side wiring was Bondmaster M-688 with CH-16 catalyst and white pigment added. It was first applied directly to the painted (tile coat) surface but shrunk during thermal-vacuum and loosened the paint. This problem was solved for Nimbus-I, -II, and -B by removing the paint under the tie point and bonding directly to the aluminum. Since these arrays were built, experience with other arrays (Lunar Orbiter and a classified program) has shown that RTV is preferred for this application. It has greater flexibility at low temperatures, therefore less likely to break, requires no paint stripping, and is easier to repair. Following a review of the application with the Thermal group, it was decided to use it on Nimbus-B2. Nimbus test experience confirms the results achieved on other programs. We foresee no problems in its use.

5. Action Item No. 5

a. Problem: Set up appropriate meetings to review the substrate and tool drawings to allow the RCA Corporation, GE Co, NASA, and Goodyear Technical Team to stay informed.

b. Action Taken: The Goodyear Aerospace Corporation (GAC) schecule for completion of the substrate tool was set as February 3, 1969. Daily communications with Goodyear and GE will be maintained. Preparations for review of the finished tool by the RCA Corporation, GE Co, and NASA at the GAC facility when the tool is finished are in process.

6. Action Item No. 6

a. Problem: Formalize the inspection data for previous solar platforms (serial no. 13, 14, 15, and 16) and related transition sections and clarify the test data.

b. Action Taken: The data listed in Table 1 summarizes the data presented at the review. The notes were added to define the column headings. The two sets of data were obtained from tests performed at different times.

7. Action Item No. 7

a. Problem: Document the inspection procedures for the tool and substrate inspection and incorporate into the substrate drawing system.

b. Action Taken: The RCA Corporation representative at the GAC facility was instructed to document all tool measurement and inspection procedures and was instructed to reference these documents in the substrates drawing system.

8. Action Item No. 9

a. Problem: Perform the necessary analysis and define the thermal requirements for acceptance of the solar array.

b. Action Taken: A review was made of the thermal requirements for acceptance of the solar array. Telemetry data shows the lower temperature during flight of Nimbus-II was -60°C. However, the telemetry sensor was a thermistor, and since sensors of this type have been known to suffer loss of calibration at low temperatures, we now believe it more prudent to use the temperature profile specified on the basis of recent α/e data. Accordingly, the recommended temperature profile is -75°C to +50°C.

TABLE 1. SOLAR PLATFORM TEST DATA, NIMBUS-B AND -B2

Assembly Ser No See Note 1	Platform (See Note 2)						Transition (See Note 2)				Phy Characteristics		
	Measurement Plane and Tol				See Notes		Measurement Plane and Tol				Weight (lbs)		Torque
	Hor ±0.002	Vert ±0.002	Hor ±0.004	Vert ±0.004	3 ±0.004	4 ±0.004	Hor ±0.002	Vert ±0.002	Hor ±0.004	Vert ±0.004	Plat	Trans	18 in lbs max
13	+0.002	+0.004	+0.002	+0.004	+0.001	+0.002	+0.001 -0.004	+0.002	+0.001 -0.003	-0.006 -0.007	16.90	4.32	9.0
14	+0.004 -0.002	+0.0015 +0.0035	+0.004 +0.000	+0.0005 -0.0035	+0.001	+0.0095 +0.0025	+0.002 +0.002	-0.003 +0.002	+0.002 -0.002	0.000 -0.008	16.90	4.33	6.75
15	+0.002	+0.001	+0.003	+0.004	+0.001	+0.004	+0.002	+0.002	+0.003	+0.003	16.93	4.68	11.25
16	+0.002	+0.003	+0.002	+0.004	+0.001	+0.004	+0.0015	+0.002	+0.003	+0.005	16.74	4.32	15.75

Note 1. Double readings for No. 13 and 14 indicate measurements taken at different times.

Note 2. Center lines must be coincident within cited tolerance for Platform and transition section, respectively.

Note 3. Motor bracket mounting surfaces must be co-planar with cited tolerances.

Note 4. Hinge center line must be parallel with motor-mount bracket surface within the tolerances cited.

9. Action Item No. 10

a. Problem: Supply the GE Co. with a qualified capacitor for installation in the engineering model control module. Include the test history of the subject capacitor.

b. Action Taken: A qualified capacitor was supplied to the GE Co, on January 24th. Product Assurance records show no previous failures of this part, hence it is the original part built into the module. There were no unusual tests run on this module which would overstress the part. These records also show, however, that the part was not preconditioned. (All flight model parts were preconditioned.)

SECTION 2

SOLAR ARRAY

A. GENERAL

Each solar array consists of two solar cell platforms comprised of a solar-cell mounting structure (substrate), solar-cell modules, a transition section, a latching assembly, a motor drive and gear reduction unit, and a control-shaft clamp.

B. NIMBUS-B2 ARRAY

Electrical and thermal-vacuum qualification tests of the solar array were completed satisfactorily on December 11, 1968; and the solar array was delivered to the General Electric Company. A final test report describing the tests conducted, calibration data, and the test results (including anomalies) is contained in Appendix I.

C. NIMBUS-D ARRAY

1. Solar Cell Humidity Tests

Humidity tests of the Nimbus-D solar cells, conducted on a sample basis, was completed on March 20, 1969. Prior to environmental exposure, the current output at 0.46 volts and 28°C was measured and recorded. Two groups of five samples per 1000 cells were then selected. One group of sample cells was exposed to an environment of 95-percent relative-humidity (min) at 25 ± 5°C for 14 days; the second group of sample cells was set aside for additional tests if required. After environmental exposure, the sample cells were inspected for electrical and mechanical defects. An electrical defect was identified as a current degradation of 3 mA when compared to the pre-humidity tests. A mechanical defect is defined as one large blister or peel (0.03 inch) or two small blisters (0.02 inch). Any one of the above failures was sufficient to reject the manufacturers lot from which the cell was selected.

The first test contained 50 cells representing approximately 10,000 cells. After exposure two cells exhibited current degradation in excess of 3 mA and manufacturers lots 07571 and 07486 were placed on hold for additional tests. The remaining cells were released to manufacturing for fabrication of solar cell modules. A second set of sample cells representing the rejected lots were subjected to a second test.

The second test contained 13 cells; 5 cells represented 500 spare cells, 8 cells represented the rejected lots (five from lot 07571, three from lot 07486). Examination of the cells representing the 500 spare cells indicated no failures. Examination of the sample cells representing the rejected lots indicated no failures due to humidity tests. One cell from lot 07571 was cracked during the post-humidity test. Since the remaining sample cells (4) adequately represented the manufacturers lot, the cells were released to manufacturing.

A detailed description of the tests and the results are contained in Appendix II.

2. Substrate Procurement

The Nimbus-D solar array substrate procurement program, leading to the delivery of a flight quality unit, is divided into six phases:

Phase I	Process Development
Phase II	Mold Design and Fabrication
Phase III	Fabrication and destruct transition and platform
Phase IV	Development of measuring technique (dimensional)
Phase V	Evaluation of Destruct Units, and
Phase VI	Production of Flight Hardware

Evaluation of the destruct unit produced satisfactory results and the Goodyear Aerospace Corporation was authorized to fabricate the first flight unit (serial no. 017). A detailed description of the tests and the test results of phases I through V are contained in Appendix III.

3. Solar-Cell Module Fabrication

Fabrication of the 10- and 6-solar modules was completed by March 28, 1968 and electrical test was 80 percent complete.

4. Plans for the Next Report Period

Fabrication of the first flight quality substrate will be completed and acceptance tests will be conducted. Upon completion of the first unit, fabrication of the second flight quality unit will be initiated.

Electrical test of the remaining solar cell modules will be completed, and bonding of the solar-cell modules to the substrates will be started when the substrates are delivered.

SECTION 3

STORAGE MODULE

A. GENERAL

Each storage module consists of a two-piece magnesium housing, 23 nickel-cadmium storage cells, and an electronic board. Eight storage modules are supplied with each flight system.

B. NIMBUS-B2 STORAGE MODULES

All the storage modules were shipped to the integration contractor for spacecraft integration and test on September 19, 1968. In February 1969, two storage modules (serial numbers 003 and 008) were delivered to RCA for use during final acceptance tests of the Nimbus Battery Conditioning Data Logger Unit.* During the acceptance test, a relay failed in the crossbar scanner of the data logger and battery voltages were applied to the telemetry circuits. The telemetry circuit affected and the voltage applied are listed in Table 2. The application of battery voltages to the telemetry circuits caused an immediate failure of the battery voltage telemetry circuit in storage module No. 003 and placed a high voltage stress on the balance of the telemetry circuits. The voltages applied to the telemetry circuits of storage module No. 008 were not large enough to effect the telemetry performance. Repair and test of the storage module was completed on March 13, 1969 and the units were returned to the General Electric Company for use as spares for the Nimbus-B2 Spacecraft. Calibration and test data are contained in Appendix IV.

C. NIMBUS-D STORAGE MODULES

1. Procurement

a. Storage Cells

The third and final shipment of 25 storage cells was delivered to the RCA Corporation during January 1969. The total number of cells received to

*RCA, Astro-Electronics Division, Instruction Manual Nimbus Battery Conditioning Data Logger Unit, Contract 028-G20212, Princeton, N.J. February 28, 1969.

TABLE 2. TELEMETRY CIRCUIT TESTS VOLTAGES

Telemetry Circuit	Pin Connection	Highest Applied Voltage	
		S/N 003	S/N 008
Battery Discharge Current Telemetry Output	J2-2	-28.91V	-1.41V
Battery Charge Current Telemetry Output	J2-3	-31.30V	-2.83V
Battery Voltage Telemetry Output	J2-4	-32.74V	-4.25V
Battery Temperature Telemetry Output	J2-5	-32.73V	-5.66V
NOTE: Voltages listed above are referenced to the telemetry return. The telemetry return and power return (battery positive) were tied together during test.			

date was 308; the number returned to the vendor was four. The results of acceptance tests conducted at the RCA Corporation, Astro-Electronics Division during incoming inspection and the test data obtained at the General Electric Co, Battery Products Division, were satisfactory. The tests performed at each location were based on the availability of tests equipment, and the tests were not repetitive except in two cases (Capacity at 0°C, Capacity at 25°C). Where the tests were repetitive, the results were within limits of the test equipment. The test results are contained in Appendix V, Par A.

b. Storage Module Castings

The balance of the castings (four units) passed incoming inspection and they were released to manufacturing. Procurement of the storage module castings was completed as of March 15, 1969.

2. Manufacturing

a. Heat Sinks

Fabrication and test of the remaining heat sinks (seven units) was completed by February 28, 1969 and the units were released for storage module

fabrication. Early in January 1969, the 2N2016 transistor (used in the shunt dissipator circuit on the heat sink assembly) had to be replaced, as multiple failures were being experienced during both the heat sink assembly test sequence and the screening test sequence. A summary of these failures is as follows:

- Screening - Prior to release to controlled stores, each transistor was screened in accordance with RCA Specification 1721353. This specification includes a 300-hour power burn-in and a dew point test. The first lot purchased for Nimbus-D program was screened using Revision R of specification 1721353; the second, third and fourth lots were screened using Revision T of specification 1721353. The screening rejects are listed in Table 3.

TABLE 3. SHUNT DISSIPATOR TRANSISTOR SCREENING TEST RESULTS

Lot	Lot Quantity	Dew Point Failures	ΔI_{CBO} Failures
1	12	3	2
2	8	3	3
3	12	5	4
4	13	5	3

- Assembly Testing - All heat sink assemblies were tested in accordance with RCA Test Procedure 1750979, Revision E. Leakage current measurements through the temperature range of -25°C to +35°C was added to the Nimbus D heat sink test sequence to detect dew point leakages in the 2N2016 transistor (Paragraph 7.0 of 1750979). Six 2N2016 transistors (three from lot No. 1, two from lot No. 2, and one from lot No. 3) failed the heat sink test sequence. The failure modes were:

  (a) Excessive leakage current as a function of temperature,

  (b) Excessive leakage current not associated with temperature variations, and

  (c) Beta changes.

The associated Test Descrepancy Reports No are TDR's 3920, 3221, 3922, 3929, 3930, and 3965. As a result of these failures a replacement transistor (Solitron SDT 9903, RCA Drawing 1970655-1) was selected and qualified for use. A detailed description of the replacement part selection, special tests, and results are contained in Appendix V, Par B.

b. Storage Module

(1) Fabrication. Fabrication of the eight-flight storage modules (serial No. 022 through 029) was completed by the end of February. Fabrication of the three spare-flight storage modules is in process.

(2) Unit Test. - Pre-potting tests, completed satisfactory by March 5, 1969, consisted of the following.

- Circuit Alignment and Electrical Test
- Conditioning Tests
- Short Tests
- Capacity Tests

As a result of multiple failures (refer to Par 2a, Heat Sinks), circuit alignment and electrical tests of four storage modules (022 through 025) were repeated after replacement of the shunt dissipator transistor. There was no significant difference in the data obtained with the new shunt dissipator transistors. The pre-potting tests results are contained in Appendix V, Par C.

3. Plans for the Next Report Period

Assembly and pre-pot electrical tests of the three spare flight storage modules (serial No. 030, 031, and 032) will be completed. Potting, post-potting electrical tests, and vibration tests of the eight flight storage modules will be completed and the storage modules will be integrated with the control module for power subsystem tests.

SECTION 4

CONTROL MODULE

A. GENERAL

The control module contains the electrical circuits that regulate the d-c voltage outputs for the spacecraft loads, limits the solar array voltage to safe load levels, provides telemetry signals for system evaluation, and provides the interface between the solar array, storage module, and spacecraft loads. The configuration of the Nimbus-D and Nimbus-B control module is identical except for the temperature telemetry circuit added to the Nimbus-D control module. Refer to "Quarterly Technical Report No. 2," (R3340) issued July 15, 1968.

B. NIMBUS-D CONTROL MODULE

1. Unit Tests

Unit test of control module (Serial No. 06) was completed during the report period. The test sequence and test results are contained in Appendix VI.

2. Predicted Control Module Input Characteristics

A predicted I-V characteristic for the Nimbus-D array was generated on the basis of test data obtained from a typical solar cell at 28°C (see Figure 1). The cell data was degraded for the beginning of life (BOL) conditions listed in Table 4 and a voltage drop of 1.8 volts was used to account for resistance across the array blocking diodes and the slip rings. The predicted I-V characteristics shown will be simulated to represent the Nimbus-D array during thermal vacuum tests of the power supply subsystem (control module and 8 storage modules).

TABLE 4. BEGINNING-OF-LIFE SOLAR CELL DEGRADATION

Design Factor	Nominal Value	Parameter Affected
Glassing Loss	5%	I_{sc}
UV Degradation	3%	I_{sc}
Series Resistance	1%	V_{pm}

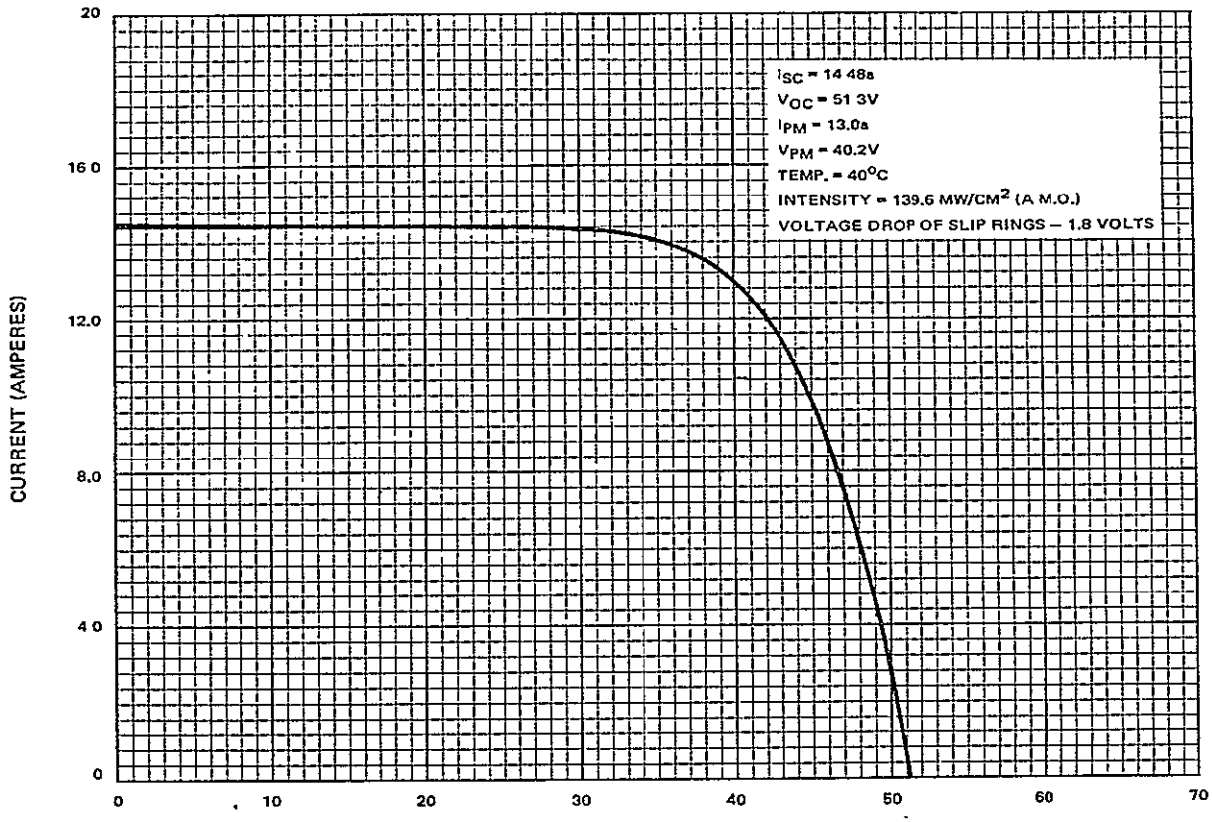

Figure 1. Predicted Beginning-of-Life I-V Characteristics at Control Module Input

3. Plans for Next Report Period

During the next report period, the control module and the eight storage modules will be integrated into a subsystem and system tests using the predicted I-V characteristics in place of an array will be started.

SECTION 5

ENGINEERING RELIABILITY

Reliability and Quality Assurance Engineering continued to provide consultations on the resolution of technical part problems encountered during procurement and preconditioning.

During the report period, 20 Test Discrepancy Reports (TDR's) were issued during test of the control module and the 11 storage modules.

One Non-Standard Part was approved for space flight hardware of the Nimbus-D Power Supply Subsystem. In this case, a Solitron SDT 9903 transistor (RCA 1970655-1), was approved for use in the shunt dissipator circuit instead of the 2N2016 transistors. Refer to Appendix V, Par B for details.

APPENDIX I

NIMBUS-B2 SOLAR ARRAY TEST REPORT

A. INTRODUCTION

This Appendix represents the results of the assembly and acceptance test programs for the Nimbus-B2 Solar Array (two platforms, Serial Nos. 15 and 16). Environmental exposures selected for the acceptance test program are intended to simulate flight conditions so that successful completion of the specified tests adequately demonstrates the capability of the platforms to perform their intended function in flight.

Test logs for each platform were maintained through the assembly and test period (April 1964 to December 1969) by the cognizant assembly and test personnel. Significant data from the acceptance test program has been included in this report. Complete documentation is retained in the files of the Space Power Group, the Environmental Simulation Group and the Environmental Test Group at RCA.

B. SUMMARY

Solar array performance during the acceptance test program (initiated July 28, 1968 and completed December 10, 1968) met all the test requirements specified. Illumination tests, conducted prior to and after thermal vacuum exposures, are used to evaluate solar cell performance. Illumination tests performed after thermal vacuum tests showed degradation of module boards H, K, and L which were suspect at the start of testing. Ten 10-cell modules were replaced - less than 1-percent of the total solar cells. Illumination tests, conducted prior to and after thermal-vacuum exposure, demonstrated that the array is capable of delivery 501 ±37 watts at 34 volts during normal orbital operation, see Figure I-1.

The thermal vacuum test (100 cycles on the Nimbus-B program) was increased to 225 cycles for the Nimbus-B2 program. Orbital heat fluxes remained unchanged at 0.857 watts per square inch during satellite day and 0.077 watts per square inch during satellite eclipse. Complete electrical tests were conducted of all electrical circuits during thermal exposure. Electrical tests conducted during thermal-vacuum exposures (225 cycles) indicated that the temperature telemetry circuits had stable voltage versus temperature characteristics. The predicted accuracy of these circuits is ±2°C at end-of-life conditions. A temperature variation of 3.2°C between the solar cells and the temperature telemetry thermistor (created when the spacecraft is placed in a 600 nm, high-noon orbit) is

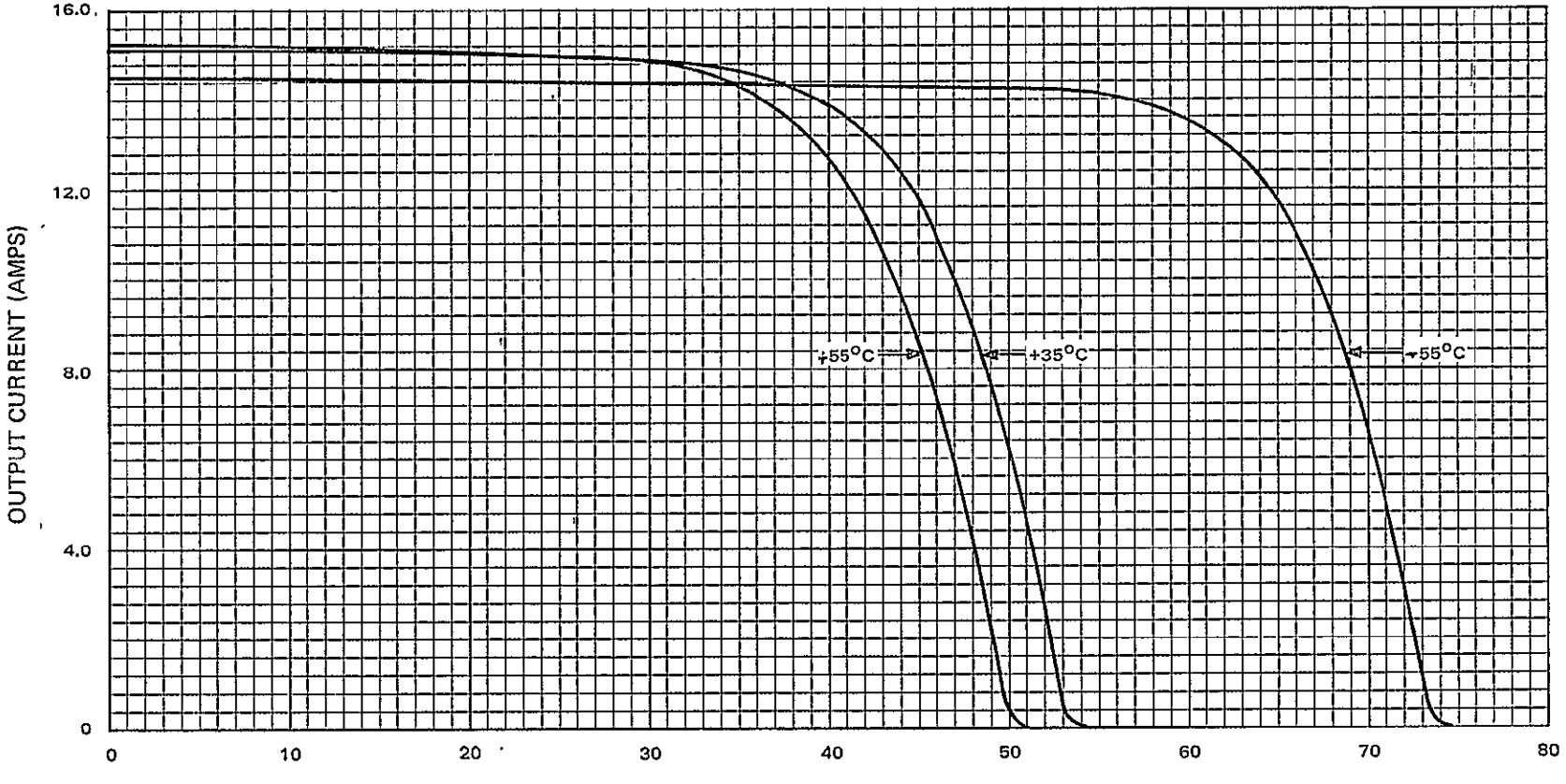

Figure I-1. Nimbus-B2 I-V Characteristics vs Temperature at Output Side of Blocking Diodes

caused by the thermal gradient through the solar platform substrates. A direct temperature readout for the solar cells of the array in the above orbit can be obtained from Figures I-2 and I-3. Typical voltage versus telemetry voltage characteristics for the voltage telemetry circuits on module boards A, F, G, and J are shown in Figure I-4.

Three separate acceptance tests were performed on the flight deployment-drive motor assemblies to demonstrate their ability to meet launch and orbital requirements. Each motor drive assembly (containing redundant motors) deployed the array within 30.6 seconds with only one motor energized and within 27.0 seconds with both motors energized. The maximum specified deployment time is 36.0 seconds. The test voltage is 24.0 volts dc with no current values specified. Weight and balance tests indicated that the center of gravity and center of rotation are displaced by 0.1387 in. due to eccentricity. Also, a total of 0.442 inches maximum exists between the center of rotation due to deflection. As a result, the platforms (Serial No. 15 and 16) will remain unbalanced in orbit by a maximum of 10.7 in. lbs. due to eccentricity. The total weight of the two platforms which includes two deployment drive-motor assemblies and the General Electric Co. latching hardware is approximately 77.2 lbs.

Vibration tests were limited to the deployment motors; vibration of the array was not included in the RCA acceptance test program.

A chronological sequence of events describing acceptance test program for the solar array is listed in Table I-15.

C. GENERAL DESCRIPTION

The Nimbus-B2 array contains two solar platforms, each consisting of a substrate containing the solar-cell modules, a transition assembly containing a control shaft clamp and latching assembly, and a deployment drive motor assembly consisting of a motor, gear reduction unit, and deployment mechanism.

The solar platform and transition substrates are honeycomb-structures of aluminum foil providing high torsional stiffness and low inertia and weight. Each solar platform is 38.4 inches wide by 96.0 inches long and is shaped to clear the main structure of the spacecraft. The solar platform has one flat face (sun side) for solar cell mounting and a reverse face (earth side) that double tapers from the rotational axis to the outer edges. Along the rotational axis, a deep torque tube beam is constructed of high density honeycomb and aluminum sheets. The honeycomb is covered with an aluminum sheet 0.003 inch thick to minimize weight.

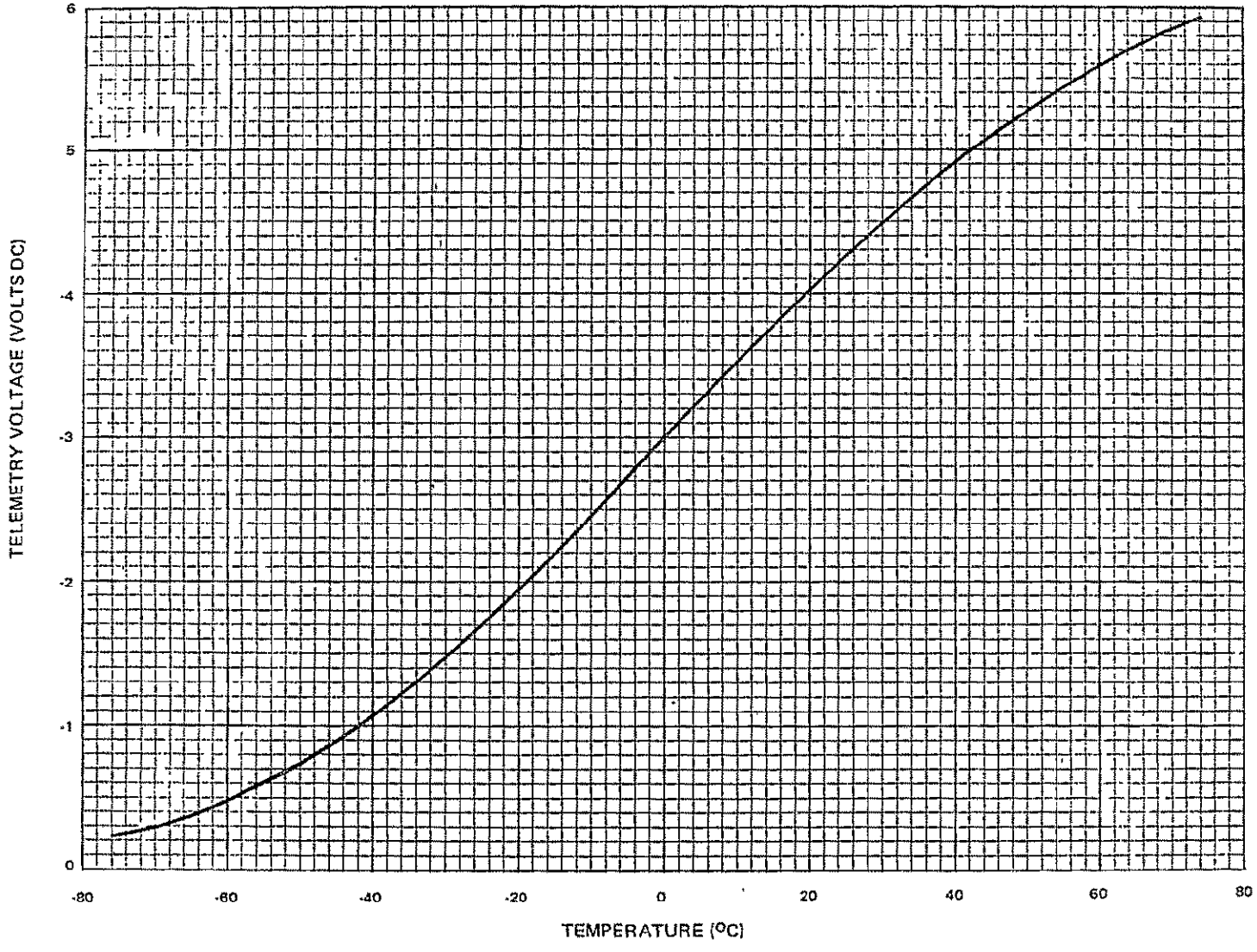

Figure I-2. Temperature Telemetry Calibration, Serial No. 5, 3.2°C Gradient Shifted

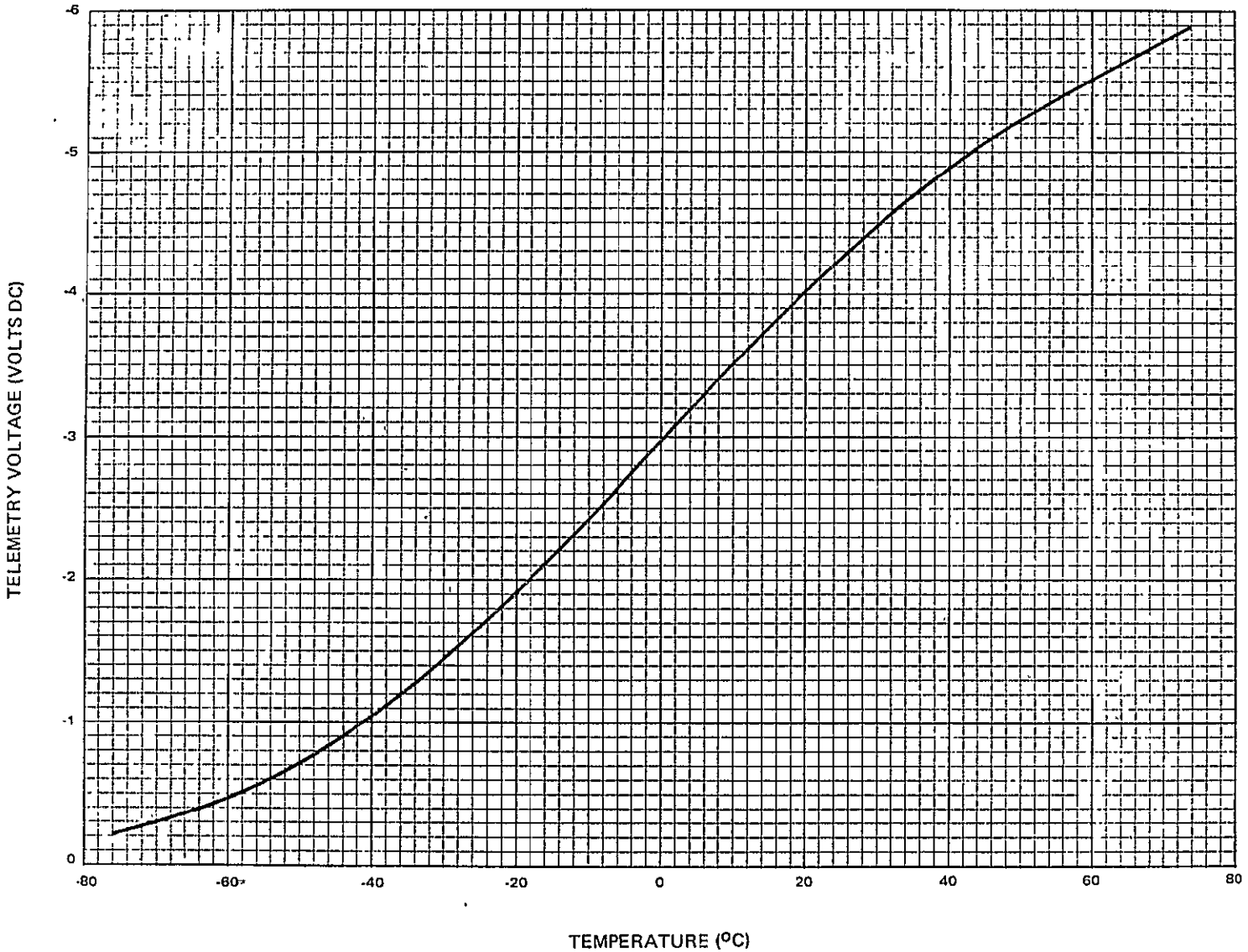

Figure I-3. Temperature Telemetry Calibration, Serial No. 6, 3.2°C Gradient Shifted

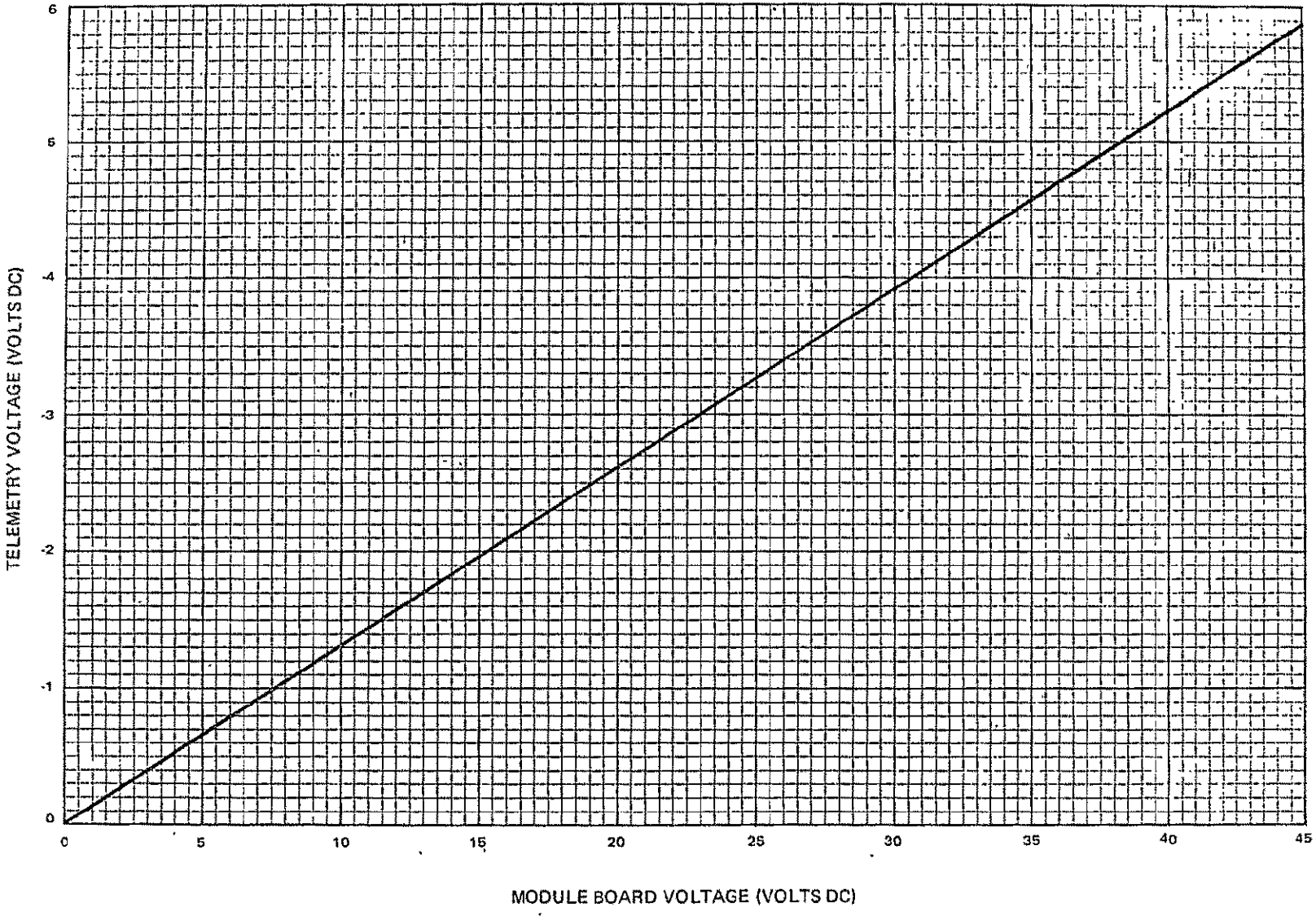

Figure I-4. Typical Voltage Telemetry Curve for Boards A, F, G, and J

Temperature drops are minimized across the different densities of the substrate because of the double taper construction, that provides excellent thermal conductivity to the earth-side surface and subsequent cooling of the heated sun-side. Absorptivity and emissivity of the sun-side and earth-side surfaces are such that an average equilibrium temperature of approximately 40 to 45°C will prevail during the satellite day.

Once in orbit, the platforms are opened by deployment motor-drive assemblies mounted near the hinge line between the transition section and the platform. From the folded position the solar platform is driven to the open position (approximately 135 degrees) in less than 36 seconds. The solar platforms are locked into the open position by the hinge latch, and then rotated together to orient the solar cells (sun-side) toward the sun.

The sun-side of each platform contains six solar-cell module boards. Four of the boards contain 98 ten-cell modules, a fifth board contains 97 ten-cell modules, and the sixth contains 97 six-cell modules for a total of 5,472 solar cells. The solar cells in each module are connected in parallel, the modules are connected in series, the boards are connected in parallel, and the two solar platforms are connected in parallel to form the Nimbus-B2 array.

The basic solar cell consists of a p-type silicon wafer unto which phosphorus has been diffused to form an n-layer. Special, optically coated, six-mil thick, fused silica platelets are bonded to the outside faces of the solar cells. The upper surface of each platelet is coated with a vacuum deposited anti-reflective material; the lower surface is coated with a vacuum deposited blue-red reflective material.

The earth-side of each platform contains the following components:

- Two voltage telemetry circuits,
- Two voltage telemetry overvoltage protection circuits,
- One temperature telemetry sensor,
- Six blocking diode component boards,
- Five board thermocouples,
- One terminal strip, and
- One harness cable.

The deployment drive-motor assembly consists of a drive motor and gear train. The drive motor consists of two redundant high speed motors mechanically coupled in series and electrically connected in parallel. Both motors drive a 5-stage planetary gearhead which reduces the motor speed from 15,000 rpm to approximately 3 rpm under a no-load condition. The gearhead output shaft is

coupled into the gear train by means of a spur gear. Each motor is capable of performing a full deployment successfully. The deployment drive-motor assembly is designed to overcome a mechanical resistance of up to 63 in-lbs. at the solar platform hinge line and still complete a full deployment.

D. Test Procedures

A summary of the tests conducted and a reference to the applicable test procedure are provided for the following:

- Module tests
- Weight and balance test
- Electrical Acceptance test
- Deployment Drive-Motor Assembly acceptance tests
- Deployment tests
- Thermal Vacuum tests
- Illumination tests.

1. Module Tests

a. Temperature Telemetry Calibration

The temperature telemetry circuit, 1964596, is calibrated prior to being assembled on the solar platform. Test procedure, TP-CA-1962593 is used for establishing the telemetry voltage versus temperature characteristics. The temperature telemetry characteristics are measured from +70°C to -80°C whereas the anticipated operating temperature of the solar platforms in flight are approximately +55°C and -60°C.

b. Voltage Telemetry Calibration

Acceptance testing of the voltage telemetry circuit, 1702461, is performed in conjunction with the environmental tests performed on the solar platforms. Calibration of the voltage telemetry circuit is not necessary due to simplicity of operation. The voltage divider circuit is not temperature sensitive.

c. Overvoltage Protection Test

The overvoltage protection circuit, 1962593, is electrically checked at the same time the temperature telemetry circuit is calibrated using test procedure TP-CA-1962593. The temperature range of +70°C to -80°C, identical to that used for the temperature telemetry calibration test is used. A voltage of -24.5 Vdc which exceeds the zener voltage by approximately 15 volts is applied during the test in order to demonstrate the circuit limiting characteristics.

2. Weight and Balance Test

The weight and balance test, outlined in test procedure 1721438, is performed to establish the center of gravity locations due to deflection and weight distribution.

3. Electrical Acceptance Test

Electrical acceptance tests were performed according to test procedure TP-EA-1975606 on each solar platform before final wiring and component board encapsulation tasks were accomplished. These tests include d-c isolation, solar cell circuit (board level) continuity, and illumination. The 10-cell module boards on each platform are illuminated under the same conditions of intensity and temperature, and the electrical output of each board is then compared on a relative basis to the outputs of the other 10-cell module boards on that platform. All boards are acceptable if the difference in short circuit currents (I_{sco}) and open circuit voltages do not exceed the 15 ma and 1.0 volt dc, respectively. Illumination data on the six cell module boards (one per platform) was not obtained due to the limitations of the tungsten illuminator.

Additional requirements of identical I-V characteristics, are placed upon the illumination data obtained from the 10-cell module boards. Any deviations from the above requirements are noted and evaluated using the trouble shooting techniques described in the test procedure.

4. Deployment Drive Motor

Each of four deployment drive motors, two flights and two spares, are subjected to a series of rigorous flight acceptance tests. Each test is designed to provide a complete data package from which the drive motor can be evaluated for its efficiency of operation and capability to perform the task of platform deployment. These tests, described in test procedures 1721444 and TP 1751589, include speed-torque tests, cold temperature environment test, vibration, thermal vacuum and deployment tests. Deployment tests are performed to verify two parameters. First, that the transition and platform assemblies have been properly joined at the hinge line, to provide for minimum clearance between hinge interfaces and maximum ease of deployment. Secondly, the deployment test will verify the final requirement placed upon the deployment motor by demonstrating a full 135° deployment within the allowable 36 seconds. Automatic motor shut-off is also demonstrated at this time.

5. Illumination Tests

Indoor and outdoor illumination tests, described in test procedure TP-IL 1975606, are performed on each platform to evaluate solar cell performance. Indoor, illumination tests are performed before and after the thermal vacuum

test under a tungsten light source set to air mass zero (AMO), one sun intensity using Nimbus standard solar cells. An outdoor illumination test is performed as a final test on the platforms before shipment to the integration contractor.* The outdoor illumination test data obtained through actual sunlight illumination is corrected to the same conditions of intensity and temperature as those used during indoor illumination test using standard correction coefficients and techniques. All data is compared for possible degradation due to environmental testing and for correlation between indoor and outdoor illumination tests.

6. Thermal Vacuum Tests

The thermal vacuum test, described in test procedures TP-TV-1975606 and TP-TE-1975606, consists of 225 thermal cycles at a pressure of 1×10^{-5} torr or less. Each thermal cycle is 108 minutes in duration and is thermally simulated by exposing each platform to 0.857 watts/in^2 equivalent orbital daytime incident heat flux for 73.2 minutes and 0.077 watts/in^2 equivalent orbital eclipse heat flux for 34.8 minutes. The test was performed utilizing the ten-foot diameter thermal-vacuum facility. Incident heat fluxes were provided through the use of tungsten wire arrays facing the solar-cell side of each platform. The required tungsten array heater power inputs were determined during a calibration test (refer to Appendix VII) conducted prior to installing the Nimbus platforms in the chamber. Temperatures on the platforms were allowed to seek their own levels but were monitored to prevent over-exposure. Simulation of the thermal sink of outer space was obtained through the use of shrouds operated at liquid nitrogren temperatures. Orbital daytime earth albedo effects are not simulated.

E. TEST RESULTS

Final test results, test anomalies, and repairs required to meet required specifications are presented in the following paragraphs.

1. Temperature Telemetry Calibration Data

Temperature telemetry calibration for telemetry circuits 4, 5 and 6 (serial numbers 4, 5, and 6, respectively) was conducted between July 25, 1968 and July 28, 1968. Each circuit was exposed to temperatures between -80°C and +70°C with stabilization every 10°C. The telemetry output voltage versus temperature characteristics are shown on Figures I-5, I-6, and I-7, respectively. There were no test anomalies. Telemetry circuit No. 5 was bonded to platform No. 16 (serial No. 16) on August 15, 1968; telemetry circuit No. 6 was bonded to platform No. 15 (serial No. 15) on July 29, 1968. On November 1, 1968,

---

* General Electric Co., Philadelphia, Pennsylvania

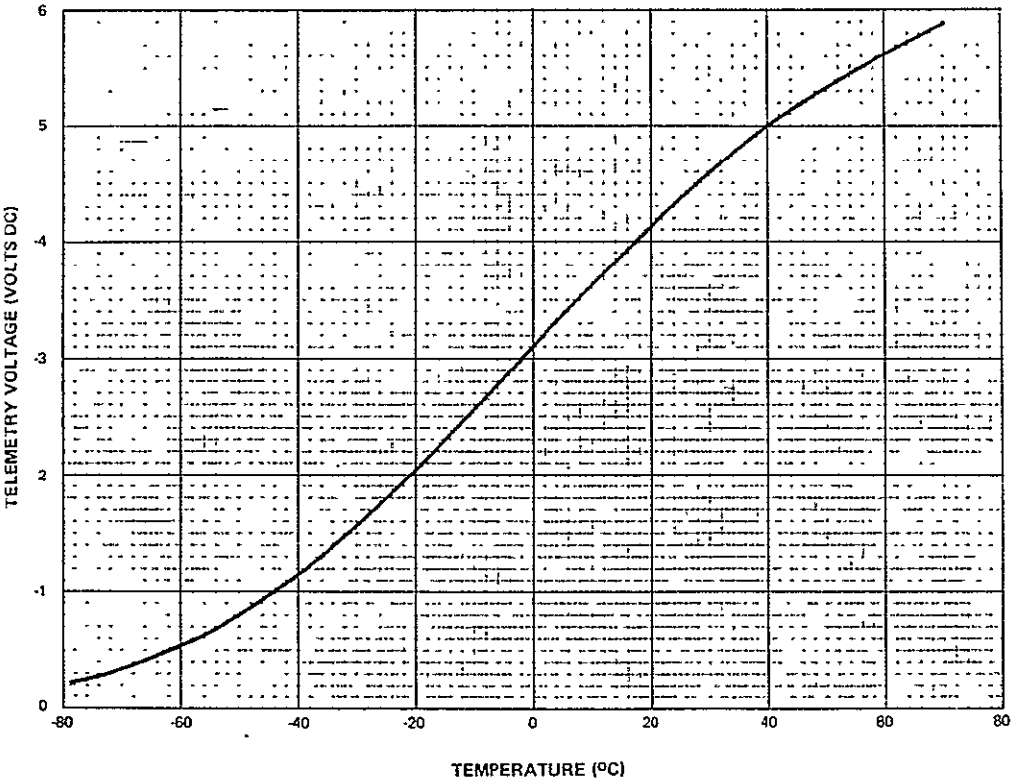

Figure I-5. Temperature Telemetry Calibration Curve, Serial No. 4

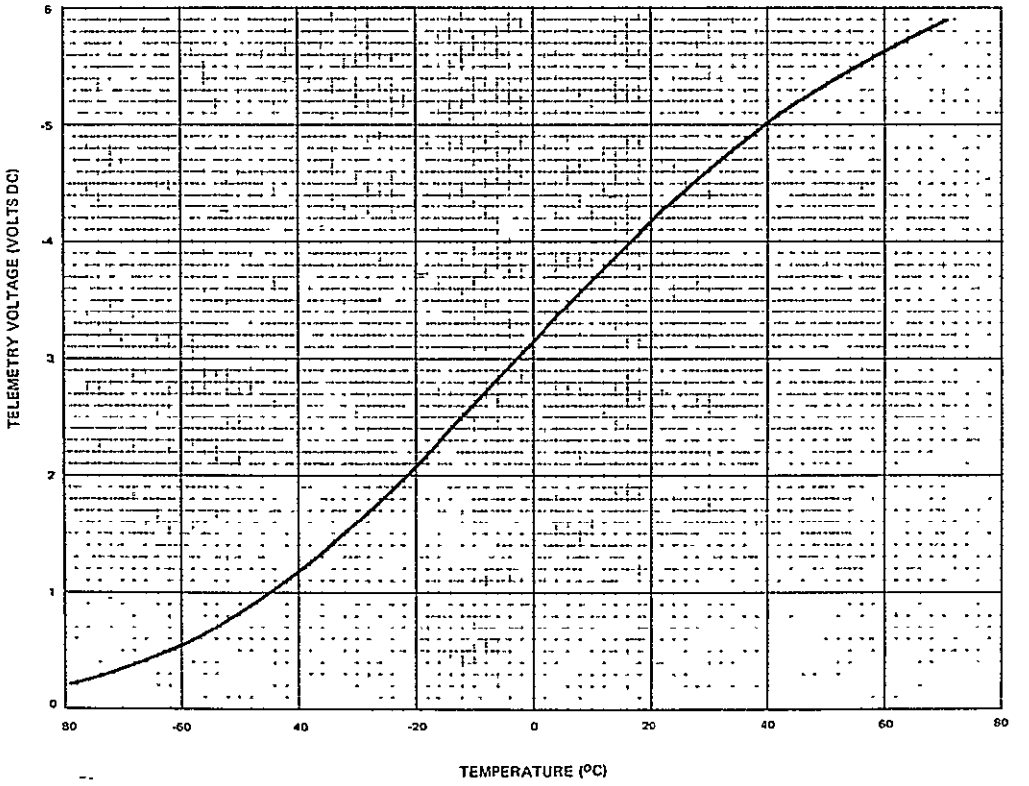

Figure I-6. Temperature Telemetry Calibration Curve, Serial No. 5

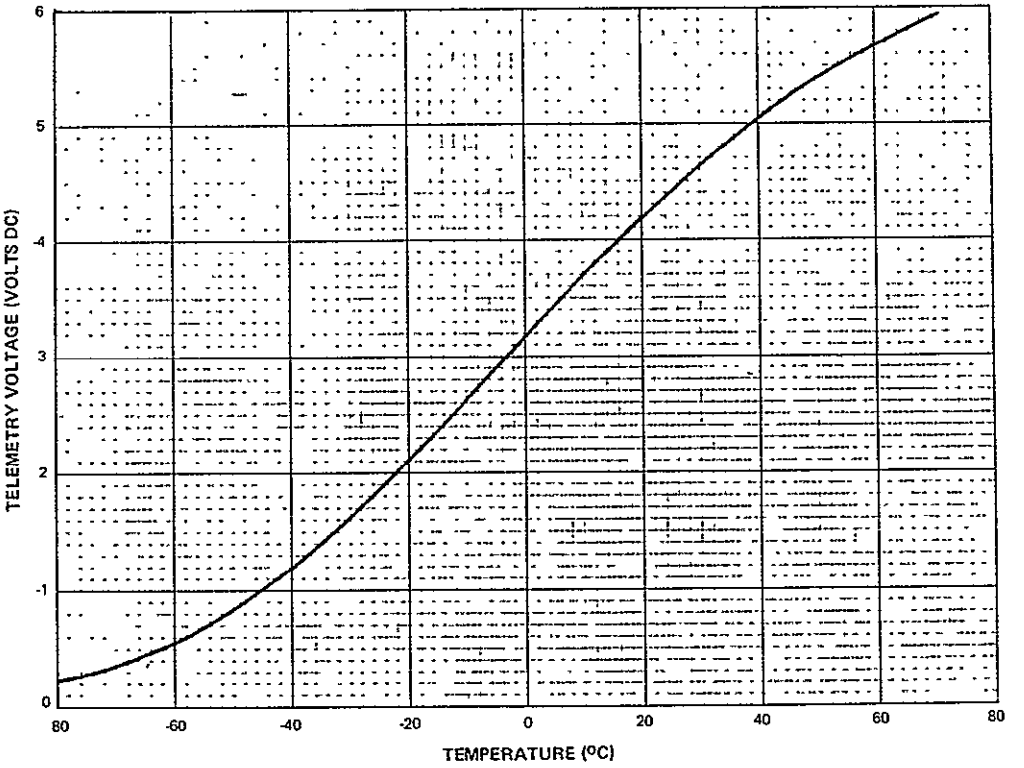

Figure I-7. Temperature Telemetry Calibration Curve, Serial No. 6

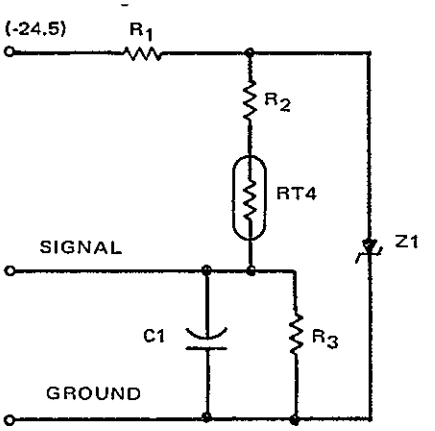

Figure I-8. Temperature Telemetry Schematic

telemetry circuit No. 4 was recalibrated to compensate for an engineering change performed on September 26, 1968. The engineering change was required as capacitor C1 (see Figure I-8) was originally installed with the wrong polarity. Based on the results of the recalibration (see Figure I-9) it was determined that no current was leaking through the capacitor C1 while it was reversed in the telemetry circuit and therefore, recalibration of telemetry circuits No. 5 and 6 was not necessary.

Figures I-2 and I-3 are 3.2°C shifted temperature telemetry curves. These telemetry curves are valid for determining solar cell temperatures from direct telemetry after the Nimbus spacecraft is placed in orbit.

2. Voltage Telemetry Performance Test Data

Calibration of the voltage telemetry circuit is not performed because of its simplicity of operation and temperature insensitive, precision resistor components. It is checked on a performance basis during thermal-vacuum testing of the solar platforms. A typical voltage telemetry transfer characteristic is shown in Figure I-4. During the night portion of thermal vacuum cycle 71, an attempt was made to evaluate the voltage telemetry overvoltage protection circuit (see Figure I-10) on Board A by shorting the negative terminal of Board A to the voltage telemetry output (simulating an open circuit). The overvoltage protection circuit is designed to operate when an open circuit exists across the voltage telemetry output resistor. The overvoltage protection circuit, was exposed to a potential of approximately 70 volts of board A. At the instant of shorting, the 70-volt potential went to zero and voltage telemetry output dropped from 8.4 volts to approximately 3 volts. The proper voltage telemetry signal could not be restored after that. Evaluation of the failure mode and test circuit showed that when board A was shorted across the voltage telemetry output resistor, the power supply output capacitor was allowed to discharge. Since the test circuit did not have any provisions for current limiting, the current ratings of blocking diode CR1, and Zener diode CR3, were exceeded. Further investigation at the completion of the thermal vacuum tests indicated that Zener diode CR3 was damaged and blocking diode CR1 was overstressed. Both diodes were replaced.

In addition to the evaluation tests performed on the overvoltage protection circuit, a simple dynamic resistance check was made on the voltage telemetry output resistor. A 5-volt potential was placed across the resistor while a current reading was made. The measured current was compared against the expected current calculated by using the 5-volt potential and the known resistance value. Both current values were within 0.2 ma, indicating the voltage telemetry output resistor was undamaged.

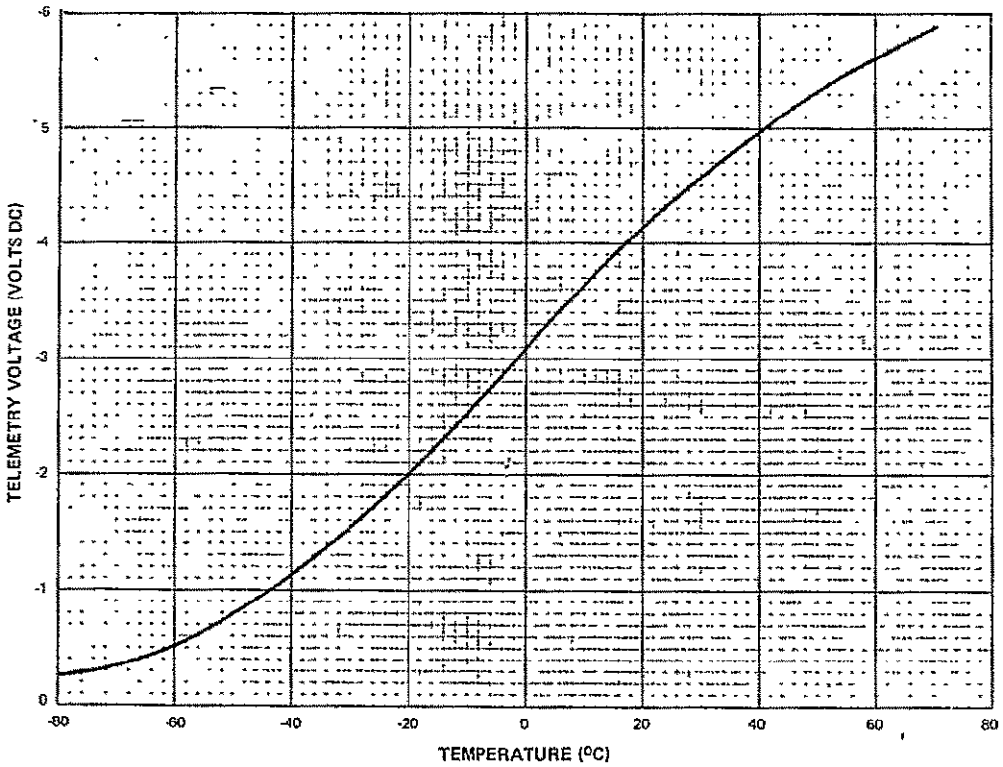

Figure I-9. Temperature Telemetry Curve, Serial No. 4, Post Repair

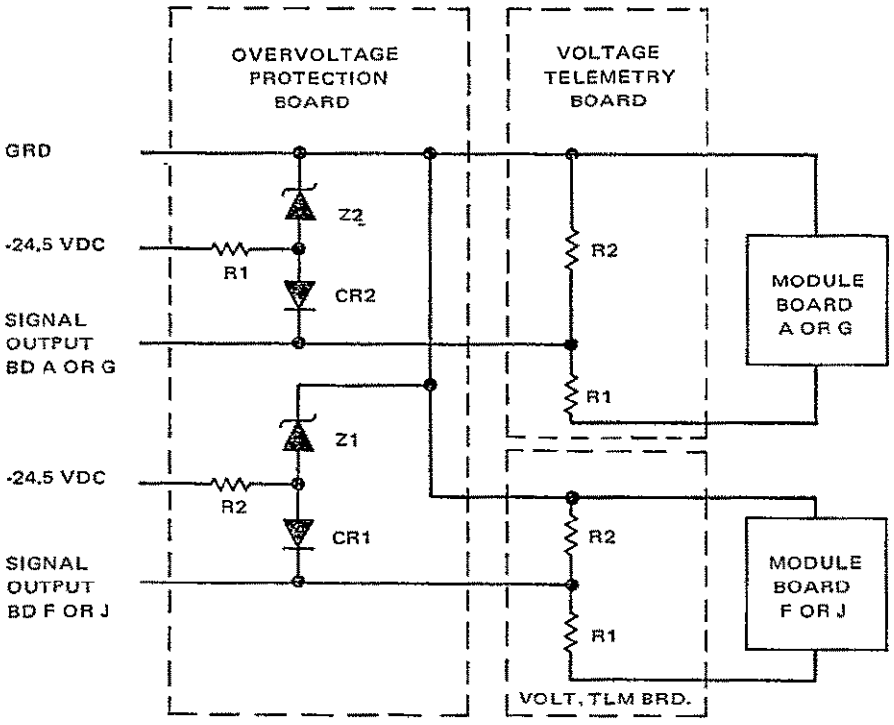

Figure I-10. Overvoltage Protection Schematic

A second failure occurred during rework of the overvoltage protection circuit. Failure analysis indicated the Zener diode CR3 was damaged because of a poor heat sink during rework operations. Diodes CR1 and CR3 were replaced a second time. Post rework testing verified proper functioning of the overvoltage protection circuit.

3. Voltage Telemetry Overvoltage Protection Test Data

Functional tests of the voltage telemetry overvoltage protection circuit (see Figure I-10) were performed over the temperature range of -80°C to 70°C at atmospheric pressure. The specified output voltages (2) for each board is -9.4 ±0.6 volts dc the actual output voltages for each temperature gradient are listed in Table I-1. There were no test anomalies. Overvoltage protection circuit No. 3 was bonded to platform No. 16 on August 15, 1968; overvoltage protection circuit No. 2 was bonded to platform No. 15 on July 29, 1968.

TABLE I-1. VOLTAGE TELEMETRY OVERVOLTAGE PROTECTION TEST DATA

	Voltage Telemetry					
	Serial No. 1		Serial No. 2		Serial No. 3	
Temp °C	Output No. 1 (Vdc)	Output No. 2 (Vdc)	Output No. 1 (Vdc)	Output No. 2 (Vdc)	Output No. 1 (Vdc)	Output No. 2 (Vdc)
27	9.67	9.61	9.66	9.72	9.68	9.58
71	9.57	9.51	9.55	9.61	9.58	9.48
41	9.64	9.57	9.62	9.68	9.65	9.55
2	9.73	-9.66	9.72	9.77	9.74	9.64
-18	9.78	9.71	-9.77	9.82	9.79	9.69
-48	9.87	9.79	9.85	9.91	9.88	9.69
-79	9.95	9.88	9.94	9.98	9.95	9.86

A malfunction of overvoltage protection circuit No. 3, associated with board A was experienced during thermal vacuum testing. Refer to Para. E2 for a detailed report.

4. Weight and Balance Test Data

The weight and balance test of platform No. 15 and 16 was completed on September 19, 1968 with the following results, the solar array will remain unbalanced in orbit by a force of 10.7 in. lbs due to eccentricity.

a. Test Description and Results

The mounting arrangement shown in Figure I-11 contains a 6-inch Starrett protractor head with a spirit level that is attached to the platform shaft. The protractor head, balanced with counterweights could easily detect variations of less than 0.5 degree. A Torqmeter (TQ-12-B torque wrench) with a ±75 in-lbs range was used to measure the unbalancing torque. The results of the tests are recorded on Figures I-12 and I-13.

These empirical curves are described by the equation:

$$T = \omega R \sin \Theta + \frac{\omega r}{2} \sin 2\Theta \qquad (1)$$

where

T = total unbalance torque at angle Θ.

W = total weight of platforms including GE Co. latchline hardware.

R = distance between center of gravity and center of rotation due to eccentricity.

r = maximum distance between center of gravity and center of rotation due to deflection.

The above equation* is the result of the addition of two sinusoidal curves with one curve having half the frequency of the other. This is caused by the center-of-gravity of the platforms being displaced from the center of rotation and by the center of gravity moving due to the platform deflection during rotation. The unbalance torque direction of the curves indicates that the center-of-gravity lies below the center of rotation towards the tapered surface of the platforms from zero to 114 degrees. The total weight of the platforms, including the two deployment motor assemblies and General Electric Co. latching hardware, was 77.2 lbs. Platform No. 15 weighed 39.1 lbs, platform No. 16 weighed 38.1 lbs. The weight difference is due to the latchline hardware design.

* The derivation of this equation is shown in Paragraph E-4b.

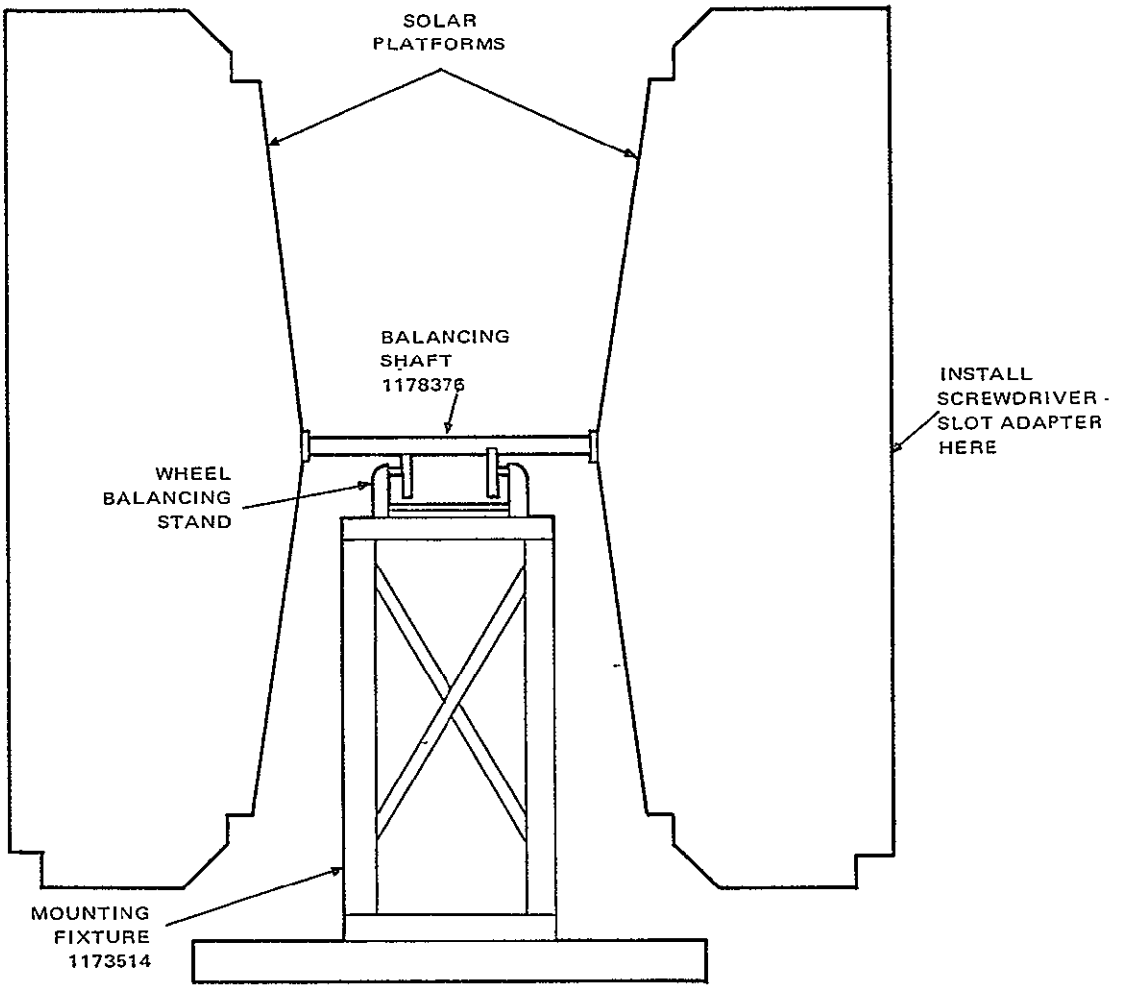

Figure I-11. Solar Platform Balance Test Setup

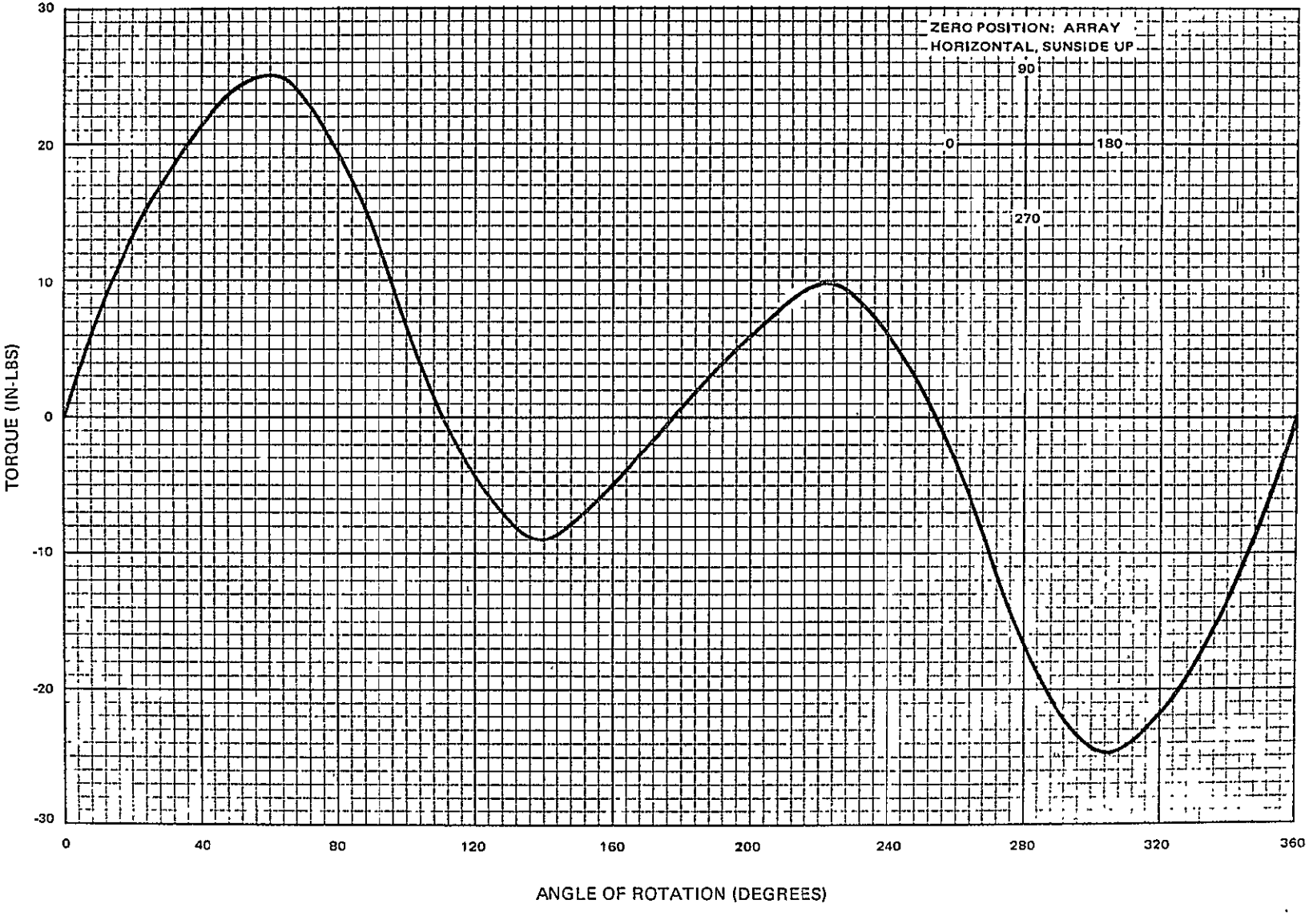

Figure I-12. Solar Array Balance, Clockwise Rotation

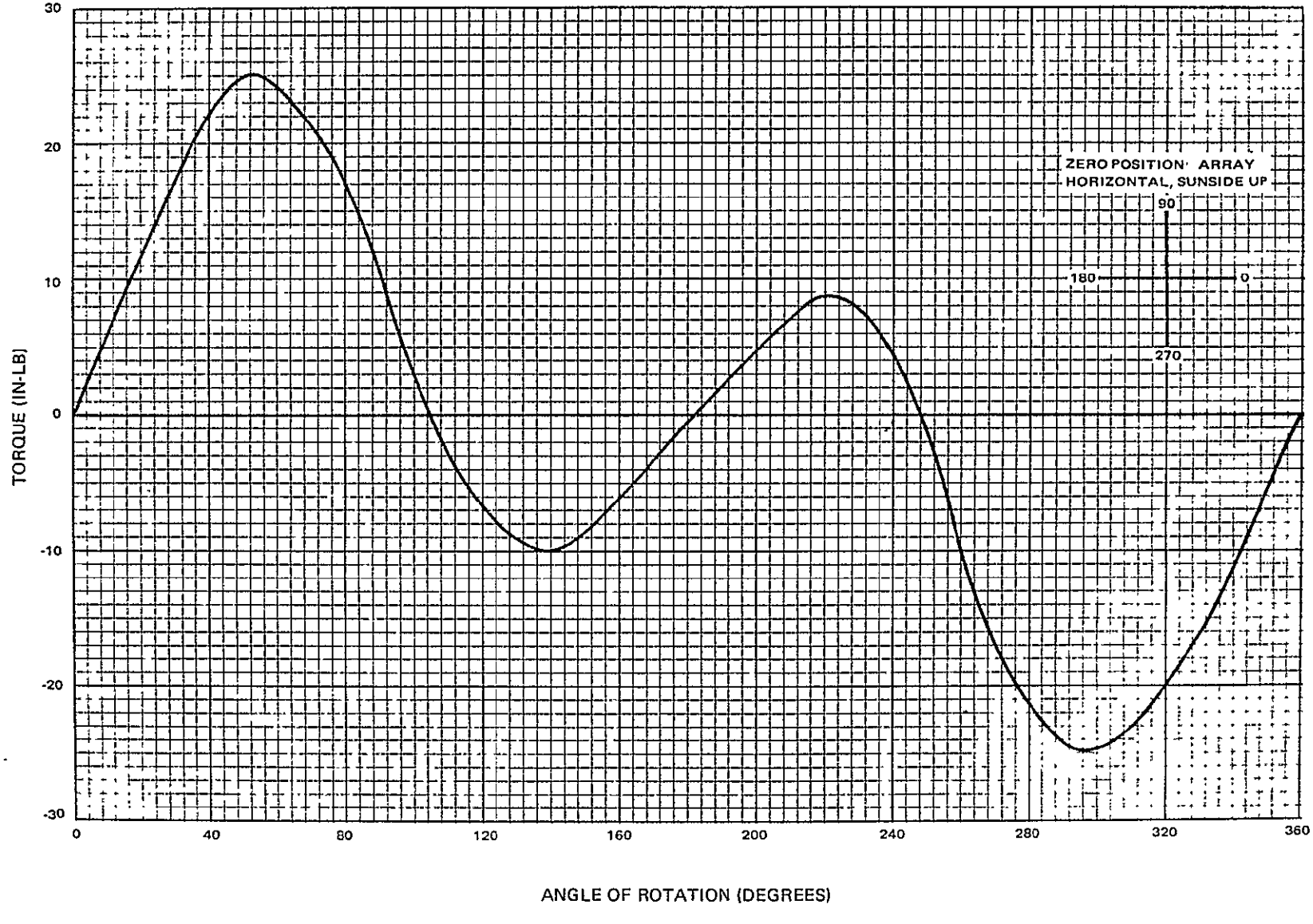

Figure I-13. Solar Array Balance, Counter Clockwise Rotation

Values of R and r are determined by choosing values of T and Θ from Figure I-13.

T_1 = 25 in-lbs at = 53°

T_2 = -10 in-lbs. at = 140°

Therefore,

$$T = \omega R \text{ sine } \Theta + \frac{\omega r}{2} \sin 2\Theta \quad (2)$$

$$25 = 77.2\ R \sin 53° + \frac{77.2r}{2} \sin 2\,(53°) \quad (3)$$

$$25 = 61.6\ R + 37.1\ r \quad (4)$$

and

$$-10 = 77.2\ R \sin 140° + \frac{77.2r}{2} \sin 2\,(140°) \quad (5)$$

$$-10 = 49.6\ R - 38.0\ r \quad (6)$$

Solving for R and r gives:

R = -0.1387 inches between the center of gravity and the center of rotation due to eccentricity.

r = 0.442 inches maximum between the center of gravity and the center of rotation due to deflection.

Separate curves of the unbalance torques due to eccentricity of the center-of-gravity and due to the deflection of the platform are plotted in Figure I-14.

The curve for center-of-gravity eccentricity is represented by:

$$T_1 = \omega R \sin \Theta \quad (7)$$

$$T_1 = 77.2\ (0.1387) \sin \Theta \quad (8)$$

$$T_1 = 10.7 \sin \Theta \quad (9)$$

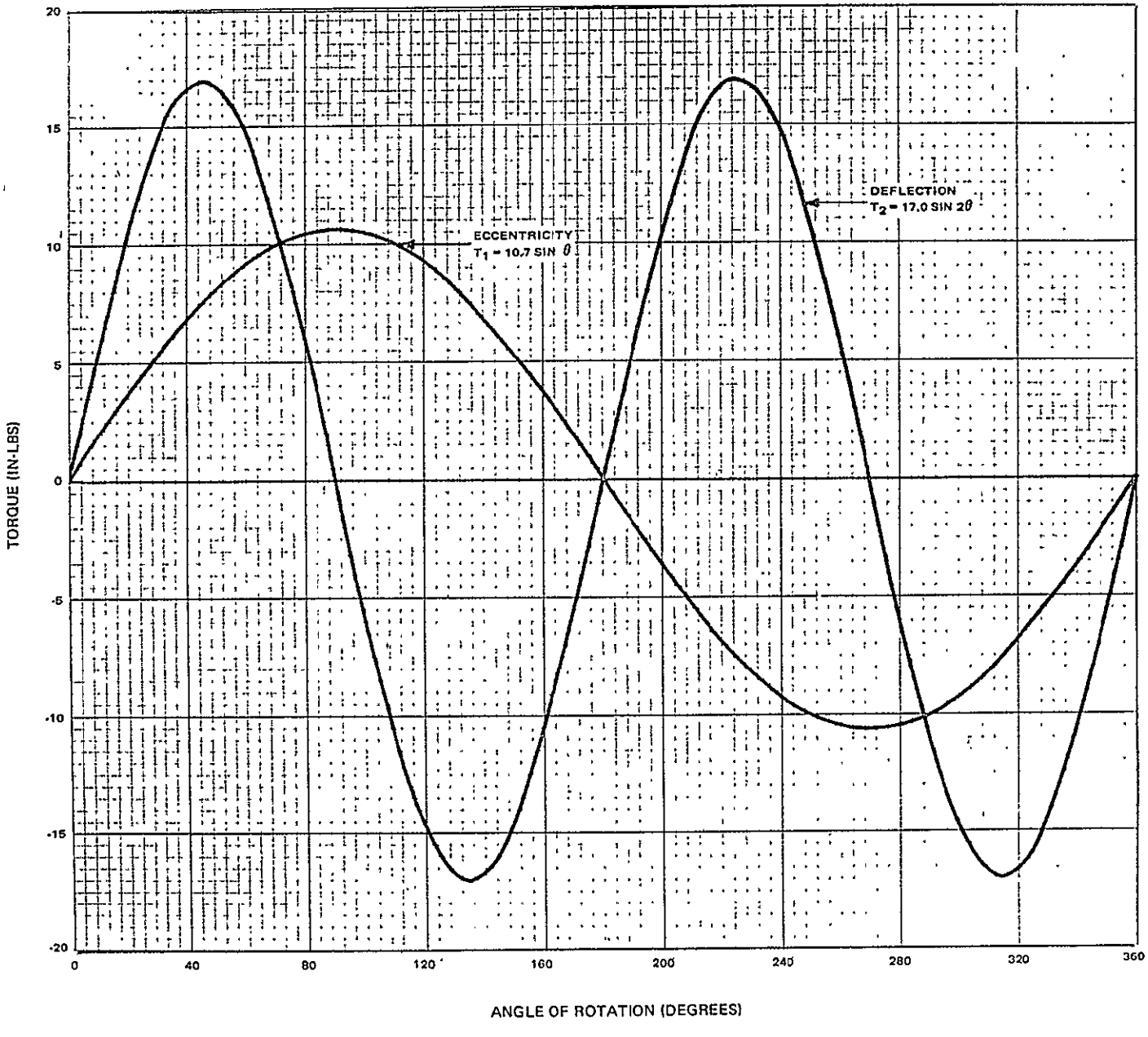

Figure I-14. Solar Array Eccentricity and Deflection Curves

The curve for deflection is represented by:

$$T_2 = \frac{\omega r}{2} \sin 2\Theta \tag{10}$$

$$T_2 = \frac{77.2\ (0.442)}{2} \sin 2\Theta \tag{11}$$

$$T_2 = 17.0 \sin 2\Theta \tag{12}$$

The location of the center-of-gravity about the center of rotation through 360° and perpendicular to the solar surface is determined by the following formula and is plotted in Figure I-15.

$$L = R + X$$

where X is the distance between the axis of rotation and the center-of-gravity along a line normal to the platform sun surace at any angle Θ.

Therefore, the deflection at any angle Θ is

$$X = r \cos \Theta \tag{13}$$

and

$$L = R + r \cos \Theta \tag{14}$$

$$L = 0.1387 + 0.442 \cos \Theta \tag{15}$$

As a result of this test, platform No. 15 and No. 16 will remain unbalanced in orbit by a maximum of 10.7 in. lbs. due to eccentricity.

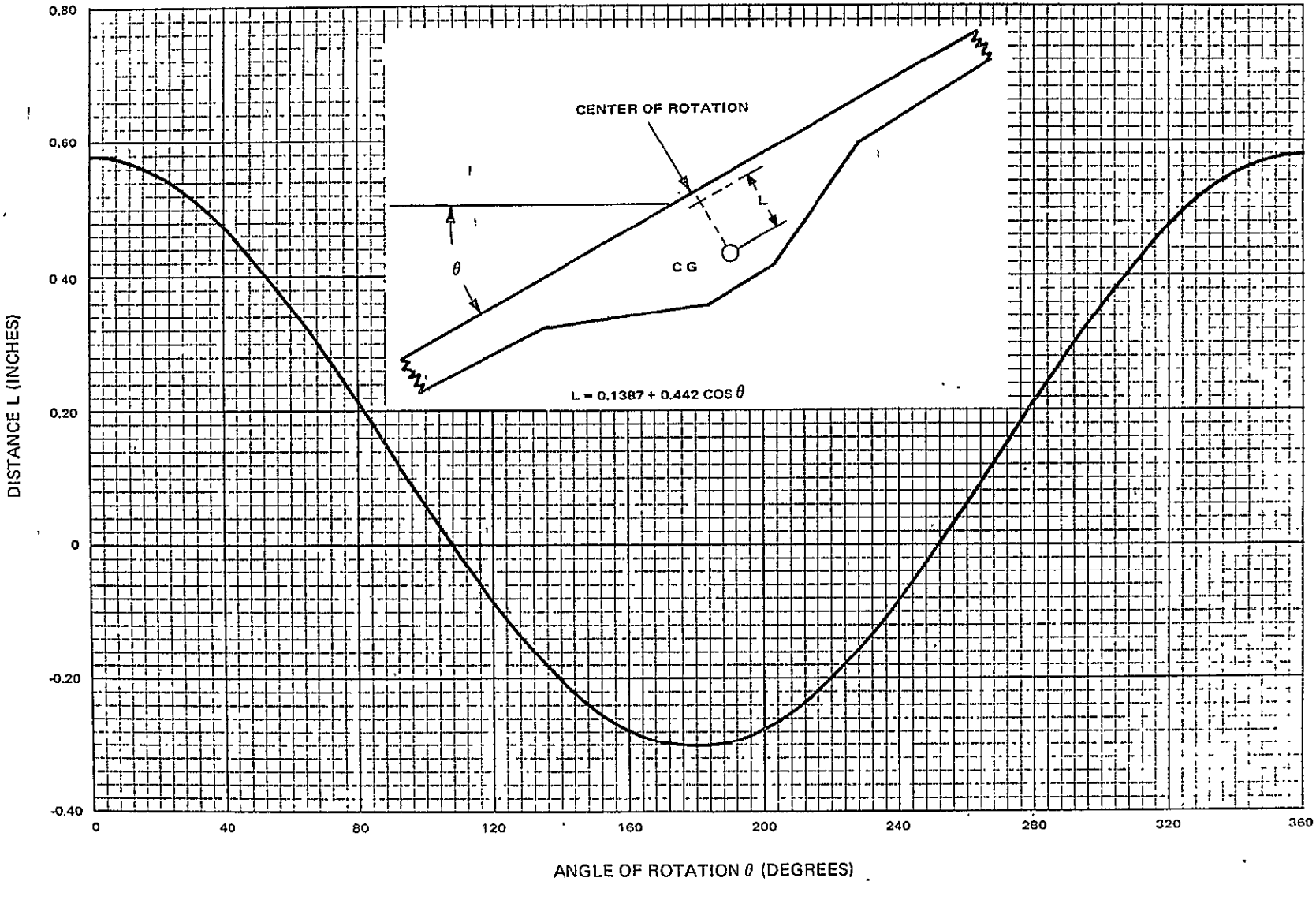

Figure I-15. Solar Array Center of Rotation Versus Center of Gravity

b. Reference Data

The derivation of equation 1 in Paragraph E-4a is based on the torque due to the eccentricity of the center-of-gravity to the center of rotation. It is described by $\omega R \sin \Theta$ for any angle of rotation.

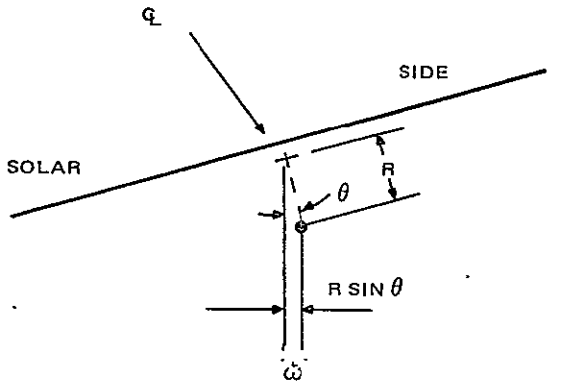

$T_1 = \omega R \text{ sine } \Theta$

Torque can be described as the results of deflection and force at any angle. The deflection at any angle is r cos Θ.

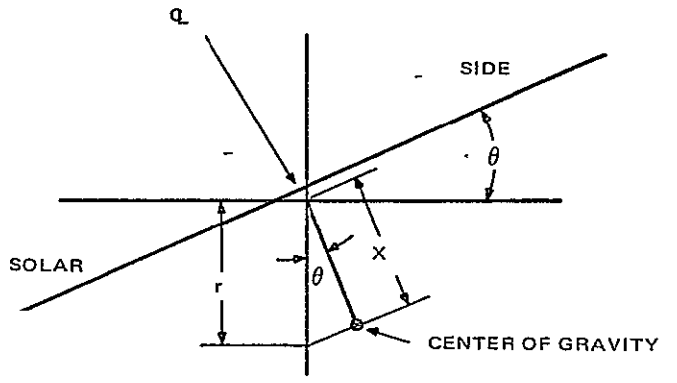

$\dot{x} = r \cos \Theta$

The force at any angle is $\omega \sin \Theta$.

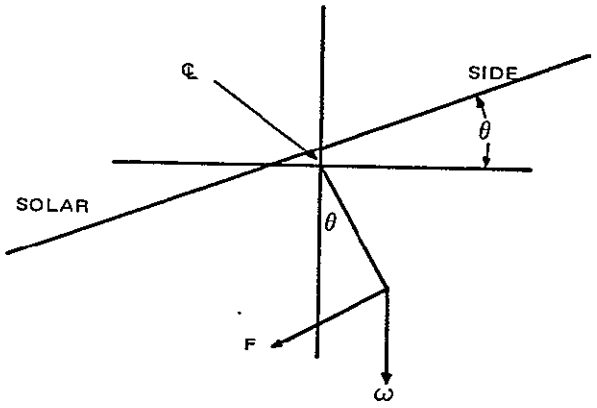

$$F = \omega \sin \Theta$$

The torque at any point due to deflection is

$$T_2 = Fx = \omega \sin \Theta \, r \cos \Theta$$

$$T_2 = \frac{\omega r}{2} \sin 2\Theta$$

The total unbalance torque due to the deflection and eccentricity of the center-of-gravity is $T_1 + T_2$.

$$T = T_1 + T_2$$

$$T = \omega R \sin \Theta + \frac{\omega r}{2} \sin 2\Theta$$

5. Electrical Acceptance Test Data

Electrical acceptance tests of each platform consist of DC isolation (short-to-shin) test, continuity test and illumination tests. Electrical acceptance tests, of platform Nos. 15 and 16, conducted before final wiring and encapsulation, were completed on August 6, and 22, 1968, respectively.

a. DC Isolation

DC isolation tests, conducted with the test setup shown in Figure I-16, are satisfactory when the leakage current is 0 amperes at 36.5 volts dc. Test data for each solar-cell board is listed in Table I-2.

TABLE I-2. DC ISOLATION TEST DATA

Parameter	BOARD											
	A	B	C	D	E	F	G	H	J	K	L	M
Current (ma)	0	0	0	0	0	0	0	0	0	0	0	20
Voltage (Vdc)	36.5	36.5	36.5	36.5	36.5	36.5	36.5	36.5	36.5	36.5	36.5	1.5

Board M failed due to a short existing between an intercell connection tab and the platform substrate. The tab was excessive in length and had been bent around the insulated edge of the platform into the end C channel. The short was eliminated by removing the excessive tab length. All intercell connection tabs on both platforms were checked for excessive length and shortened as required.

b. Continuity Tests

Continuity tests, using the test setup shown in Figure I-16, are satisfactory when the current equals 1 ampere at the board voltage for the 10-cell module boards (boards A to E and G to L) and 0.6 amperes at the board voltage for the 6-cell module boards (boards F and M). A variation of approximately ±5 percent in the board voltages is expected due to ambient light and temperature variation. The test results are listed in Table I-3.

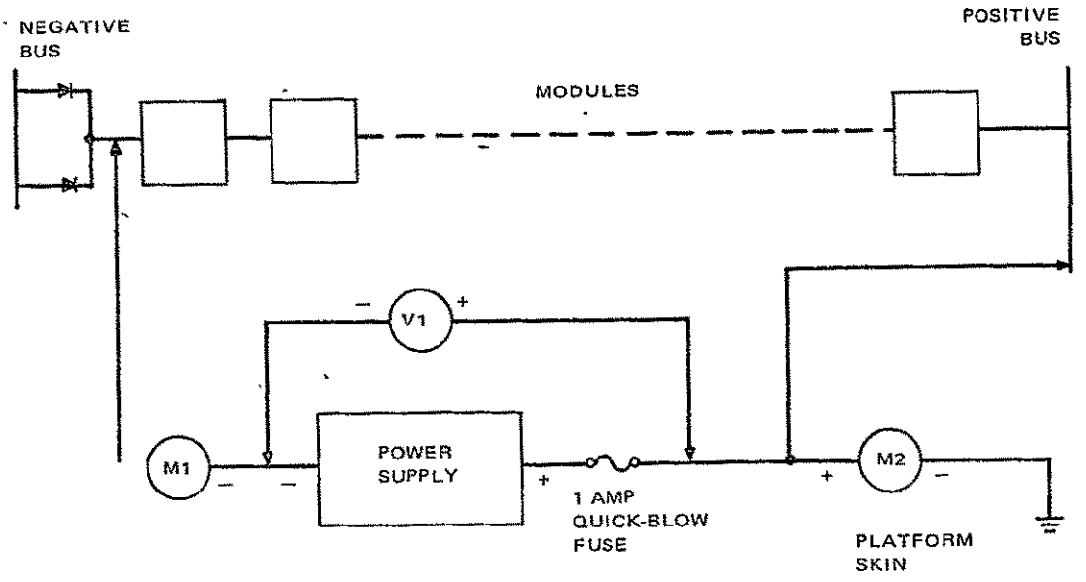

Figure I-16. DC Isolation and Continuity Test Setup

TABLE I-3. CONTINUITY TEST DATA

Board	A	B	C	D	E	F	G	H	J	K	L	M
Current	1.0	1.0	1.0	1.0	1.0	0.6	1.0	1.0	1.0	1.0	1.0	0.6
Voltage	69.3	68.5	68.3	69.1	69.9	67.3	68.2	68.7	67.7	69.1	68.4	66.9

c. Illumination

Illumination tests, using the test setup shown in Figure I-17, are satisfactory when I_{sc} variations of the board do not vary more than 15 ma and the V_{co} variations of the boards do not vary more than 1 volt dc. Test results for all the boards except the long boards (F and M) are shown in Table I-4. The last requirement, identical shape of I-V curve (knee), are shown on Figures I-18 through I-29.

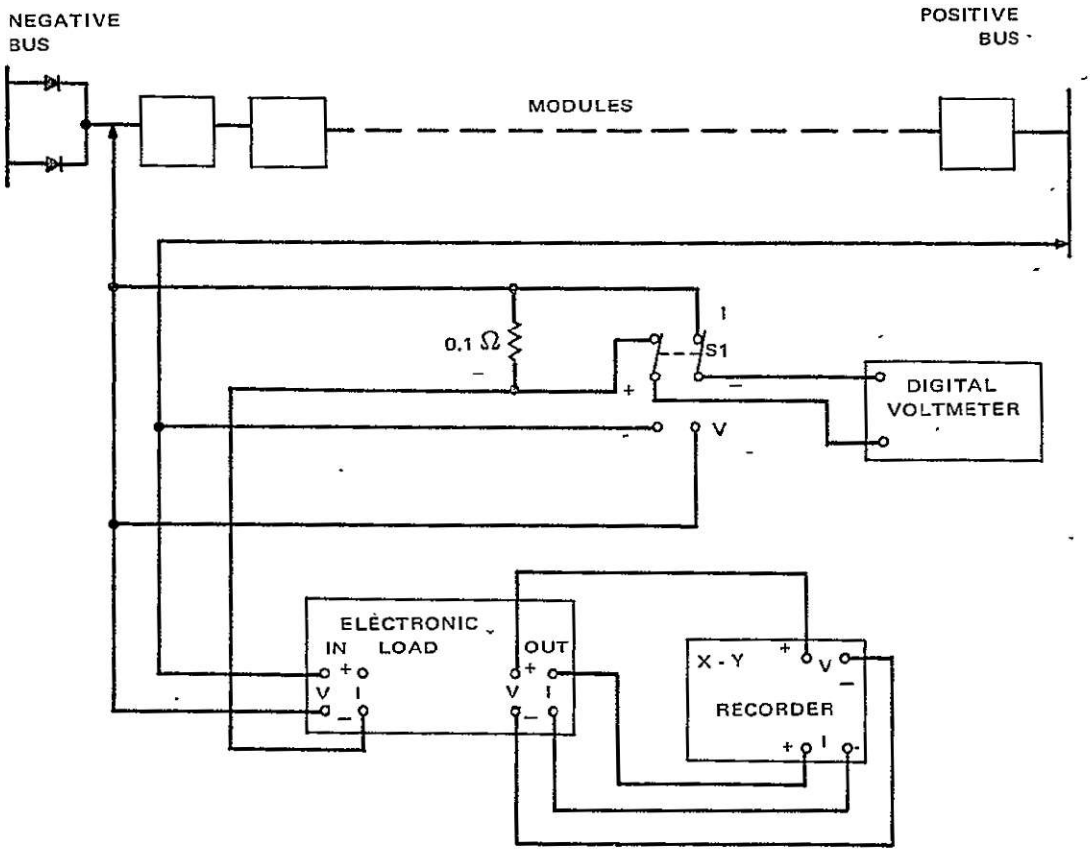

Figure I-17. Illumination Test Setup

TABLE I-4. ILLUMINATION TEST DATA

Parameter	BOARD									
	A	B	C	D	E	G	H	J	K	L
I_{sc} (Amp)	1.178	1.210	1.188	1.184	1.179	0.719	0.719	0.715	0.712	-
V_{oc} (Vdc)	55.0	54.7	54.2	54.77	54.59	54.8	54.5	54.3	54.9	-

Data comparison is applicable only between boards A to E and G to L due to different platform test dates and conditions. The six-cell module long boards (F and M) were not illuminated due to illuminator limitations.

Boards B, H, and L failed to meet the test requirements. Board B exceeded the 15 ma requirement, however, since the I_{sc} was greater than the average board I_{sc} and the I-V curve shape was identical to boards A, C, D and E it was accepted.

Board H was unacceptable because of a soft knee condition existing in its I-V characteristics. Trouble shooting indicated module No. 52 had excessive resistance as shown in Figure I-27. This module was replaced.

An error in intermodule wiring on board L could not be corrected adequately during the illumination test and platform No. 15 was returned to the fabrication facility for rework.

6. Deployment Drive Motor Acceptance Test Data

Flight acceptance testing of the two flight motors was performed in November 1967. At that time these motors were designated as spares for the Nimbus-B program. The original motors assigned to Nimbus D were returned to the vendor for refurbishment and designated as spares for Nimbus-B2 program. Flight and spare deployment-drive motor assembly serial numbers are tabulated in Table I-5.

TABLE I-5. DEPLOYMENT MOTOR-DRIVE ASSEMBLY IDENTIFICATION

Platform S/N	Flight S/N	Spare S/N
15	F/VS-2	15
16	FF/MMS-2	16

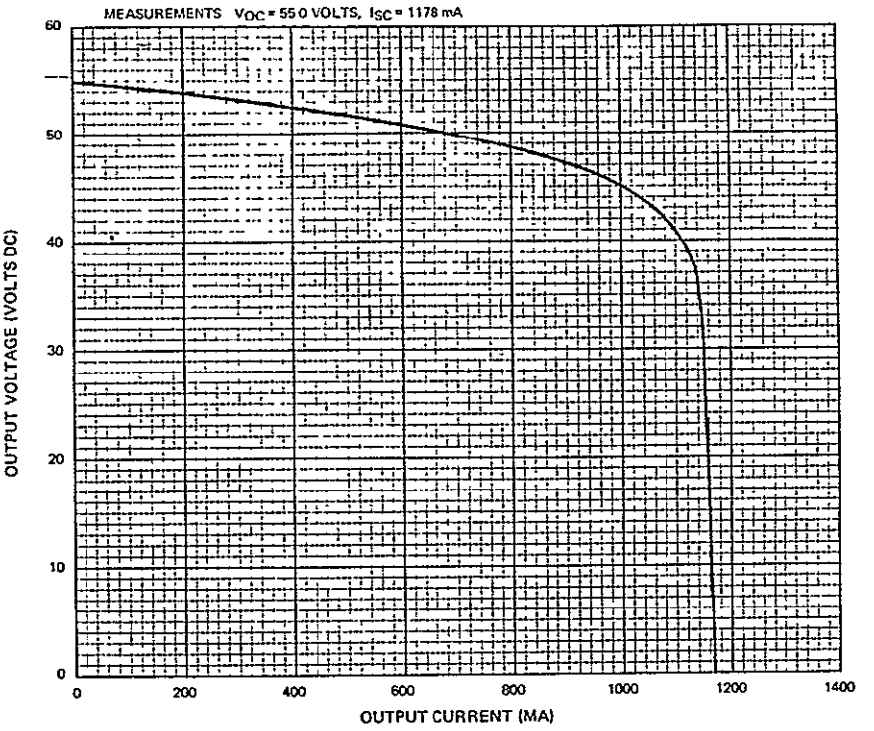

Figure I-18. Post-Fabrication I-V Characteristic, Board A

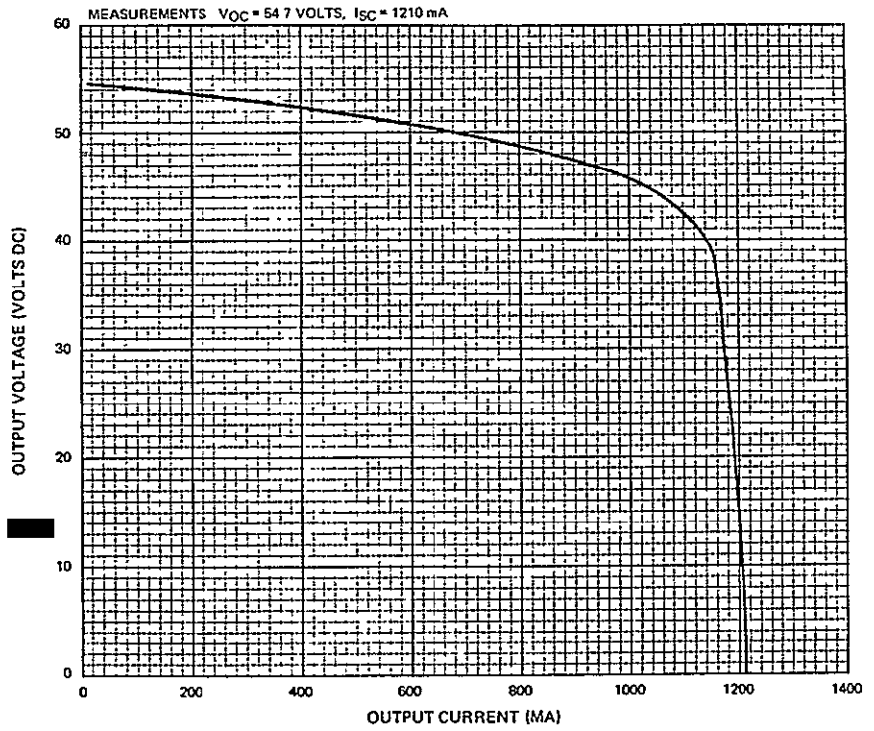

Figure I-19. Post-Fabrication I-V Characteristic, Board B

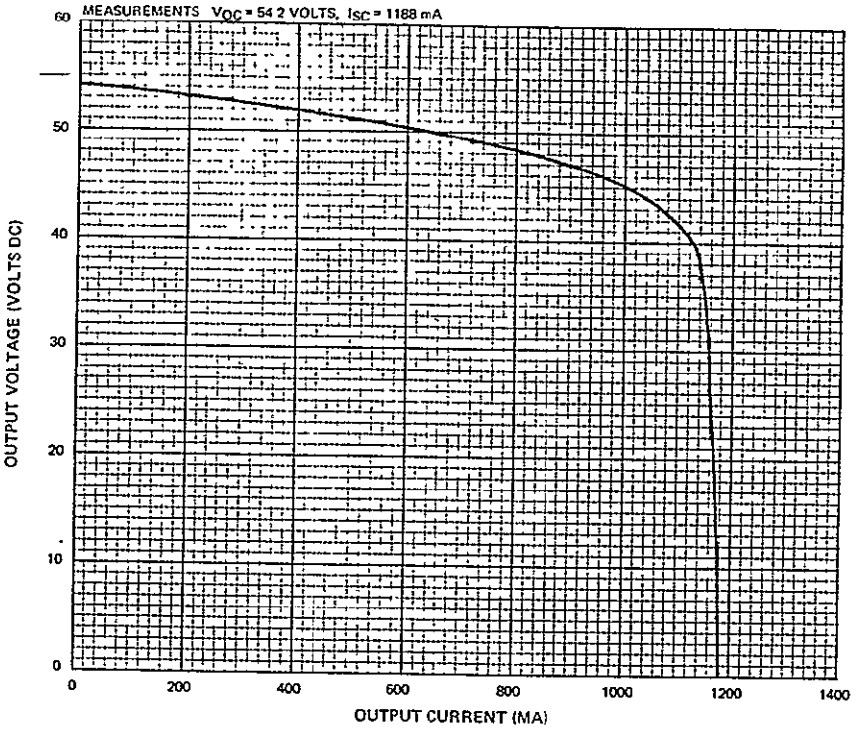

Figure I-20. Post-Fabrication I-V Characteristic, Board C

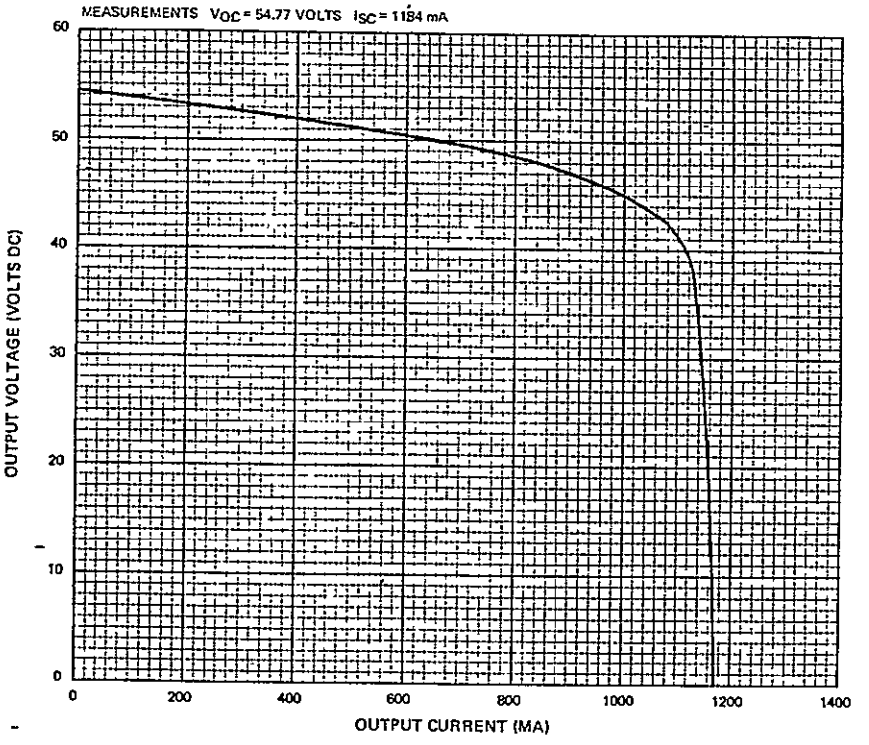

Figure I-21. Post-Fabrication I-V Characteristic, Board D

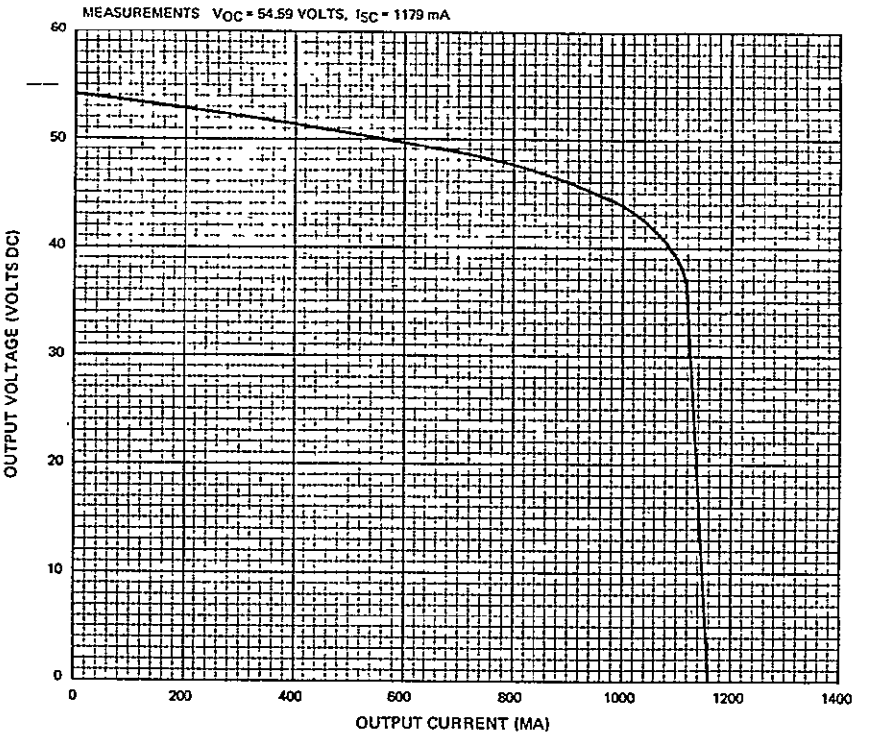

Figure I-22. Post-Fabrication I-V Characteristics, Board E

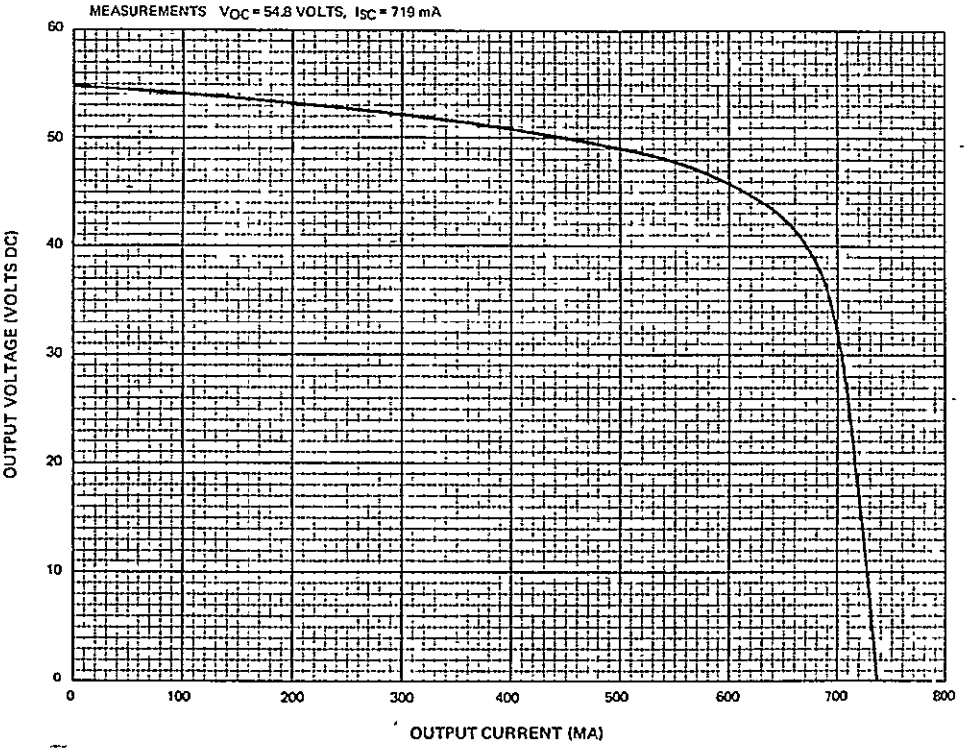

Figure I-23. Post-Fabrication I-V Characteristic, Board G

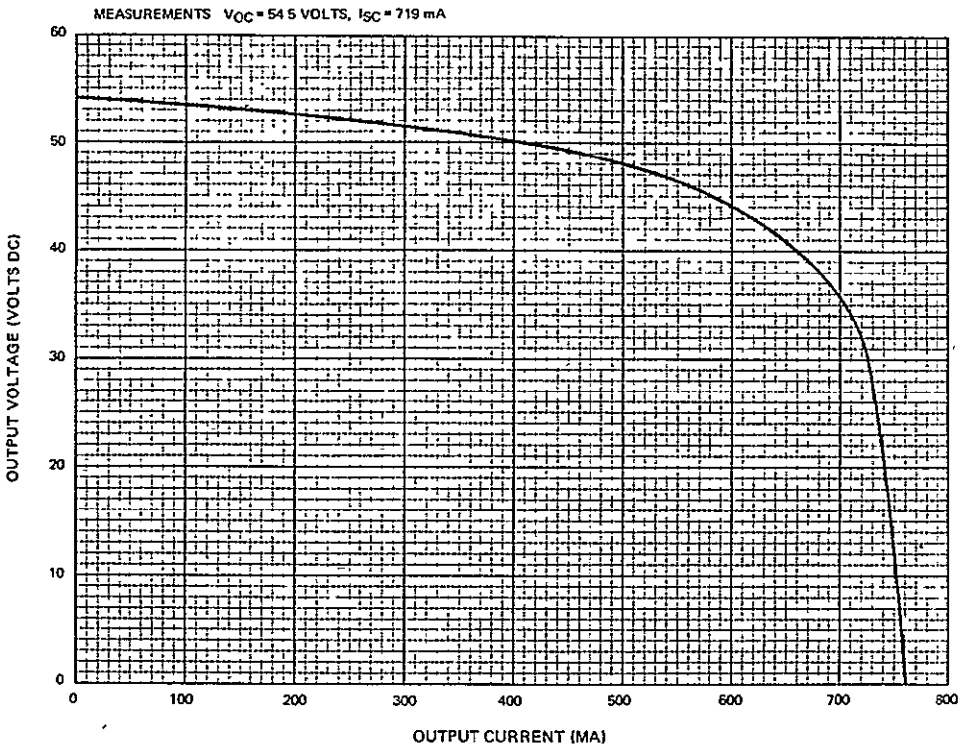

Figure I-24. Post-Fabrication I-V Characteristics, Board H

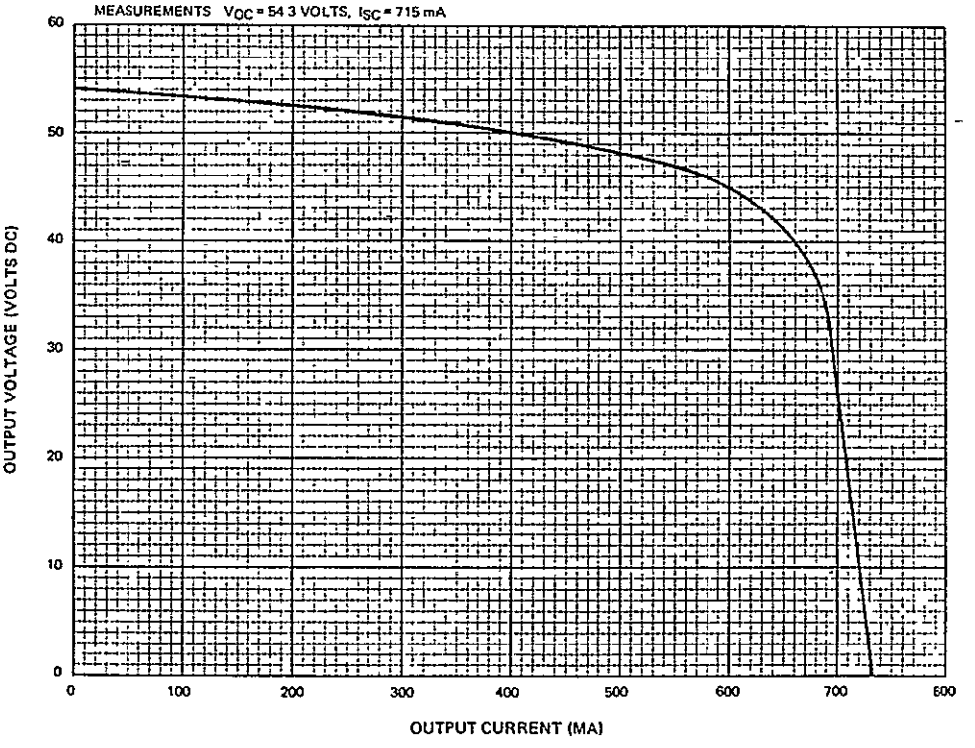

Figure I-25. Post-Fabrication I-V Characteristics, Board J

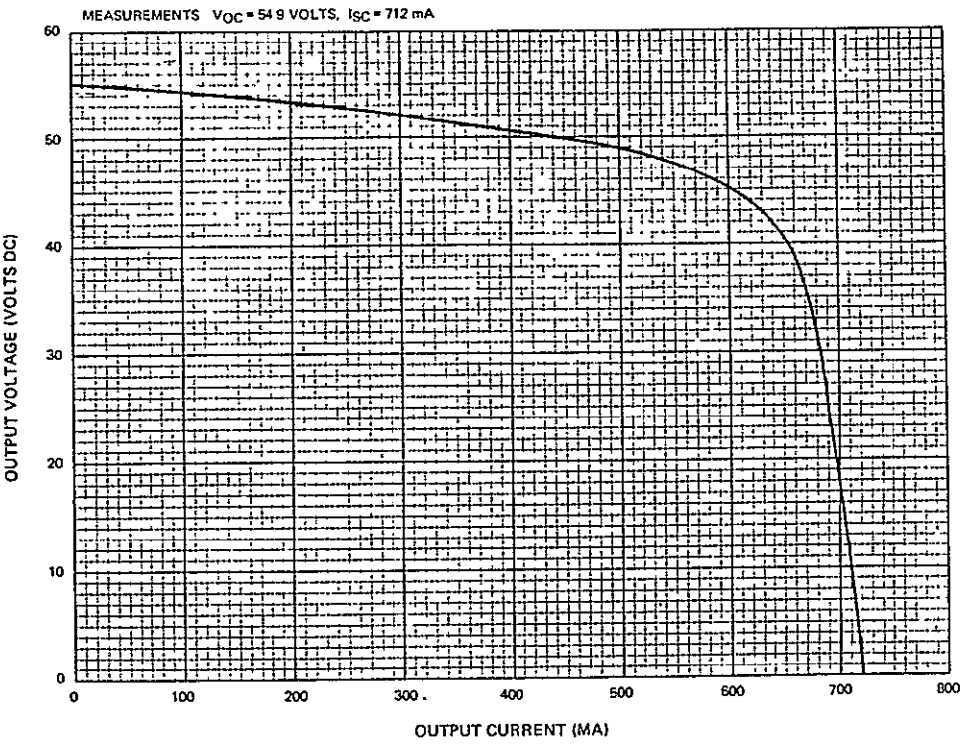

Figure I-26. Post Fabrication I-V Characteristics, Board K

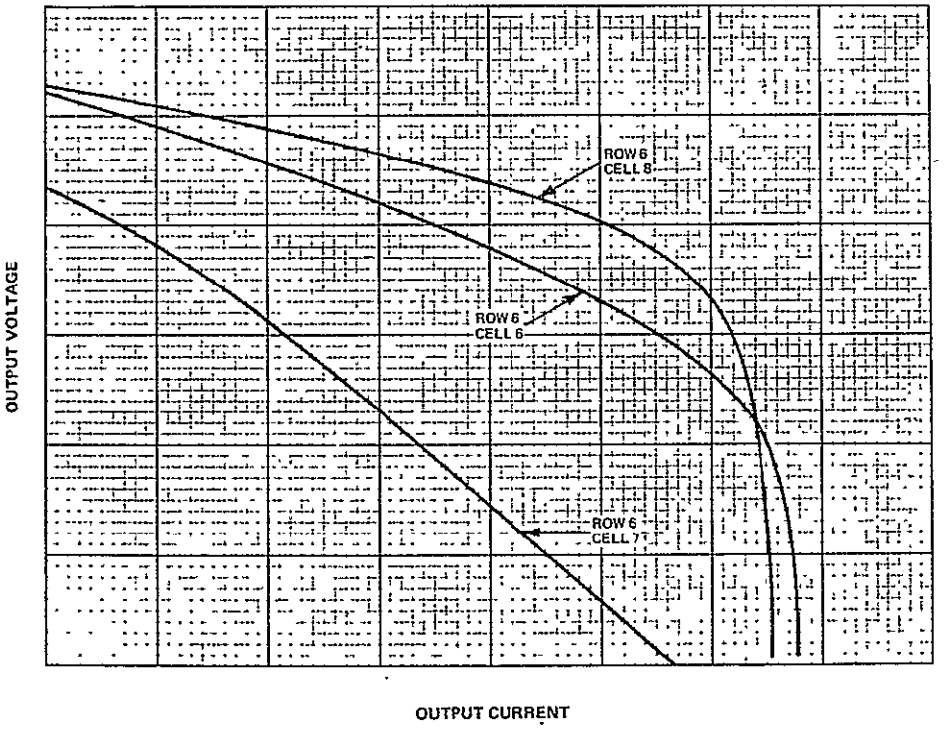

Figure I-27. Module 52, Board H, I-V Characteristics for Cells No. 6, 7, and 8

Acceptance tests were conducted in accordance with the test flow shown in Figure I-28 with the following exception, the spare deployment motor drive assemblies were not subjected to deployment tests.

a. Speed Torque Test Data

Four speed torque tests were performed on each of the deployment drive-motor assemblies. During each test the motor speed is measured with respect to a pre-determined load. The test results must be within ±10 percent of the torque speed curve shown on Figure I-29. There were no test anomalies during any of the tests; data for the initial and final tests are listed in Tables I-6 and I-7.

b. Cold Temperature Test Data

Cold temperature tests are conducted under a no load condition for 45 seconds at the temperature shown in Table I-8. The test is satisfactory if the instantaneous current change at each temperature does not vary more than ±10 percent. Test results are listed in Table I-8.

c. Vibration Test Data

Vibration tests, conducted to the levels listed in Tables I-9 and I-10, were satisfactory. No electrical tests are required during vibration exposures.

d. Thermal Vacuum Test Data

Thermal vacuum tests are performed on a continuous basis for 29 hours. Each motor is energized for 45 seconds per hour under a torque load of 63 in-lbs. This torque load is allowed to vary by ±10 in-lbs.

Motors serial number F/VS-2 and FF/MMS-2 were tested between December 13, 1967 and December 14, 1967. Both units performed within the requirements stated above. On January 6, 1969, thermal vacuum testing was started on the spare motors, serial numbers 15 and 16. After 21 hours of testing, the test fixture braking system froze and caused each drive motor to turn in the hold down arrangement. Only minor damage occurred to the motors. As each motor turned, the motor electrical lead and insulation were cut by the motor case resulting in a short. Both motors were repaired by removing the damaged portion of the electrical lead (approximately 1/2 inch).

The thermal vacuum test was resumed after cleaning and resetting the load fixture. Two hours into the retest, a second brake failure occurred on serial number 15. Motor damage and repair was identical to that described above. The braking pulley was replaced with an alternate and testing was resumed. No further malfunctions occurred for the duration of the test.

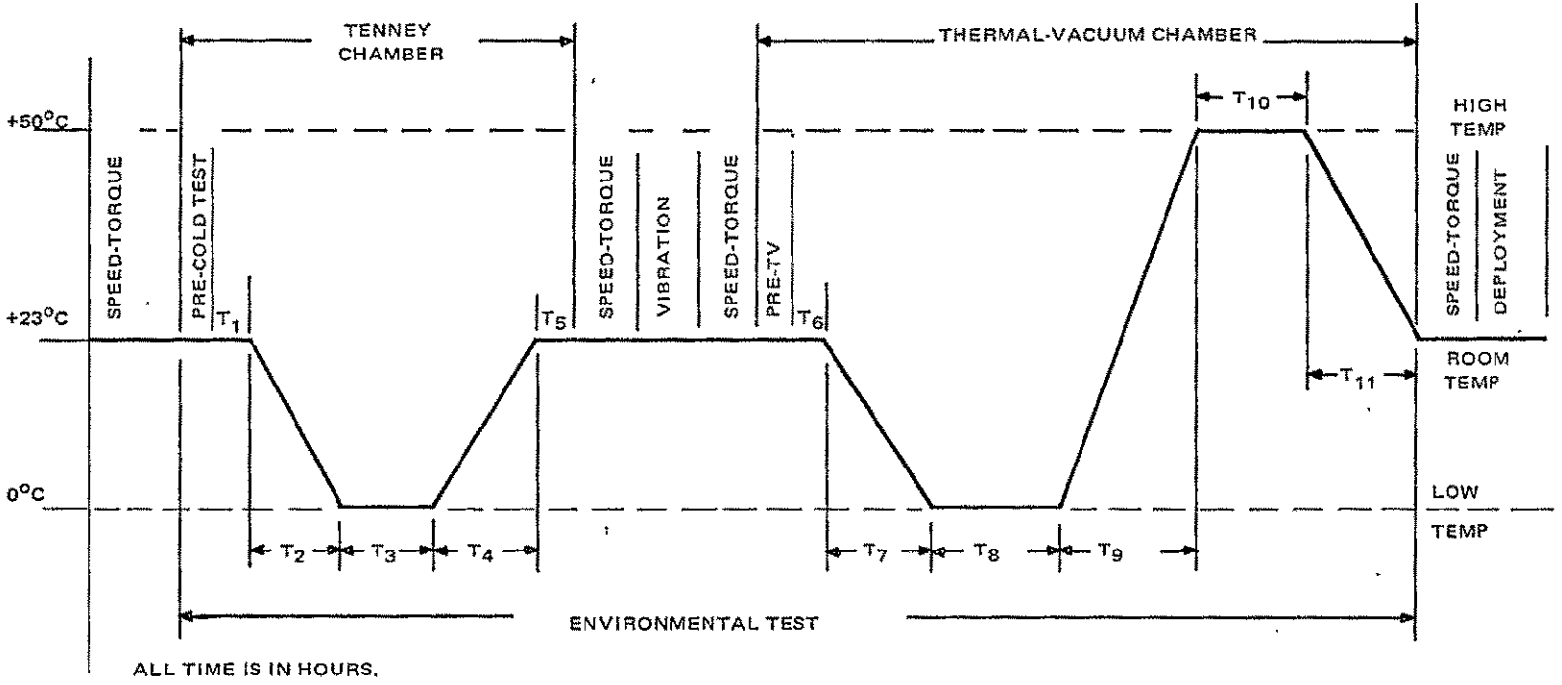

Figure I-28. Deployment Motor-Drive Assembly Test Flow Diagram

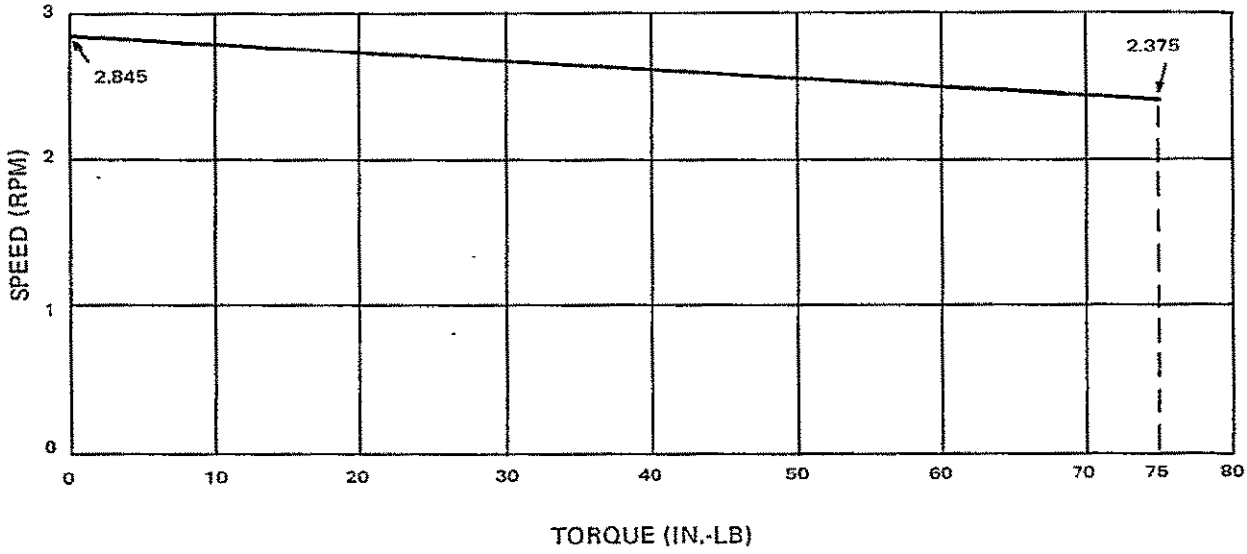

Figure I-29. Deployment Motor-Drive Assembly Torque-Speed Characteristics at -24.0 Volts dc

TABLE I-6. INITIAL SPEED-TORQUE TEST DATA

Force (in-lbs)	Motor-Drive Serial Number							
	F/VS-2		FF/MMS-2		No. 15		No. 16	
	I_{ma}	RPM	I_{ma}	RPM	I_{ma}	RPM	I_{ma}	RPM
0	171	2.70	150	2.76	185	2.76	200	2.78
15	223	2.62	202	2.66	225	2.73	240	2.73
30	264	2.54	242	2.58	270	2.65	275	2.68
45	306	2.47	289	2.50	320	2.52	325	2.56
60	345	2.41	335	2.42	375	2.41	370	2.52

TABLE I-7. FINAL SPEED TORQUE TEST DATA

Force (in-lbs)	Motor-Drive Serial Number							
	F/VS-2		FF/MM-2		No. 15		No. 16	
	I_{ma}	RPM	I_{ma}	RPM	I_{ma}	RPM	I_{ma}	RPM
0	180	2.69	165	2.75	180	2.80	190	2.84
15	235	2.60	220	2.69	220	2.73	230	2.74
30	275	2.53	260	2.59	265	2.65	280	2.71
45	325	2.46	305	2.52	320	2.58	320	2.62
60	370	2.36	355	2.46	365	2.46	370	2.54

TABLE I-8. COLD TEMPERATURE TEST DATA

Motor Drive Assembly Serial Numbers							
F/VS-2		FF/MMS-2		No. 15		No. 16	
Temp.°C	I_{ma}	Temp.°C	I_{ma}	Temp.°C	I_{ma}	Temp.°C	I_{ma}
27.7	175	27.7	155	25.0	165	25.0	170
8.2	191	8.0	175	11.0	180	11.0	180
0.0	-	0.0	-	0.0	195	0.0	190
-3.8	205	-4.1	191	-8.0	180	-8.0	175
24.0	180	24.0	165	-25.0	170	-25.0	165

TABLE I-9. SINUSOIDAL VIBRATION LEVELS

Frequency (Hz)	Amplitude - g (0 to peak)	
	Thrust Axis	Transverse Axes
5-14	0.5 inch double amplitude	0.5 inch double amplitude
14-2000	5	5
Amplitude is limited to 0.5 inch double amplitude. The sweep rate is 2 octave per minute.		

TABLE I-10. RANDOM VIBRATION LEVELS

Axis	Frequency Band (Hz)	Spectral Density (g^2/Hz)	RMS Level (g's)
Thrust	20-2000	0.07	11.7
Transverse	20-2000	0.07	11.7
Duration of each test was 2 minutes per axis.			

e. Deployment Test Data

A total of three deployment tests have been performed on the flight motor serial numbers F/VS-2 and FF/MMS2. The first was performed on the Nimbus-B platforms on December 15, 1967. The second and third tests were performed on September 13, 1968 and October 30, 1968 as part of the Nimbus-B2 platforms. A third test was performed because the transition assemblies were detached from the platforms to perform the platform thermal vacuum tests. Deployment motor-drive test data is listed in Table I-11, I-12, and I-13. Neither spare motor was subjected to a deployment test because spare deployment motor mounts were not available. These motors were acceptable, however, based upon the performance data package and past history of all deployment tests, a failure has never been experienced on this type motor.

7. Illumination Test Data

a. Indoor Illumination

Pre-thermal I-V characteristics of the 10-cell module boards (6-cell module boards-long, cannot be illuminated under the Lunar Orbiter illuminator), obtained between September 25, and September 27, 1968, are shown on Figures I-30 through I-39.

TABLE I-11. NIMBUS-B DEPLOYMENT MOTOR DRIVE TEST DATA

Serial No. and Motor No.	Run No.	Running Voltage (Vdc)	Minimum Current (ma)	Maximum Current (ma)	Latch Time (sec)	Shutoff Time (sec)
F/VS-2						
Motor No. 1	1	24.3	170	340	28.2	30.5
	2	24.3	170	340	27.7	29.8
	3	24.3	165	340	28.1	29.8
Motor No. 2	1	24.4	165	340	28.9	30.6
	2	24.4	160	335	28.4	30.4
	3	24.4	160	330	28.6	30.3
Motor No. 1 & 2	1	24.4	160	330	25.6	27.1
	2	24.4	160	330	25.5	27.0
	3	24.4	160	330	25.6	27.0
FF/MMS-2						
Motor No. 1	1	24.3	160	360	27.9	30.1
	2	24.3	155	350	27.8	29.9
	3	24.3	150	350	27.7	29.7
Motor No. 2	1	24.3	150	340	27.1	29.1
	2	24.3	145	335	27.0	28.9
	3	24.3	145	335	26.7	28.9
Motor No. 1&2	1	24.2	165	330	25.5	27.2
	2	24.3	150	330	25.1	26.9
	3	24.3	150	330	25.2	26.7

TABLE I-12. NIMBUS-B2 DEPLOYMENT MOTOR DRIVE TEST DATA, ORIGINAL TEST

Serial No. and Motor No.	Run No.	Running Voltage (Vdc)	Minimum Current (ma)	Maximum Current (ma)	Latch Time (sec)	Shutoff Time (sec)
F/VS-2						
Motor No. 1	1	24.0	160	260	27.0	29.2
	2	24.0	160	260	26.9	29.2
	3	24.0	160	260	27.0	29.1
Motor No. 2	1	24.0	160	260	26.4	28.4
	2	24.0	158	255	26.2	28.5
	3	24.0	155	258	26.0	28.2
Motor No. 1&2	1	24.0	160	250	24.1	26.1
	2	24.0	158	255	24.0	26.2
	3	24.0	155	255	24.1	26.2
FF/MMS-2						
Motor No. 1	1	24.0	155	285	25.5	27.9
	2	24.0	145	280	25.4	27.8
	3	24.0	145	270	25.6	27.8
Motor No. 2	1	24.0	140	270	26.0	28.4
	2	24.0	138	260	26.0	28.3
	3	24.0	138	260	25.8	28.1
Motor No. 1&2	1	24.0	138	245	23.8	26.0
	2	24.0	137	245	23.9	25.8
	3	24.0	137	245	23.9	26.1

TABLE I-13. NIMBUS-B2 DEPLOYMENT MOTOR DRIVE TEST DATA, POST THERMAL VACUUM

Serial No. and Motor No.	Run No.	Running Voltage (Vdc)	Minimum Current (ma)	Maximum Current (ma)	Latch Time (sec)	Shutoff Time (sec)
F/VS-2						
Motor No. 1	1	24.0	140	295	29.0	30.9
	2	24.0	140	290	28.6	30.4
	3	24.0	160	295	28.4	30.4
Motor No. 2	1	24.0	160	300	27.4	28.9
	2	24.0	160	295	27.3	29.0
	3	24.0	155	295	27.3	29.2
Motor No. 1&2	1	24.0	160	300	25.0	26.8
	2	24.0	155	295	25.3	26.7
	3	24.0	155	290	25.2	26.7
FF/MMS-2						
Motor No. 1	1	24.0	150	300	27.0	29.2
	2	24.0	145	295	26.7	28.6
	3	24.0	145	290	26.8	28.9
Motor No. 2	1	24.0	140	295	27.5	29.6
	2	24.0	140	275	27.5	29.5
	3	24.0	140	280	27.2	29.1
Motor No. 1&2	1	24.0	140	275	25.1	26.8
	2	24.0	140	270	25.2	27.0
	3	24.0	135	270	25.1	26.9

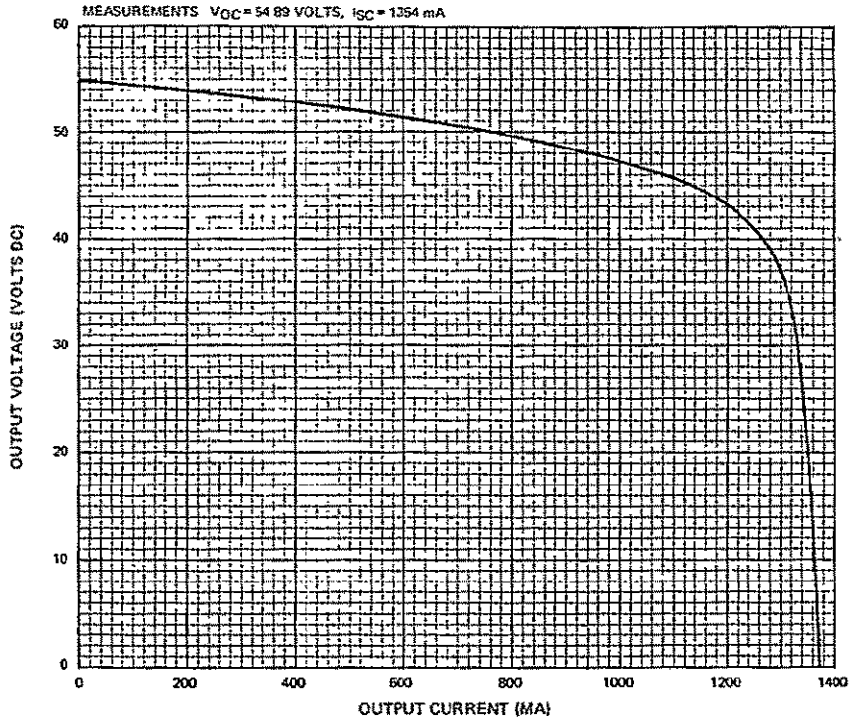

Figure I-30. Pre-Thermal Indoor I-V Characteristics, Board A

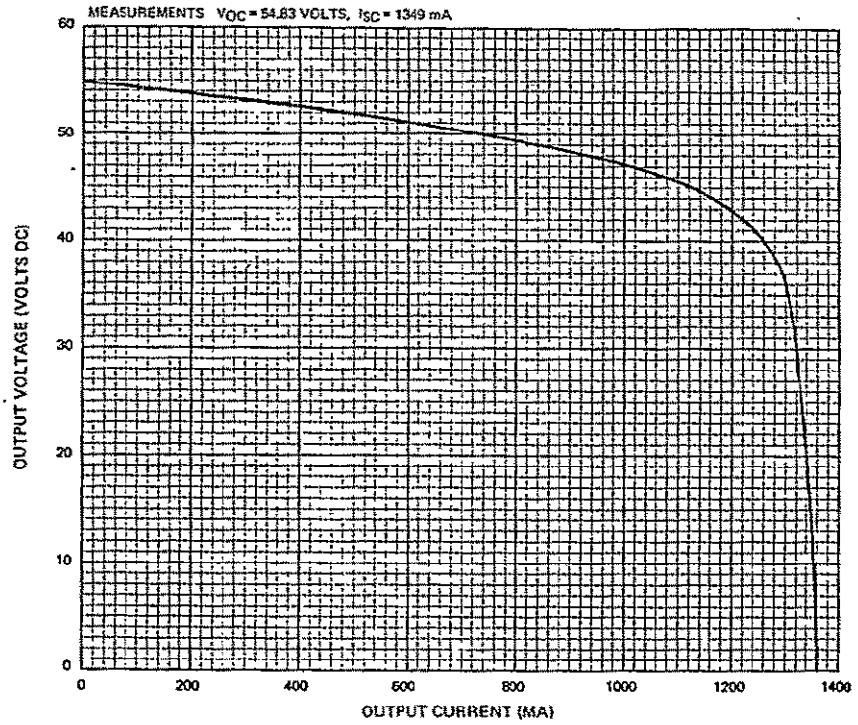

Figure I-31. Pre-Thermal Indoor I-V Characteristics, Board B

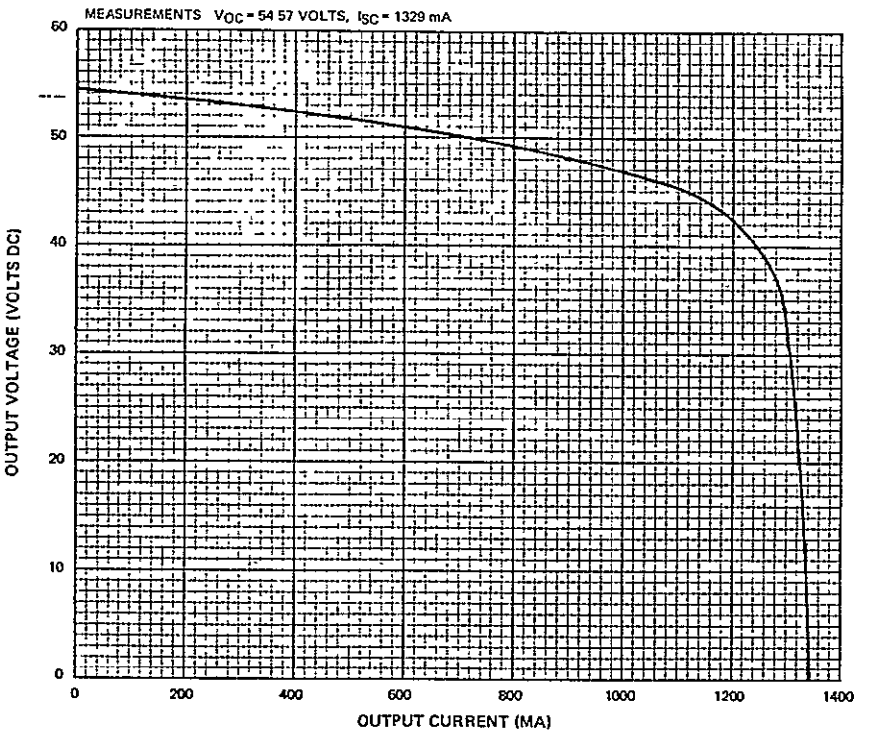

Figure I-32. Pre-Thermal Indoor I-V Characteristics, Board C

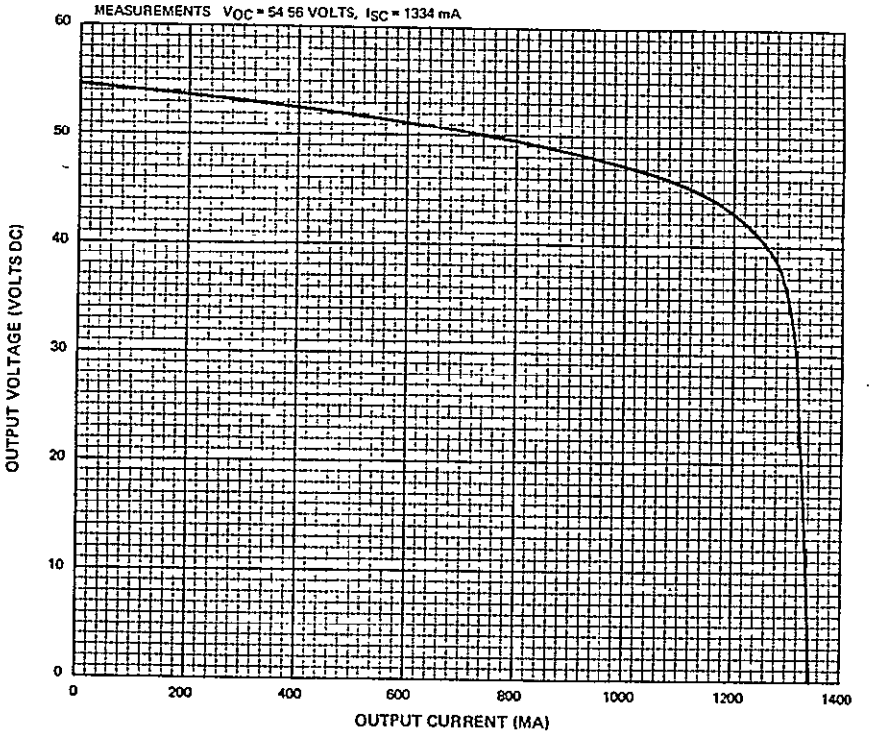

Figure I-33. Pre-Thermal Indoor I-V Characteristics, Board D

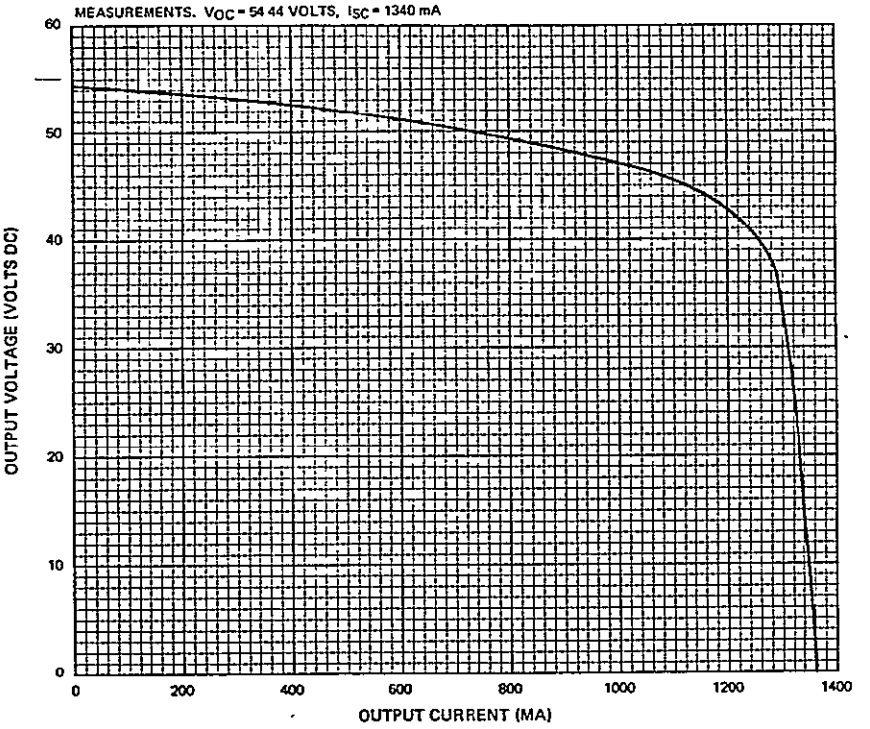

Figure I-34. Pre-Thermal Indoor I-V Characteristics, Board E

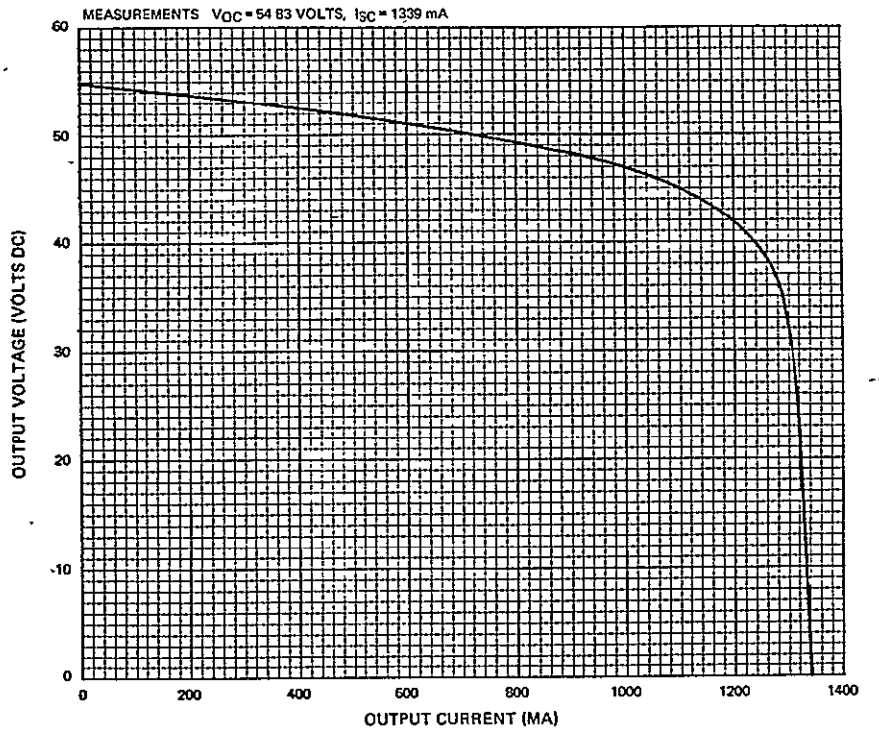

Figure I-35. Pre-Thermal Indoor I-V Characteristics, Board G

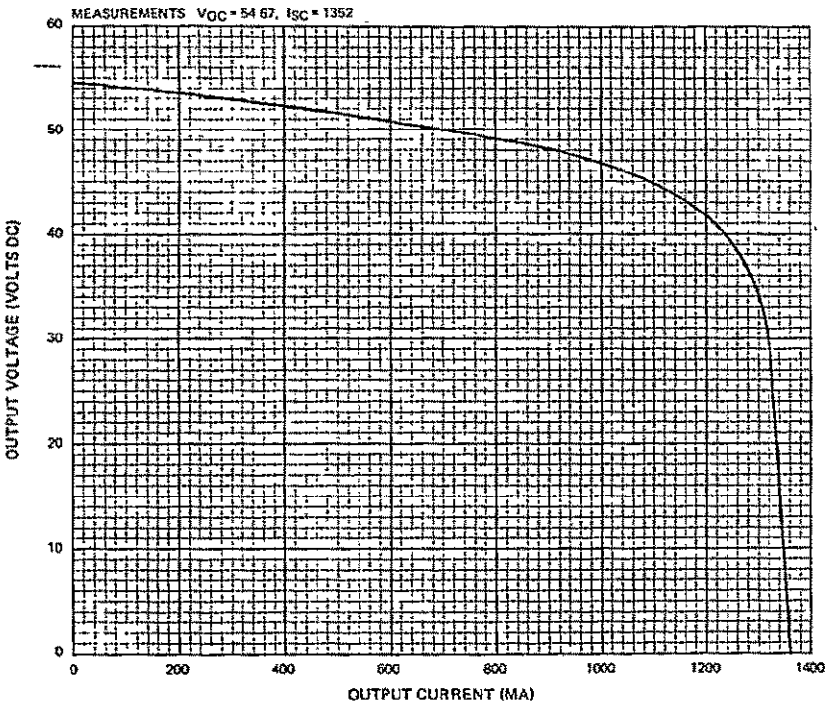

Figure I-36. Pre-Thermal Indoor I-V Characteristics, Board H

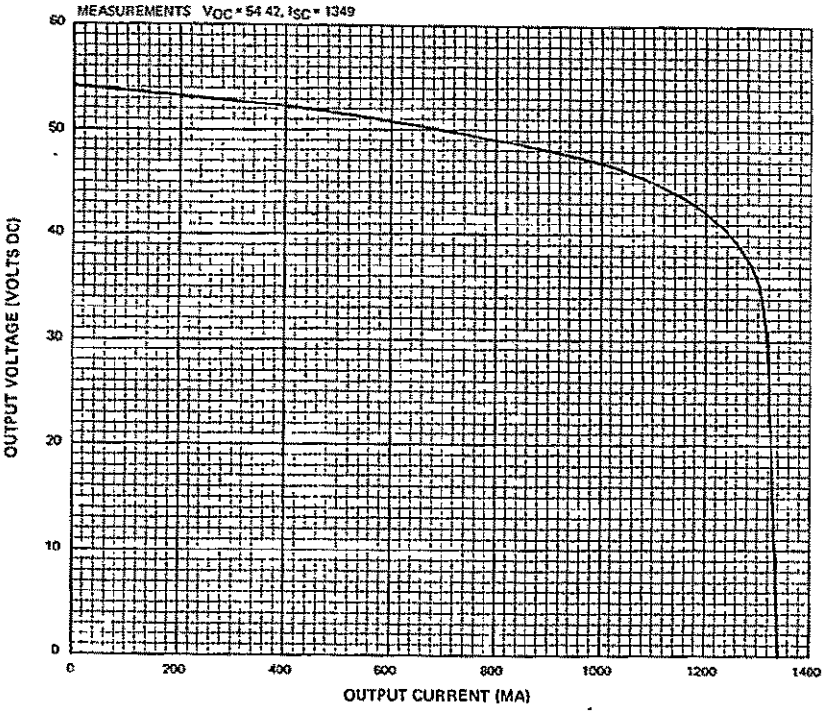

Figure I-37. Pre-Thermal Indoor I-V Characteristics, Board J

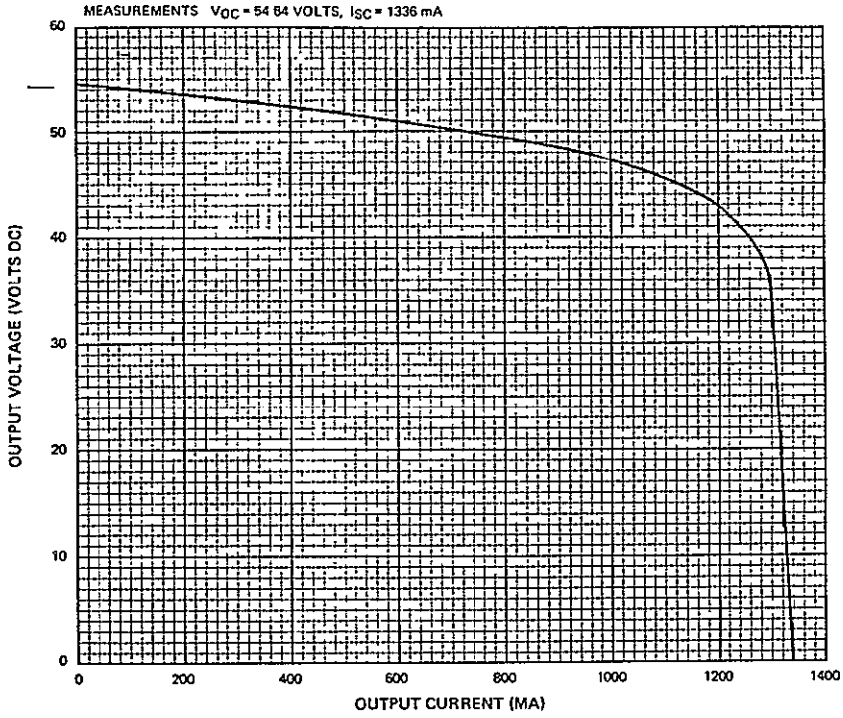

Figure I-38. Pre-Thermal Indoor I-V Characteristics, Board K

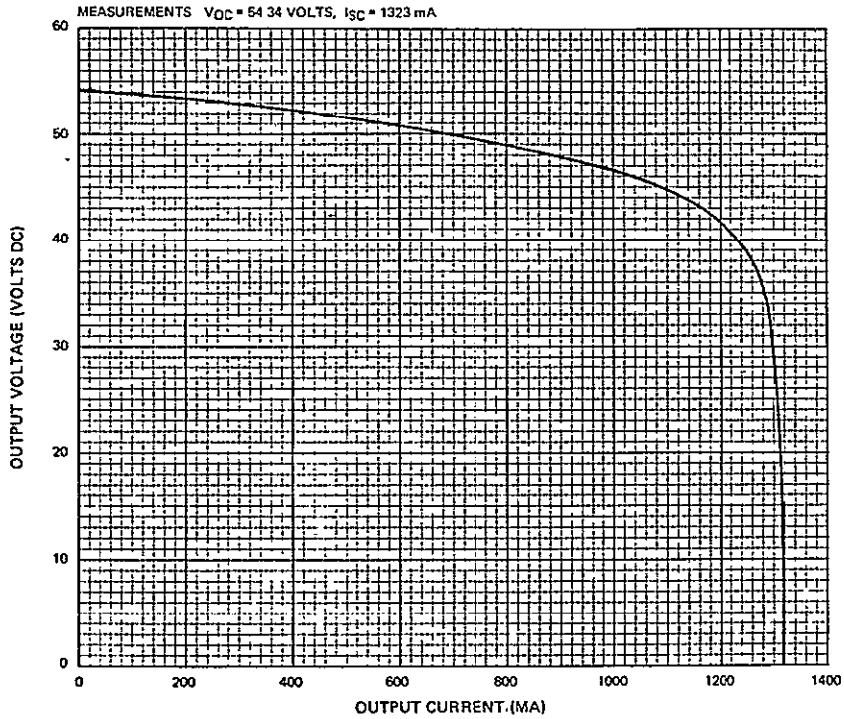

Figure I-39. Pre-Thermal Indoor I-V Characteristics, Board L

Boards E and L failed to meet the test requirements of TP-IL-1975606 paragraph 5.1.2, Step 22. Trouble shooting showed that module No. 2 on board E (see Figure I-40) and module No. 85 on board L were defective and were replaced with high output modules. Module No. 73 on board E was also replaced because of a damaged tab. Figures I-41 and I-42 show the I-V characteristics of Boards E and L after being reworked.

Post-thermal I-V characteristics, obtained between October 24 and November 11, 1968, are shown on Figures I-43 through I-52. Comparison of I-V characteristics to pre-thermal vacuum test data indicates boards H, K and L had deteriorated at the knee of the I-V curve. Board H had a soft knee and boards K and L failed to meet the continuously changing positive slope requirement.

Trouble shooting of the three boards resulted in replacement of the following modules:

Board	Module No.
H	4, 15, 17 and 20
K	2, 6, and 7
L	80, 81, and 85

I-V characteristics obtained after solar-cell module replacement are shown on Figures I-53 through I-55. These boards were questionable on the basis of data obtained during pre-thermal tests. However, troubleshooting was delayed until after thermal vacuum tests on the basis of Nimbus-B Q-board tests. If additional degradation occurred during thermal-vacuum tests, the boards that displayed the greatest deterioration would be reworked using the limited number of spare modules. At the completion of thermal vacuum tests only the questionable boards showed further signs of deterioration.

In order to obtain an I-V characteristic curve for the solar array, 120 percent of the average 10-cell module board for each illumination test was added to the sum of the 10-cell module boards to account for the two 6-cell module boards which could not be illuminated. The anticipated solar array outputs pre- and post-thermal vacuum tests are shown in Figures I-56 and I-57.

Comparison of the two curves indicates that an increase of approximately 0.25 amps at 34 volts after the thermal-vacuum test. This is accounted for by replacement of the defective modules and test repeatability. Test repeatability is within ±2 percent.

b. Outdoor Illumination

Outdoor illumination tests, performed on December 8, 1968, were conducted under the following test conditions:

Average board temperature	11.3°C
Average intensity	115.4 mw/cm^2

The outdoor illumination data, shown on Figures I-58 through I-69, was corrected to 35°C at an air mass zero intensity of 139.6 mw/cm^2. Each of the twelve corrected I-V characteristics were added together to obtain the solar array characteristics shown in Figure I-70. Comparison of Figure I-70 and the post-thermal vacuum illumination curve, Figure I-57, indicates the differences listed in Table I-14.

TABLE I-14. INDOOR/OUTDOOR I-V CHARACTERISTIC SUMMARY

Parameter	Post I-V	Outdoor	Difference
I_{sc}	15.19	15.66	0.47 amps
I at 34.0 Vdc	14.80	15.23	0.43 amps
V_{oc}	54.47	53.59	0.88 volts

An approximate 3-percent difference exists between short circuit and -34 volt reference currents because of a discrepancy in the test equipment.

A discrepancy (unusually high current values) was noted during initial illumination tests on the Nimbus-D Q-board on November 18, 1968. These values exceeded those predicted by approximately 8 percent. The source of the discrepancy was not determined until December 19, 1968 when it was noted that the short circuit current reading on the DVM would fluctuate when one of the banana plugs connecting the test circuit to the precision resistor was moved, see Figure I-17. The set screw was tightened and the short circuit current dropped to within 1-percent of the predicted value. It was also noted that during eight illumination tests on the Nimbus-D Q-board, the difference between the actual and the predicted current values varied from 1- to 8-percent. The same test equipment was used during Nimbus-B2 outdoor illumination tests. Based on the results of the Nimbus-D Q-board program, it is assumed that the resistance introduced by the loose connection also caused the Nimbus-B2 outdoor data to be 3 percent high.

A difference also exists between open circuit voltages. This difference is attributed to a temperature tolerance of ±3°C placed upon the average outdoor temperature of the module boards. The average temperature (11.8°C) was used to correct each module board to 35°C. A delta temperature of 3.8°C will shift the array V_{oc} 0.88 volts.

The basic purpose for outdoor illumination tests is to provide a basis for comparison and evaluation of the indoor test data. The assumption that the 6-cell module boards (long boards) are 60 percent of the average 10-cell module board is verified here. By shifting the array outdoor I-V curve orthogonally to the current-voltage axes it can be shown that the indoor and outdoor curve shapes are essentially the same. Since the environment under which indoor illumination tests are performed is controlled, the I-V characteristics measured indoors are accurate and acceptable. Therefore, the post-thermal vacuum array I-V curve, see Figure I-57, is the predicted Nimbus-B2 beginning-of-life I-V characteristics on the input side of the array blocking diodes. Figure I-1 shows the predicted I-V characteristics on the output side of the blocking diodes at temperatures of 50°C, 35°C and -55°C. Individual platform level I-V characteristics could not be measured outdoors due to equipment problems and unfavorable weather conditions.

8. Thermal Vacuum Test Data

The thermal vacuum acceptance test was initiated on September 30, 1968 and completed on October 21, 1968. Testing was interruped at cycles 5 and 145 for mechanical failures of the test equipment. A summary of electrical testing before, during, and after the thermal vacuum test follows:

a. Intermodule Continuity Test Data

Continuity of all boards was successfully maintained throughout the thermal vacuum test.

b. Voltage Telemetry Test Data

Pre-thermal vacuum electrical tests were unsatisfactory on boards F and G. In both cases an error in wiring was found and corrected. During the first five orbital cycles all telemetry data was acceptable. At cycle number five testing was interrupted because of breakage of a fiberglass support rod (refer to Appendix VII). At the completion of repair work an electrical check showed all telemetry was satisfactory.

A second electrical check was made during the first retest cycle. The telemetry signal from Board F was zero. Upon verification of board continuity it was decided to continue the thermal vacuum test. Checks made after completion of testing showed the failure resulted from a broken test lead inside the test chamber.

Board A voltage telemetry failed to give satisfactory readings after cycle 71. This failure was the result of a open Zener diode on the overvoltage protection circuit, refer to Paragraph E-2. Voltage telemetry from Boards G and J was acceptable throughout the 225 simulated orbits.

c. Voltage Telemetry Overvoltage Protection Test Data

Refer to Voltage Telemetry Overvoltage Protection test results in Paragraph E-2.

d. Temperature Telemetry Test Data

Temperature telemetry measurements were made at various temperatures throughout the thermal vacuum testing. All telemetry voltages were translated into temperatures using the calibration curves previously obtained and shown in Figures I-5 and I-6. These temperatures were within the allowable ±3°C of thermocouple readings taken at the telemetry sensing points.

e. D.C. Isolation Test Data (Short to Skin)

During the thermal vacuum test, no leakage current could be measured from any solar cell board at a maximum potential of 83.0 volts.

f. Interboard Leakage Test Data

Leakage resistance between the boards on each platform was measured at the start and completion of the thermal vacuum test. Leakage measurements were performed at a pressure of less than 1×10^{-5} torr and a temperature of 25°C. The leakage resistance between boards was found to be greater than 10 megohoms for each board.

F. POWER SUMMARY

The solar array operating point of 34 volts, the sunlight intensity at 139.6 mw/cm^2, and the array temperature at 35°C was selected. The power output of the solar array is 501 watts (derived from Figure I-57) on the input side of the array blocking diodes. The power varies with the following conditions:

- array operating point - this point varies between 32 and 36 volts depending on the spacecraft load profile and the state of charge of the storage modules.
- array temperature - the array temperatures for a typical orbit varies between -70°C and +50°C.
- intensity level - the sunlight intensity cycles between 134.7 mw/cm^2 and 144.5 mw/cm^2 during the year.

Under these conditions, plus the variations associated with the test of the platforms, the output power variation is estimated at ±37 watts.

Array power degradation as a function of orbital life is not part of the scope of this report. The power output of 501 ±37 watts presented is for the first day in orbit and does not consider ultraviolet degradation and radiation damage, both of which seriously reduce the array output.

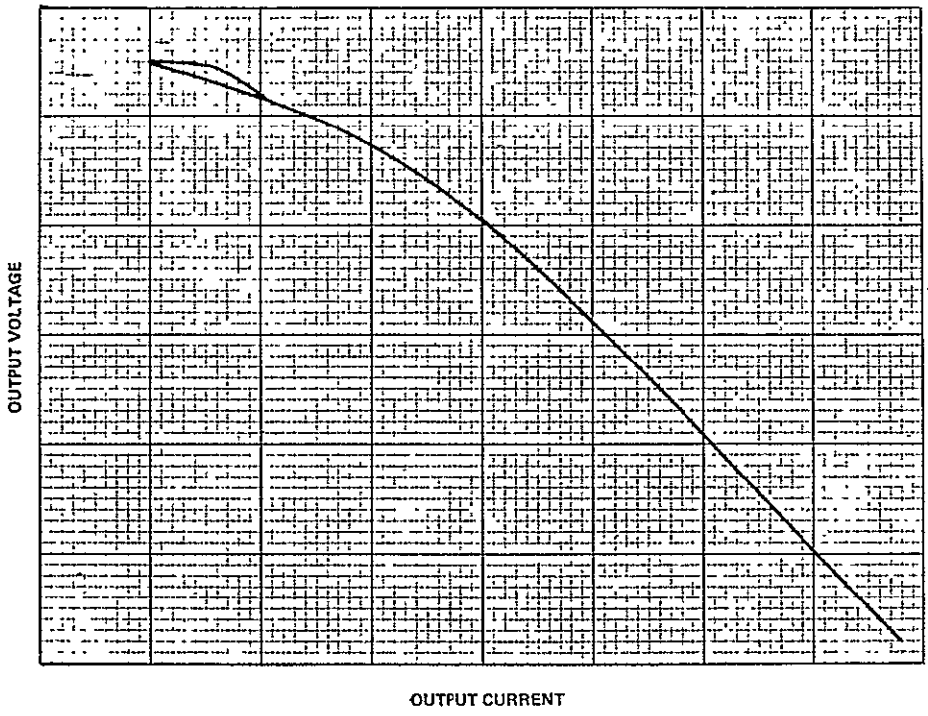

Figure I-40. Module No. 2, Board E I-V Characteristics

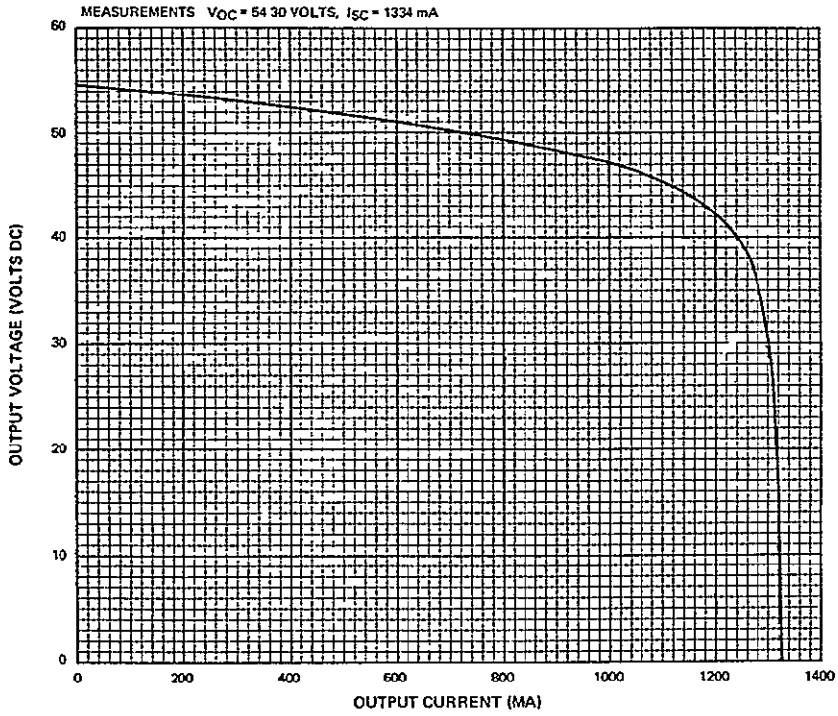

Figure I-41. Pre-Thermal Indoor I-V Characteristics, Board E After Rework

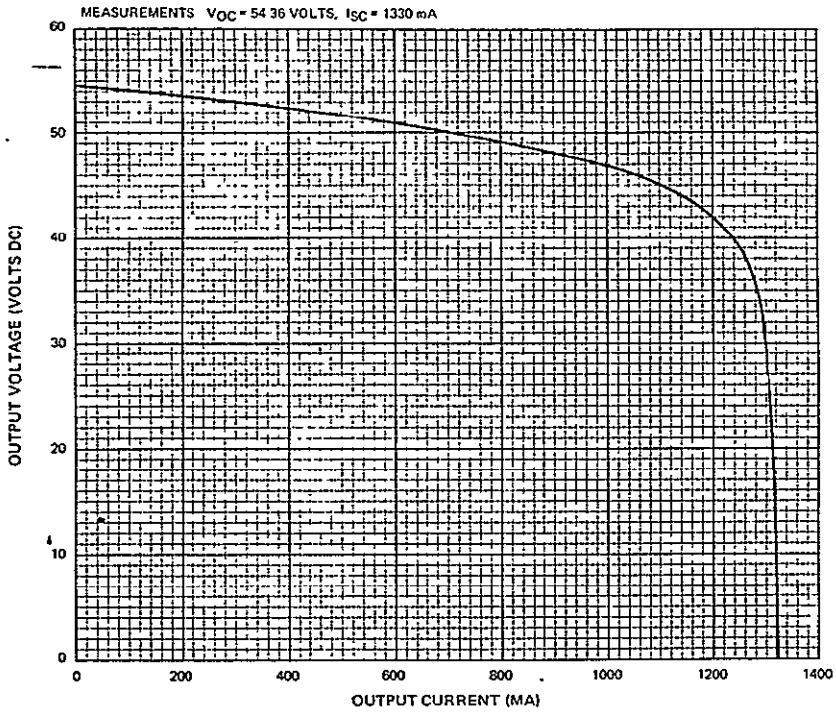

Figure I-42. Pre-Thermal Indoor I-V Characteristics, Board L After Rework

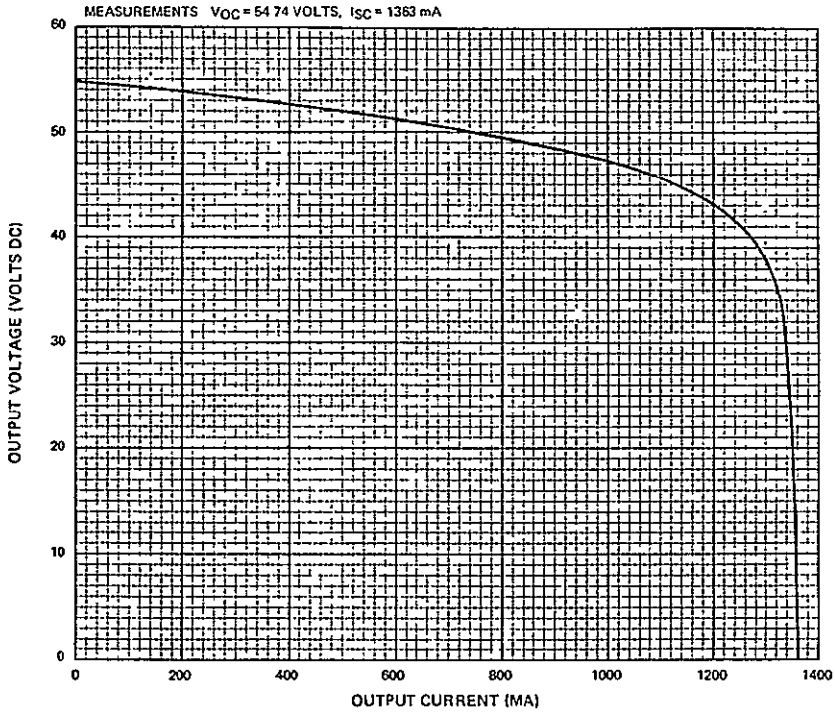

Figure I-43. Post-Thermal Indoor I-V Characteristics, Board A

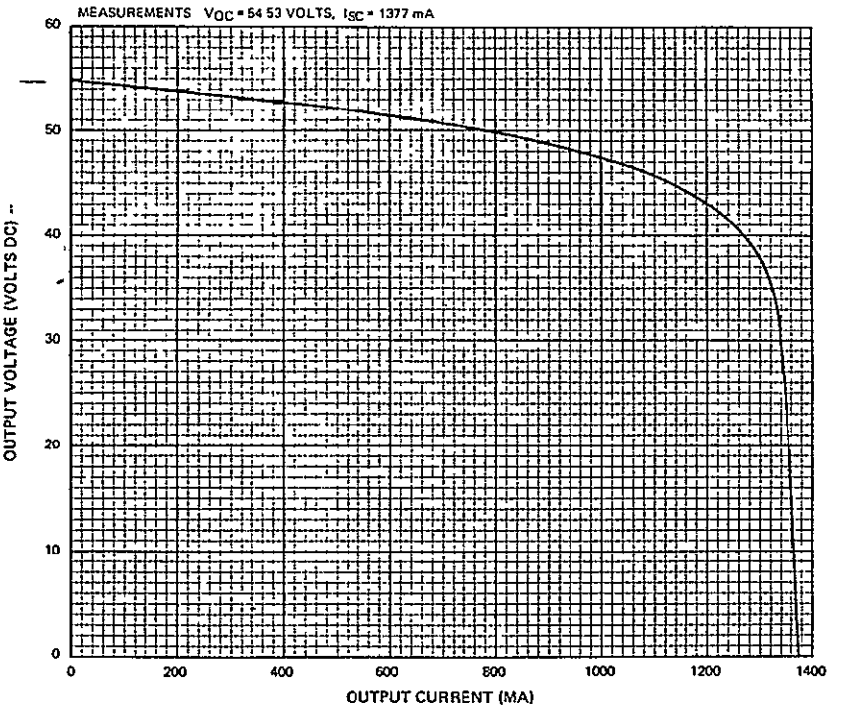

Figure I-44. Post-Thermal Indoor I-V Characteristics, Board B

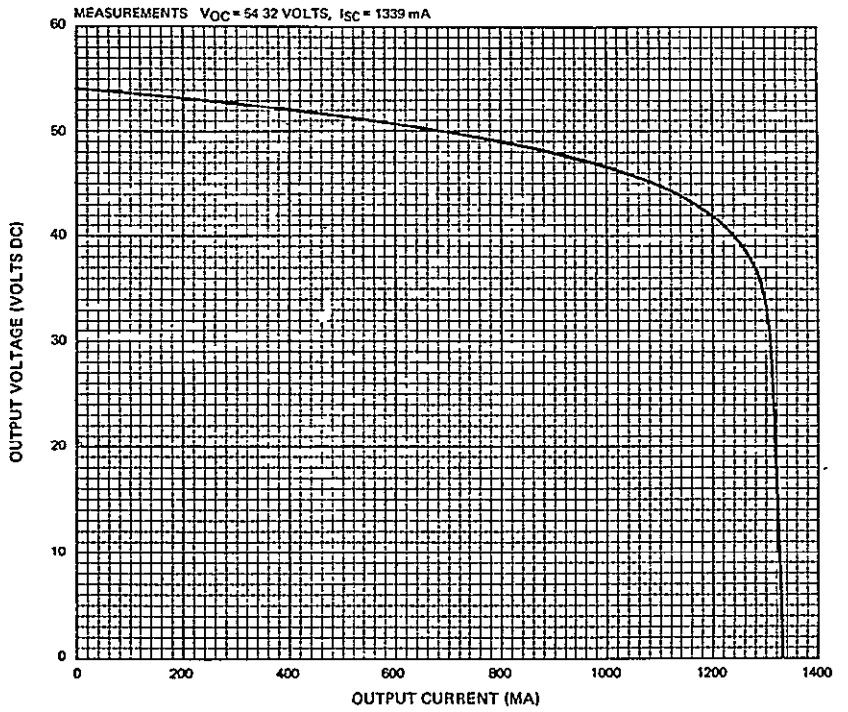

Figure I-45. Post-Thermal Indoor I-V Characteristics, Board C

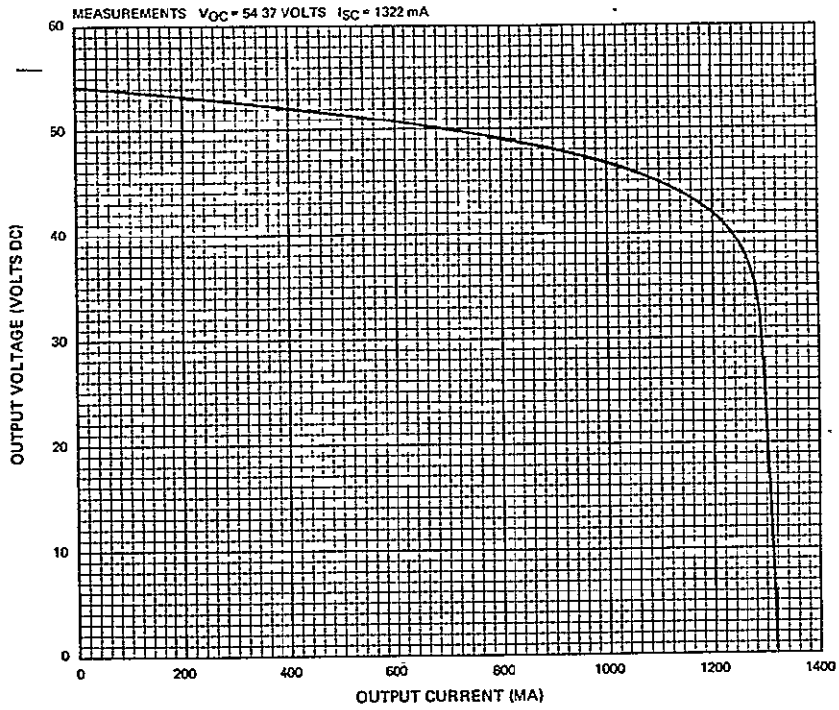

Figure I-46. Post-Thermal Indoor I-V Characteristics, Board D

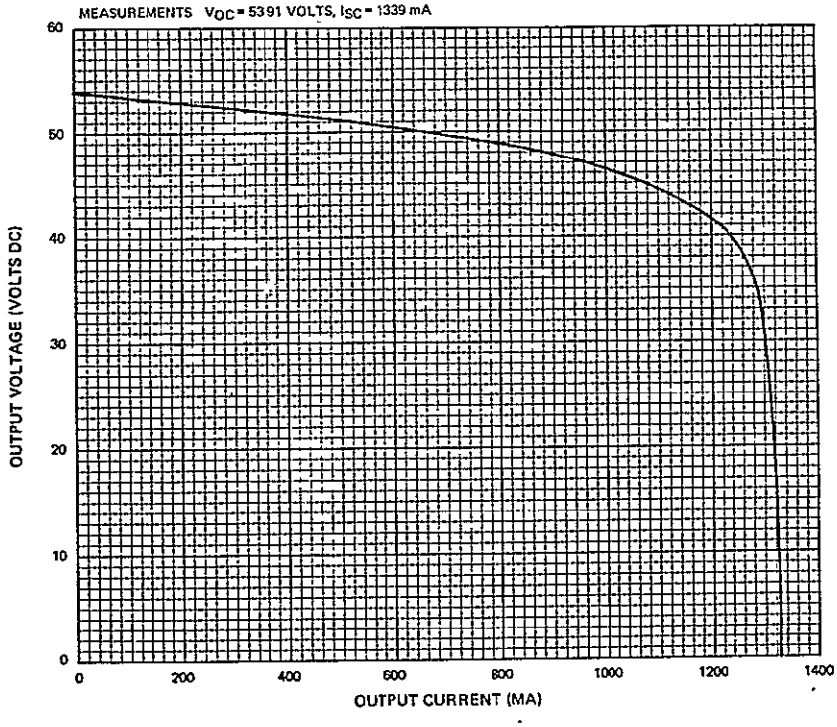

Figure I-47. Post-Thermal Indoor I-V Characteristics, Board E

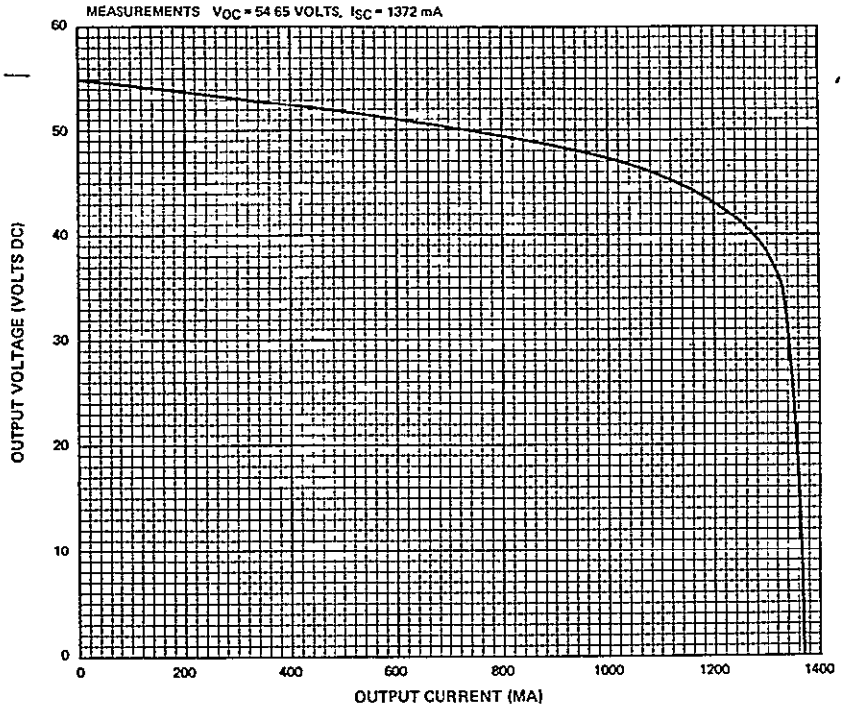

Figure I-48. Post-Thermal Indoor I-V Characteristics, Board G

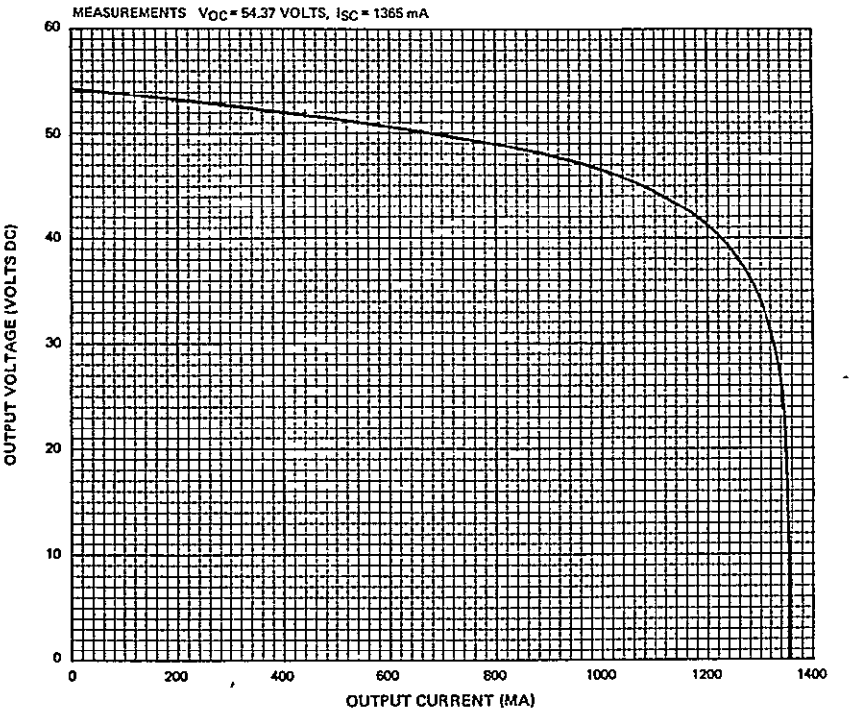

Figure I-49. Post-Thermal Indoor I-V Characteristics, Board H

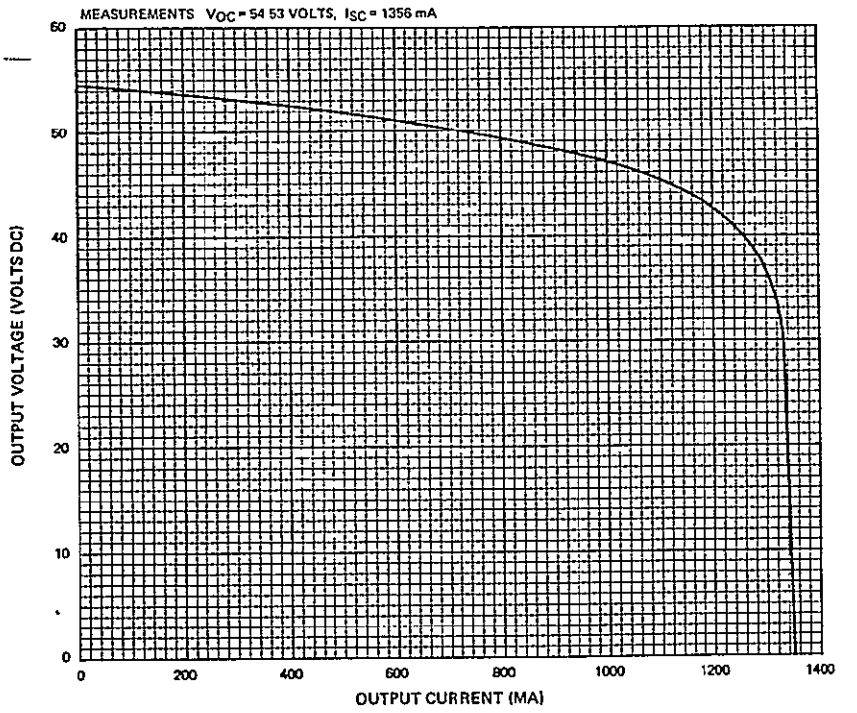

Figure I-50. Post-Thermal Indoor I-V Characteristics, Board J

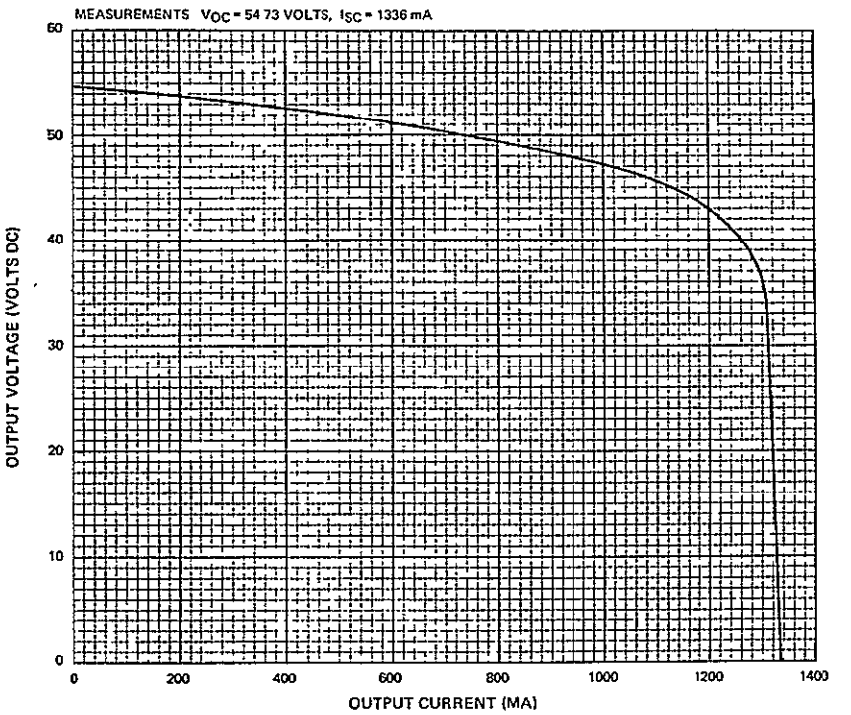

Figure I-51. Post-Thermal Indoor I-V Characteristics, Board K

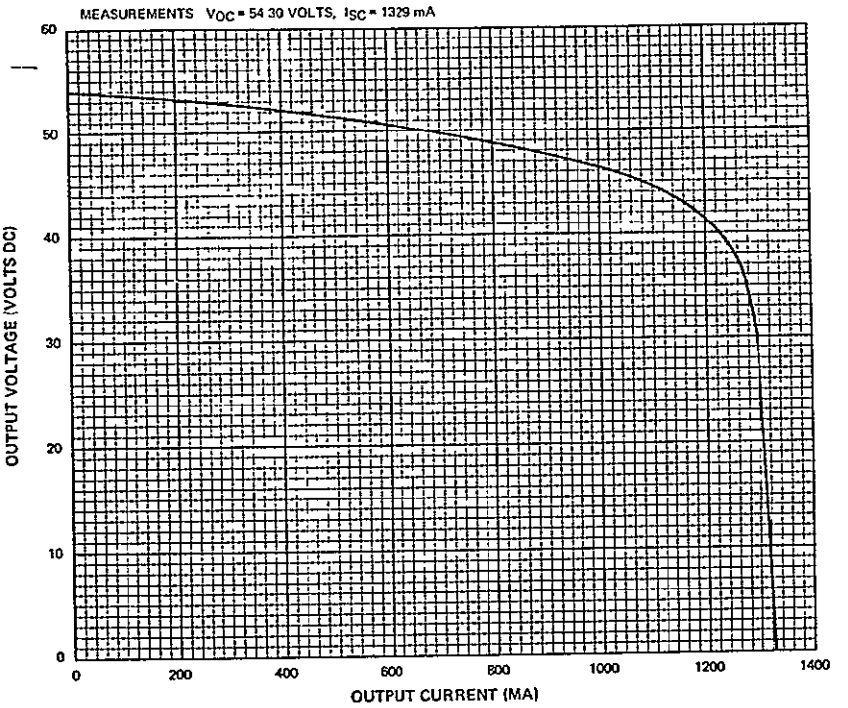

Figure I-52. Post-Thermal Indoor I-V Characteristics, Board L

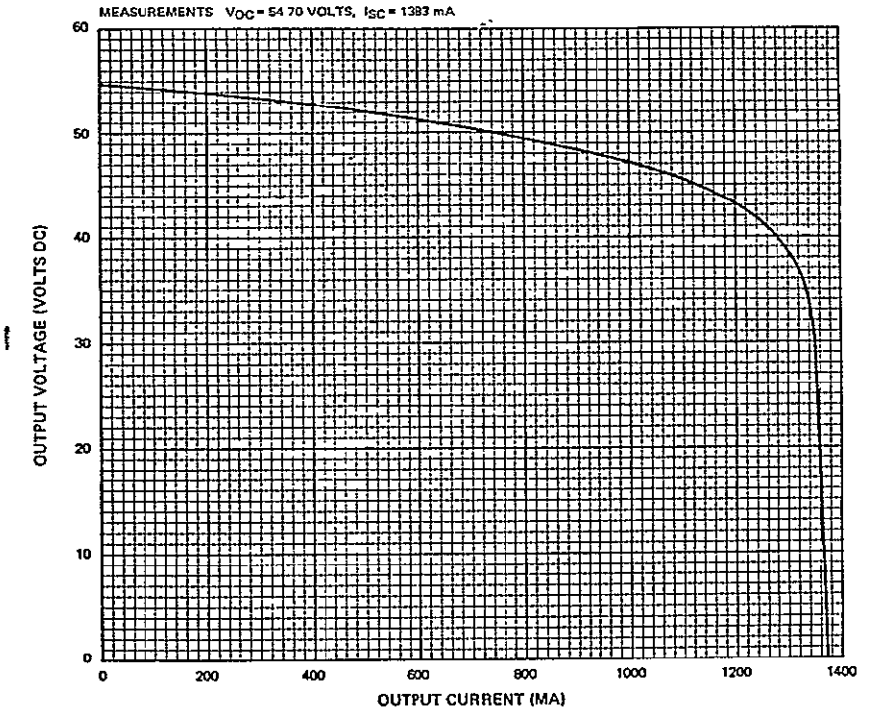

Figure I-53. Post-Thermal Indoor I-V Characteristics, Board H After Rework

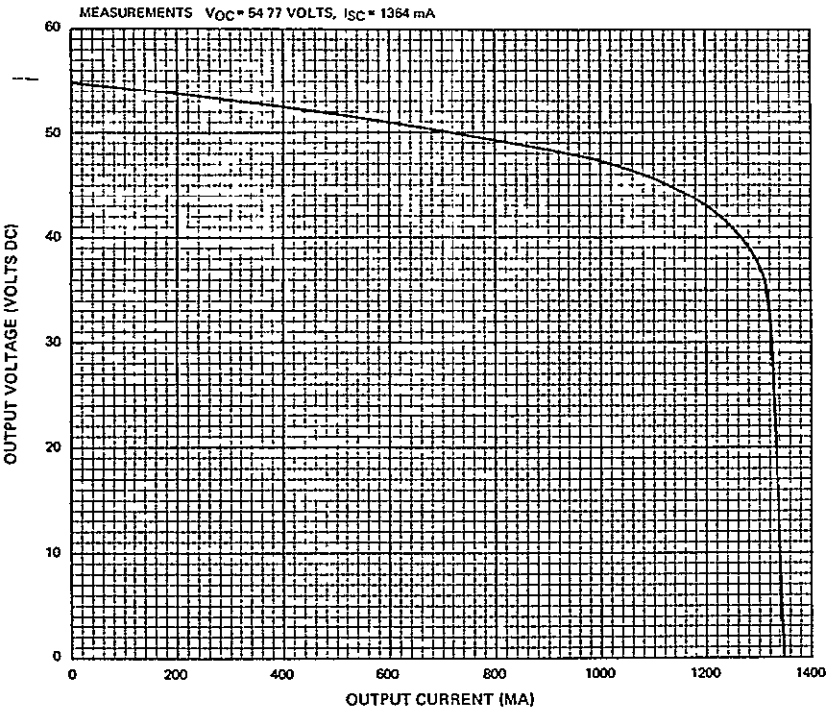

Figure I-54. Post-Thermal Indoor I-V Characteristics, Board K After Rework

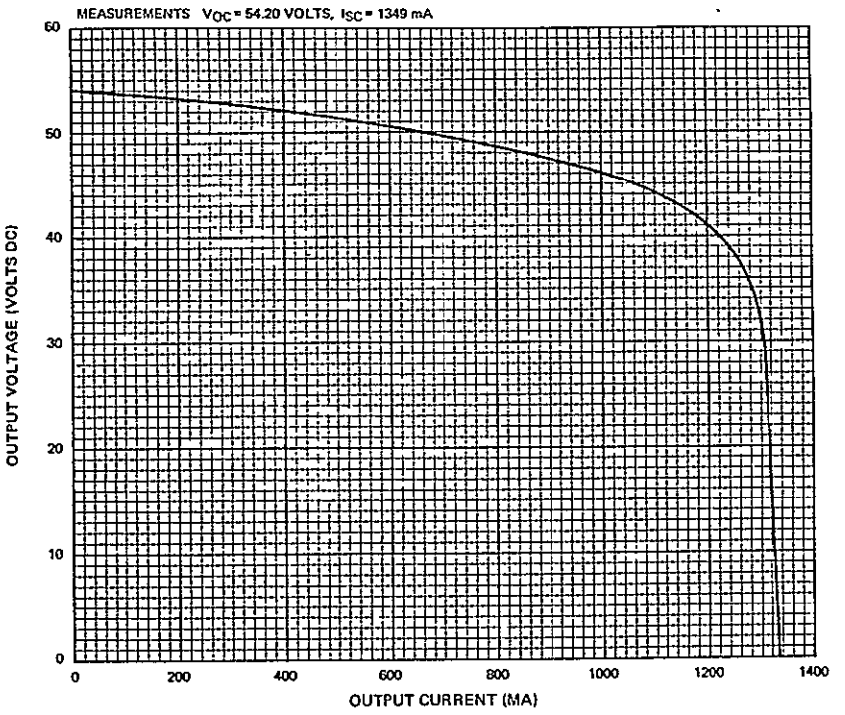

Figure I-55. Post-Thermal Indoor I-V Characteristics, Board L After Rework

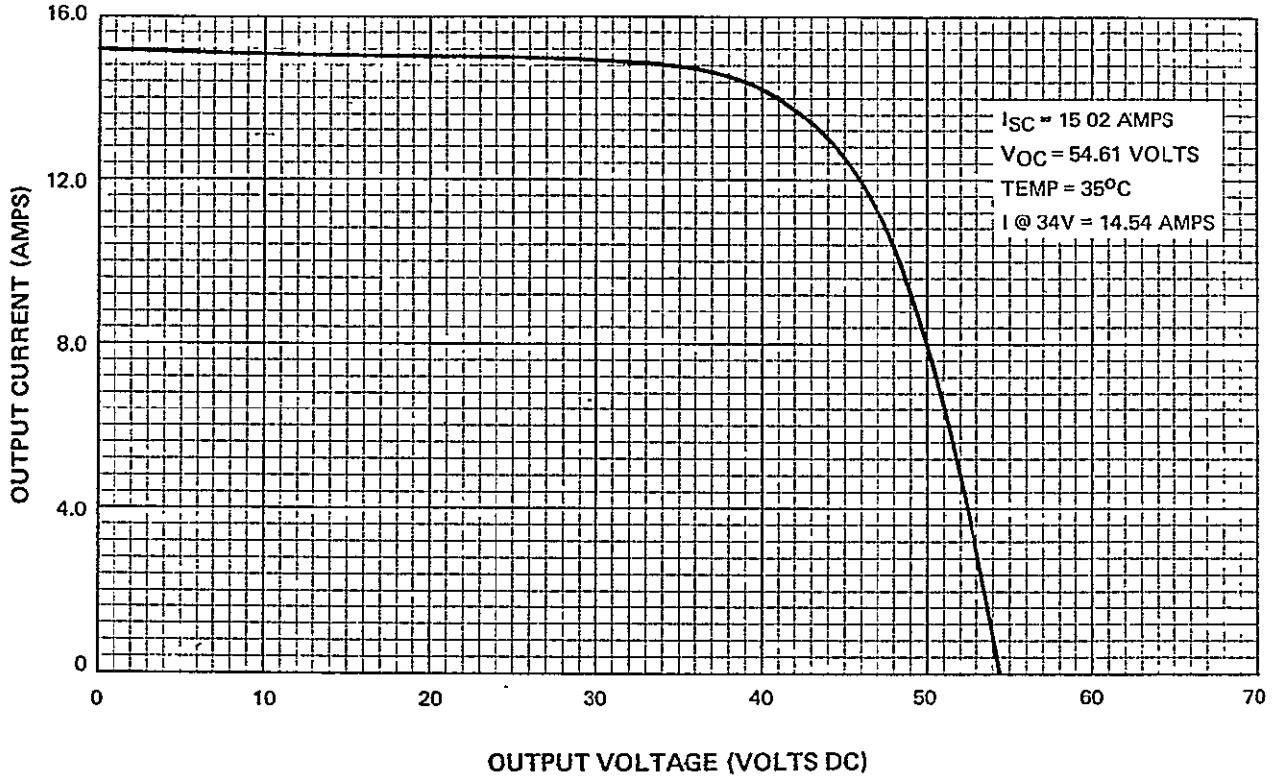

Figure I-56. Predicted Solar Array I-V Characteristics,

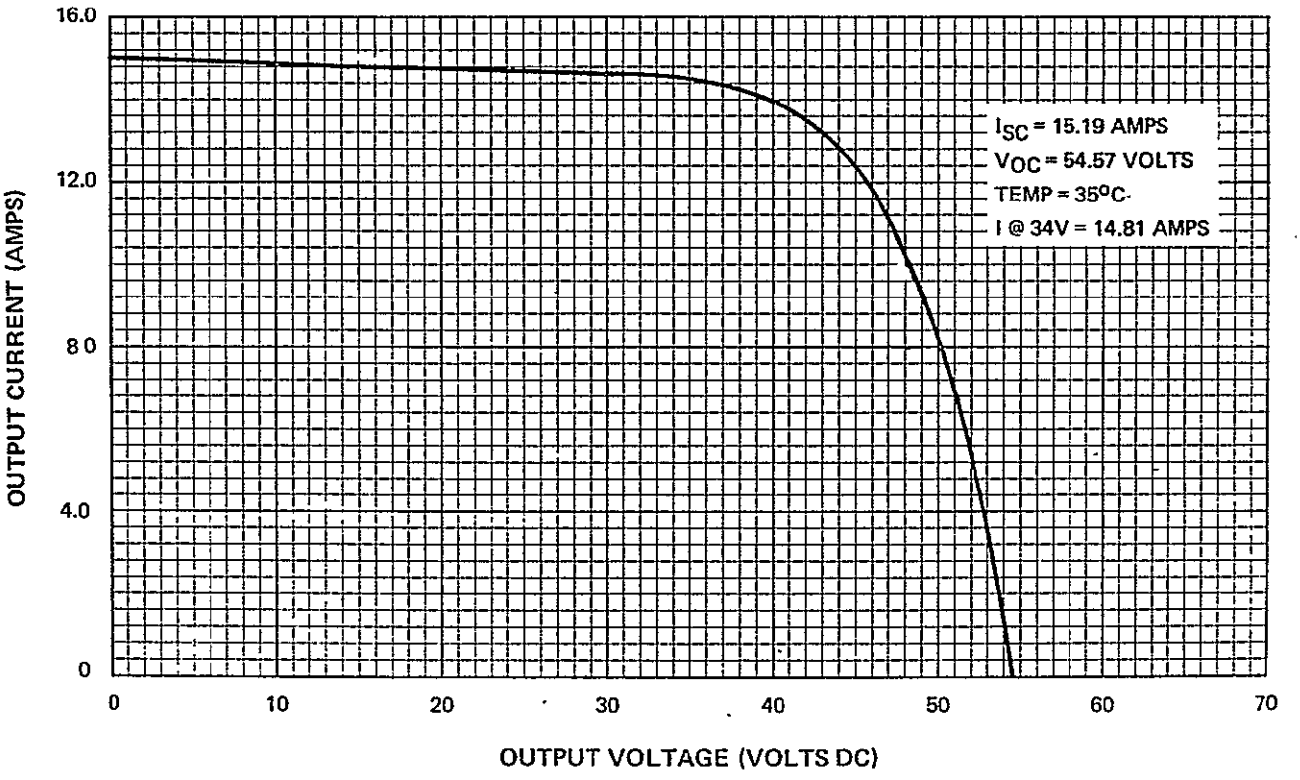

Figure I-57. Predicted Solar Array I-V Characteristics, Post-Thermal Vacuum

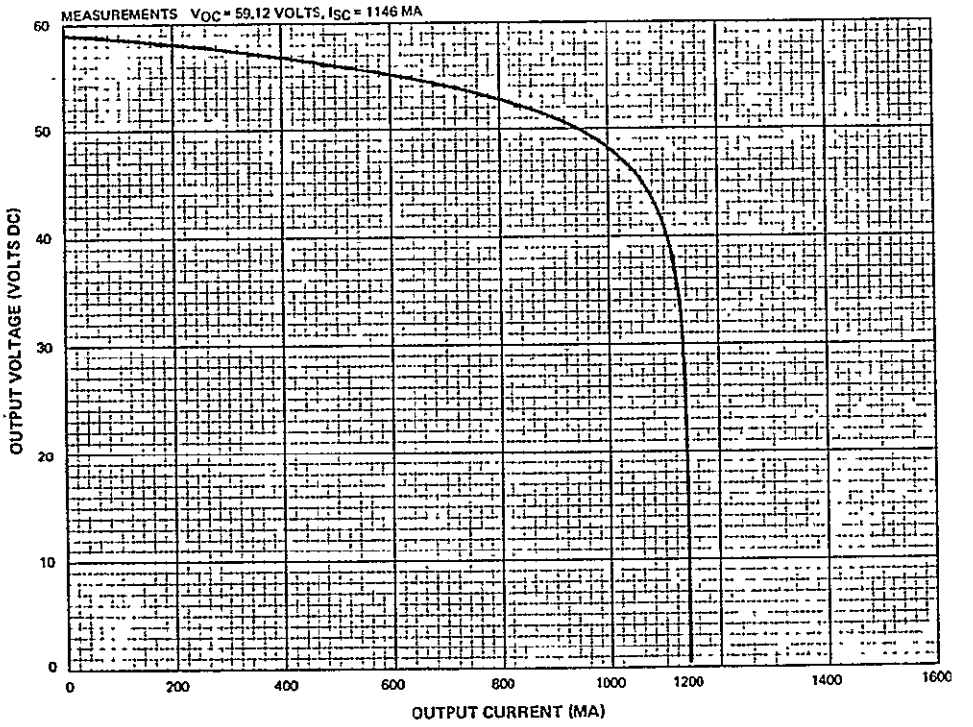

Figure I-58. Outdoor I-V Characteristics, Board A

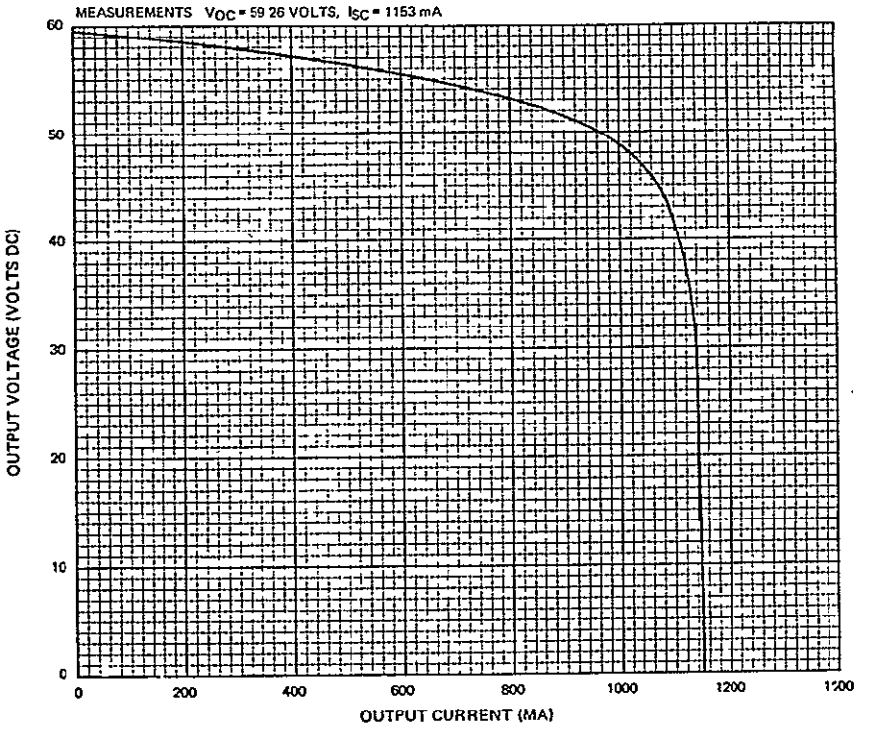

Figure I-59. Outdoor I-V Characteristics, Board B

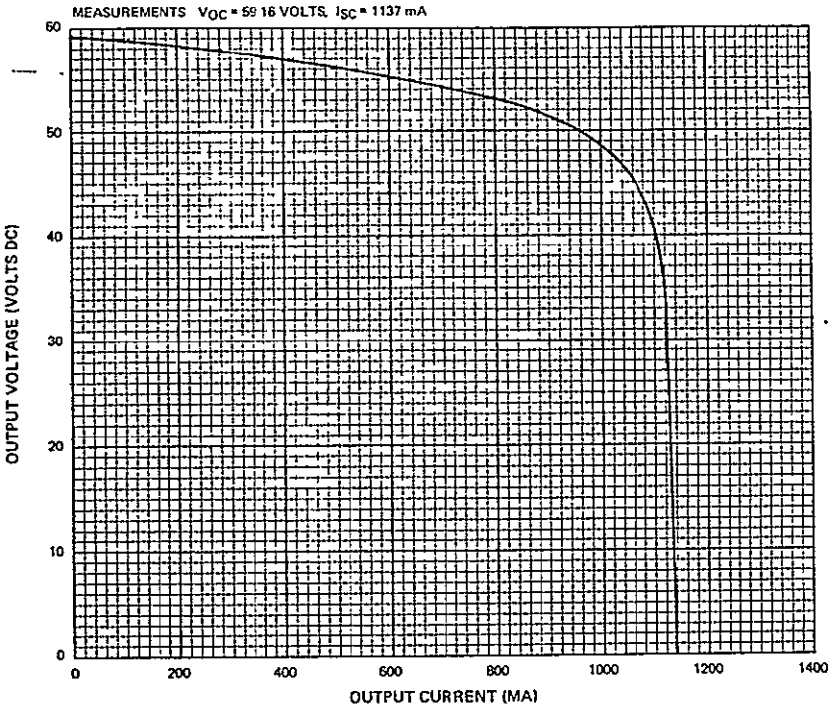

Figure I-60. Outdoor I-V Characteristics, Board C

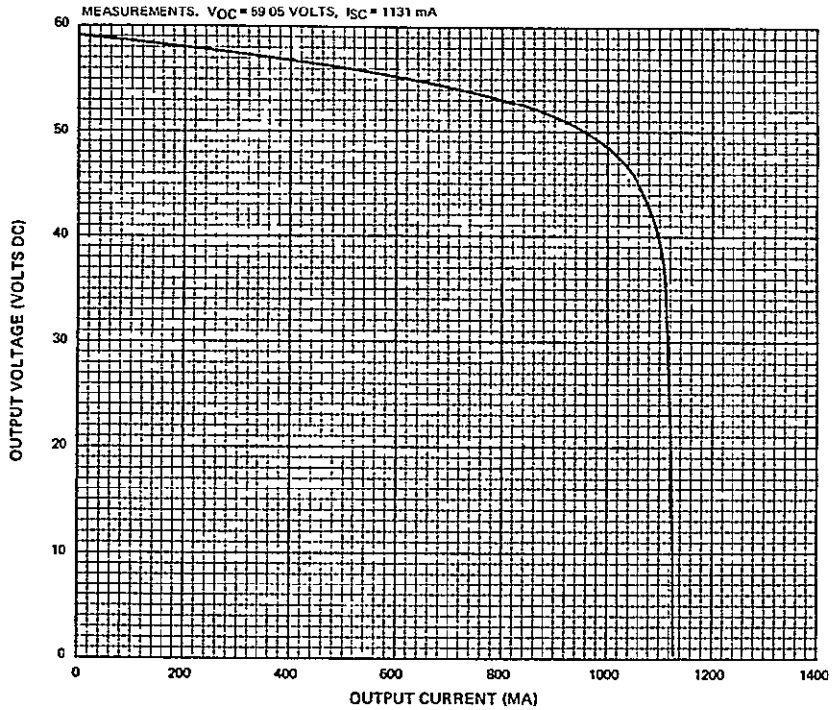

Figure I-61. Outdoor I-V Characteristics, Board D

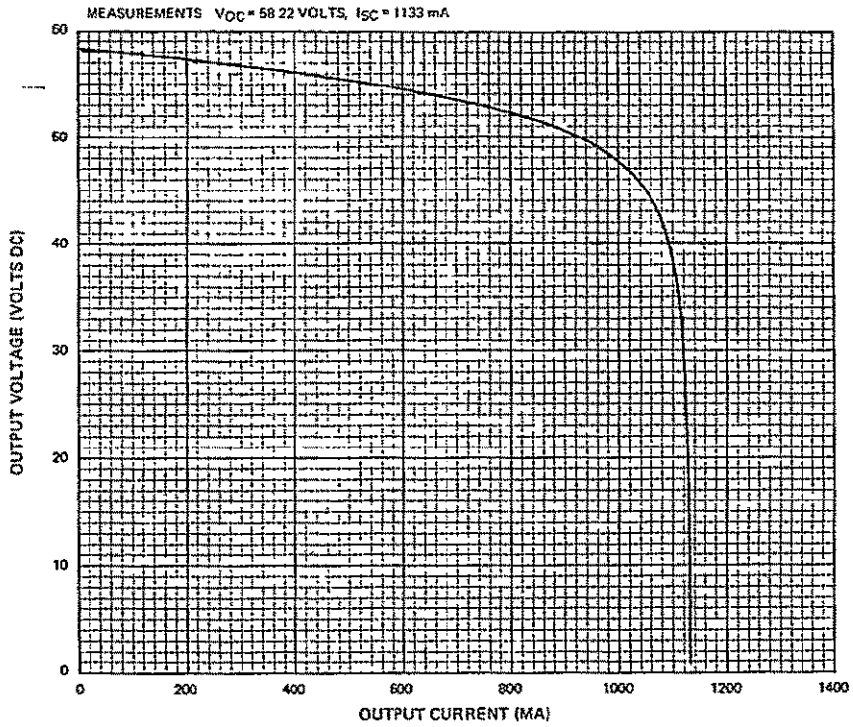

Figure I-62. Outdoor I-V Characteristics, Board E

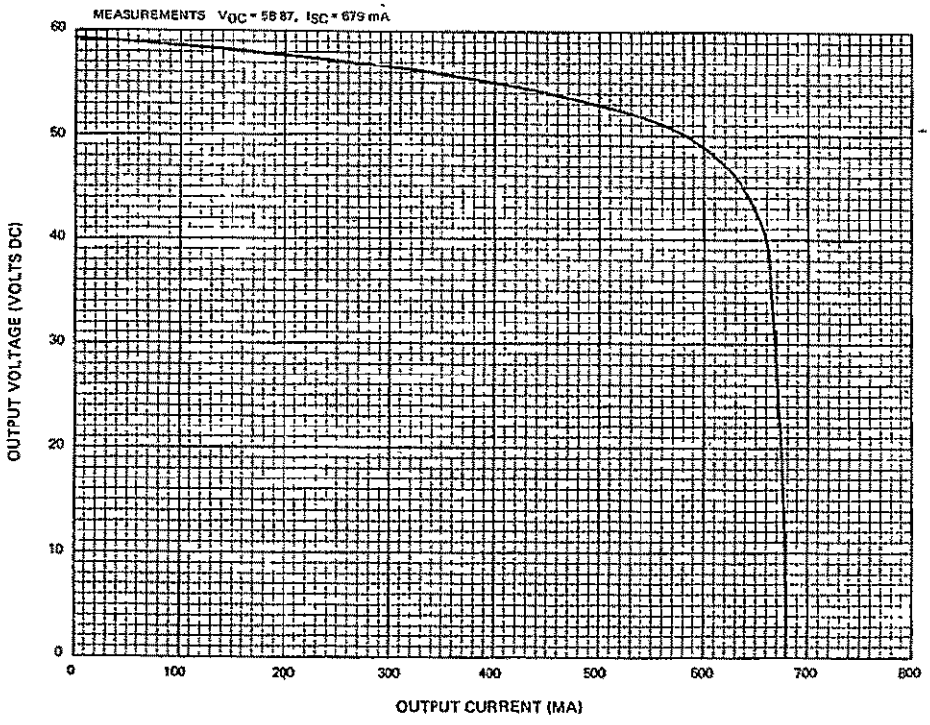

Figure I-63. Outdoor I-V Characteristics, Board F

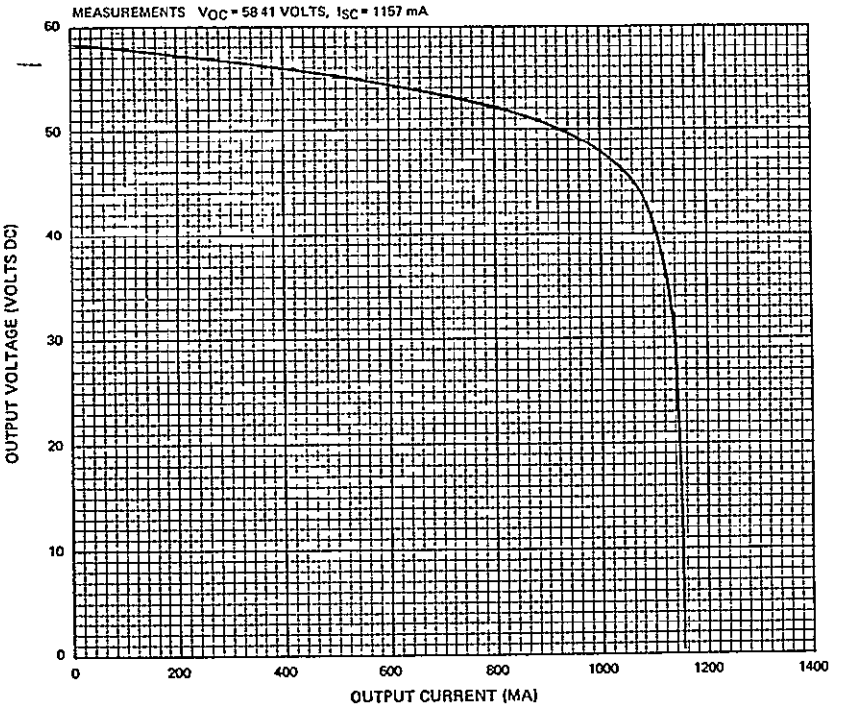

Figure I-64. Outdoor I-V Characteristics, Board G

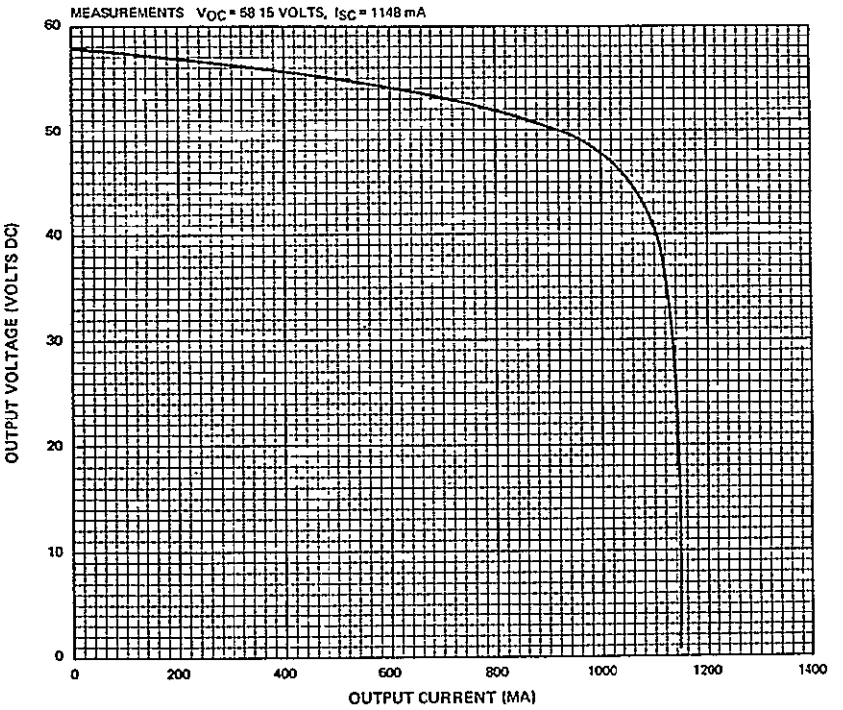

Figure I-65. Outdoor I-V Characteristics, Board H

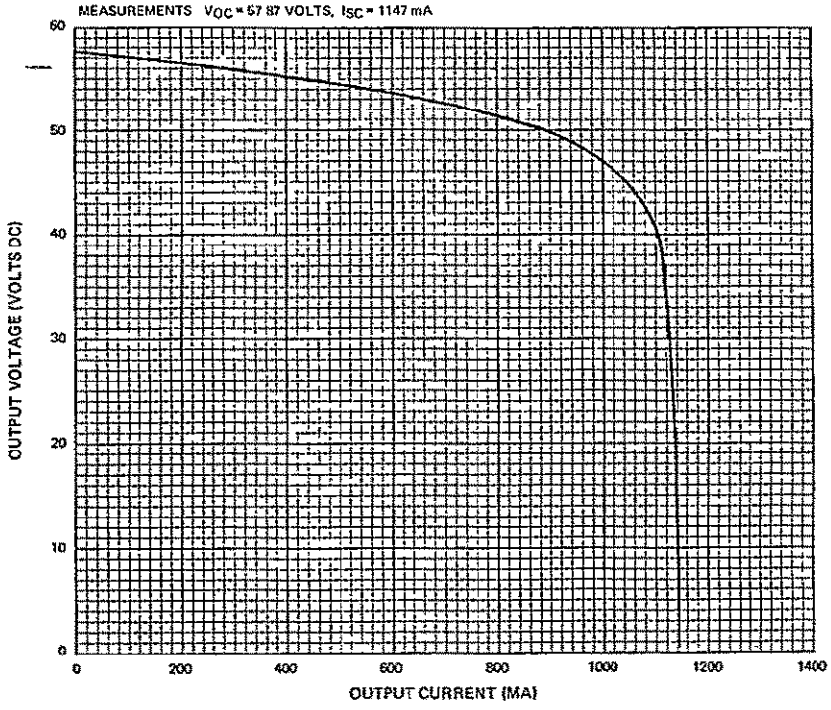

Figure I-66. Outdoor I-V Characteristics, Board J

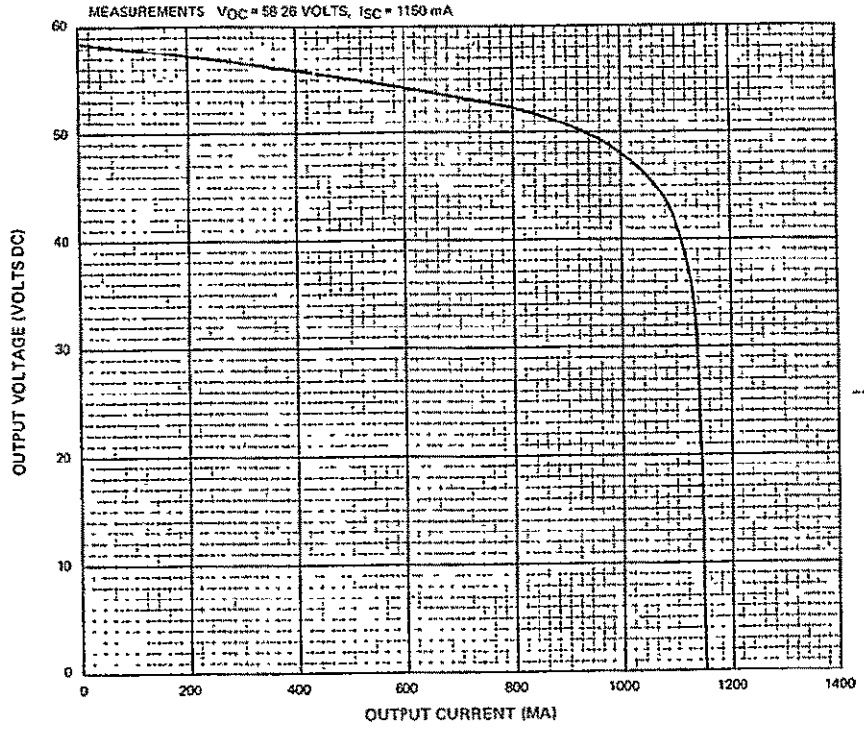

Figure I-67. Outdoor I-V Characteristics, Board K

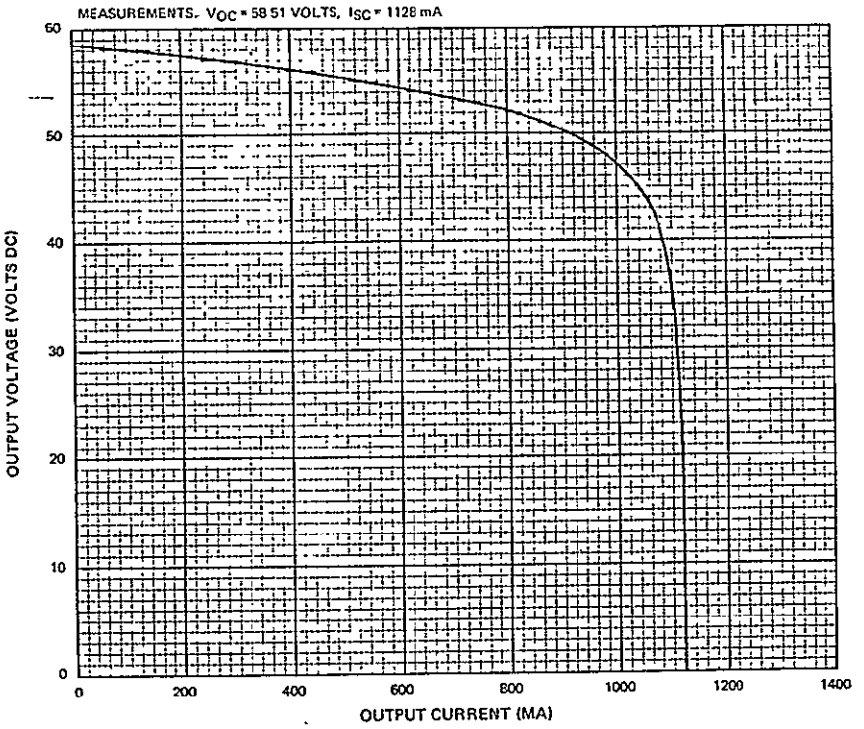

Figure I-68. Outdoor I-V Characteristics, Board L

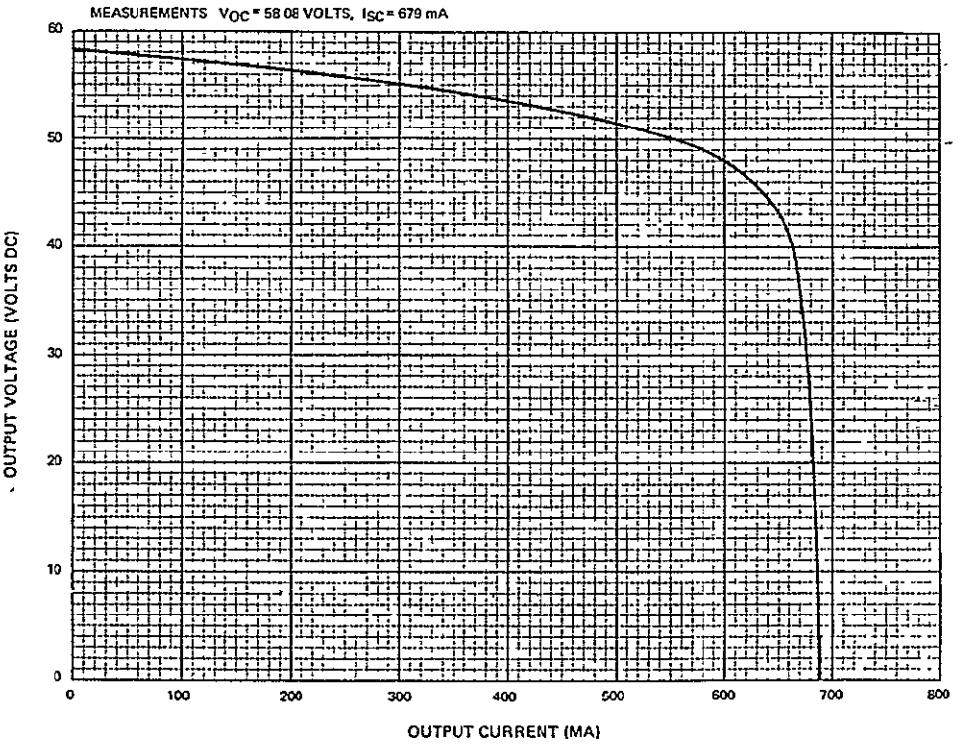

Figure I-69. Ourdoor I-V Characteristics, Board M

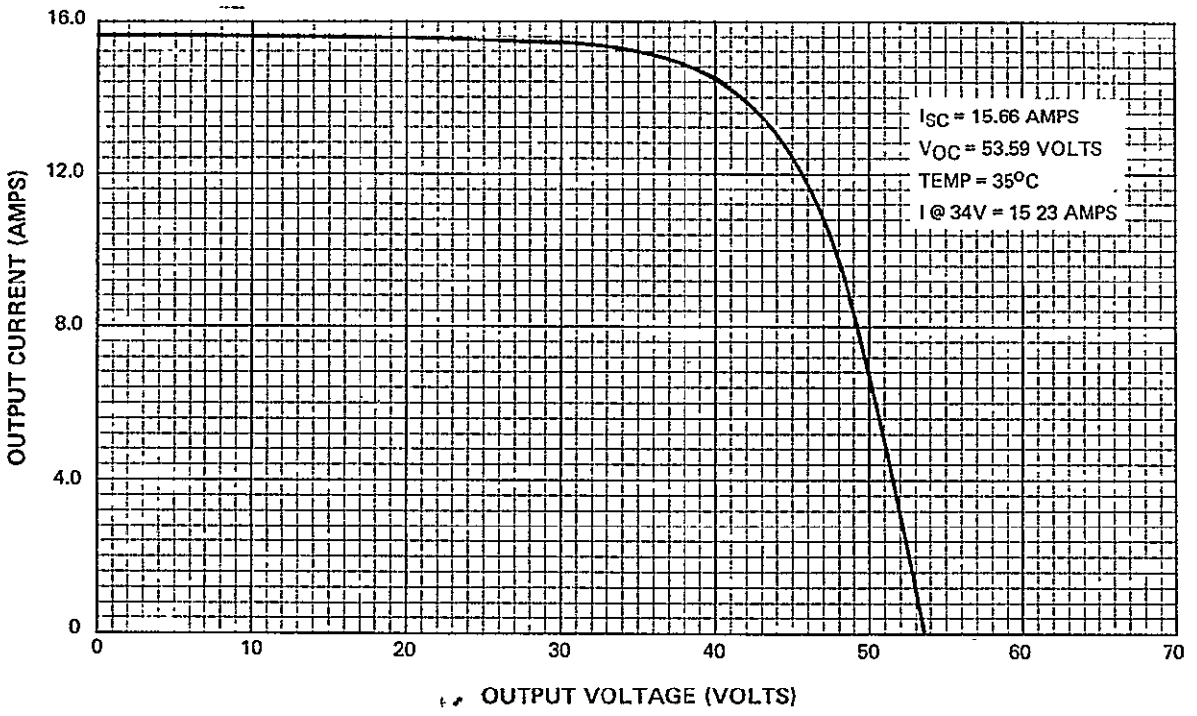

Figure I-70. Solar Array I-V Characteristics, Outdoor Illumination at Air-Mass-Zero and Temperature Corrections

TABLE I-15. CHRONOLOGICAL SEQUENCE OF EVENTS

Date	Events	Results	Comments
9-15-67	NAS5-10470 Contract Date. - The solar-cell modules and substrates were supplied as GFE by NASA. (Time of storage was approximately 4 years).		The solar cell modules were fabricated by the Electronic Components division of the RCA Corp. The substrates (Serial No. 015 and 016) were fabricated by the Martin-Marietta Corp. Baltimore, Md.
10-30-67	Start solar-cell module evaluation		
11-30-67	Complete solar-cell module evaluation		Reference "Quarterly Technical Report No. 1 (R-3272) Section 2, Par. C-2."
12-1-67	Initiate Q-Board Fabrication		
12-29-67	Completed Q-Board Fabrication and started Q-board tests		
5-27-68	Completed Q-Board Tests		Reference "Quarterly Technical Report No. 2 (R-3440)Section 2, Par. C-2."
6-14-68	Started fabrication of platform Ser. No. 15		
6-18-68	Started fabrication of platform Ser. No. 16		
6-18-68	Nimbus-D solar cell modules and substrates diverted to Nimbus-B2 program		
7-28-68	Fabrication and calibration of temperature telemetry boards completed		Reference Par. E-1
8-6-68	Electrical confidence tests of platform Ser. No. 15 completed		Reference Par. E-5

TABLE I-15. CHRONOLOGICAL SEQUENCE OF EVENTS (Continued)

Date	Events	Results	Comments
8-22-68	Electrical confidence tests of platform Ser. No. 16 completed		Reference Par. E-5.
9-13-68	Deployment tests completed on platforms Ser. No. 15 and 16		Reference Par. E-6
9-19-69	Weight and Balance Test completed of platform Ser. No. 15 and 16		Reference Par. E-4
9-20-69	Fabrication of platforms Ser. No. 15 and 16 completed.		
9-25-69	Start Pre-thermal illumination tests		
9-28-69	Complete Pre-thermal illumination tests		Reference Par. E-7
9-30-69	Platforms installed in thermal vacuum chamber and pumpdown started		Pressure 1.0×10^{-5} torr
10-1-69	5 cycles completed, thermal vacuum tests stopped		Unacceptable thermal gradient on platform Ser. No. 16. Reference Appendix VII
10-14-69	Thermal vacuum tests interrupted. Pressure maintained.		Environmental test facility equipment failure. Reference Appendix VII
10-15-69	Continued thermal vacuum tests		
10-11-69	Completed thermal tests	Satisfactory	
10-24-69	Started post-thermal illumination tests		
10-30-69	Completed post-thermal illumination tests	Satisfactory	Reference Par. E-7.
11-21-68	Started outdoor illumination tests		Interrupted due to poor weather conditions

TABLE I-15. CHRONOLOGICAL SEQUENCE OF EVENTS (Continued)

Date	Events	Results	Comments
12-7-68	Completed outdoor illunination tests	Satisfactory	Platform illumination tests were not performed as weather conditions deteriorated and space-craft integration was in jeopardy.
12-11-68	Packed both platforms and delivered to the General Electric Co. per NASA direction		

APPENDIX II

HUMIDITY TEST REPORT

A. GENERAL

Two separate humidity tests were conducted on solar cells procured for the Nimbus-D solar array. Test number 1 contained 50 cells representing five cells from each manufacturer's shipping lot. Test number 2 contained 18 cells; 10 cells (sample groups 1 and 2) represented 500 cells procured to replace the cells used for Q-board qualification and to replace the lots that failed during test number 1; eight cells (sample group Nos. 3 and 4) represented the two manufacturers lots that failed test number 1. All of the solar cell samples of test number 1 were also retested in test number 2.

B. ELECTRICAL, VISUAL, AND HUMIDITY TESTS

Each sample solar cell selected was visually inspected and electrically tested prior to and after humidity exposures. Visual inspection consists of inspecting each sample cell at 105 power magnification and mapping any physical characteristics such as blisters, peels, cracks, or chips. Electrical tests consisted of securing current voltage (I-V) characteristics of each cell under a filter color wheel. The current output at 0.46 volts is then compared to the vendors current rating. The specified allowable current degradation due to humidity tests is 3 milliamperes at 0.46 volts dc. Humidity tests consist of exposing the sample cells to 100-percent humidity for 14 days. Test number 1 was conducted between 3:00 PM December 20, 1968 and 3:00 PM January 3, 1969; test number 2 was conducted between 3:00 AM March 5, 1969 and 9:00 AM, March 20. The additional 18 hours of test number 2 compensates for the period of time that the humidity dropped below 95 percent. The wet and dry bulb temperature were monitored every two hours except on weekends and holidays. If the humidity was above 95 percent when 2-hour measurements were resumed, the shutdown time was added to the accumulated test time.

C. TEST RESULTS AND CONCLUSIONS

1. Test No. 1 Results

Visual inspection was conducted after humidity exposure and compared to the pre-humidity data recorded on maps. Cell number 15 had some small blisters 0.002-inch in diameter on the grid lines; no other degradation was observed.

The cells were then cleaned and electrically tested. The results, compared to the vendor data, are listed columns 2 through 3 in Table II-1. Two cells (Nos. 3 and 32) indicated a current degradation in excess of 3 milliamperes at 0.46 volts. These cells, subsequently inspected at 375 power magnification, showed signs of mechanical degradation. The fixture contacts had peeled material from the negative contacts and some material from some of the grid lines peeled during the cleaning operation. All of the cells passed the mechanical requirements specified for acceptance but three cells showed signs of degradation when inspected at 375 power magnification. As a result of these tests, manufacturer's lots 07571 and 07486 were placed in a hold pending further resolution.

2. Test No. 2 Results

Visual inspection was conducted after humidity exposures and compared to the pre-humidity data recorded on maps. Cell number 12 was cracked during post-humidity tests; the remainder of the cells (refer to Table II-1) did not show any mechanical degradation. The cells were then cleaned and electrically tested. The results, compared to the vendor data, are listed in Table II-2. One cell (number 12) showed current degradation in excess of 3 milliamperes at 0.46 volts. The remaining cells were satisfactory. Since four cells were adequate to represent the group, lot 07571 along with lot 07486 was released for use in the fabrication of solar cell modules. The solar cell test lot used during test number 2 for information purposes. Current data (I at 0.46 volts) is shown in column 5 of Table II-1.

3. Test Anomaly Summary

A summary of the test anomalies are tabulated in Table II-3.

TABLE II-1. I-V CHARACTERISTICS, TEST NO. 1
SAMPLE CELLS

Cell No.	Current (mA) at 0.46 Volts DC				Difference Col. 3 minus Col. 4 (mA)
	CRL Measurements Post-Manufacturing	RCA Measurements			
		Pre-Humidity	Post-Humidity No. 1	Post Humidity No. 2	
1	128	125.8	127.0	126.8	+1.2
2	120	119.0	122.8	122.7	+3.8
3	130	129.3	125.0	123.1	-4.3
4	120	127.2	127.2	127.6	0
5	130	127.6	129.6	132.0	+2.0
6	132	131.8	131.2	132.1	-0.6
7	128	127.4	126.9	127.9	-0.5
8	128	128.0	128.1	127.8	+0.1
9	122	120.5	122.0	122.9	+1.5
10	132	130.4	130.2	131.1	-0.2
11	128	121.0	123.8	124.2	+2.8
12	120	117.6	119.6	119.0	+2.0
13	120	128.6	128.7	118.3	+0.1
14	120	113.6	120.6	121.0	+7.0
15	126	122.6	126.1	126.8	+3.5
16	120	122.9	122.9	123.3	0
17	130	129.6	128.1	129.9	-1.5
18	120	128.4	128.0	117.6	-0.4
19	120	128.6	126.0	126.2	-2.6
20	126	127.4	127.6	123.9	+0.2
21	132	129.7	128.3	128.0	-1.4
22	120	117.4	117.3	116.0	-0.1
23	124	123.5	125.0	126.4	+1.5

TABLE II-1. I-V CHARACTERISTICS, TEST NO. 1
SAMPLE CELLS (Continued)

Cell No.	Current (mA) at 0.46 Volts DC				Difference Col. 3 minus Col. 4 (mA)
	CRL Measurements Post-Manufacturing	RCA Measurements			
		Pre-Humidity	Post-Humidity No. 1	Post-Humidity No. 2	
24	124	122.4	122.6	121.2	+0.6
25	120	129.2	129.2	119.8	0
26	130	125.6	124.1	124.1	-1.5
27	130	130.9	128.6	128.6	-2.3
28	130	130.0	130.0	129.2	0
29	128	123.0	123.3	123.7	+0.3
30	124	123.4	122.2	123.0	-1.2
31	130	130.0	129.8	130.0	-0.2
32	124	122.5	118.5	116.2	-4.0
33	128	128.9	126.9	127.4	-2.0
34	128	128.4	125.5	125.1	-2.9
35	120	129.3	128.6	118.8	-0.7
36	128	126.9	127.0	126.7	+0.1
37	124	123.5	124.9	125.7	+1.4
38	124	120.0	118.9	118.2	-1.1
39	126	127.3	126.6	125.2	-0.7
40	122	122.0	124.5	125.2	+2.5
41	126	120.8	121.5	122.3	+0.7
42	120	119.9	118.5	108.8	-1.4
43	126	126.8	127.2	128.7	+0.4
44	126	124.8	123.8	123.6	-1.0
45	128	127.6	129.2	129.6	+1.6
46	120	120.3	122.6	122.6	+2.3

TABLE II-1. I-V CHARACTERISTICS, TEST NO. 1
SAMPLE CELLS (Continued)

Cell No.	Current (mA) at 0.46 Volts DC				Difference Col. 3 minus Col. 4 (mA)
	CRL Measurements Post-Manufacturing	RCA Measurements			
		Pre-Humidity	Post-Humidity No. 1	Post-Humidity No. 2	
47	128	126.2	126.2	125.3	0
48	132	131.5	131.4	132.2	-0.1
49	120	120.6	122.5	125.1	+1.9
50	124	124.0	123.3	122.0	-0.7

TABLE II-2. I-V CHARACTERISTICS, TEST NO. 2 SAMPLE CELLS

Sample* Group No.	Cell No.	Current (mA) at 0.46 Volts DC			Difference Col. 3 minus Col. 4 (mA)
		CRL Measure Post-Manuf.	RCA Measurement		
			Pre-Humidity	Post-Humidity	
No. 1	1	134	33.0	132.6	-0.4
	2	134	131.0	130.8	-0.2
	3	134	130.8	130.0	-0.8
	4	124	123.9	123.3	-0.6
	10	124	119.5	124.7	+5.2
No. 2	6	134	130.1	130.5	+0.4
	7	134	132.7	132.3	-0.4
	8	124	122.3	122.3	0
	9	124	120.3	120.6	+0.3
	5	124	101.5	100.2	-1.3
No. 3	11	128	127.7	127.2	-0.5
	12	128	127.9	121.8	-6.1
	13	128	127.6	126.7	-0.9
	14	128	127.1	126.6	-0.7
	15	128	129.2	129.0	-0.2
No. 4	16	130	130.4	130.2	-0.2
	17	130	131.4	131.0	-0.4
	18	130	131.8	131.0	-0.8

*Sample groups No. 1 and No. 2 represent manufacturer's lots 07635 and 07721; sample groups No. 3 and No. 4 represent manufacturer's lots 07571 and 07486 respectively, (refer to Test No. 1, Paragraph 1C (1).

TABLE II-3. TEST ANOMALY SUMMARY

Table No.	Cell No.	Symptom	Comments
1	3, 32	Excessive current degradation	Refer to Paragraph 1c (1).
	14	Large positive current change	Pre-humidity test connections questionable.
	15, 32	Mechanical change	Small blisters and peeling. Refer to Paragraph 1c (1).
	34	S_iO coating crazed	No change during test.
2	1	Broken cell	Broken after final visual inspection.
	10	Large positive current change	Pre-humidity test connections questionable.
	5	Low current	Cell cracked during pre-humidity test.
	12	Excessive current degradation	Cell cracked during post-humidity electrical test.

APPENDIX III

NIMBUS-D SOLAR ARRAY SUBSTRATE
FABRICATION REPORT

A. INTRODUCTION

The Nimbus-D solar-array substrate fabrication program is divided into six separate phases. The tasks performed during each phase are as follows:

Phase I. - Process Development

- Prepared samples to aquaint the vendor with the test methods and procedures invoked by the RCA Corp.
- Prepared sample lots to establish a production-process technique and define limitations.
- Defined the thermal profile to further clarify the production-process technique.
- Prepared sample coupons during fabrication of destruct platforms and transition to further clarify the production-process technique.

Phase II. - Mold Design and Fabrication

- Prepared a mold design for the fabrication tools of the transition and platform section based on drawings supplied by the RCA Corp.
- Reviewed and approved the mold design (by Structures Engineering Group of the RCA Corp.).
- Fabricated a destruct transition in the mold to verify the design.
- Inspected the destruct transition for dimensional tolerances and evaluated the mold.
- Fabricated a destruct platform in the mold to verify the design.
- Inspected the destruct platform for dimensional tolerances and evaluated the mold.

Phase III. - Fabrication of Destruct Transition and Platform

- Allowed the manufacturing group to pre-fit parts during dry-run layup.
- Formulated the fabrication process.

- Performed final adjustments to the production processing technique as dictated by factual performance during processing of parts.

Phase IV. - Development of a Measurement Technique

- Developed a method of holding and measuring the completed units during the evaluation of the destruct units.
- Determine the measurement criteria.
- Prepared a document to record the measurement data.

Phase V. - Evaluation of Destruct Unit

- Performed a complete dimensional check.
- Performed a flexural strength test using sample coupons, and segments of the destruct panel.
- Performed peel tests.
- Checked the lap-shear samples for tensile strength.
- Joined the transition and platform sections, and measured the torque required to open the platform.
- Determined the useability of the completed assembly when compared to the requirements of the RCA Corp. and General Electric Co. interface drawings.

Phase VI. - Production of Flight Hardware

- Fabricate a flight quality unit and sample coupons from the same materials and process.
- Evaluate the completed units (dimensional and interface) requirements.
- Test the sample coupons.
- On the basis of the forgoing test data, accept or reject the unit.

Phases I through V were completed during the report period and the Goodyear Areospace Corp. (GAC) was authorized to fabricate the first flight unit, serial No. 017 (1756030-501, Platform; and 1756055-501, transition). A detailed discussion of the substrate materials and Phases I through V are contained in this report.

B. SUBSTRATE MATERIALS

The Nimbus-D Solar Array substrate design is based on materials of construction that will yield a lightweight structure having the required structural strength and a combined weight of 21 pounds, maximum. The materials used in construction are as follows:

- Sun side skin. - An aluminum alloy foil (type 5052-H-19) 3.7 mils thick, to which a 2-min film of Teddar is bonded.
- Earth side skin. - An aluminum alloy foil (type 5052-H-19) 3.7 mils thick.
- Honeycomb Core. - An aluminum alloy (type 5052) of the following characteristics

  a. 1/4" cell × 0.001" web, perforated alloy with a density of 2.3
  b. 3/16" cell× 0.001" web, perforated alloy with a density of 3.1
  c. 1/8" cell × 0.001" web, perforated alloy with a density of 4.5
  d. 1/8" cell × 0.002" web, perforated alloy with a density of 8.1

- Adhesive. - The adhesive (American Cyanamid FM-1000) is a modified epoxy-polyamide with unsupported-film characteristics. The specified adhesive film is 6-mils thick with a weight of 0.045 lb. per square foot.
- Primars. - The primars (American Cyanamid BR-1009-8, and 1009-49) are solvent solutions of a polyamide epoxy resin that are used to pre-treat the mating surfaces of the skins.
- Foam. - The foam (American Cyanamid H7-424, Type III) is an unsupported epoxy phenolic-aluminum filled sheet. It is used for splicing sandwich core, inserts, and edging.

C. PROCESS DEVELOPMENT

During the process development phase, considerable time was spend producing sample lots, employing production equipment, and simulated production molds, in an effort to derive data that would lead to an acceptable processing technique. After preparation of a tentative processing specification (GAC-RDB-5342) which encompassed all facets of the process, a final series of samples were made on the production tool. In conjunction with this investigation, a thermal run was performed on the bonding tools to establish handling restraints imposed by the tooling.

Peel test data obtained during evaluation of the samples are shown in Figures III-1 through III-3. A review of the test data indicates that the failure mode is predominantly torn webs (see Figure III-2). This indicates that the adhesive bond-to-skin and core exceeded the strength of the honeycomb webs.

In view of the fact that the Goodyear Aerospace Corp. testing equipment did not have a head speed of 4 inches per minute, it was necessary to change the test conditions specified in RCA specification 1846329 (90 Degree Peel Test, Ultralight Adhesive Bonded Honeycomb Structures). Special tests were then conducted by the RCA Corp. at 2 and 4 inches per second to determine the impact, if any, on the test results or the resultant autographs. Figure III-3 contains the curves and values recorded. The test data and behavior of the samples indicated that a head speed of two inches per minute would be acceptable for the peel test at the Goodyear Aerospace Corp.

Based on the results obtained during the physical testing of the samples produced, an approval of the process specification was given to the Goodyear Aerospace Corp.

D. MOLD DESIGN AND FABRICATION

Based on RCA Corp. drawings 1756030, 1756055, and 1756054, tool designs for the solar platform and transition were completed and approved by the Mechanical Design Group of the RCA Corp. The tools, built in accordance with the specified design, consist of a one-inch jig plate base to which was bolted a picture frame conforming to the platform outline. The critical portions of the mold are the flatness and the hinge holding bar. Upon completion, the molds were inspected and approved by both GAC and the RCA Corp.

In compliance with the program plan, a destruct unit of each type was produced using the tooling, process specifications, and specified materials. Dimensional checks of the fabricated transition section disclosed that the part would not meet specified tolerances. A recheck of the tooling was done using an optical system which pinpointed three deviations from the tool design drawings. The deviations were as follows:

- The baseplate of the tool was warped,
- the hinge line bar was warped, and
- the hinge knuckles were not within the specified tolerances.

Based on these findings it was necessary to redesign and rework the existing molds.

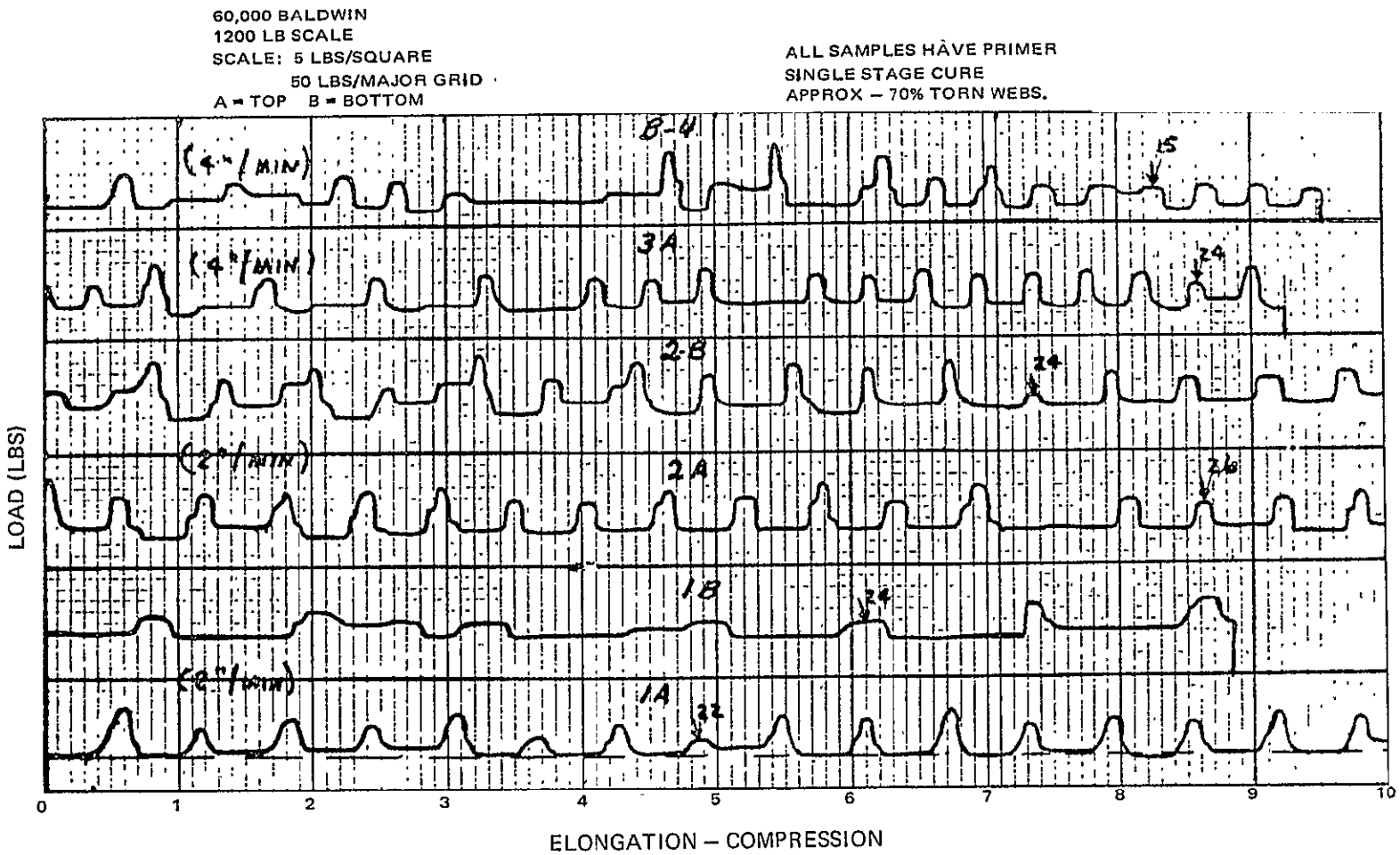

Figure III-1. Peel Test Data, Process Verification, Lot No. 1 (Sheet 1 of 2)

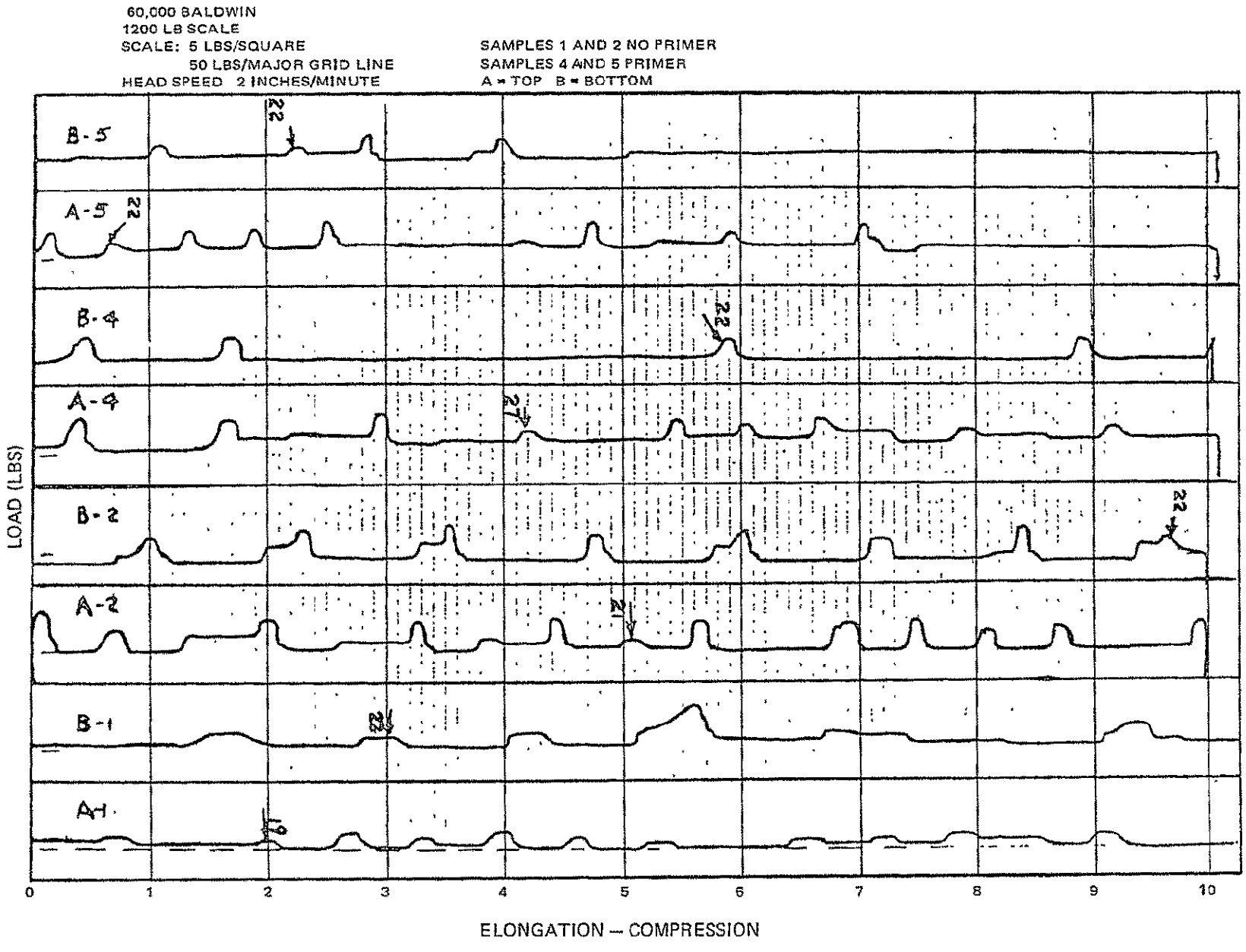

Figure III-1. Peel Test Data, Process Verification, Lot No. 1 (Sheet 2 of 2)

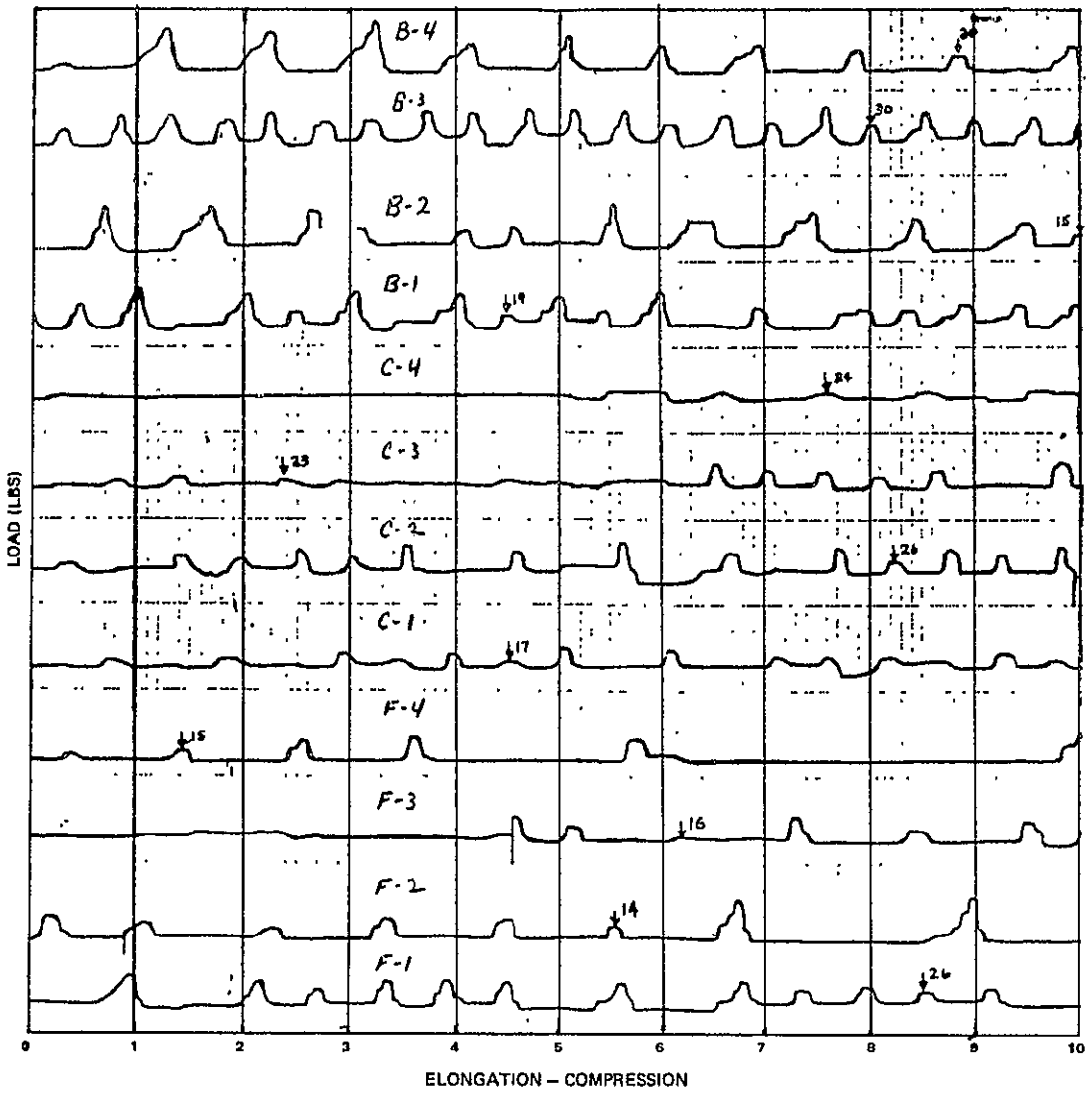

60,000 BALDWIN
1200 SCALE
600 RANGE
2"/MIN HEAD SPEED
SCALE 5-LBS/SQ
50 LBS/MAJOR GRID LINES
GOODYEAR AERO SPACE CORP
FABRICATION PROCESS RDB 5342

LEGEND
F – FRONT OF OVEN
C – CENTER OF OVEN
B – BACK OF OVEN
EVEN NO. MOLD SIDE
ODD NO TOP SIDE

RESULTS

SAMPLE	% TORN WEBS	VALUE
F-1	>95	26
F-2	>95	14
F-3	>95	16
F-4	>95	15
C-1	>95	17
C-2	>95	26
C-3	>95	23
C-4	>95	24
B-1	>95	19
B-2	>95	15
B-3	>95	30*
B-4	>95	20

Figure III-2. Peel Test Data Process Verification, Lot No. 2

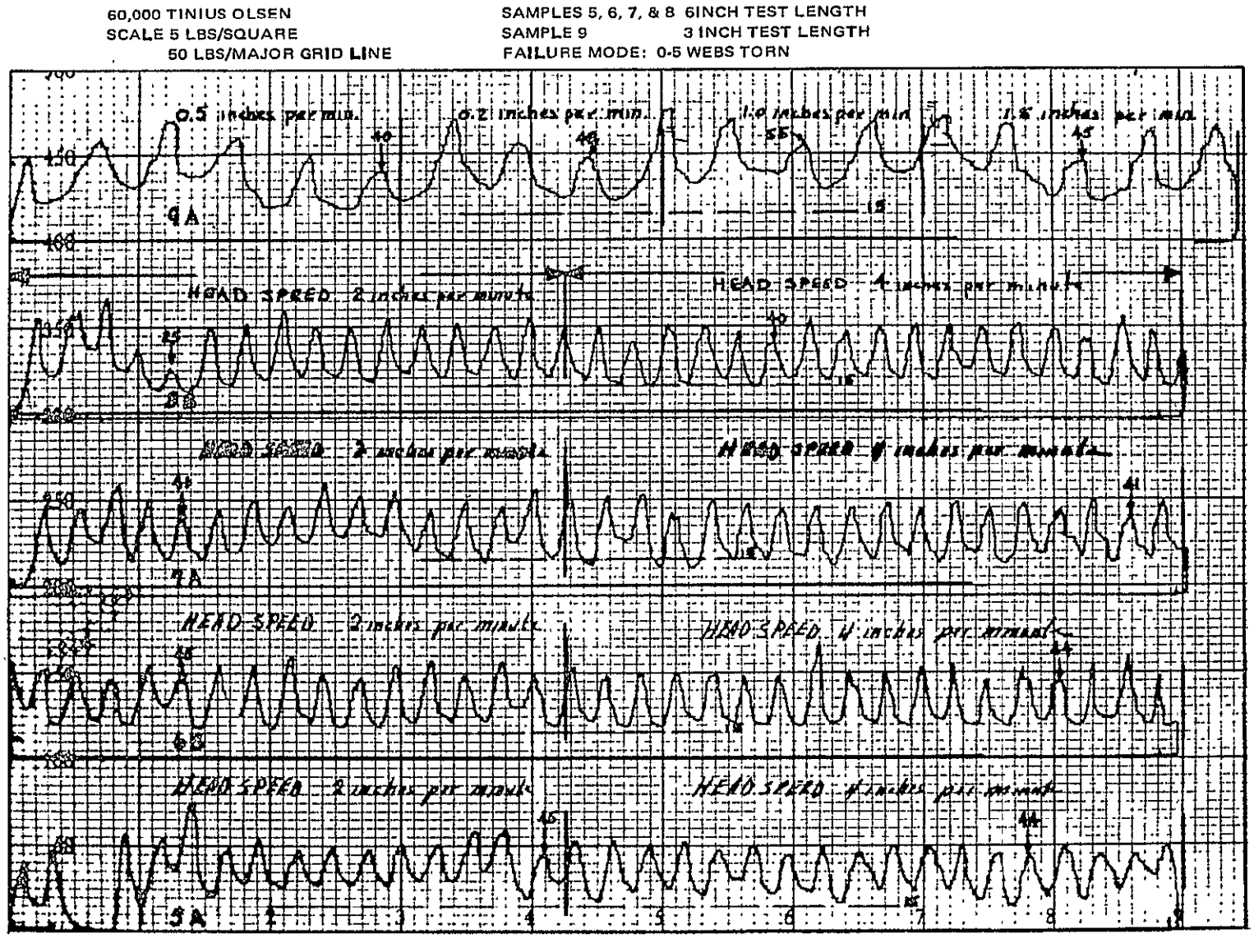

Figure III-3. Peel Test Data, Process Verification at the RCA Corp.

The rework consisted of the following operations:

- Mold Plate. - Bolting an egg-crate-type re-enforcing member onto the bottom of the mold plate.
- Hinge Bar. - The bow was reduced to approximately 60 mils by mechanical means. This action and torquing the bolts to a definate value insured flatness during molding operations.
- Hinge Holders. - The hinge holders were worked by straightening, machining, welding on new holding knuckles, redrilling and re-pinning onto the holding bar. In conjunction with this, the individual knuckles were manipulated to bring the hinge line to within the required tolerance.

At the completion of rework, the tool was checked for compliance to dimensional tolerances and the tool was found to be acceptable for use. The tool was then exposed to one thermal cycle identical to that specified for a normal cure cycle. A second dimensional check was run and the tools were released for use to build the destruct platform and flight transitions.

A documented method, including the type of measuring equipment, was prepared by GAC and is on record in their Tool Inspection Department. End and side views of the transition and platform molds are shown in Figures III-4 and III-5, respectively.

E. FABRICATION OF DESTRUCT UNITS

1. Transition

The destruct transition was assembled and bonded in the original transition tool with lay-ups, bonding, cure, and final fitting done in accordance with RCA 1750081 and GAC-RBD-5342. During the various stages of manufacture, the detailed processing operations were documented in a log book assigned to the unit.

2. Platform.

The destruct platform was assembled and bonded in the reworked platform tool with lay-up, bonding, cure and final fitting done in accordance with RCA 1750081 and GAC-RBD-5342. During the various stages of manufacture, the detailed processing operations were documented in a log book assigned to the unit.

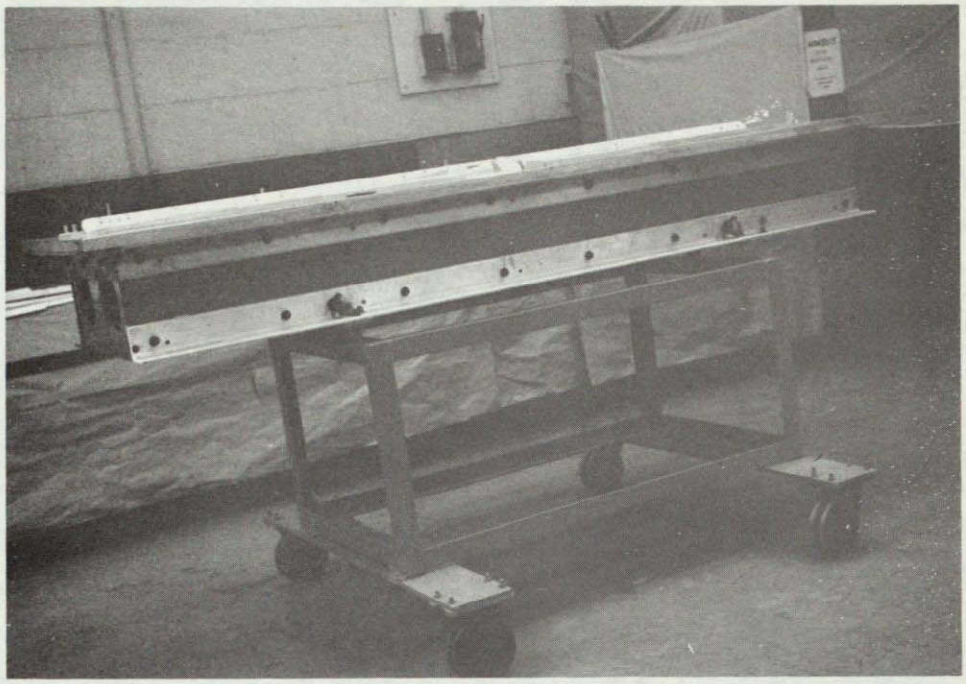

A. Side View

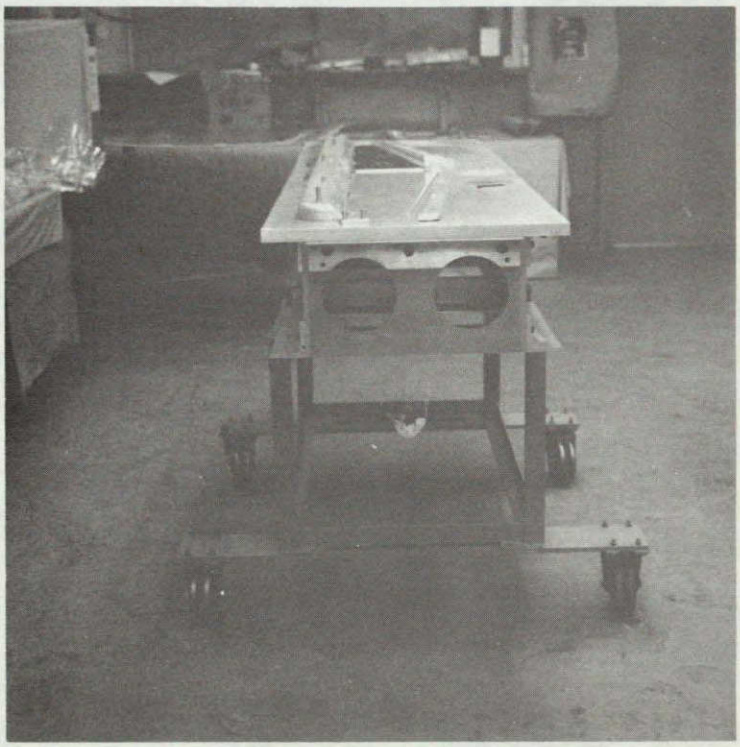

B. End View

Figure III-4. Transition Mold (RCA Dwg. 1756055-501, -502)

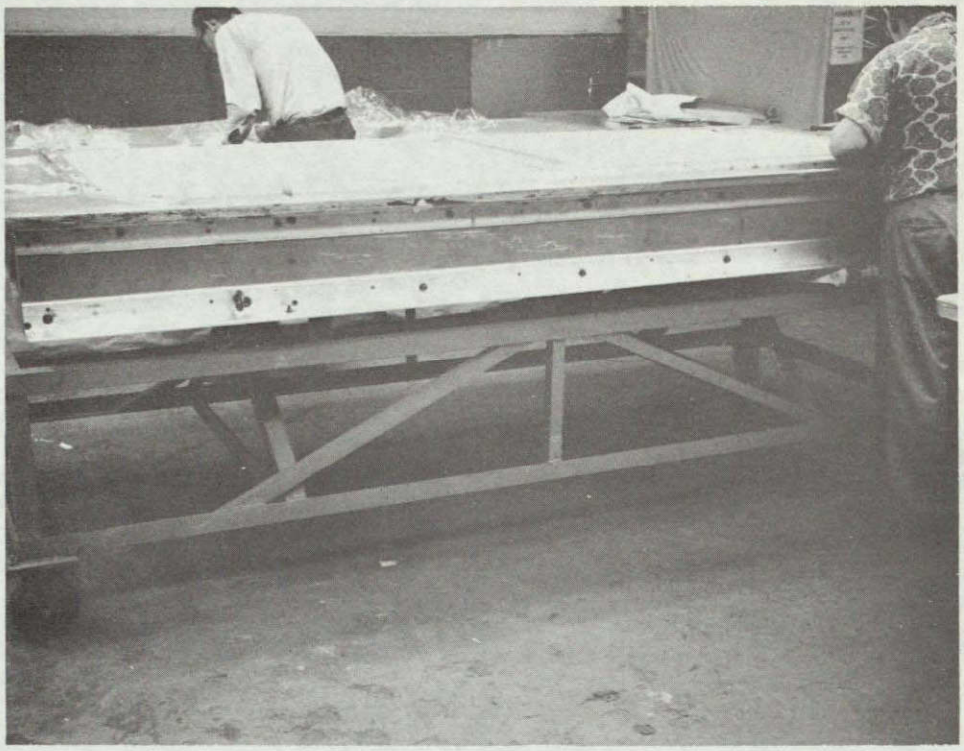

A. Side View

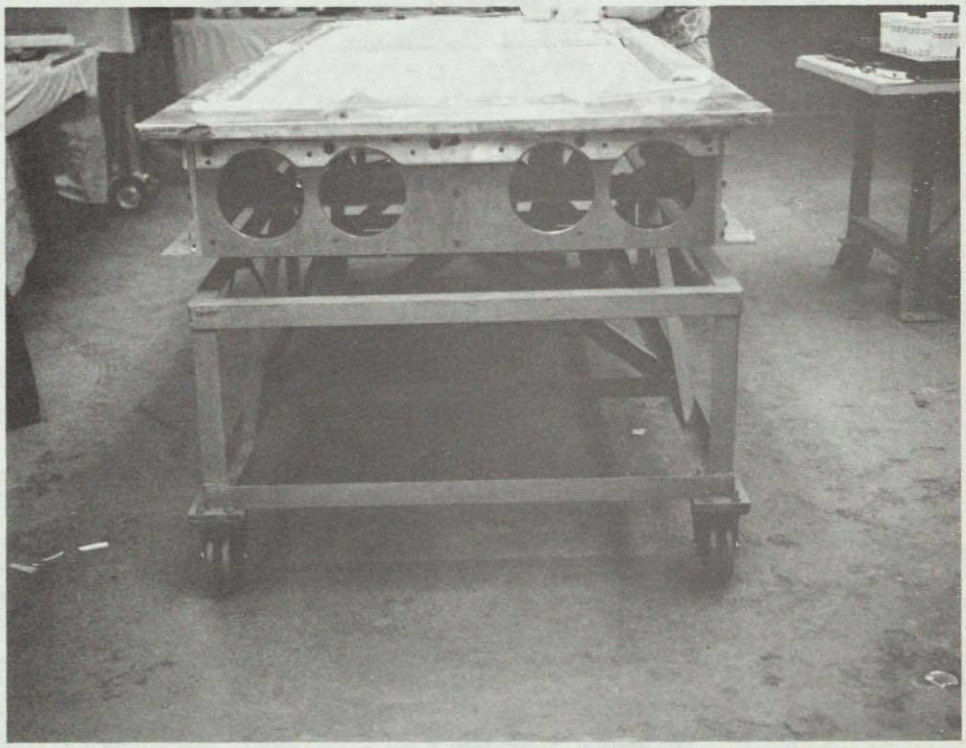

B. End View

Figure III-5. Platform Mold (RCA Dwg. 1756030-501, -502)

3. Detailed Parts

All detail parts and subassemblies were of flight level quality with the exception of the Hinge-transition toggle latch (RCA Dwg. -1756045). The discrepancy of this part was dimensional in an area that had no effect upon any mating surface employed during the bonding cycle.

During the dry run lay-ups and the actual lay-up it became necessary to alter many of the part drawings and the completed piece parts due to interference fits. In general there had been insufficient clearance left between the mating parts to accommodate the FM-1000 adhesive or the HT-424 foam adhesive. Since this is one of the functions served by the destruct unit concept, it was possible to have the balance of the parts for the flight unit reworked prior to fabrication, thus preventing schedule interference once the building cycle was initiated.

4. Documentation

Another function of building a destruct unit is to permit the updating of proposed, planning, processing techniques, and detailed processes, to reflect the actual conditions required. In this way, all documentation reflects true conditions and can be employed in the building of the flight units.

5. Cure Cycles

The most critical portion of the building cycle is the processing of the FM-1000, and H-T-424 adhesive during the assembly of the basic honey comb structure. To attain the maximum strength from the adhesive system, certain restraints on the processing was defined and monitored with great care. This cure cycle is divided into three parts, namely,

- Heat-up and cure temperatures
- Cure period, and
- Cooling cycle.

The recommended cure cycle is shown in Figure III-6.

a. Heat-up Stage and Cure Temperature

The recommended heat-up rate for the FM-1000 adhesive is shown on Figure III-7. Note that the vendor permits wide tolerance on the heat-up time. However, it is generally felt by the honey comb handling industry that it is better

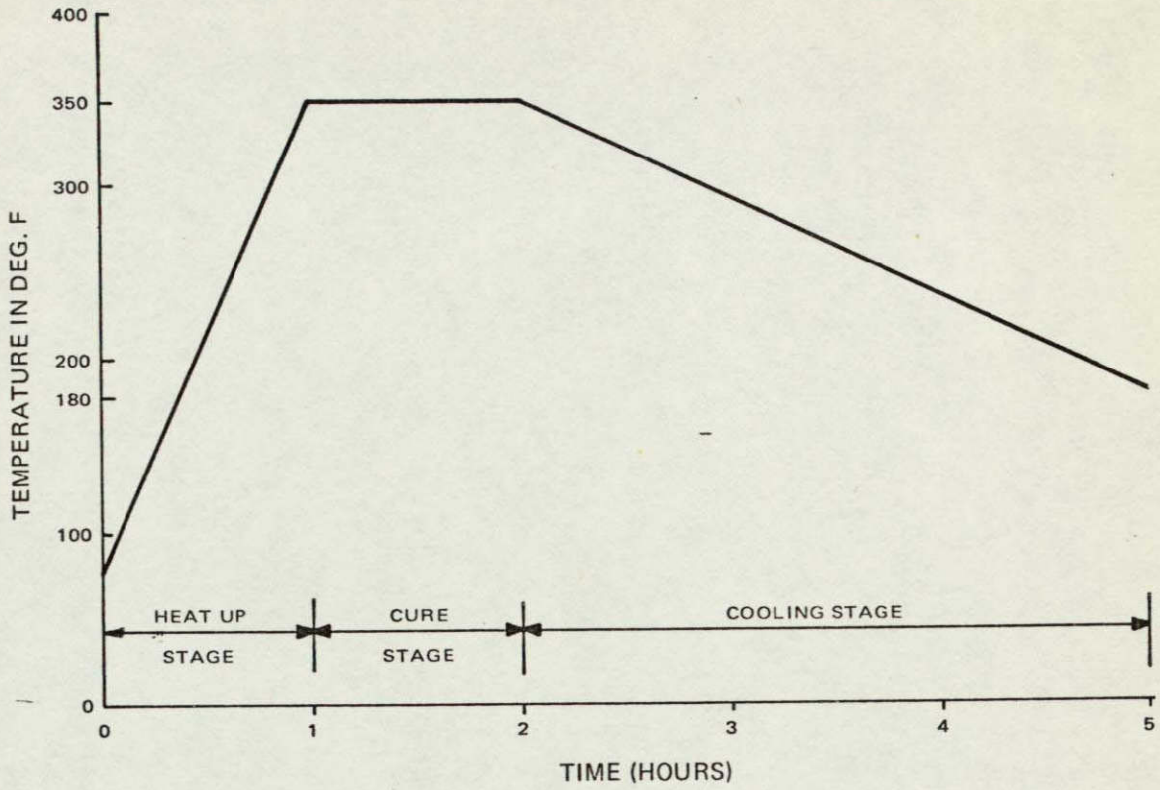

Figure III-6. Recommended Cure Cycle for FM-1000 Adhesive

to adhere to the preferred heat-up zone shown on the triangle. In brief it is to the fabricators benefit to attain the softening point of the "B" staged adhesive as quickly as possible so that wetting of the surfaces and filler forming is completed at the lowest viscosity prior to the rapid polymerization of the modified polyamide-epoxy system. Figures III-8 and III-9 shows the heat-up cycles for the destruct platform using the reworked tooling.

b. Cure Stages

The RCA Corp. employs a two-stage bonding technique when fabricating a honey comb structure containing inserts or sheet metal parts. The adhesive vendor recommends a cure of 1 hour at 350 ±-10°F. When the RCA Corp. two-stage bonding technique is used, the cure time and temperature are modified as follows:

	Temp	Time
First Cure	330-350°F	45 ±5 min
Second Cure	340-350°F	55 ±5 min

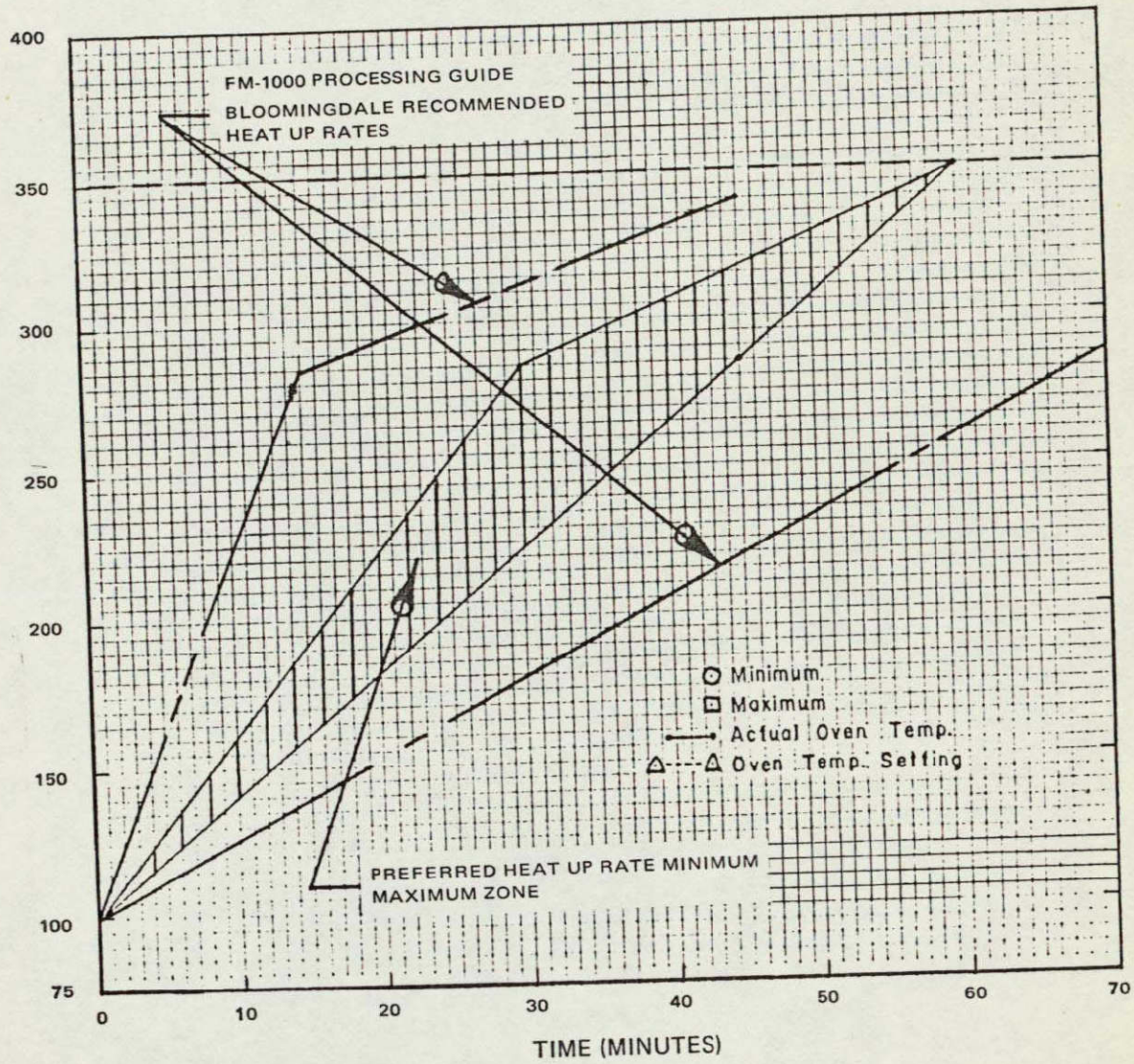

Figure III-7. Recommended and Preferred Heat-Up Rates for FM-1000 Adhesive

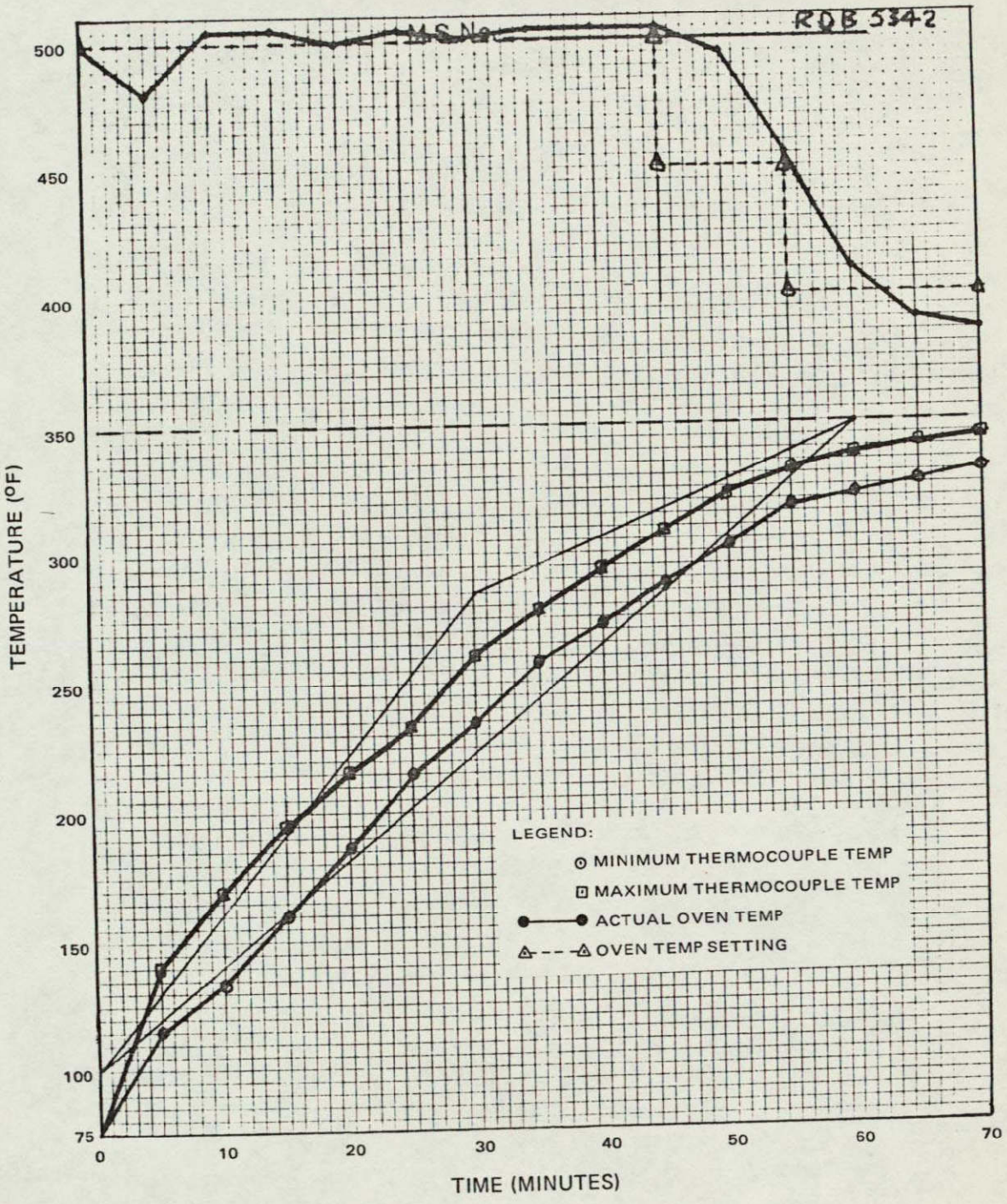

Figure III-8. Destruct Unit Heat-Up Rate, First Cure

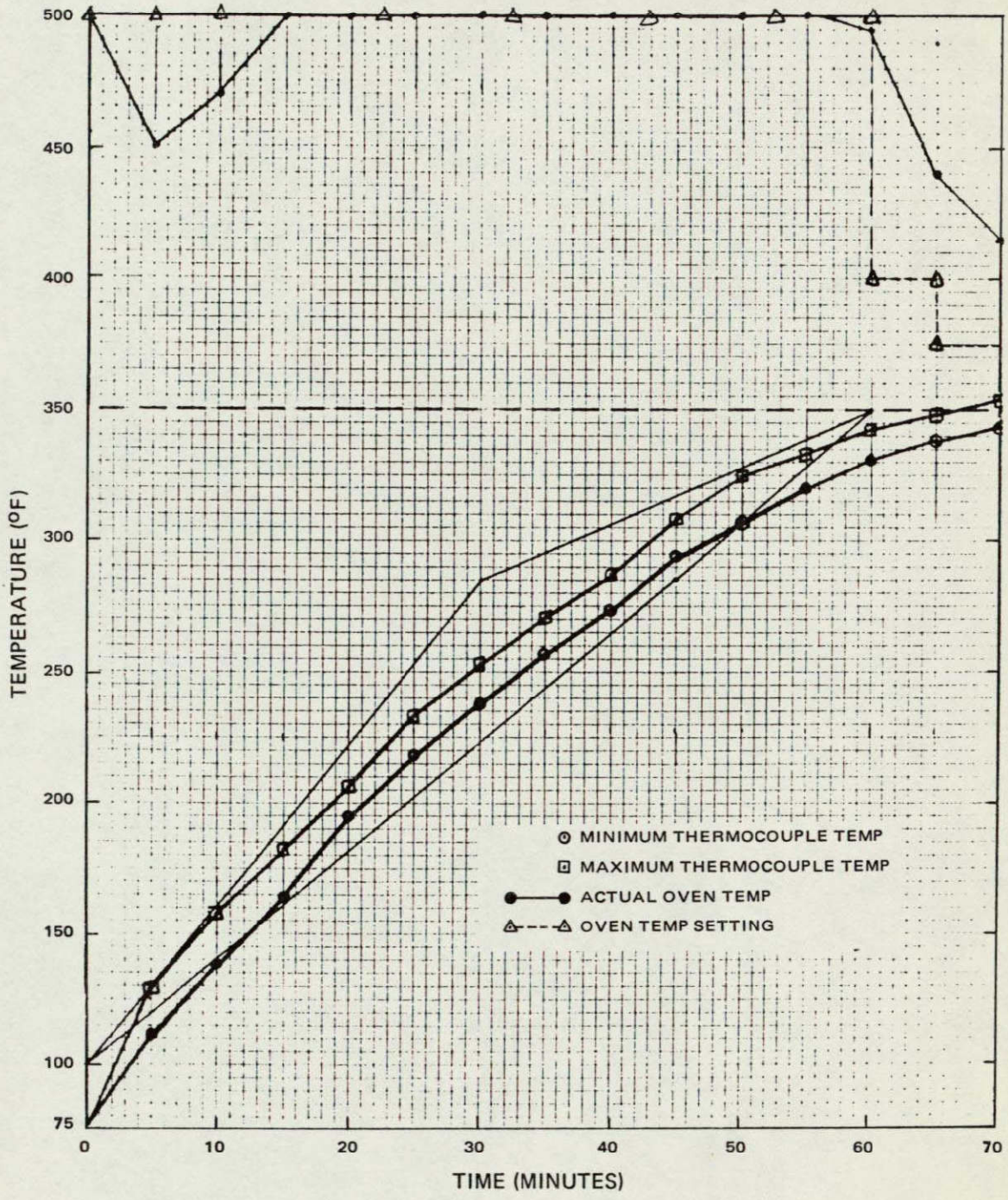

Figure III-9. Destruct Unit Heat-Up Rate, Second Cure

c. Cooling Stage

The critical parameters of this stage are as follows:

- maintain the pressure on the bonded assembly until the temperature of the bond reaches 180°F,
- maintain a uniform temperature on both sides of the honey comb structure during the cooling cycle.

The pressure requirement is necessary as the heat distortion temperature (HDT) of this adhesive system is 180°F. Therefore, the pressure of the bond line must be maintained until the lowest thermocouple reaches 180°F. The uniform temperature requirement is required to prevent uneven stresses upon the assembly due to thermal coefficients of expansion caused by a non-uniform cooling profile.

F. DEVELOPMENT OF MEASUREMENT TECHNIQUES

1. General

Due to the flexible nature of the completed platform and transition, which has a definite bearing upon the ability to reproduce dimensional check values, it was necessary to develop a measuring system and technique. The basic problem was to develop a holding method which would permit the unit being measured to assume its normal contour with no effect from its own weight and not restrict the unit in any way. The platform presented the greatest problem since even a draft through a doorway can cause it to deflect in the order of a few mils. The holding fixtures and test equipment used to obtain the dimensional data are shown on Figures III-10 through III-12.

It was necessary to employ physical and optical instruments to obtain the required data. Figures III-11 and III-12 show the type of instruments utilized during the dimensional check.

In Figure III-12, the electronic gauge shown was utilized to detect if the setting of the platform was affected in any way. This was necessary since the measurement of the hinge line required reading of the hinge line to a tolerance of ±4 mils at the end of the platform.

2. Documentation

During the initial efforts to obtain the required dimensional data, a formal document was prepared for the expressed purpose of recording the dimensional data. This document, Inspection Dwg., Solar Platform, is designated as RCA Dwg. No. 1976408.

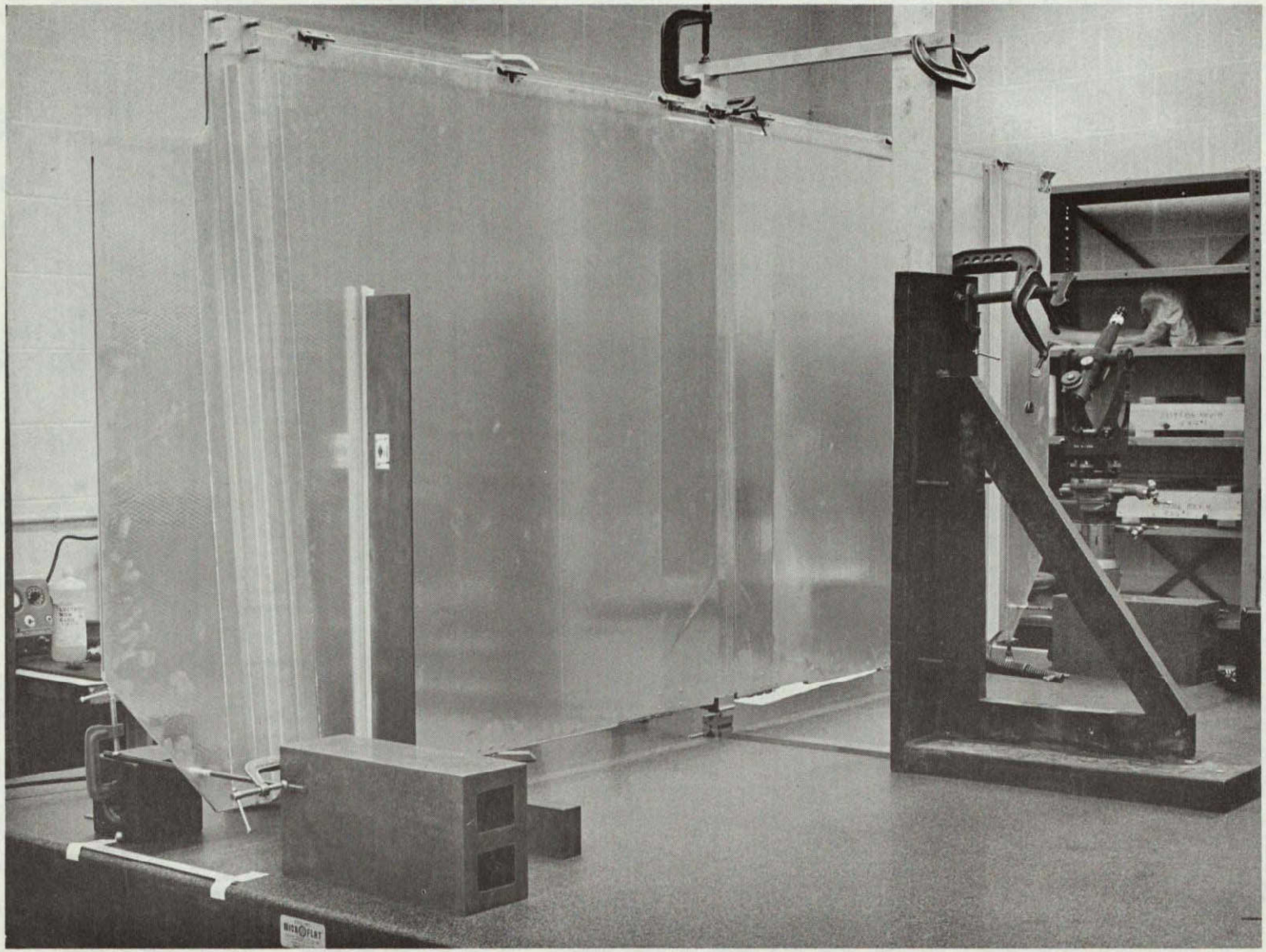

Figure III-10. Holding Ficture for Dimensional Check, Earth Side Shown

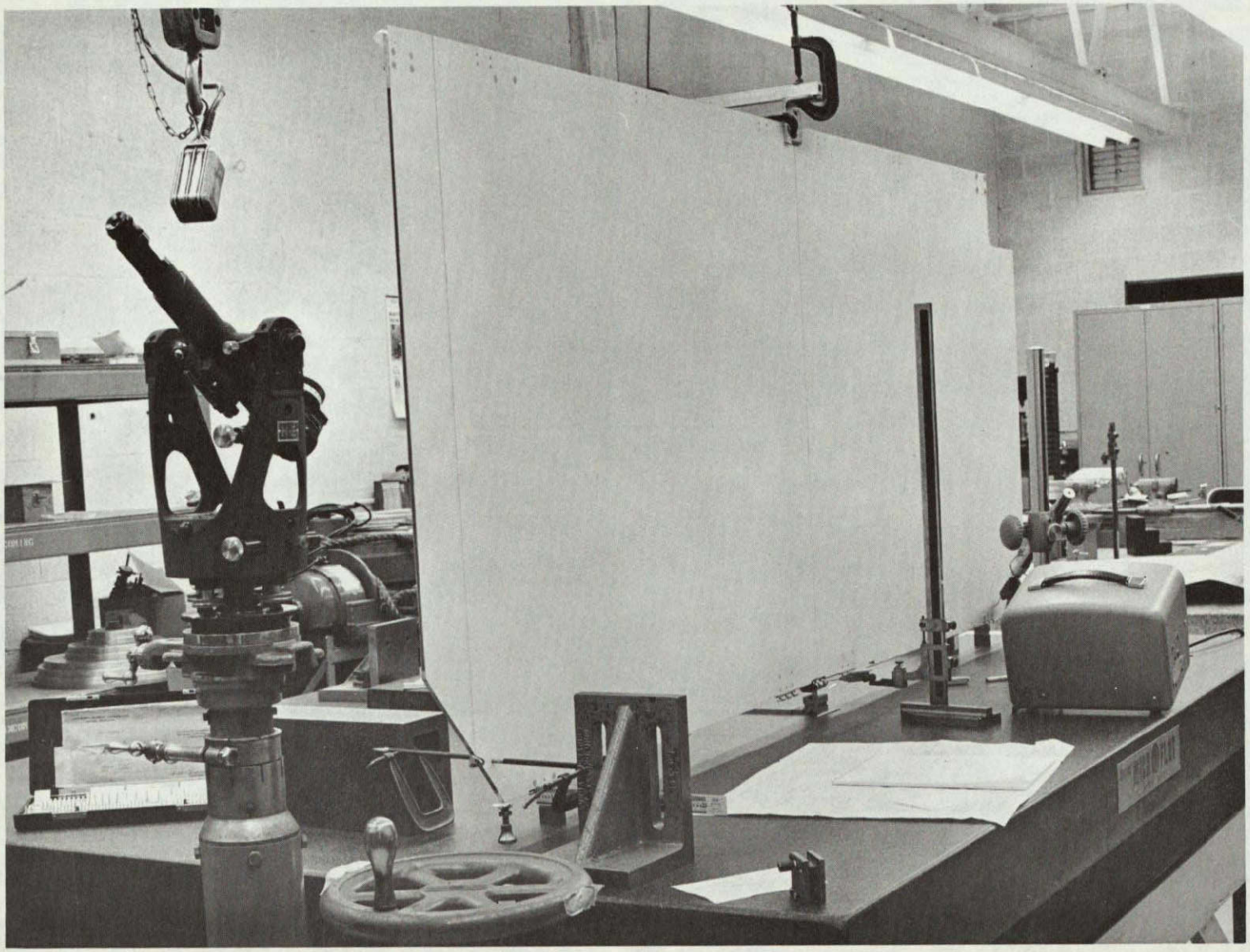

Figure III-11. Holding Ficture and Optical Instrumentation for Dimensional Check, Sun Side Shown

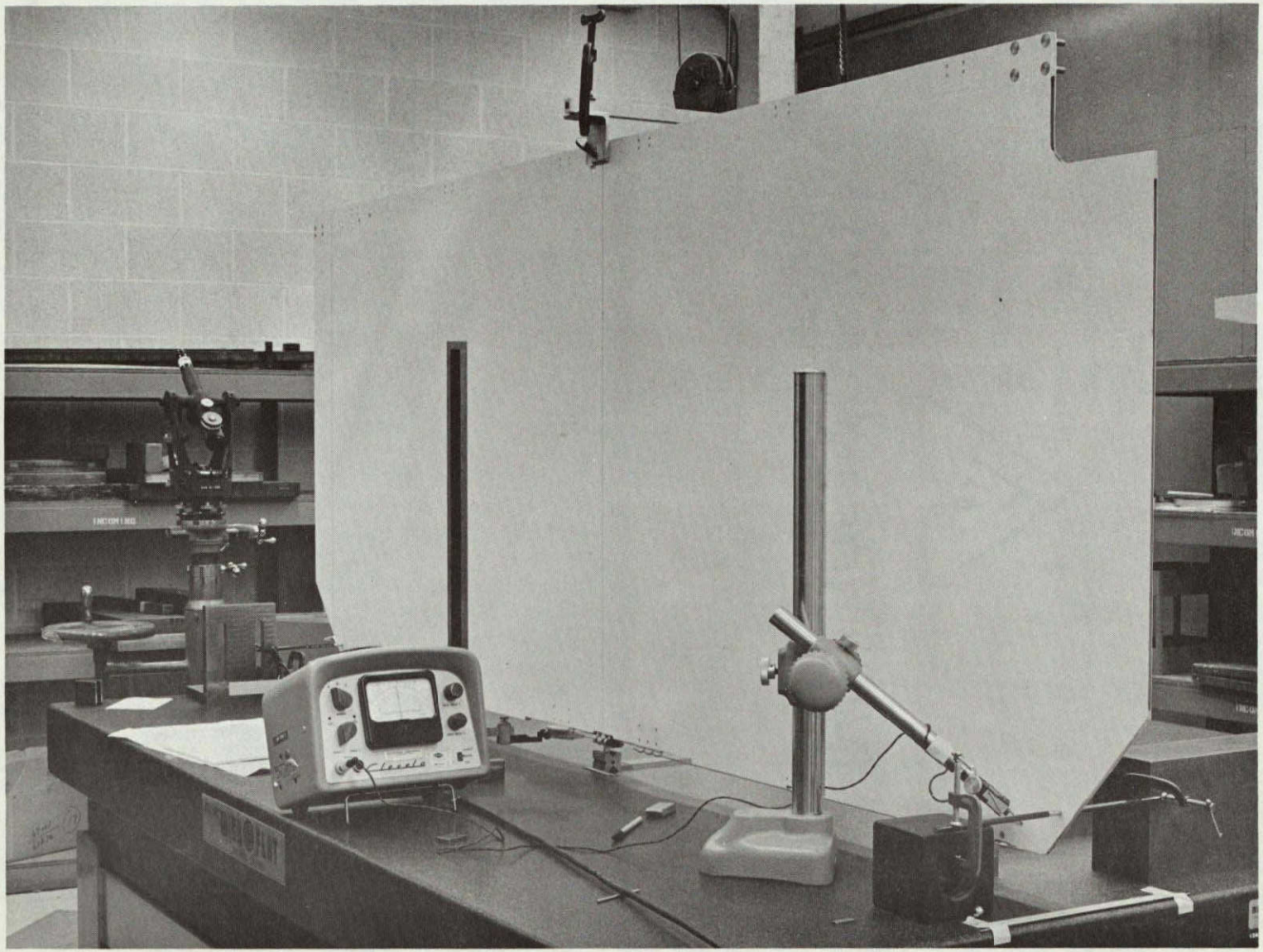

Figure III-12. Holding Ficture and Electronic Instrumentation, For Dimensional Check, Sun Side Shown

G. EVALUATION OF DESTRUCT UNIT

The evaluation of the destruct unit requires the analysis of all measurable properties, documented control data, recorded dimensional data and the ability to comply with the requirements of the RCA Specification 1750081. Test data was obtained from segments of the destruct panel (see Figure 13); and sample coupons and lap shear specimens prepared simultaneously with the destruct unit.

1. Flexural Strength Test

The flexural strength was determined by a test method specified in Mil-Std-401. Figure III-14 shows the dimensions of the sample and test set up. The required value for this test is 30 pounds per inch of width. All samples tested from the destruct unit exceeded this minimum value. Test data is contained in Table III-2.

2. Lap Shear Strength Test

There are four lap shear specimens processed for each bonding operation of the platform. The precise steps are the first bond of honey comb, the second bond of honey comb, and bonding of the structural bar channels onto the solar array platform. All cleaning, priming and curing is identical with those used on the units being produced. All lap shear values exceeded the minimum value of 1000 PSI. Test data are listed in Table III-1.

TABLE III-1. DESTRUCT UNIT LAP-SHEAR TEST DATA

Cure	Sample No.						
	1	2	3	4	High	Lo	Avg
No. 1	6250	6135	6025	6040	6250	6025	6112
No. 2	6055	6092	6358	6553	6553	6055	6264

3. Peel Strength Tests

The peel test involves the action of separating a face sheet of the honey comb sandwich from the honey comb itself. The method used is a 90 degree peel test performed in accordance with RCA Dwg. 1846329 (90° Peel Test-Ultralight Adhesive Bonded Honey comb Sandwiches). Acceptance test criteria are shown in Figure III-15; test data are listed in Table III-2.

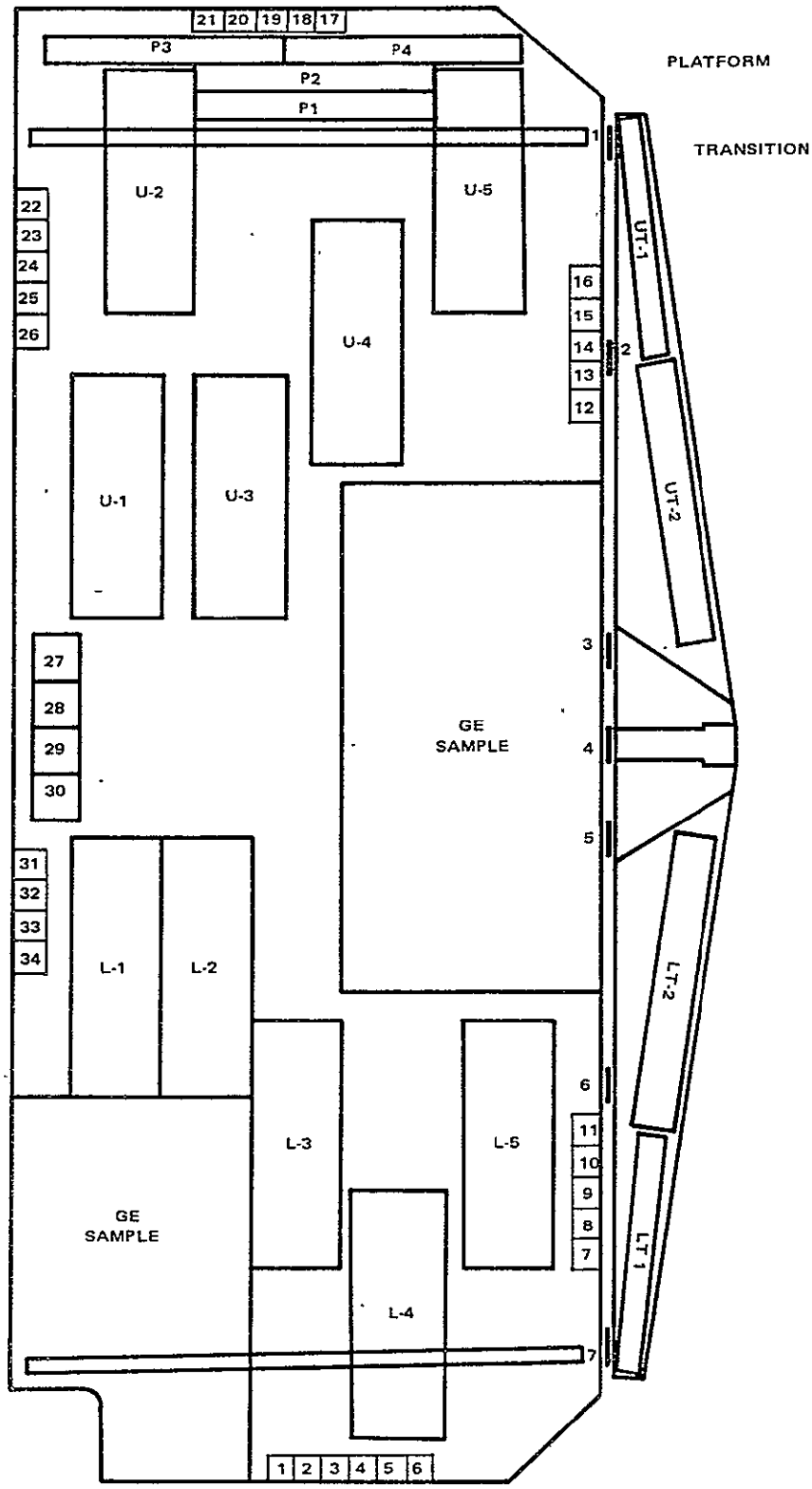

Figure III-13. Destruct Panel, Sample Test Pattern

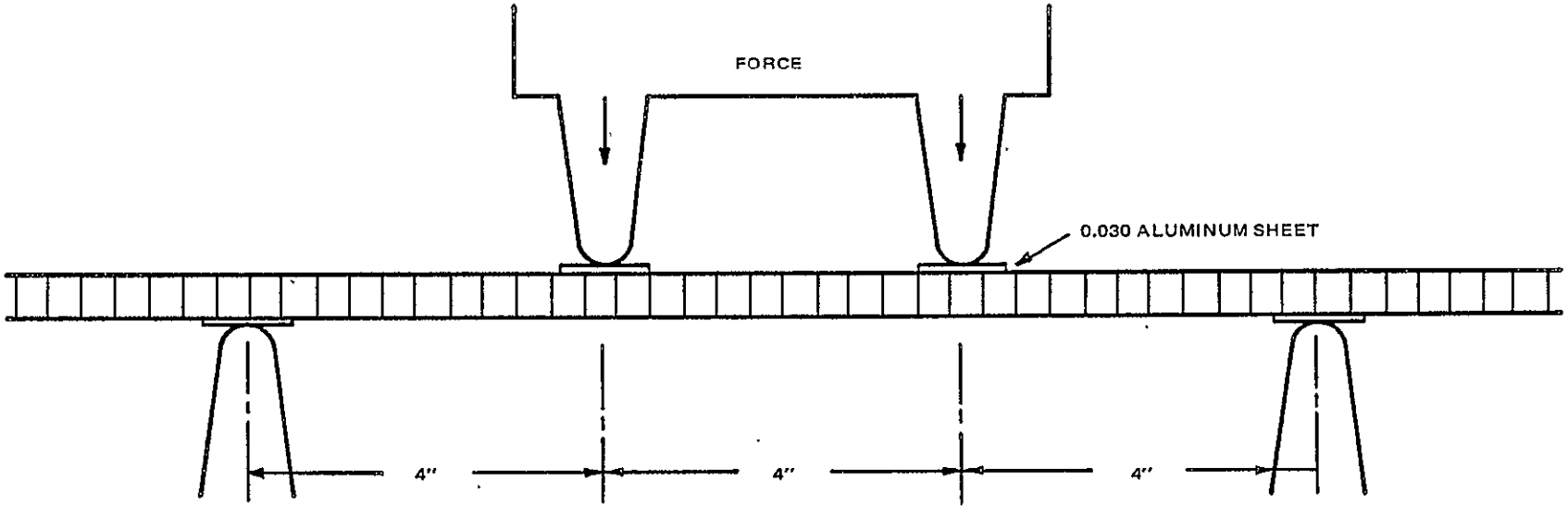

$$\text{VALUE/INCH WIDTH} = \frac{\frac{F}{2} \times 4 \text{ MOMENT ARM}}{3 \text{ WIDTH}}$$

Figure III-14.. Flexure Test Setup

TABLE III-2. DESTRUCT UNIT PEEL TEST DATA

Test	Destruct Platform Sample									Destruct Trans. Sample		Platform Sample Coupon		Transition Sample Coupon	
	U-1	U-2	U-3	U-4	U-5	L-1	L-2	L-3	L-4	UT-2*	LT-2*	3 FB	4 BM	†	†
90° PEEL TEST															
Pull Force															
Sun Side (lbs)	29	23	17	20	20	31	20	20	45	37	15	30	40	38	30
Earth Side (lbs)	29	25	24	25	25	21	21	25	20	37	20	45	38	20	17
Torn Webs															
Sun Side (No.)	6	23	9	9	9	6	29	29	12	0	0	0	0	0	0
Earth Side (No.)	43	43	43	43	43	43	43	43	43	0	0	12	13	0	0
Sun Side (%)	10	40	15	15	15	10	50	50	20	0	0	0	0	0	0
Earth Side (%)	75	75	75	75	75	75	75	75	75	0	0	20.6	22.3	0	0
Flexure															
Sun Side (lbs)	102			81	68		106		81	90		120	117		98
Earth Side (lbs)		62	117			118		83			82			104	
Value/Inch Width*															
Sun Side (psi)	68			66.6	44		70.6		53	60		80			65.3
Mold Side (psi)		41.3	77.3			78.6		54.6			54.6		78	69.3	

Legend:

U - Sample taken from upper section of destruct platform
L - Sample taken from lower section of destruct platform
UT - Sample taken from upper section of destruct transition
LT - Sample taken from lower section of destruct transition
P - Sample taken from platform test coupon
T - Sample taken from transition test coupon

*See Figure III-14.

†Destruct transition completed prior to rework of transition mold.

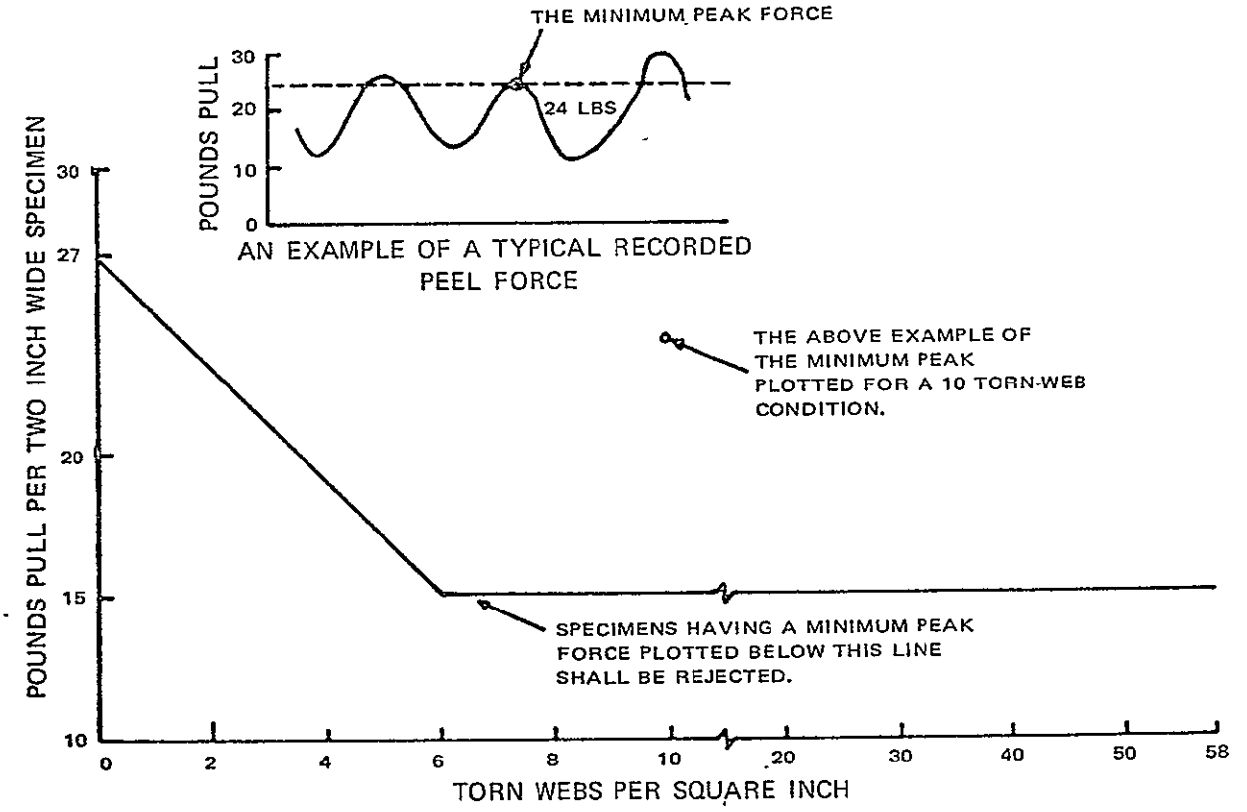

Figure III-15. Peel Test Requirements

a. Platform Tests

All samples cut from the platform exceeded the acceptance value. However, the peel sample from the test coupon failed on one skin. After an investigation at the time, it was determined that an operator cut skins from an uncleaned skin and used them on the test coupon (bag side). In all cases, the mode of failure was at the junction of the adhesive and the honey comb web.

b. Transition Tests

The test data obtained from the transition and the representative test coupon showed that three of the four requirements (refer to Table III-2) were below the acceptance limits shown on Figure III-15.

The data obtained from this unit was used to modify the processing technique and the molds. As background information it should be noted that these samples were

were produced on the original mold prior to the rework and were not representative of the final processing technique.

4. Dimensional Test Data

a. Platform Data

The destruct platform was dimensionally checked in compliance with methods described in para. F. There are two categories of measurements namely, general overall dimensions and interface dimensions.

The majority of the dimensions in the first category were either within the specified tolerance or within 10 mils of the specified values. After a review of the parts, the requirements, and the dimensions, it was determined that the unit was acceptable. The discrepancies were reviewed by the RCA Corp. Material Review Board (MRB). The critical dimensions in the second group are the hinge line (vertical and horizontal), latch line, and flatness. Test results are listed in Table III-3.

TABLE III-3. INTERFACE DIMENSION TEST RESULTS

Parameters	Specified (in)	Measured Values (in)	
		Platform	Transition
Hinge Line (Vert.)	±0.004	0.095	0.011
Hinge Line (Hor.)	±0.004	0.0118	0.026
Flatness (Hinge Line)	0.030 TIR*	0.095	0.132
Flatness (Latch Line)	0.030 TIR*	0.106	—
*Total Indicator Run-out.			

Although these values deviated from the specified values, it was found during subsequent tests that the unit could be used without penalty for the intended application. During discussions with General Electric Co. representatives, it was determined that the unit could function within the limits of the G.E. Co. interface requirements.

b. Transition Data

The destruct transition wad dimensionally checked in compliance with methods described in para. F. Here again, there are the two categories of measurements namely, general overall and interface dimensions.

A majority of the dimensions in the first category were within the specified tolerances or within 10 mils of the specified values. After a review of the parts, requirements, and the dimensions, it was determined that the unit was acceptable. The discrepancies were reviewed by an RCA-Corp. Material Review Board. The critical dimensions of the transition section, the specified values, and the measured results are listed in Table III-3.

As in the case of the platform, it was found during subsequent tests that the unit could be used without penalty for the intended application.

c. Destruct Unit Dimensional Data

Detailed dimensional data for the destruct unit is contained in Figure III-16.

5. Torque Measurement Data

In this test the hinge lines of the platform and transition are joined and pinned in accordance with the applicable drawing. The test determines the force required to rotate the platform from the normal launch position to the deployed position. Deployment requires the platform to move through an arc of 135° while the transition is in a stationary position (See Figure III-17). The torque required to move the platform from the folded (launch position) to the deployed position shall not exceed 18-inch lbs of torque. The starting torque obtained in four tests and the average running torque are listed in Table III-4. In addition to the four torque tests, the starting and running torque at seven angular settings are listed in Table III-5.

The torque test data indicates that the destruct unit (platform and transition) fulfills the interface specification requirements. A review of the dimensional test results indicated a bow condition that could effect the torque test. The low value of torque measured when the two section were pinned to a common hinge line is attributed to the inherent flexability of the structure. The maximum measured value was 7.1 inch-lbs, less than 30 percent of the value ($<$18 inch-lbs) specified in specification 1750081.

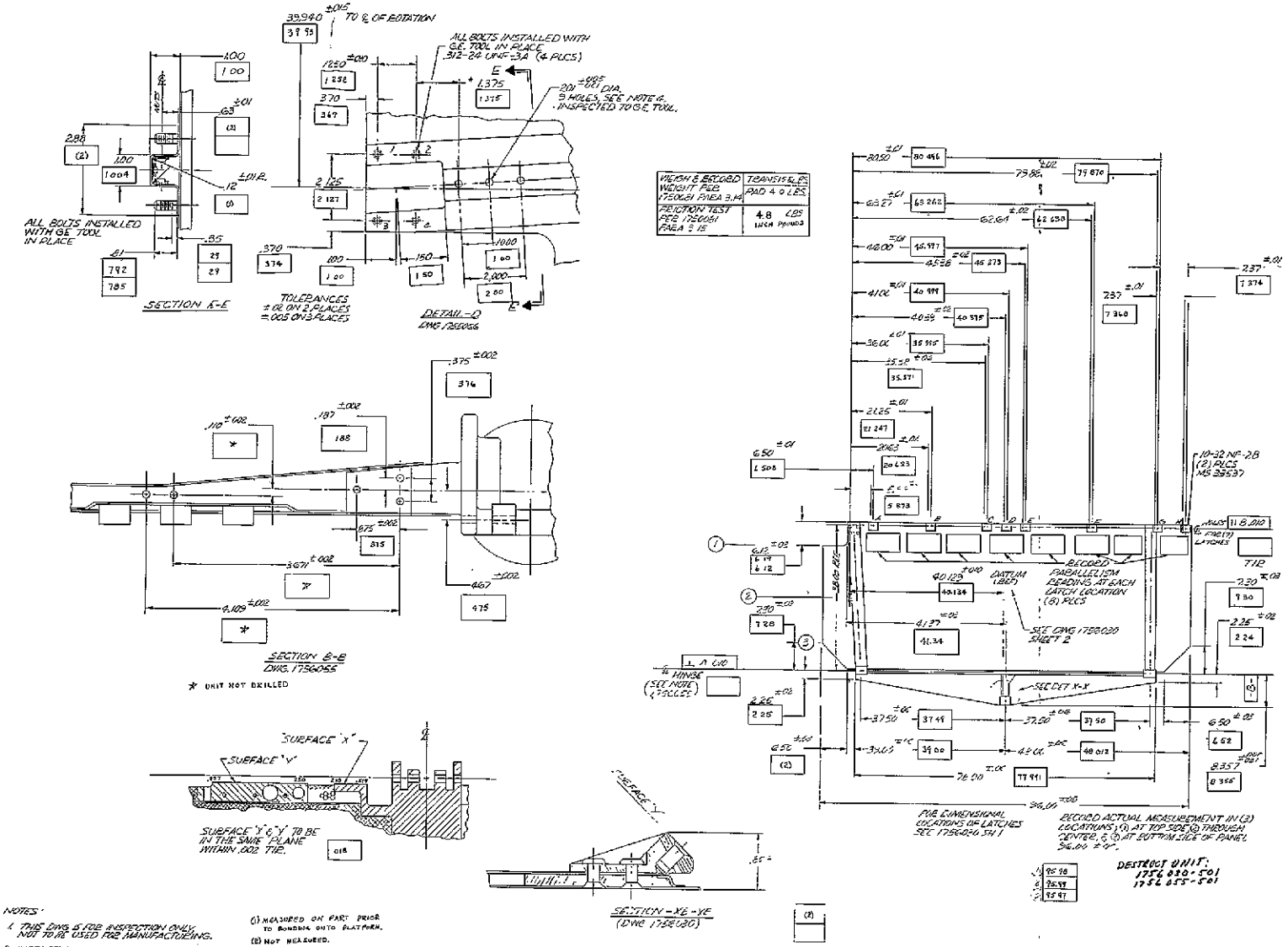

Figure III-16. Destruct Unit Dimensional Test Data (Sheet 1 of 3)

Fold Out

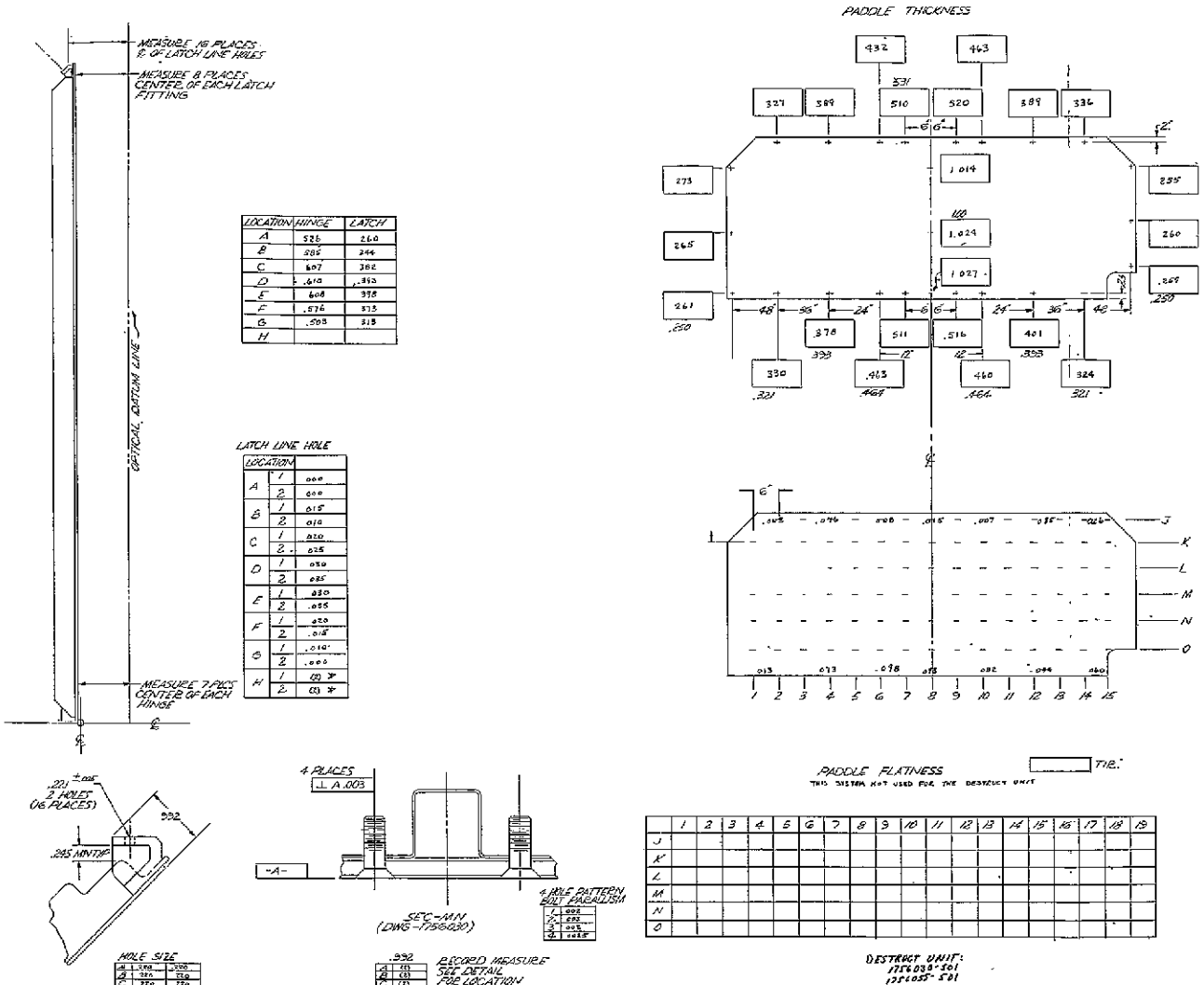

Fold Out

a

Figure III-16. Destruct Unit Dimensional Test Data (Sheet 2 of 3)

B

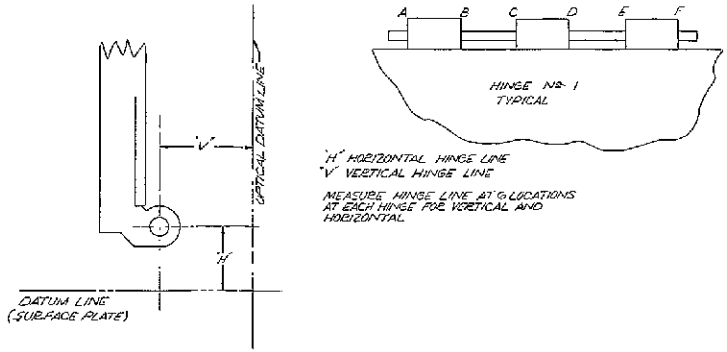

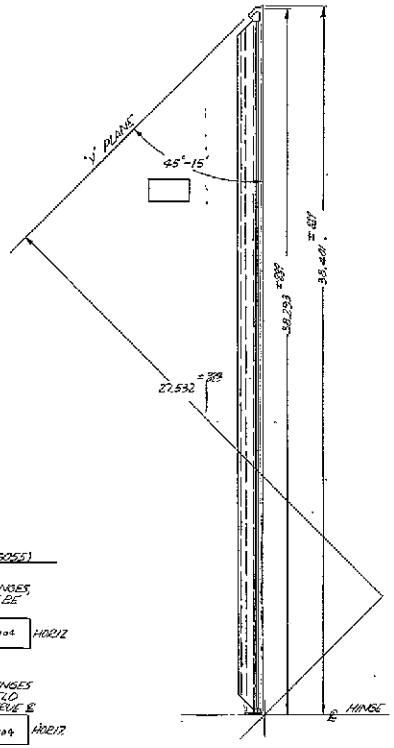

PADDLE

HINGE NO.	POSITION	VERTICAL	HORIZONTAL
	A	.256	.000
	B	.260	- .001
	C	.264	- .0019
	D	.266	- .0016
	E	.270	-.0016
	F	.274	- .0016
	A	.329	- .0004
2	B	.331	- .0004
	C	.335	- .0003
	D	.339	-.0001
	E	.341	- .0003
	F	.343	- .0007
	A	.361	- .0033
	B	.361	- .0030
3	C	.361	-.0025
	D	.360	- .0030
	E	.358	- .0035
	F	.362	- .0026
	A	.359	.000
	B	.358	+ .0001
4	C	.360	.000
	D	.360	.000
	E	.362	.000
	F	.363	+ .0015
	A	.346	- .0011
	B	.361	- .002
5	C	.360	- .0024
	D	.360	- .0027
	E	.358	- .0030
	F	.357	- .0037
	A	.331	+ .0011
	B	.333	+ .0009
6	C	.331	+ .0009
	D	.328	+ .0004
	E	.325	+ .0002
	F	.324	- .0002
	A	.271	- .0013
	B	.269	- .0019
7	C	.266	- .0019
	D	.268	- .0017
	E	.261	- .0015
	F	.259	- .0016

TRANSITION **

HINGE NO.	POSITION	VERTICAL	HORIZONTAL
	A		
	B		
1	C		
	D		
	E		
	F		
	A		
	B		
2	C		
	D		
	E		
	F		
	A		
	B		
3	C		
	D		
	E		
	F		
	A		
	B		
4	C		
	D		
	E		
	F		
	A		
	B		
5	C		
	D		
	E		
	F		
	A		
	B		
6	C		
	D		
	E		
	F		
	A		
	B		
7	C		
	D		
	E		
	F		

** DETAIL DATA NOT AVAILABLE
ONLY OVERALL DATA-SEE CHART.

PADDLE (1756020)

NOTE 3:
CENTERLINE (3 PER PADDLE) ITEMS 72, 73 & 74 MUST BE CONCURRENT WITHIN ± .002
.0025 VERT & .006 HORIZ

NOTE 4:
CENTERLINE (2 PER PADDLE) ITEM 75 MUST BE COINCIDENT WITHIN ±.004
.0042 VERT & .1163 HORIZ

NOTE 6:
SURFACE "V" OF ITEMS 76, 77, 78 & 79 TO BE COPLANER WITHIN ± .004
.172

NOTE 2:
HINGE CENTERLINE MUST BE PARALLEL WITH BRACKET SURFACE "V" PLANE WITHIN ±.004
- .014 + .036 THIS DUE TO SPAN IN PADDLE HINGE LINE LATCH LINE

TRANSION (1756055)

NOTE 4:
CENTERLINES OF HINGES ITEMS 39,30 & 41 MUST BE HELD WITHIN ±.002
.0131 VERT & .0104 HORIZ
TO TRUE ℄

NOTE 5:
CENTERLINES OF HINGES ITEM 42 MUST BE HELD WITHIN ±.004 OF TRUE ℄
.0159 VERT & .0704 HORIZ

NOTE 6:
SURFACE "V" OF ITEMS 76, 77, 78 & 79 TO BE COPLANER WITHIN ± .004
.172

NOTE 2:
HINGE CENTERLINE MUST BE PARALLEL WITH BRACKET SURFACE "V" PLANE WITHIN ±.004
- .014 + .036 THIS DUE TO SPAN IN PADDLE HINGE LINE LATCH LINE

DESTRUCT UNIT
1756030-501
1756055-501

LATCH LOCATIONS	27.532	38.258	38.401
A	27.441	38.226	38.371
B	27.473	38.240	38.396
C	27.519	38.269	38.446
D	27.558	38.269 38.275	38.492
E	27.519	38.268	38.446
F	27.473	38.269	38.398
G	27.329	38.268	38.256
H	27.268	-	-

Fold Out
Q

Figure III-16. Destruct Unit Dimensional Test Data (Sheet 3 of 3)

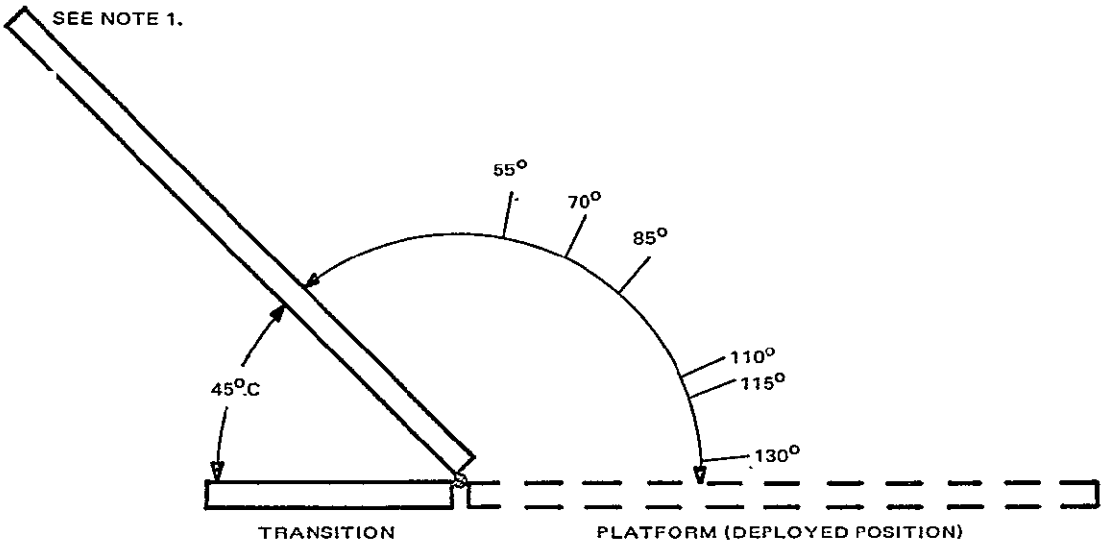

'E 1. FOR PURPOSES OF TEST, THE FOLDED POSITION IS REFERENCED 0°.

Figure III-17. Deployment Test Positions

TABLE III-4. DEPLOYMENT TEST RESULTS

Run No.	Starting Torque (in-lbs)	Average Running Torque (in-lbs)*
1	2.5	5.3
2	2.5	4.7
3	2.5	4.5
4	2.5	4.7
*Overall average torque is 4.8 inch-lbs.		

TABLE III-5. ANGULAR DISPLACEMENT TEST RESULTS

Start Angle (degrees)	Starting Torque (in-lbs)	Running Torque (in-lbs)
0	3.1	3.1
55	4.7	4.5
70	4.7	4.7
85	5.0	5.0
110	5.3	5.6
115	6.3	6.3
130	7.2	6.3

6. Weight Data

The completed solar array platform structure which includes the platform, transition and the required hardware must not exceed 21.7 pounds. The weight of the individual parts are as follows:

Item	Weight
Platform	15.53 pounds
Transition	4.00 pounds
Hinge Pins, shims and lock rings	0.07 pounds
Latching assembly, Hut clamps and misc. hardware	1.40 pounds
Total Weight	21.00 pounds

H. RECOMMENDATIONS AND CONCLUSION

1: Introduction

On all development programs, a test unit which is identified by many names (prototype, engineering model, breadboard model, feasibility model, proof model, and trial model) is built for product test and analysis. During the production of ultra-light honeycomb structures, the RCA Corp. fabricates a destruct unit to qualify the tooling, production process technique and materials. The data obtained during product analysis is used to validate the process and insure the quality of the flight units.

2. Recommendations

Test data obtained from the destruct unit indicates that the original production-process technique would not meet the specifications imposed by the RCA Corp. As a result, the following modifications were recommended and used to improve the design.

- The tools were modified to insure greater uniformity of parts for subsequent units.
- Drawing and specification errors in addition to conflicting tolerances were eliminated by Engineering Change Notices.
- The dimensional check method was improved to insure repeatability of measurements and provide for factual interpretation of the data.
- Documentation for recording the dimensional data was prepared.
- Thermal profiles of the tooling were obtained to insure uniform cure cycles.
- The production-process technique was modified to highlight critical procedures, namely cleaning, machining, and curing cycles.
- Simplify final lay up operations by preparing cured subassemblies in advance.
- Reduce the temperature differential between the top and bottom of the mold by the judicious use of thermal blankets.

3. Conclusions

Based on the experience and data obtained during the fabrication of the destruct unit the production-process technique (as modified) was approved for use in the fabrication of flight equipments.

APPENDIX IV

NIMBUS-B2 STORAGE MODULE REWORK TEST AND ALIGNMENT DATA REPORT

A. REPAIR CYCLE

The electronics board from each storage module (board 003 from storage module 003, board 009 from storage module 008) was removed and electrically examined. Board 003 contained the following defects:

- The base connection of Q-13B (RCA drawing 1849843) was open, and
- Zener diode VR5 (RCA drawing 1849843) measured 13.63 volts instead of the rated voltage of 19.45 volts.

Electronics board 009 did not have any discrepancies.

The thermistor (temperature telemetry sensor) on storage cell No. 5 of each battery was also examined. No discrepancies were detected for either thermistor.

The storage modules were reassembled with the following equipment:

- Storage Module 003. — Electronics board 009 was installed (board 003 was removed from service).
- Storage Module 008. — Electronics board 022 (spare from the Nimbus B program) was installed.

Installation of the electronic boards was selected to optimize storage module performance.

B. TEST SEQUENCE

After rework, the following tests were conducted to calibrate the telemetry circuits and verify circuit operation.

- Circuit Alignment and Electrical Test per Test Procedure TP-CT-1759580,
- Workmanship Vibration per Test Procedure TP-HVA-1759580 - Random Exposure in the Radial Axis only,

- Telemetry Calibration per Test Procedure TP-TM-1759580 - Temperature Levels of -5°C, 0°C, 5°C, 25°C, 40°C, 45°C, 50°C, and 55°C,
- Electrical Performance Test per TP-CT-1759580 - Temperature Levels of 5°C, 25°C, 45°C, and
- Trickle Charge Circuit Test per TP-CT-1759580 at 55°C.

C. TEST RESULTS

Storage module performance was satisfactory during workmanship and calibration tests. The critical parameters and test results are listed in Table IV-1. Calibration curves for the telemetry circuits are shown in Figure IV-1 through IV-12.

TABLE IV-1. TEST PARAMETERS AND RESULTS FOR STORAGE MODULES 003 AND 008

Test Parameters	Performance Data Summary					
	Module No. 003 at			Module No. 008 at		
	5°C	25°C	45°C	5°C	25°C	45°C
Maximum Charge Current (amperes)	1.105	1.102	1.103	1.107	1.106	1.109
Trickle Charge Current (amperes)	0.158	0.156	0.156	0.160	0.158	0.160
Charge Voltage Limit (volts dc)	34.6	33.7	32.7	34.6	33.7	32.7
Charge Current TLM at 1.2A (volts dc)	6.039	6.006	5.958	6.022	6.003	5.985
Discharge Current TLM at 2.4A (volts dc)	5.801	5.781	5.742	5.837	5.804	5.775
Battery Voltage TLM at 30V (volts dc)	3.137	3.137	3.138	3.103	3.101	3.100
Battery Temperature TLM (volts dc)	1.73	3.19	4.67	1.68	3.15	4.62
Shunt Dissipator Turn-On Voltage (volts dc)	38.1	38.1	38.1	38.1	38.1	38.1

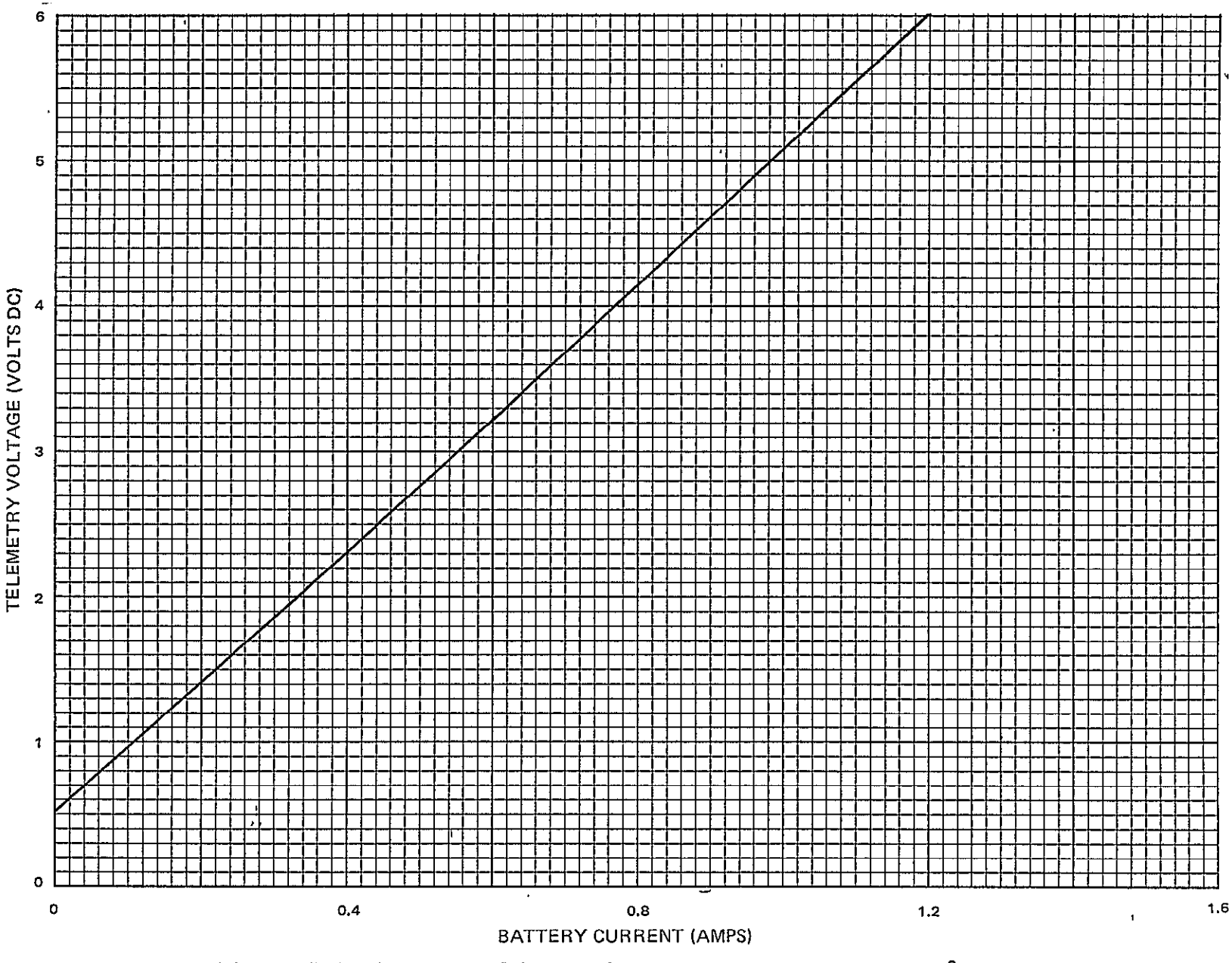

Figure IV-1. Storage Module 003 Charge-Current Telemetry at 25°C

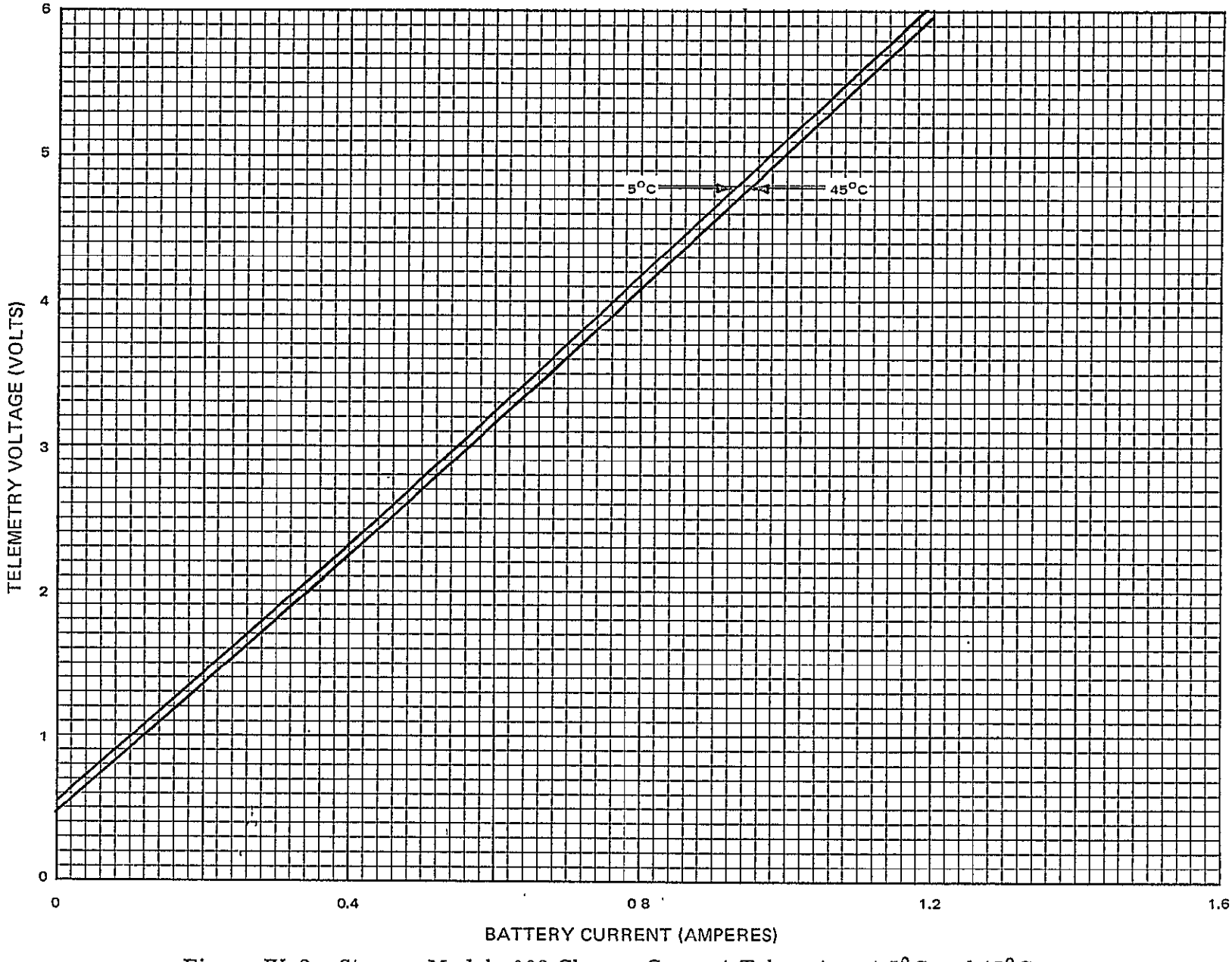

Figure IV-2. Storage Module 003 Charge-Current Telemetry at 5°C and 45°C

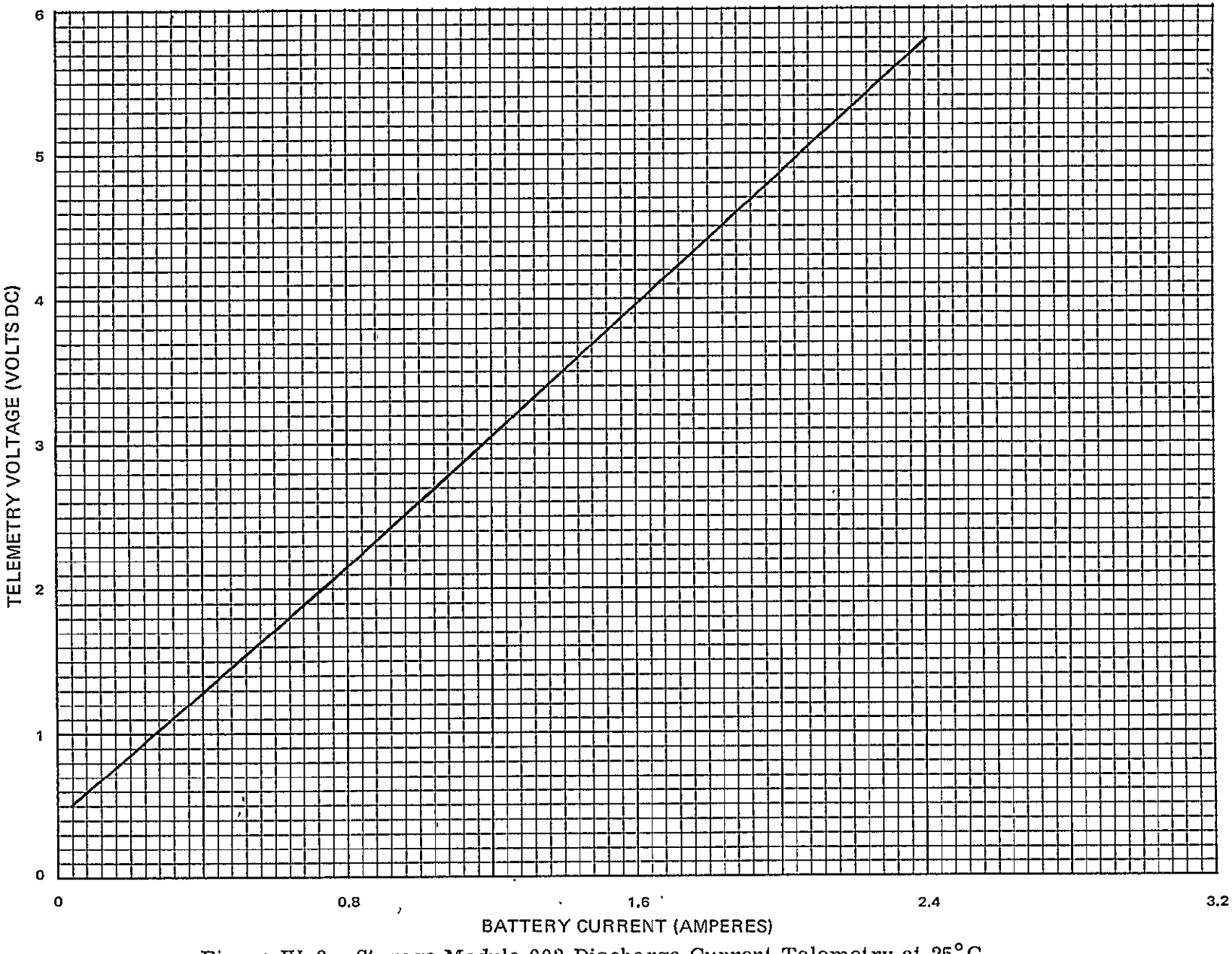

Figure IV-3. Storage Module 003 Discharge Current Telemetry at 25°C

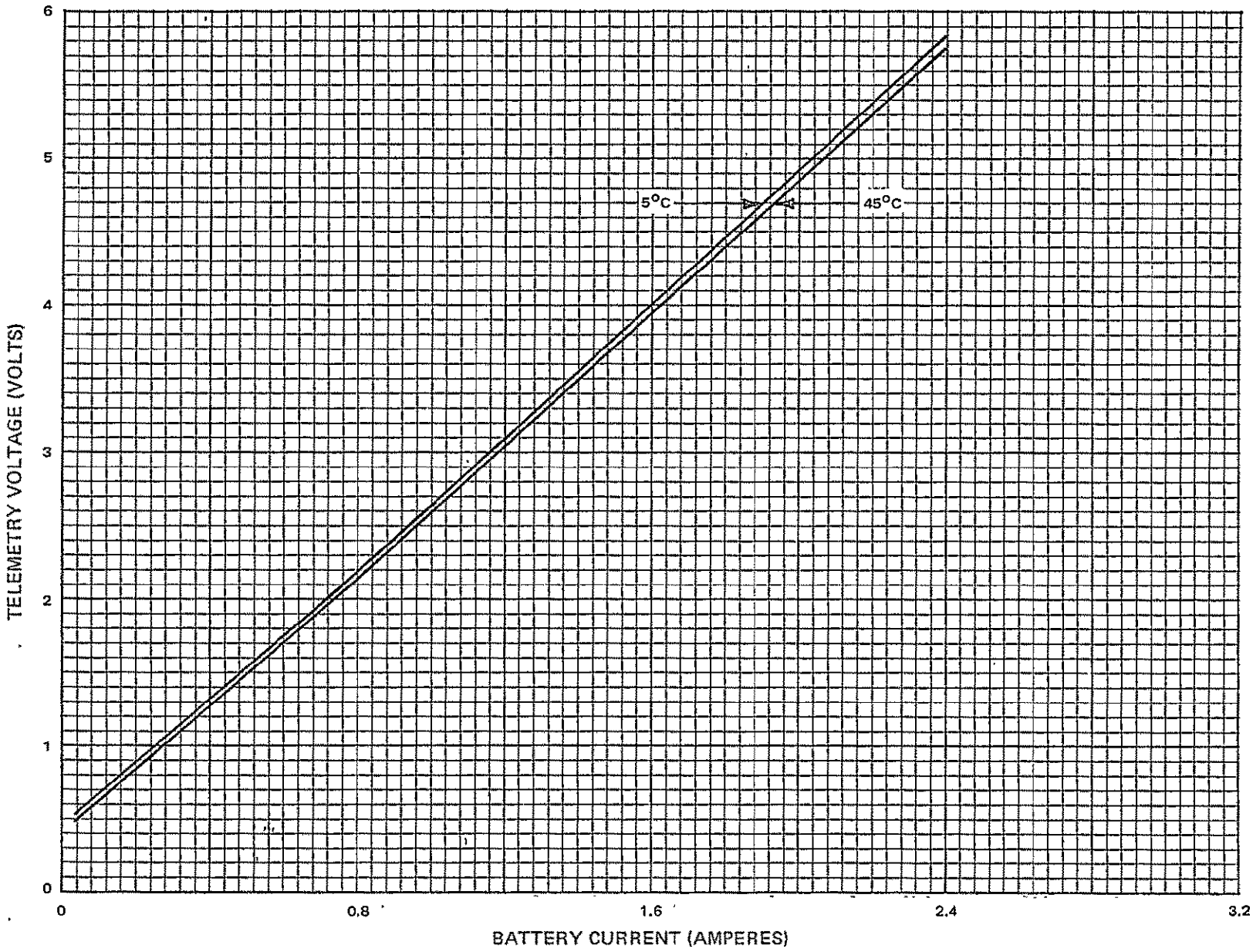

Figure IV-4. Storage Module 003 Discharge Current Telemetry at 5°C and 45°C

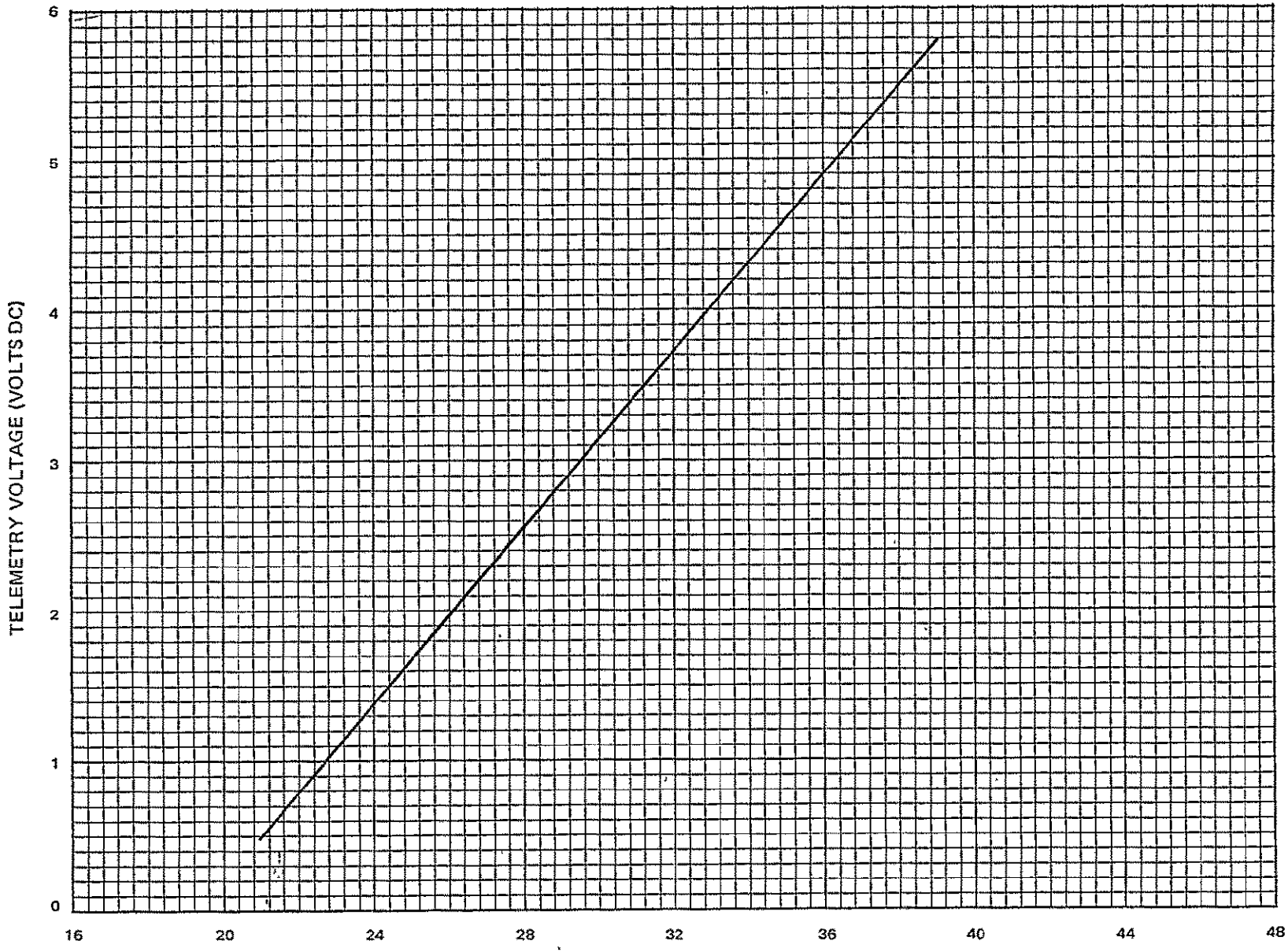

Figure IV-5. Storage Module 003 Voltage Telemetry

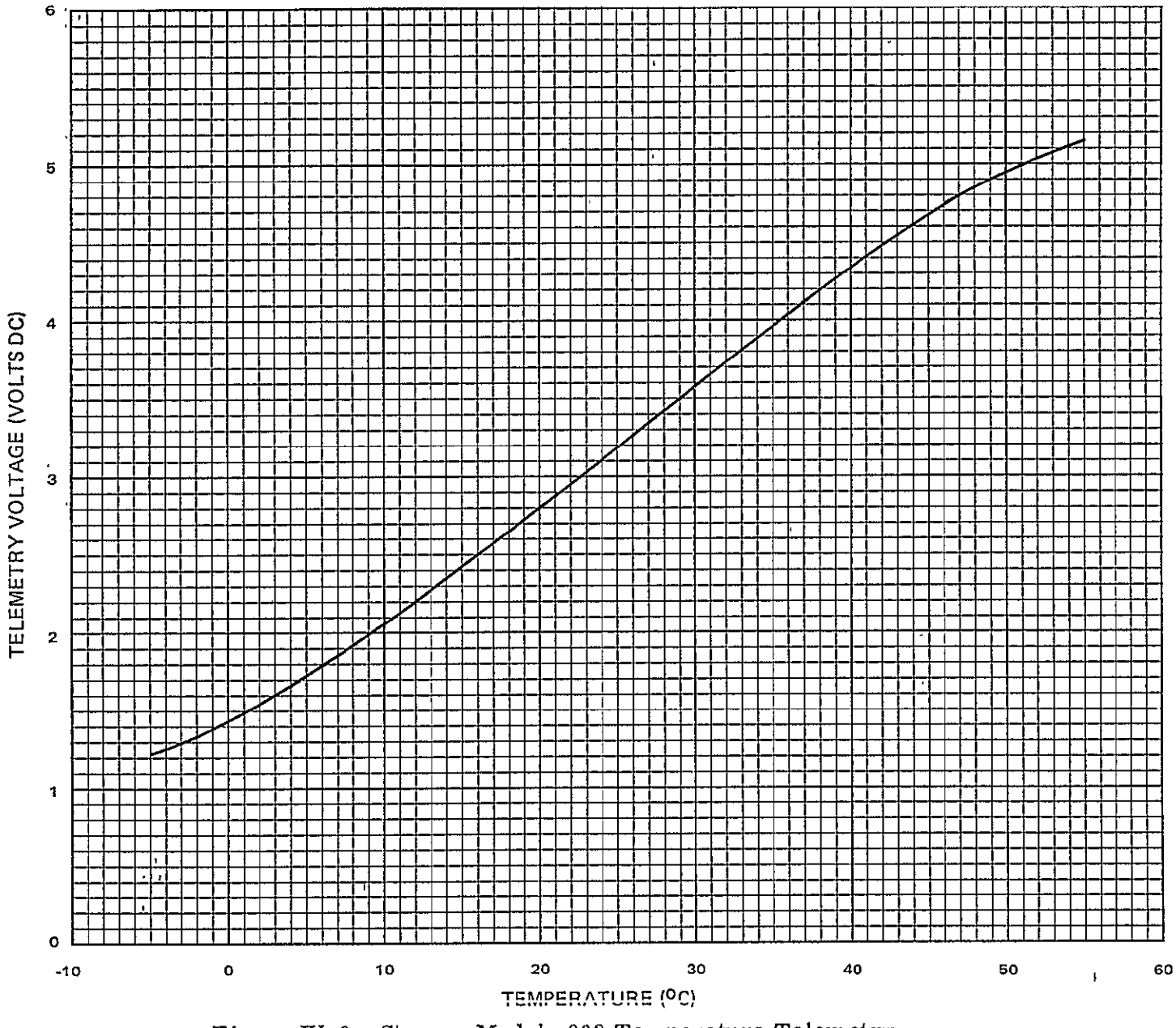

Figure IV-6. Storage Module 003 Temperature Telemetry

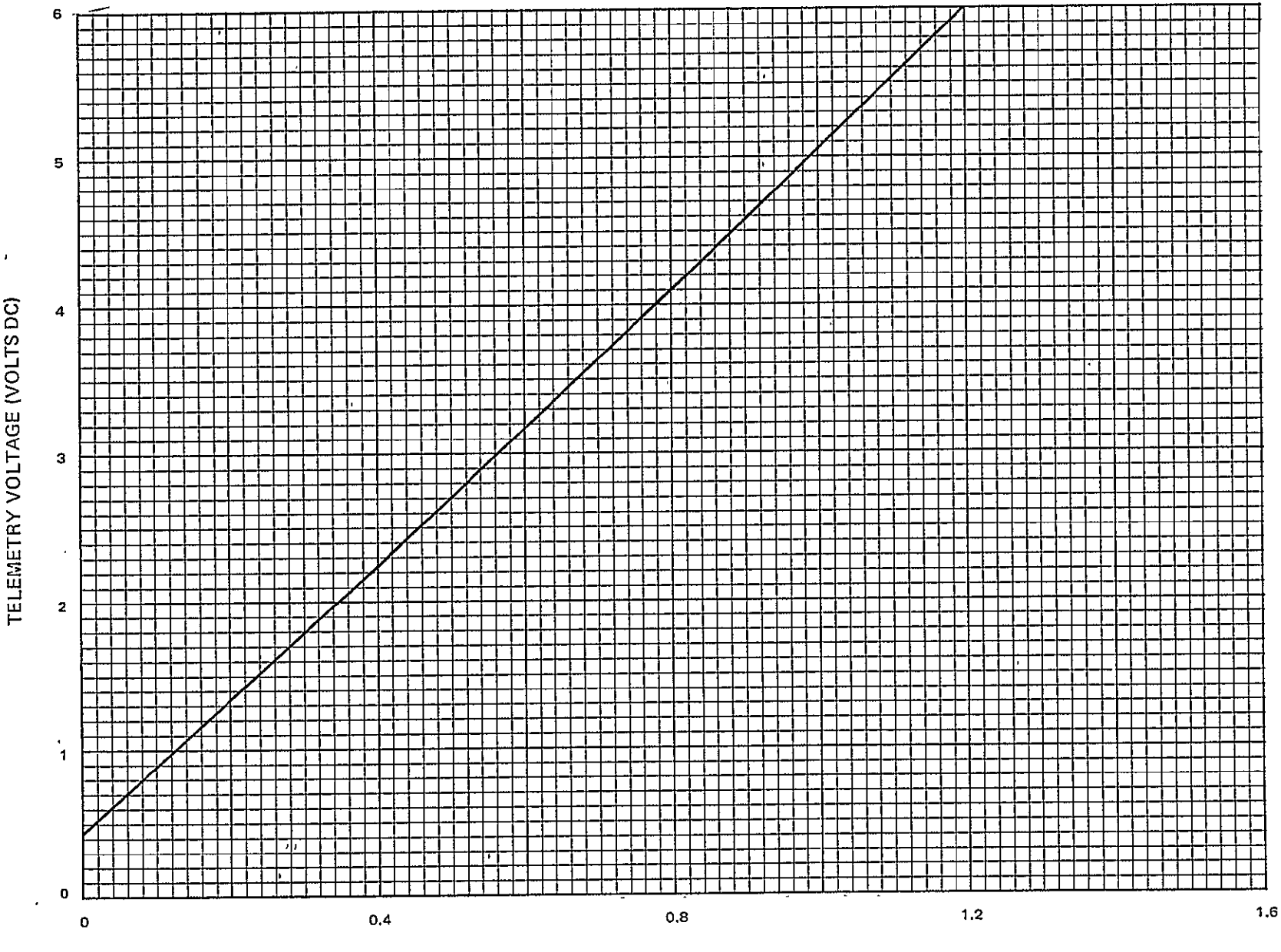

Figure IV-7. Storage Module 008 Charge Current Telemetry at 25°C

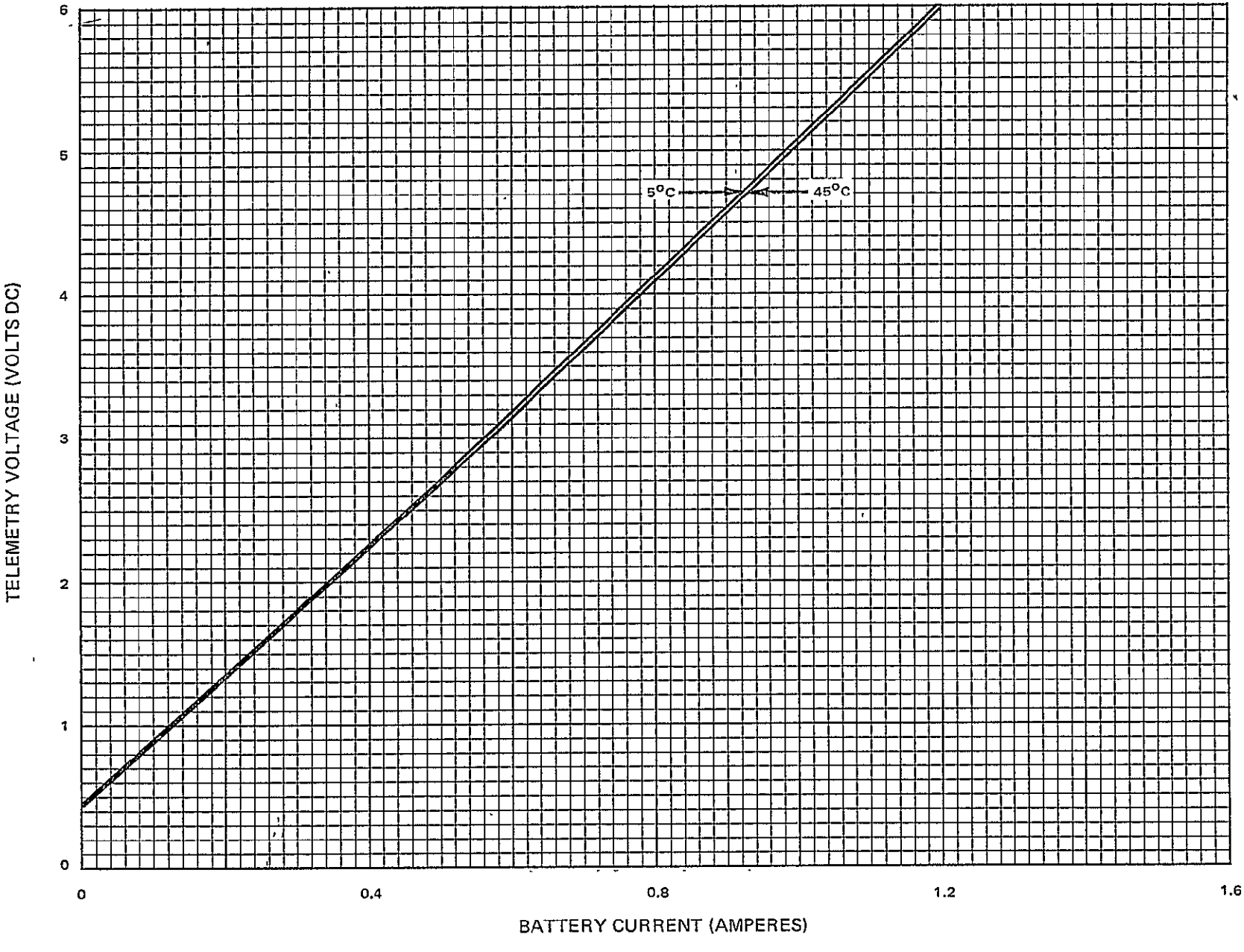

Figure IV-8. Storage Module 008 Charge Current Telemetry at 5°C and 45°C

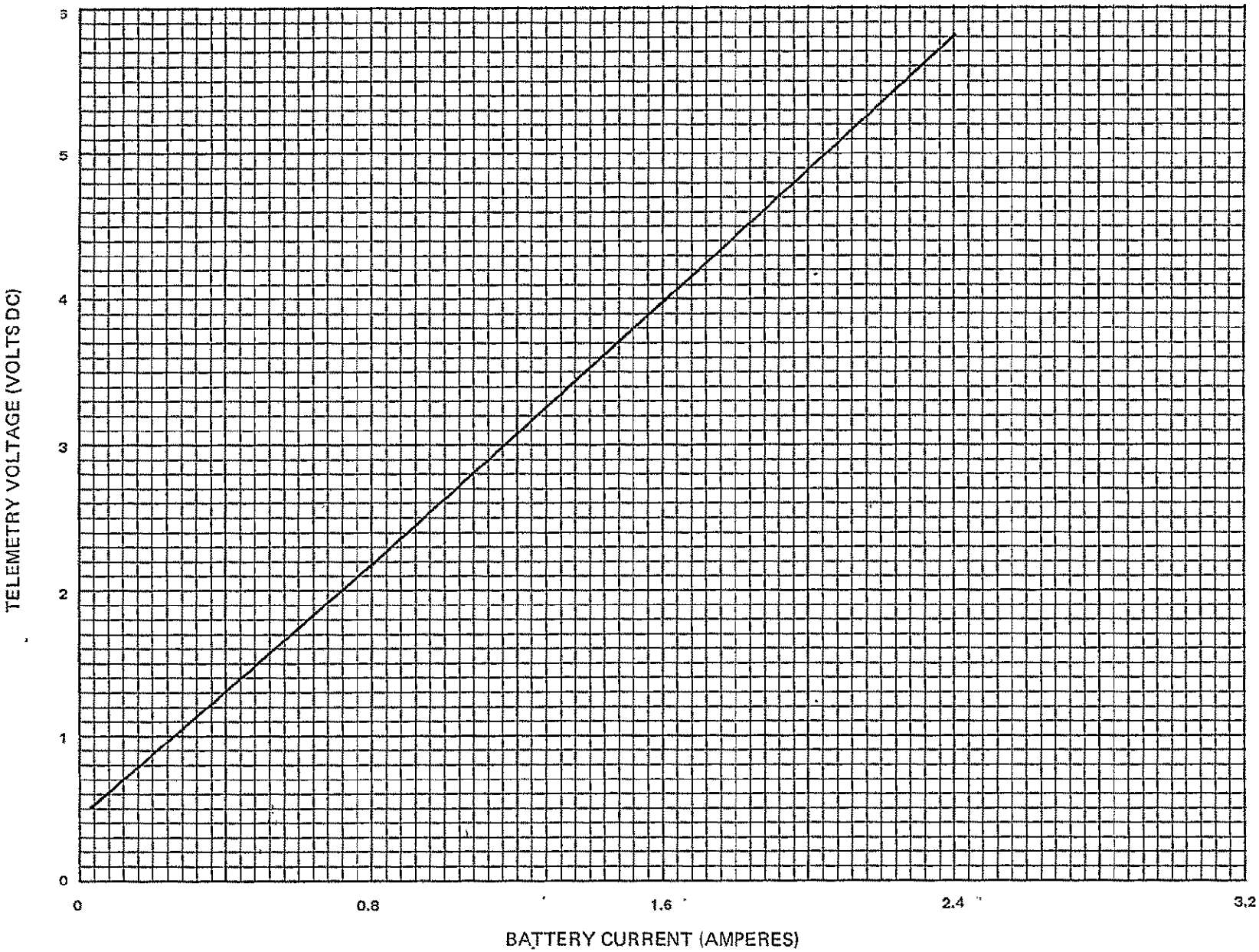

Figure IV-9. Storage Module 008 Discharge Current Telemetry at 25°C

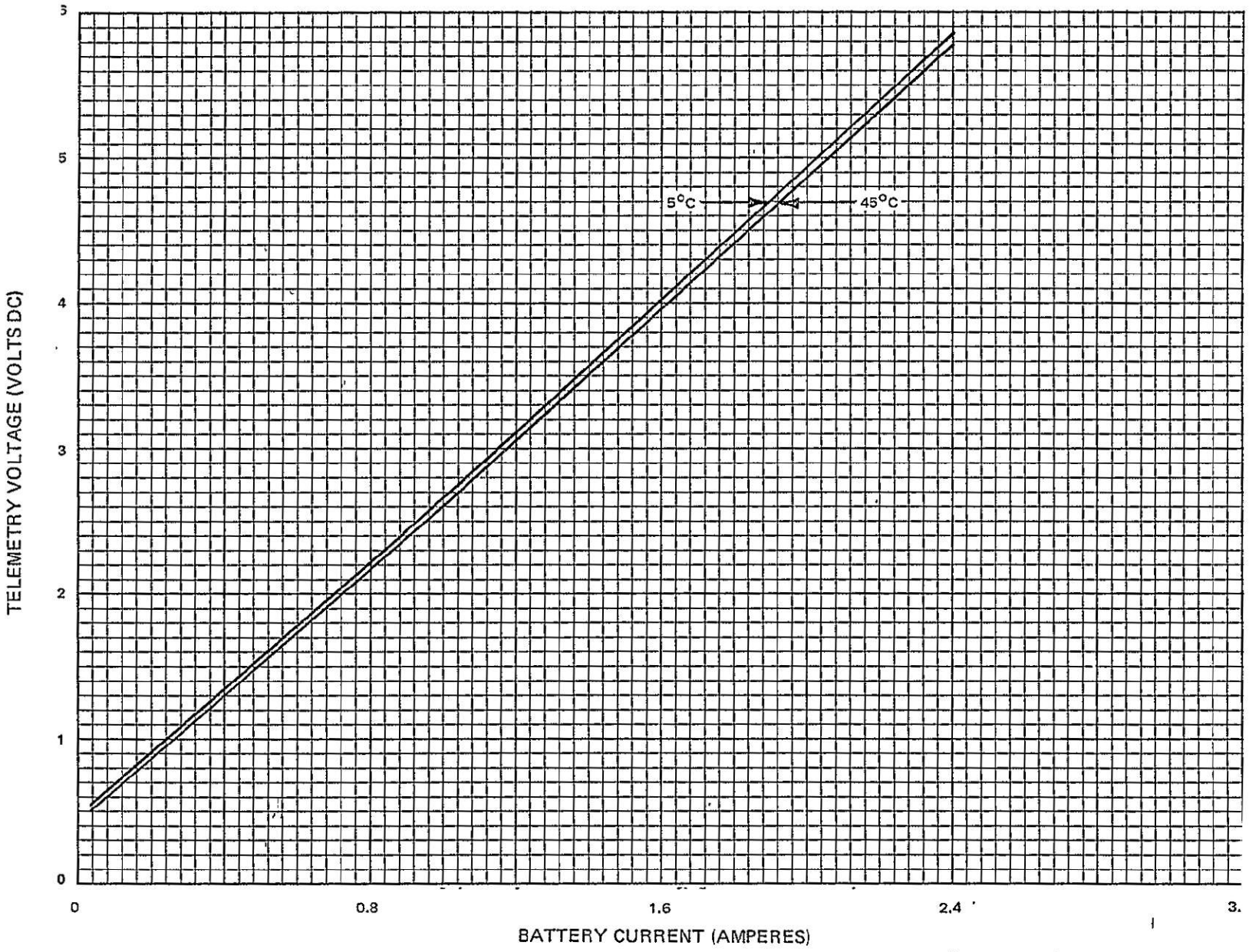

Figure IV-10. Storage Module 008 Discharge Current Telemetry at 5°C and 45°C

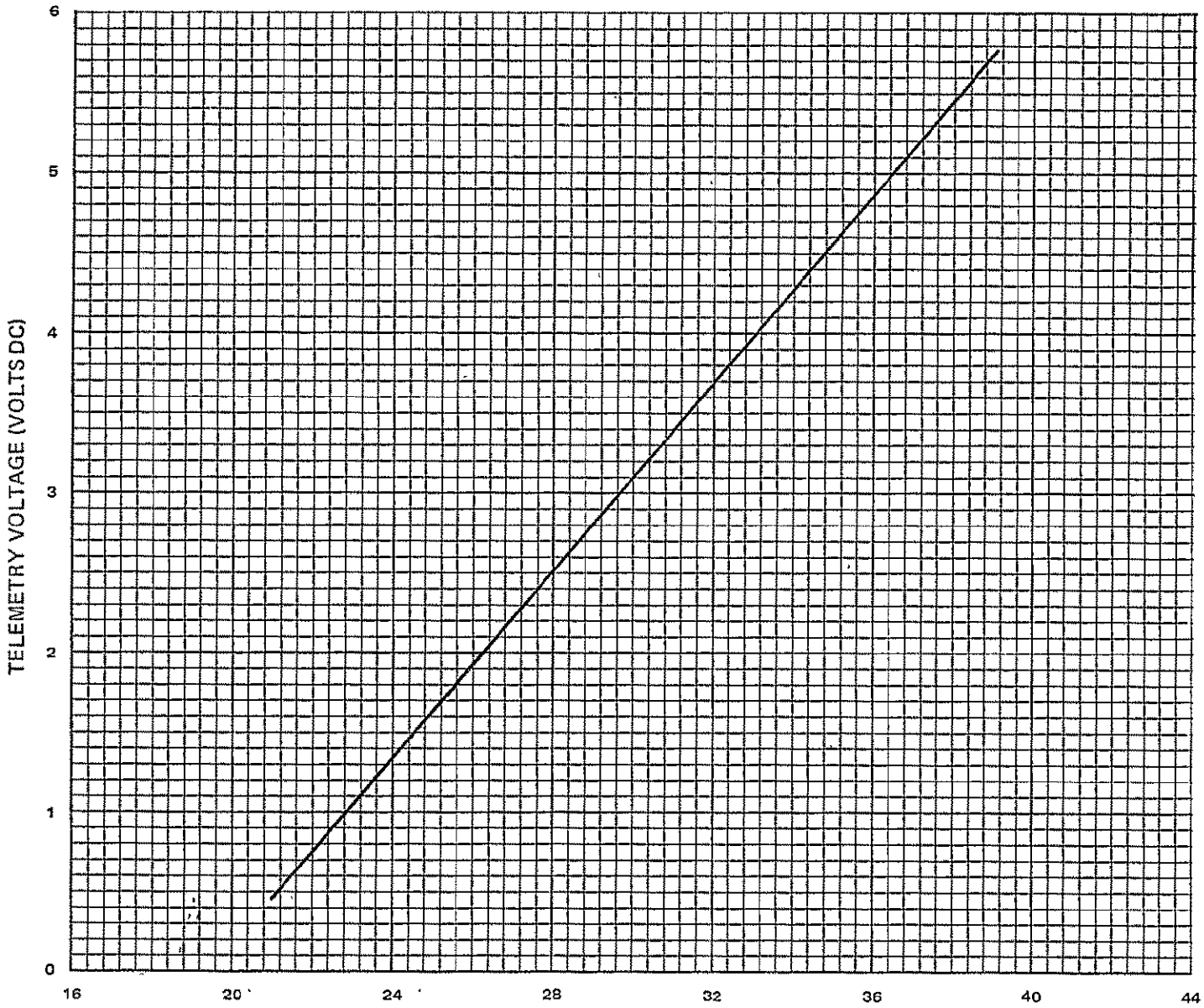

Figure IV-11. Storage Module 008 Voltage Telemetry

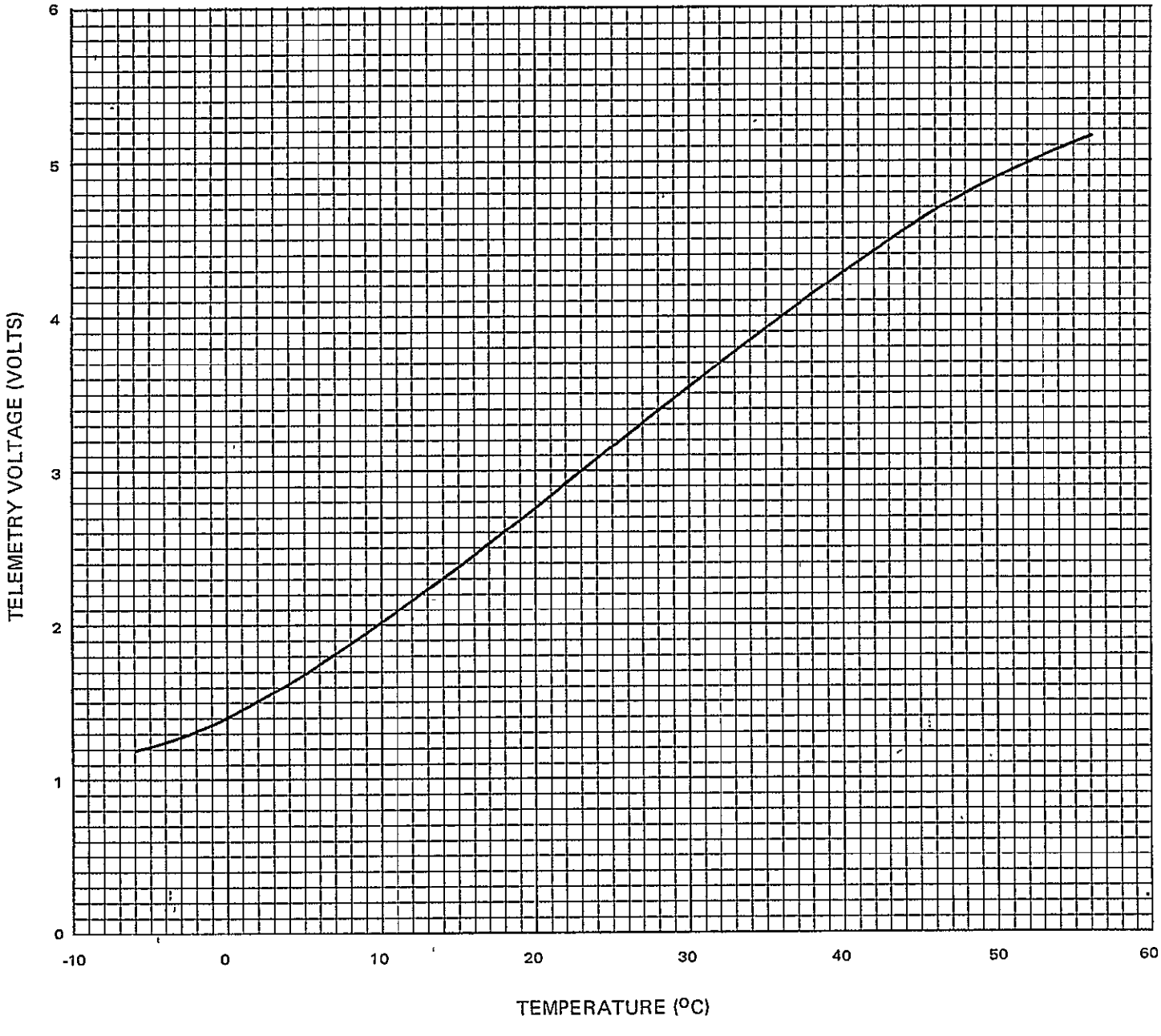

Figure IV-12. Storage Module Temperature Telemetry

APPENDIX V

NIMBUS-D STORAGE MODULE TEST AND CALIBRATION REPORT

A. STORAGE CELL DATA

The acceptance test data obtained at RCA (RCA lot 34, GE Co. shipment No. 3) are contained in Figures V-1 through V-7. Acceptance test data obtained at the GE Co. prior to delivery are contained in Figures V-8 through V-14. Based on the test results, the storage cells were released to manufacturing.

B. HEAT SINK TRANSISTOR REPLACEMENT AND TEST RESULTS

1. Replacement Part Selection

The part selected for replacement was a SDT 9903 Solitron transistor (RCA Drawing 1970655-1). The reasons for choosing this part are as follows:

- Procurement - 44 units of 1970655-1 were available in controlled stores for the I-TOS program, and were not scheduled for use on I-TOS until July 1969. The in-stock units had been successfully dew-point tested and preconditioned.
- Electrical compatability - the 1970655-1 had suitable electrical characteristics for a direct replacement without any changes in electrical design.
- Mechanical compatability - the 1970655-1 would fit on the heat sink with only minor changes to the heat sink assembly.
- Qualification - the 1970655-1 was considered fully flight-qualified by RCA. This transistor, used in the shunt dissipator circuit on I-TOS, had demonstrated excellent performance during the I-TOS vibration qualification testing.
- Thermal Performance - the 1970655-1 transistor performed satisfactory during a special "worst-case" thermal test. This test determined that the junction temperature/power coefficient was low enough to maintain the junction temperature below 100°C when mounted in the Nimbus-D storage module configuration. The discussion of the thermal test is presented in the following paragraphs.

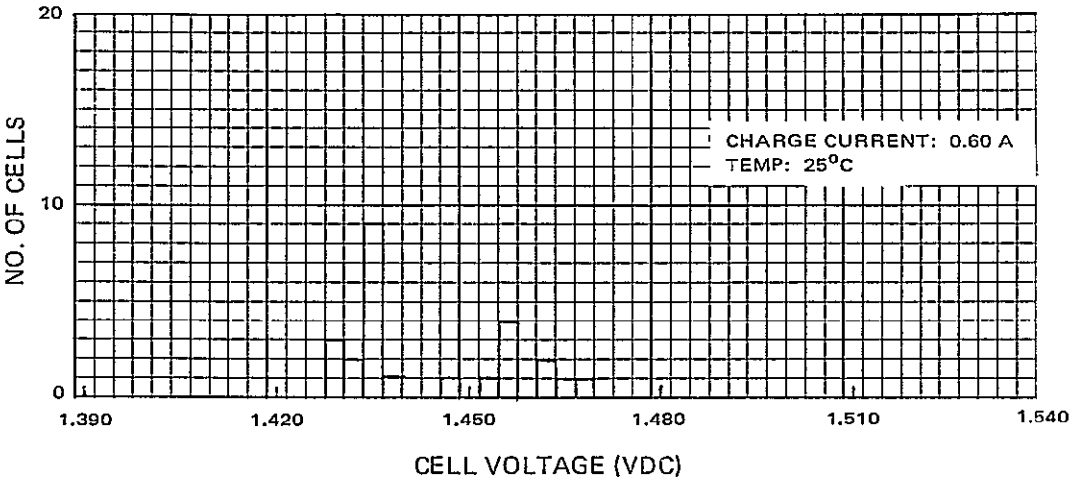

Figure V-1. Cycling Test, Maximum Voltage at End-of-Charge

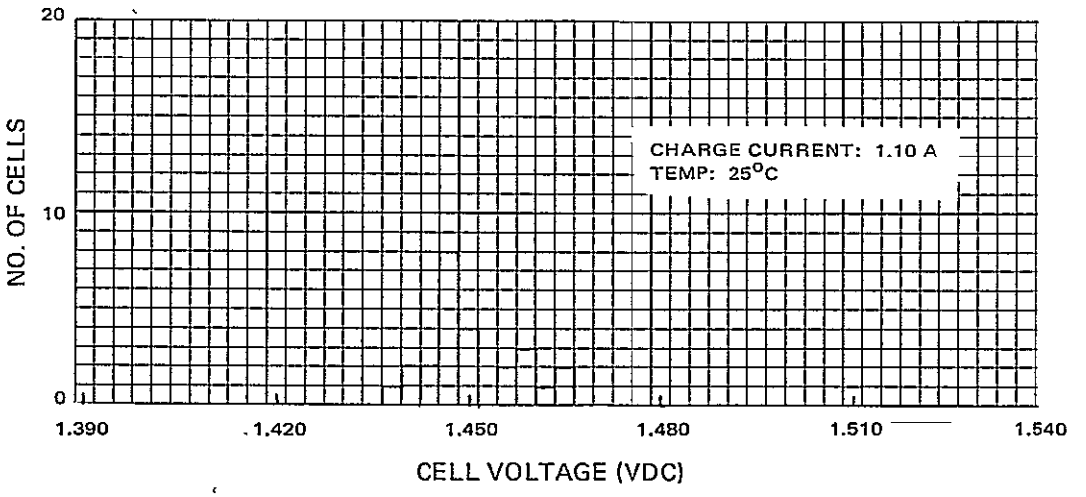

Figure V-2. Cycling Test, Maximum Charge Voltage

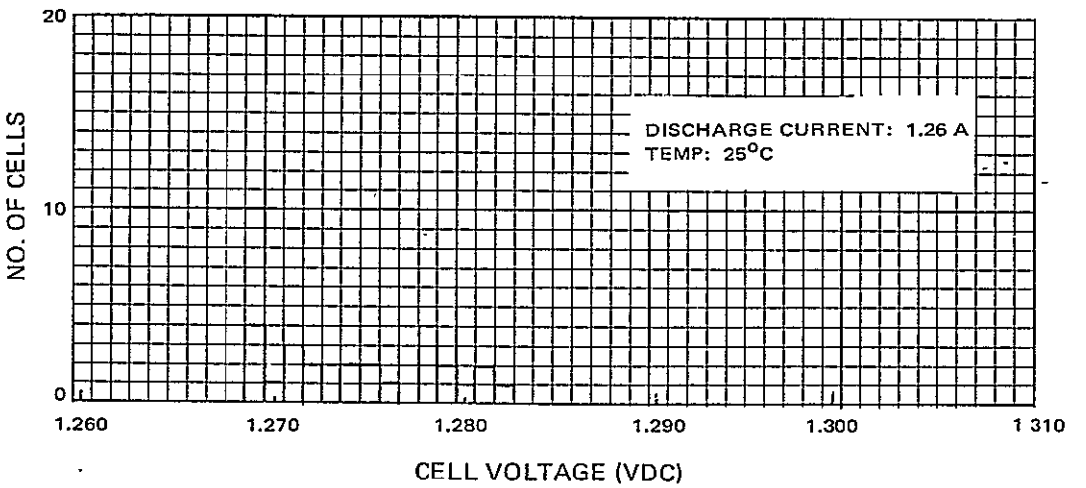

Figure V-3. Cycling Test, Minimum Discharge Voltage

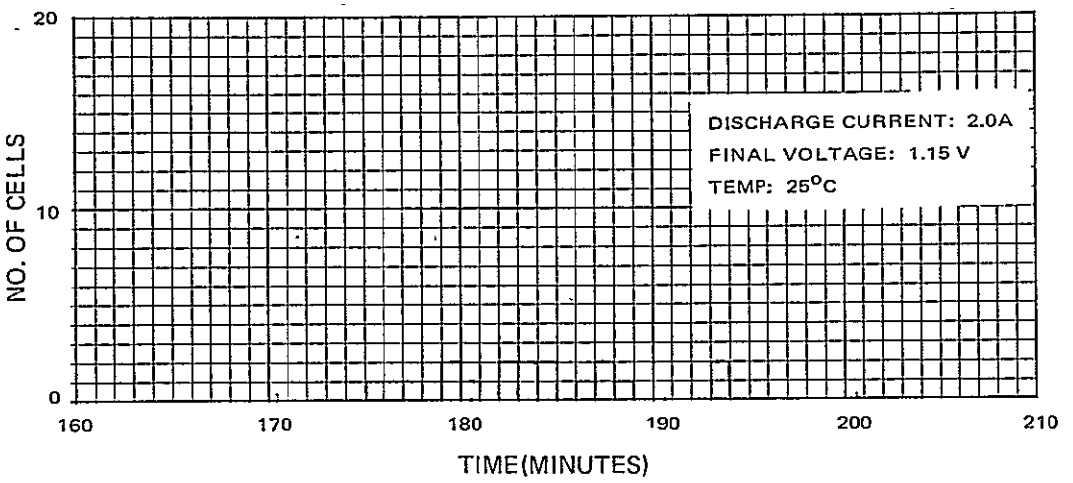

Figure V-4. Cycling Test, Residual Capacity

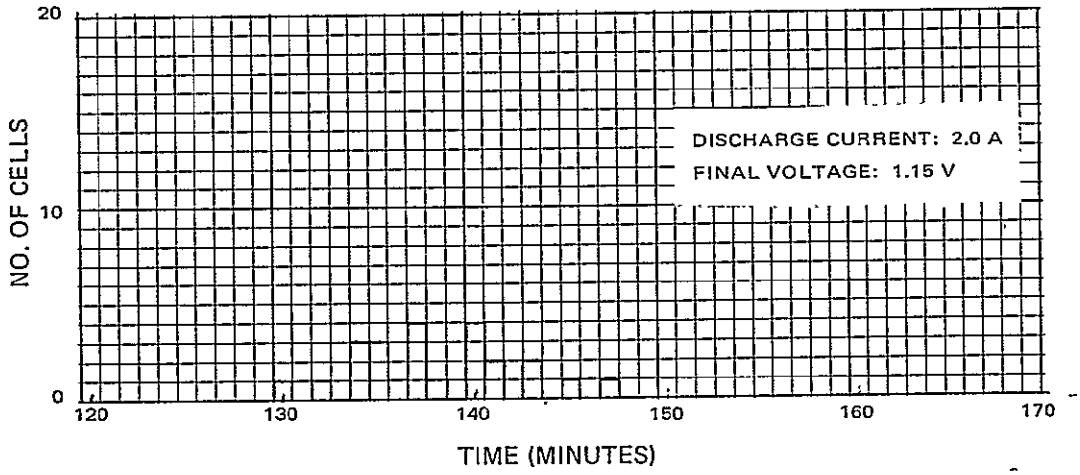

Figure V-5. Capacity Test at 40°C, RCA

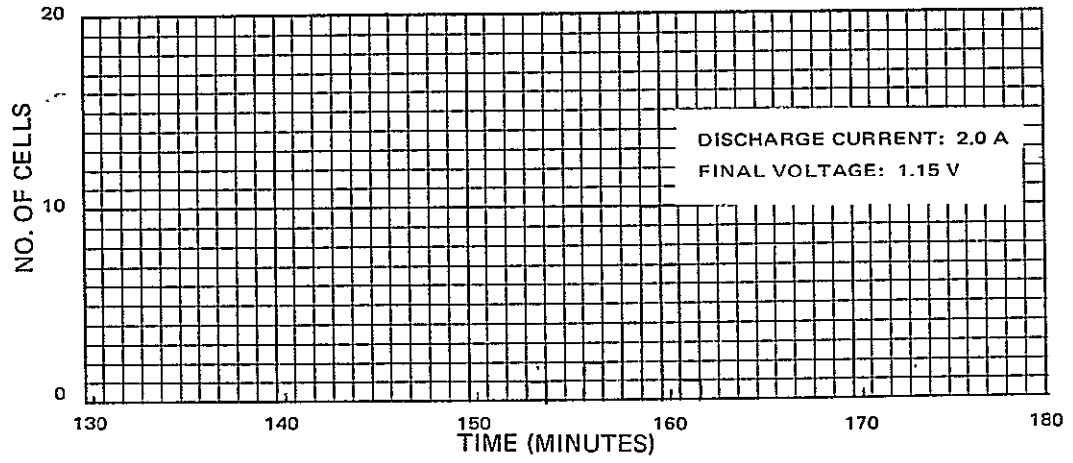

Figure V-6. Capacity Test at 25°C, RCA

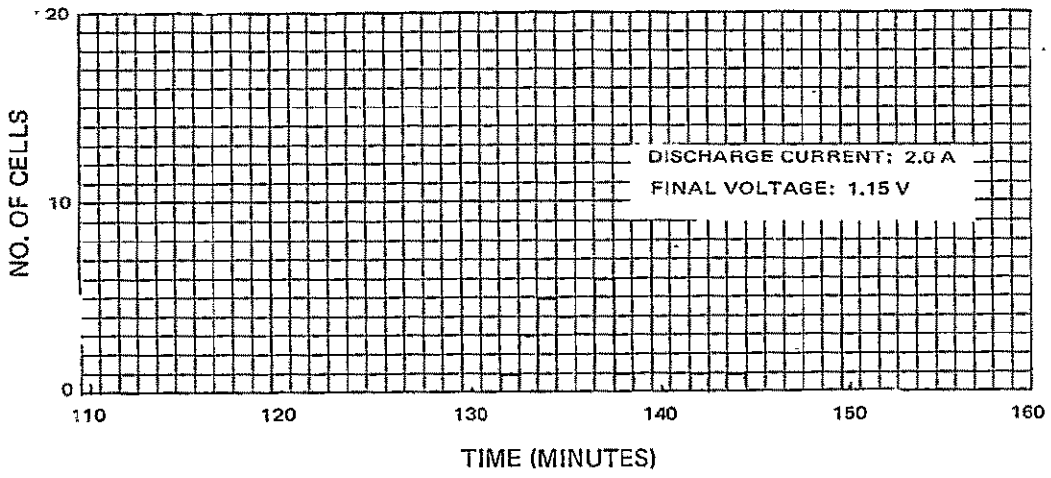

Figure V-7. Capacity Test at 0°C, RCA

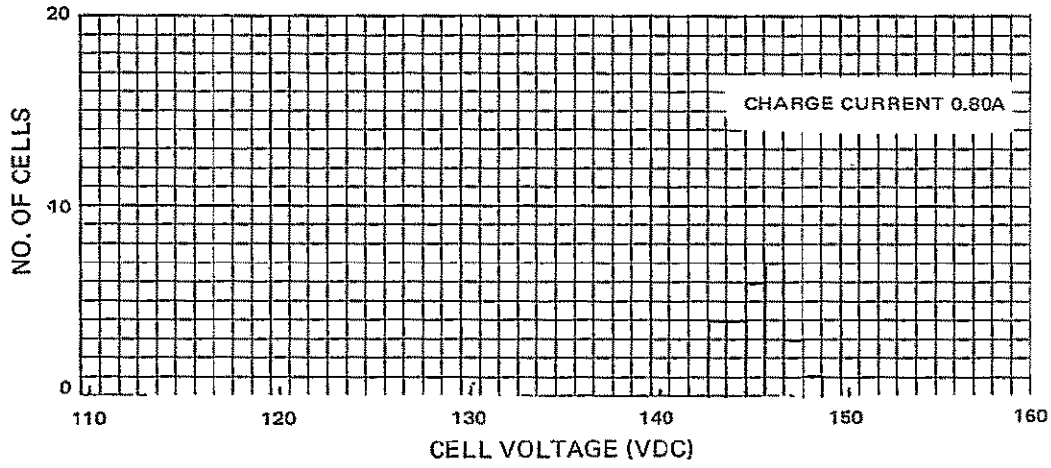

Figure V-8. Maximum Overcharge Voltage at 25°C

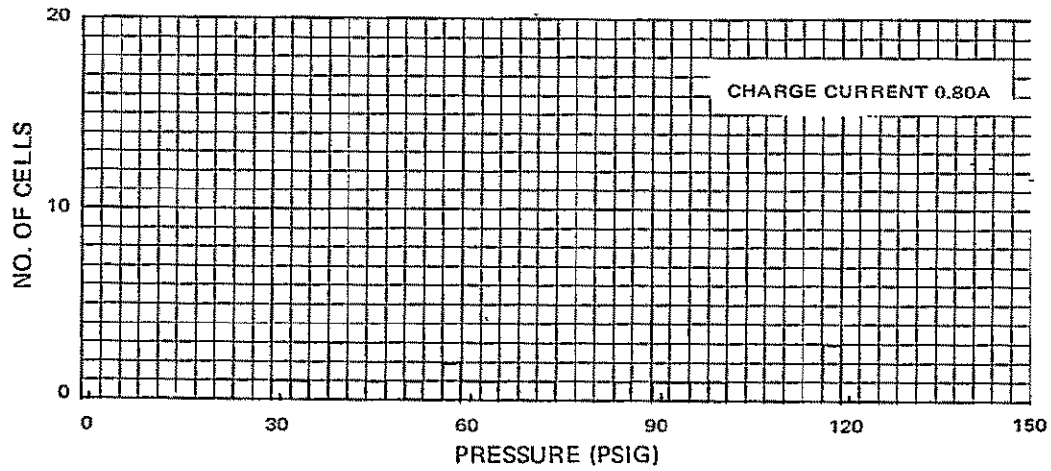

Figure V-9. Maximum Overcharge Pressure at 25°C

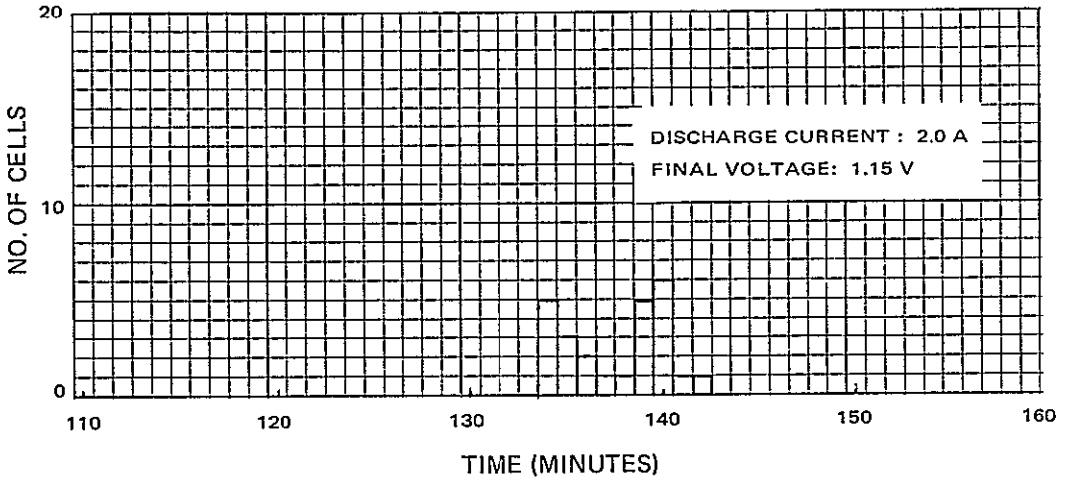

Figure V-10. Capacity Test at 0°C — GE

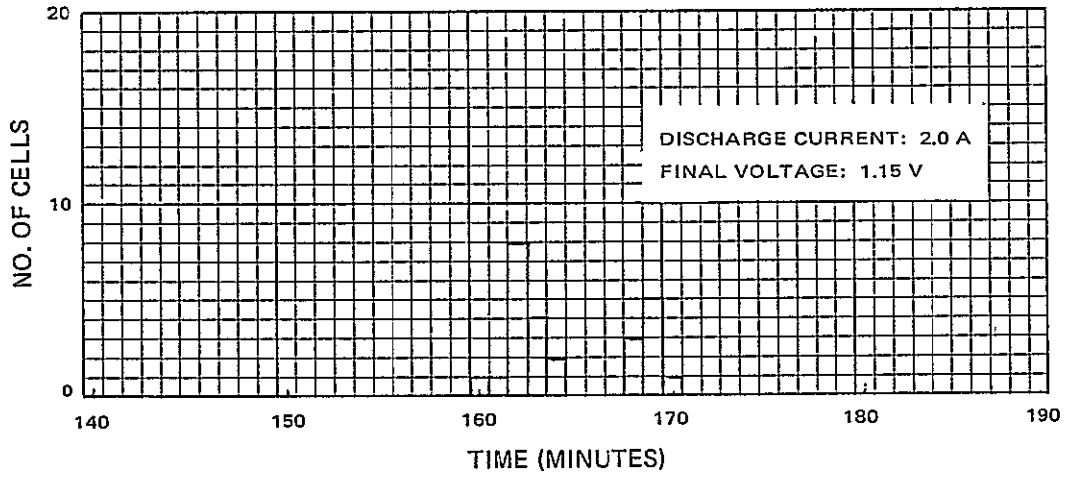

Figure V-11. Capacity Test at 25°C — GE

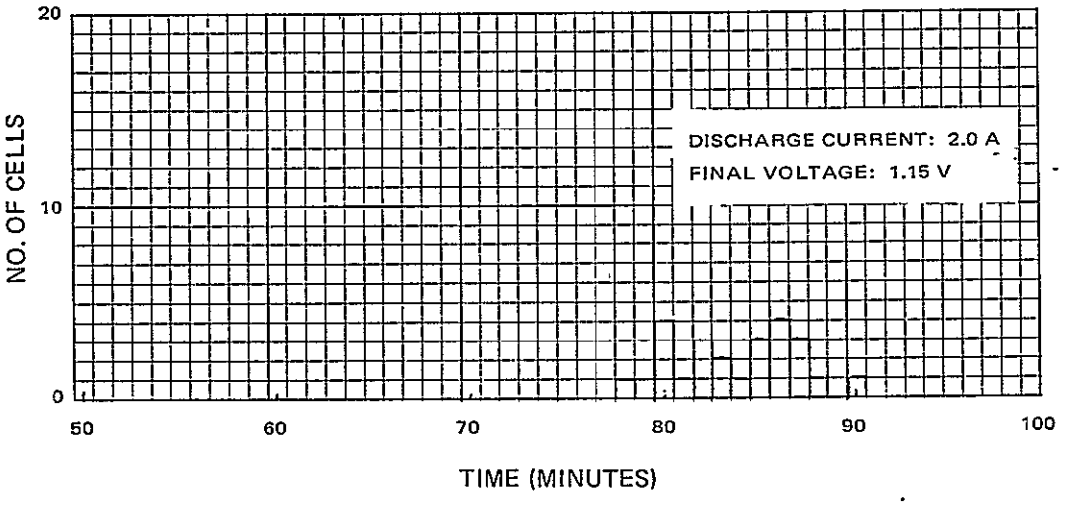

Figure V-12. Capacity Test at 50°C — GE

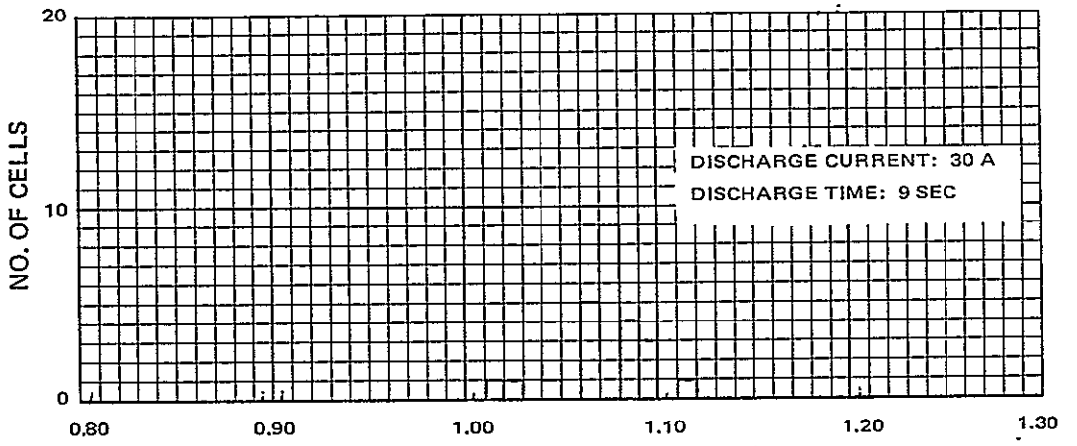

Figure V-13. Internal Resistance Test

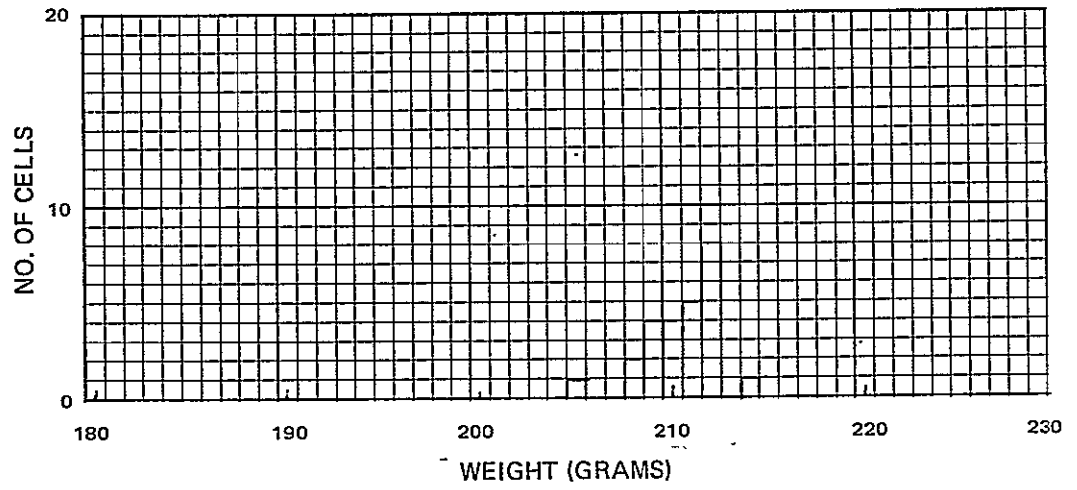

Figure V-14. Storage Cell Weight

2. Special Thermal Test and Results

A Nimbus heat sink assembly (serial No. 001) was modified by the repl ment of the 2N2016 transistor with a 1970655-1 transistor and was subjected thermal investigation. The test model was mounted to an aluminum plate (3/ 15 × 8 inches) to ensure thermal equilibrium conditions during test.

The maximum power dissipation of the transistor is determined by the electr cal circuit (see Figure V-15). Power dissipation versus collector current is shown in Figure V-16. The worst-case power is approximately 20 watts at 1. amperes.

Junction temperature is determined by preparing a calibration curve of I_{CBO} versus temperature using the test circuit shown in Figure V-17. The calibra curve is shown in Figure V-18. The temperature was measured at the transi case and was considered equivalent to the junction temperature. The points c the curve were established under temperature equilibrium conditions.

After generation of the calibration curve, the heat sink assembly was brought thermal equilibrium at 50°C (temperature of aluminum plate) with the shunt dissipator transistor powered at approximately 20 watts using the test circuit shown in Figure V-19. Variable resistor R controlled the base drive and was adjusted to maintain a collector current of 1.0 ampere. Switch S1 (DPDT) w used to connect either the calibration circuit or the normal transistor circuit. Instantaneous readouts of I_{CBO} were taken four times during a 73-minute soa and converted to junction temperature. A plot of this curve is shown in Figu V-20. The steady state junction temperature was found to be 88°C and the ca temperature was measured at 65°C.

The accepted formula for calculating junction temperature/power coeffieient :

$$\theta_{J-C} = \frac{T_J - T_C}{P_{DJ}} \qquad (1)$$

where

T_J = junction temperature

T_C = case temperature

P_{DJ} = power dissipated at junction.

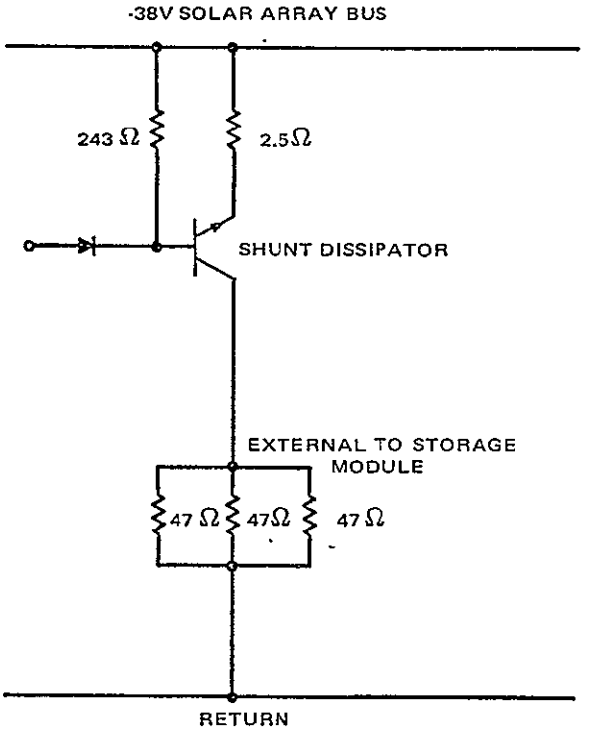

Figure V-15. Power Dissipation Test Circuit

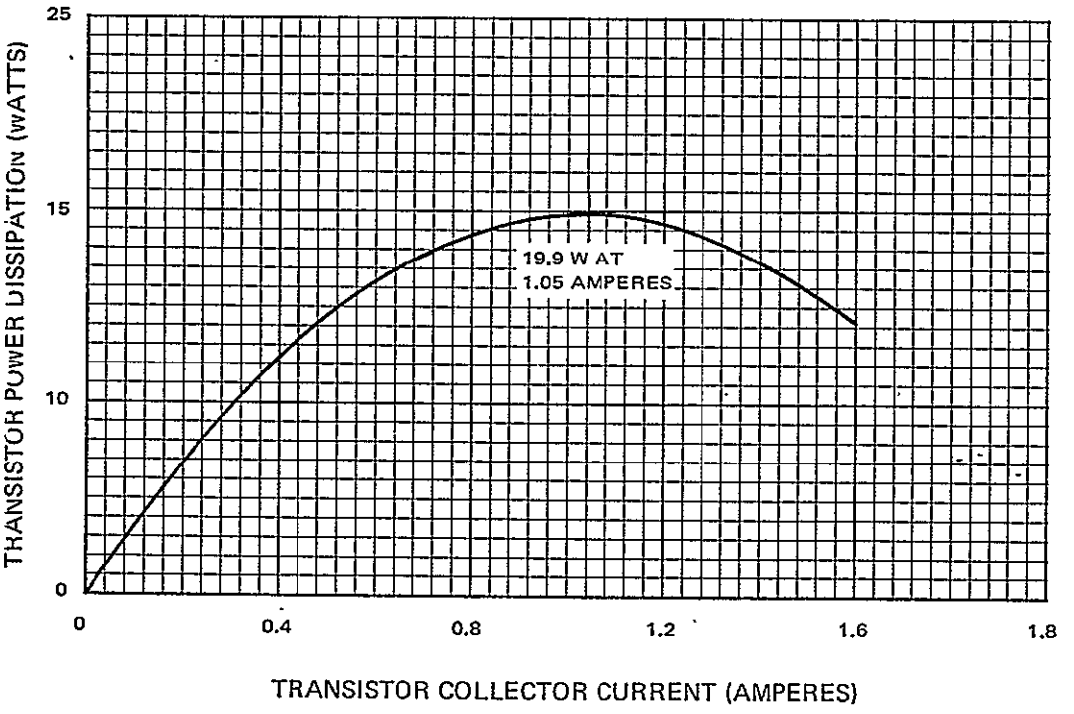

Figure V-16. Power Dissipation Characteristics

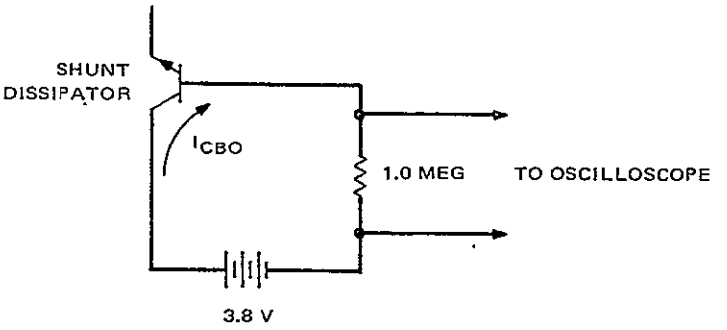

Figure V-17. Junction Temperature Calibration Test Circuit

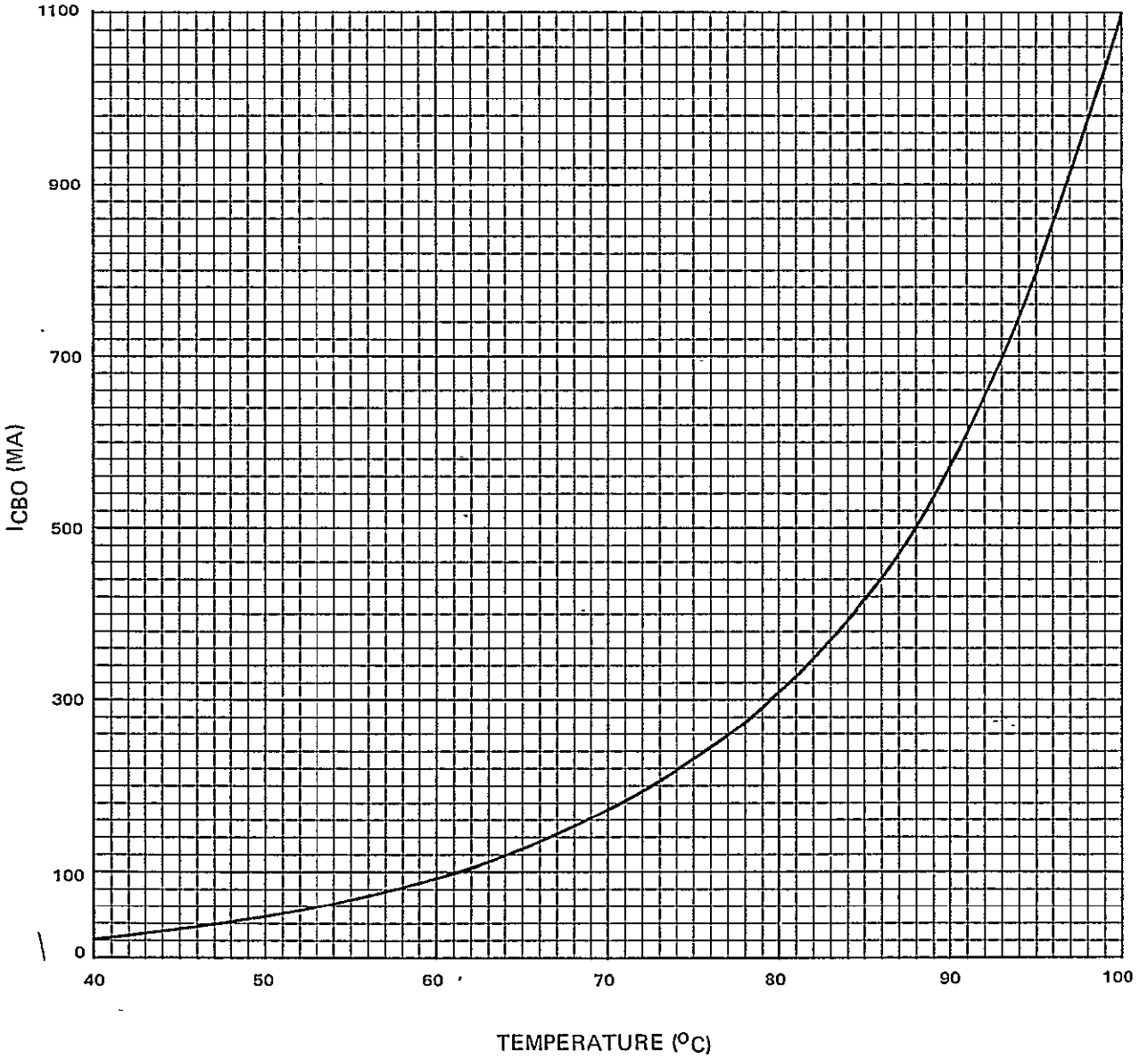

Figure V-18. Junction Temperature Calibration Curve

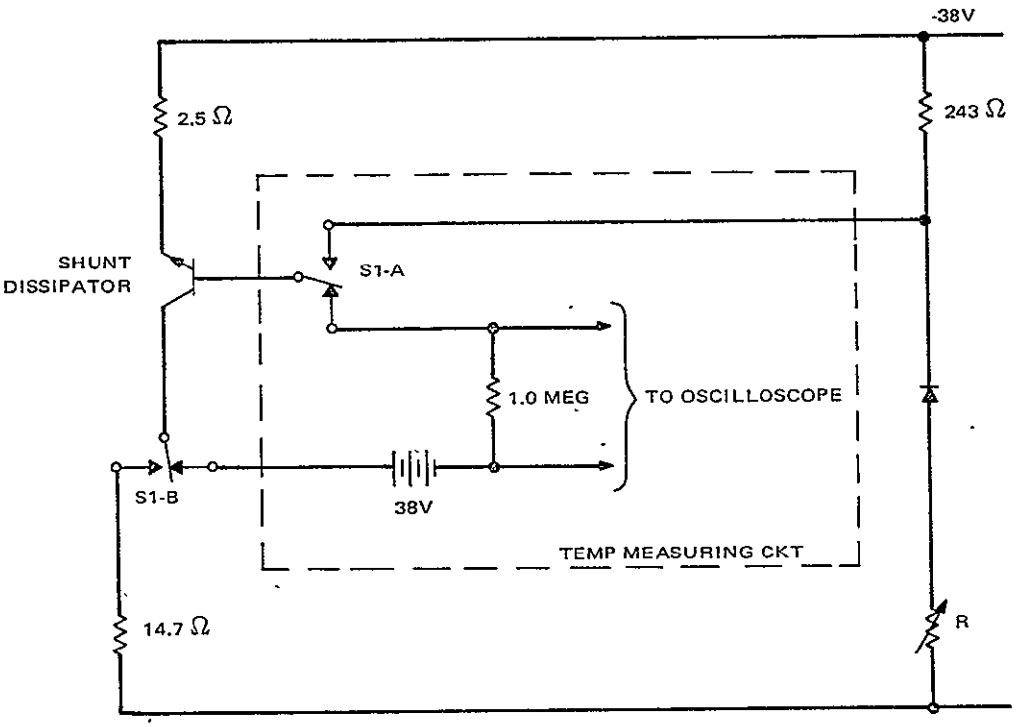

Figure V-19. Junction Temperature Test Circuit

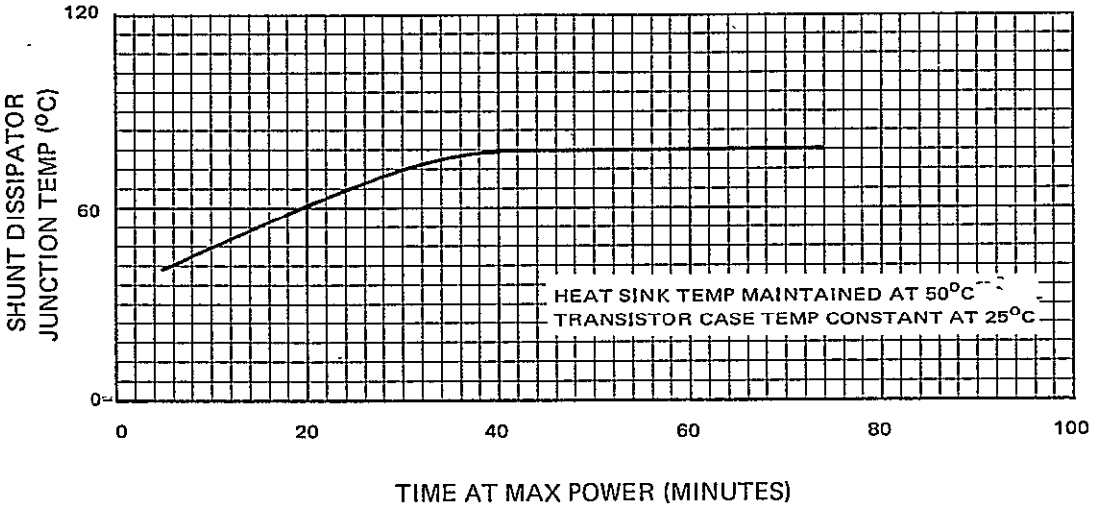

Figure V-20. Junction Temperature Characteristics

Using Equation (1) the junction temperature equals

$$\theta_{J-C} = \frac{88 - 65}{20.8} = 1.11°C/watt$$

This is less then the 1.2°C/watt max rating specified by the manufacturer.

Based on the results of the special test, RCA recommended the part change which was accepted by NASA and part replacement was started during the last week of January.

Eleven heat sink assemblies with the newly installed 1970655-1 shunt dissipator transistor passed the heat sink test requirements. The final heat sink test sequence included current leakage measurements in the temperature range of -25°C to +35°C, even though the transistors had been previously tested for leakage during screening.

C. STORAGE MODULE TEST DATA

1. General

The pre-potting electrical test sequence and the date of completion of each test for a specific storage module is listed in Table V-1. Circuit alignment and electrical test of storage modules 022 through 025 was repeated on February 25, 1969 after replacement of the shunt dissipation transistor (refer to Appendix V, Paragraph B for details). The remaining storage modules were modified with the new shunt dissipator transistor prior to the test. The results of the circuit alignment and electrical tests are listed in Table V-2. After circuit alignment and electrical test, the 23-cells of each storage module were conditioned as follows:

- a 40-hour, 200 milliampere charge
- a 240-ampere discharge until the voltage of one cell equals 1.150 volts
- a 4-hour letdown (a one-ohm resistor connected across each cell)
- a 20-hour-400 milliampere charge
- a 2.0 ampere discharge until the voltage of one cell equals 1.150 volts
- a letdown until each cell voltage was less than 20 millivolts.

TABLE V-1. STORAGE MODULE TEST SEQUENCE AND COMPLETION DATE

Test Procedure Name and Number	Storage Module (Serial No.)							
	022	023	024	025	026	027	028	029
Circuit Alignment & Electrical Test (TP-CT-1759580 Rev G)	1-7-69	1-15-69	1-27-69	1-27-69	3-3-69	3-3-69	3-5-69	3-5-69
Conditioning Test (Described in text)	1-28-69	1-25-69	1-30-69	1-30-69	1-30-69	3-6-69	3-11-69	3-11-69
Short Test (TP-BT-1759580 Rev C)	1-29-69	1-21-69	1-31-69	1-31-69	3-7-69	3-7-69	3-12-69	3-12-69
25°C Capacity Test (TP-BT-1759580 Rev C)	1-23-69	1-23-69	2-3-69	2-3-69	3-11-69	3-11-69	3-13-69	3-13-69

2. Test Results and Conclusion

The circuit alignment and electrical test data and the battery capacity are listed in Tables V-2 and V-3 respectively. Reference data for both the short test and capacity test are presented in Tables V-4, V-5, and V-6. All the test results were within the limits specified in the test procedures. There was no significant difference in the data obtained with the new shunt dissipator transistors.

TABLE V-2. CIRCUIT ALIGNMENT AND ELECTRICAL TEST DATA

Storage Module No.	Max Charge Current Amperes	Trickle Charge Current (Amperes)	Charge Voltage limit at 25°C (Volts dc)	Charge Current TM at 1.2 Amp (Volts dc)	Discharge Current TM at 2.4 Amp (Volts dc)	Batt Voltage TM at 30 Volts (Volts dc)	Batt Temp TM at Ambient (Volts dc)	Shunt Diss Turn-On Voltage (Volts dc)
022	1.100	0.148	33.58	6.005	5.790	3.109	3.120	38.1
023	1.102	0.147	33.58	6.025	5.820	3.110	3.100	38.1
024	1.100	0.154	33.58	6.033	5.807	3.138	3.110	38.1
025	1.101	0.154	33.58	5.996	5.816	3.111	3.110	38.1
026	1.101	0.152	33.58	6.003	5.790	3.107	3.120	38.1
027	1.101	0.152	33.58	6.010	5.794	3.096	3.130	38.1
028	1.100	0.150	33.58	6.027	5.770	3.136	3.130	38.1
029	1.100	0.153	33.58	6.026	5.792	3.145	3.140	38.1

TABLE V-3. STORAGE MODULE CAPACITY TEST DATA AT 25°C

Storage Module Number	Capacity (ampere/minutes)
022	316
023	317
024	328
025	326
026	327
027	323
028	330
029	331

TABLE V-4. TWENTY-HOUR OPEN CIRCUIT CELL VOLTAGES (VOLTS DC) SHORT TEST

Cell Position (number)								
	022	023	024	025	026	027	028	029
1	1.211	1.230	1.221	1.205	1.206	1.211	1.231	1.227
2	1.225	1.229	1.224	1.220	1.211	1.209	1.229	1.225
3	1.225	1.232	1.222	1.211	1.193	1.218	1.232	1.230
4	1.242	1.230	1.221	1.216	1.214	1.215	1.229	1.228
5	1.240	1.232	1.222	1.218	1.194	1.218	1.229	1.222
6	1.228	1.229	1.224	1.213	1.216	1.218	1.231	1.227
7	1.229	1.224	1.221	1.218	1.203	1.214	1.228	1.226
8	1.228	1.232	1.222	1.215	1.216	1.210	1.229	1.231
9	1.220	1.233	1.221	1.211	1.217	1.219	1.230	1.228
10	1.230	1.227	1.221	1.211	1.200	1.219	1.227	1.232
11	1.232	1.229	1.218	1.212	1.186	1.219	1.232	1.233
12	1.226	1.229	1.221	1.215	1.216	1.218	1.230	1.230
13	1.231	1.227	1.222	1.216	1.190	1.219	1.234	1.231
14	1.218	1.220	1.219	1.210	1.216	1.219	1.233	1.232
15	1.226	1.216	1.220	1.216	1.216	1.216	1.232	1.229
16	1.209	1.232	1.209	1.220	1.213	1.216	1.228	1.237
17	1.229	1.229	1.221	1.209	1.188	1.218	1.229	1.225
18	1.228	1.231	1.208	1.218	1.184	1.216	1.226	1.230
19	1.229	1.229	1.222	1.211	1.212	1.214	1.232	1.230
20	1.226	1.229	1.222	1.220	1.214	1.213	1.223	1.229
21	1.227	1.231	1.222	1.214	1.212	1.216	1.231	1.225
22	1.221	1.231	1.208	1.212	1.188	1.210	1.233	1.228
23	1.228	1.237	1.218	1.211	1.195	1.217	1.228	1.221

TABLE V-5. END-OF-CHARGE CELL VOLTAGES (VOLTS DC), CAPACITY TEST

Cell Position (number)	Storage Module Number							
	022	023	024	025	026	027	028	029
1	1.407	1.403	1.418	1.416	1.426	1.423	1.416	1.417
2	1.406	1.409	1.418	1.414	1.425	1.428	1.414	1.419
3	1.410	1.405	1.421	1.419	1.428	1.427	1.417	1.416
4	1.414	1.405	1.419	1.419	1.426	1.426	1.417	1.419
5	1.411	1.406	1.419	1.418	1.425	1.423	1.416	1.414
6	1.405	1.401	1.418	1.421	1.425	1.424	1.415	1.418
7	1.405	1.405	1.421	1.419	1.425	1.424	1.416	1.418
8	1.404	1.402	1.419	1.419	1.420	1.424	1.416	1.414
9	1.409	1.404	1.420	1.418	1.420	1.423	1.417	1.418
10	1.410	1.407	1.423	1.418	1.420	1.423	1.419	1.420
11	1.407	1.405	1.424	1.422	1.420	1.419	1.419	1.418
12	1.406	1.406	1.419	1.421	1.421	1.419	1.420	1.419
13	1.405	1.403	1.420	1.420	1.421	1.419	1.420	1.418
14	1.410	1.405	1.421	1.417	1.417	1.418	1.418	1.420
15	1.406	1.402	1.418	1.417	1.417	1.421	1.419	1.416
16	1.407	1.404	1.414	1.419	1.421	1.421	1.423	1.427
17	1.409	1.401	1.416	1.421	1.420	1.420	1.421	1.415
18	1.408	1.402	1.417	1.418	1.421	1.419	1.419	1.421
19	1.405	1.401	1.414	1.421	1.428	1.424	1.420	1.418
20	1.408	1.402	1.417	1.426	1.421	1.418	1.422	1.419
21	1.413	1.402	1.418	1.422	1.420	1.421	1.419	1.415
22	1.406	1.403	1.416	1.424	1.423	1.431	1.419	1.415
23	1.408	1.401	1.418	1.421	1.425	1.419	1.416	1.421

TABLE V-6. END-OF-DISCHARGE CELL VOLTAGES, (VOLTS DC), CAPACITY TEST

Cell Position (number)	Storage Module Numbers							
	022	023	024	025	026	027	028	029
1	1.167	1.173	1.167	1.182	1.173	1.176	1.182	1.166
2	1.176	1.167	1.180	1.186	1.171	1.173	1.180	1.164
3	1.182	1.173	1.176	1.171	1.177	1.168	1.185	1.179
4	1.176	1.176	1.169	1.174	1.190	1.179	1.177	1.180
5	1.168	1.164	1.160	1.168	1.179	1.181	1.182	1.111
6	1.179	1.178	1.174	1.161	1.188	1.192	1.179	1.182
7	1.183	1.180	1.170	1.168	1.188	1.181	1.184	1.138
8	1.180	1.179	1.166	1.174	1.186	1.183	1.180	1.188
9	1.161	1.185	1.178	1.177	1.186	1.169	1.184	1.180
10	1.185	1.178	1.143	1.172	1.182	1.165	1.175	1.177
11	1.180	1.185	1.169	1.171	1.190	1.178	1.181	1.180
12	1.182	1.179	1.174	1.164	1.180	1.180	1.177	1.168
13	1.182	1.172	1.176	1.174	1.183	1.171	1.176	1.175
14	1.168	1.174	1.168	1.162	1.176	1.173	1.176	1.179
15	1.179	1.182	1.160	1.177	1.184	1.183	1.158	1.182
16	1.101	1.184	1.178	1.172	1.184	1.177	1.163	1.182
17	1.182	1.158	1.175	1.168	1.184	1.167	1.174	1.169
18	1.178	1.160	1.169	1.156	1.183	1.184	1.161	1.155
19	1.182	1.166	1.169	1.168	1.076	1.126	1.171	1.183
20	1.178	1.176	1.174	1.159	1.170	1.179	1.163	1.170
21	1.128	1.166	1.175	1.168	1.166	1.173	1.175	1.179
22	1.146	1.168	1.153	1.168	1.157	1.183	1.173	1.174
23	1.164	1.172	1.158	1.147	1.159	1.184	1.172	1.146

APPENDIX VI

CONTROL MODULE TEST REPORT

A. GENERAL

Unit test of the control module (serial No. 6) was completed during the report period. The test sequence, test procedures, and completion date are listed in Table VI-1.

B. TEST RESULTS

All the test results were within the limits specified in the test procedures. Worst case measurements obtained during unit test are listed in Table VI-2. Efficiency and current limiting characteristic for the main regulator are shown in Figures VI-1 and VI-2. Typical output impedance characteristics for the main and auxiliary regulators are shown in Figure VI-3.

Telemetry data measured during the calibration effort was used to generate the computerized telemetry data listed in Tables VI-3 through VI-7. These tabulations are obtained by expanding measured data into smaller increments by means of linear interpolation. These telemetry tables were used to monitor telemetry circuit performance during vibration and post-vibration performance tests. The worst-case telemetry performance for the vibration and post-vibration performance tests are listed in Table VI-8.

TABLE VI-1. NIMBUS-D CONTROL MODULE TEST SEQUENCE AND COMPLETION DATE

Test Sequence	Test Procedures	Completion Date
Pre-Pot Electrical at 25°C	TP-BT-1759712	12-6-68
Telemetry Calibration at 5°C, 10°C, 25°C, 40°C, and 45°C	TP-BT-1759712-Elect.	1-10-69
Performance Test at 10°C, 25°C, and 40°C	TP-BT-1759712-Elect.	1-14-69
Vibration Test	TP-HVA-1759712-Elect. TP-EA-1846689-Environ	1-29-69
Performance Test at 25°C	TP-BT-1759712	2-4-69

Tables VI-3 through VI-7 will also be used to evaluate the telemetry parameters during the thermal vacuum test cycle of the control modules.

Two internal temperature sensors (thermistors RT-1 and RT-2) were added to the control module at the start of the Nimbus-D program (refer to Nimbus-D Quarterly Technical Report No. 2). During calibration, the performance characteristics of the two thermistors were established. Figure VI-4 shows the external test circuit and the thermistor characteristics as a function of temperature. To generate various temperature conditions the control module was operated with a main regulator current of 20 amperes at five environmental temperature levels (5°C, 10°C, 25°C, 40°C, and 45°C). The worst-case measurements were at 45°C; a 30°C increase for RT-1 and a 10°C increase for RT-2 was recorded with the regulator powered at 20 amperes.

TABLE VI-2. WORST CASE TEST MEASUREMENTS

Parameter	Test Limits	Worst-Case Measurements	
		Measured Value	Measurement Conditions
Solar Array Diode Leakage	25 ma max	3.6 ma	T = 40°C, V_u = 40 V, I_L = 2 A
Battery Diode Leakage	25 ma max	0.5 ma	T = 40°C, V_u = 40 V
Battery Diode Current Sharing	±10% of average	3.5%	T = 40°C, V_u = 32, I_{SA} = 8 A
Clock Bus Diode Voltage (From Main Bus)	less than 0.80 V	0.68 V	T = 10°C, V_R = 24.5 V, Clock Bus B
Clock Bus Diode Voltage (From Auxiliary Regulators)	less than 0.80 V	0.68 V	T = 10°C, V_A = 23.5 V, Clock Bus B
Main Regulator Voltage Regulation	24.5 ±0.5 V	24.33 V	T = 25°C, V_u = 26 V, I_L = 20 A, Regulator #1
Main Regulator Ripple Peak	100 mv (p-p)	75 mv	T = 40°C, V_u = 38 V, I_L = 20 A, Both Regulators
Main Regulator Current Limit	30 A max.	23.5 A	T = 10°C, V_u = 38 V, V_R = 12 V Regulator #1
Main Regulator Output Impedance	less than 0.1 Ω (10 to 10,000 Hz)	0.08 Ω	T = 25°C, V_u = 26 V, I_L = 5 A, I_{AC} = 1 A, F = 500 Hz, Both Regulators
Main Regulator Transient Response (Recovery Time to 24.5 ±0.5 V)	less than 3 ms	2 ms	T = 25°C, V_u = 26 V, I_L = 16 A, ΔI_L = 4 A, Both Regulators
Auxiliary Regulator Voltage Regulation	23.5 ±0.5 V	23.52 V	T = 10°C, V_u = 38 V I_R = 1 A, Both Auxiliary Regulators
Auxiliary Regulator Output Impedance	less than 1.1Ω (1 kHz to 20 kHz)	0.1 Ω	T = 40°C, V_u = 26 V, I_R = 0.5 A I_{AC} = 0.5 A (p-p), F = 5 kHz, Both Auxiliary Regulators
Auxiliary Regulator Transient Response (Max. Voltage Deviation/Recovery Time)	100 mv/10 $\overline{ms}$ max	50 mv/1 ms	T = 25°C, V_u = 38 V, I_R = 2 A ΔI_R = 0.5 A, Both Regulators
Bus Comparator Upper Voltage Limit	26.0 ±0.5 V	25.92 V	T = 10°C, V_u = 32 V, I_L = 2 A
Bus Comparator Lower Voltage Limit	23.0 ±0.5 V	22.94 V	T = 40°C, V_u = 32 V, I_L = 2 A
Shunt Dissipator Voltage	38.0 ±0.3 V	38.17 V	T = 10°C, I_{SH} = 14 A
Main Regulator ON TLM Voltage	7.500 ±0.375 V	7.178 V	T = 10°C, Regulator #1
Trickle Chg Override TLM Voltage	8.0 V max	6.483 V	T = 10°C, V_u = 32 V

Legend: T = temperature, V_u = unregulated bus voltage, I_L = load current

I_{SA} = solar array current, V_R = regulated bus voltage

V_A = auxiliary regulator voltage, I_R = auxiliary regulator current

I_{AC} = a-c current, ΔI_L = change in load current

ΔI_R = change in auxiliary regulator current, I_{SH} = shunt dissipator current

F = frequency, TLM = Telemetry, P-P = peak-to-peak

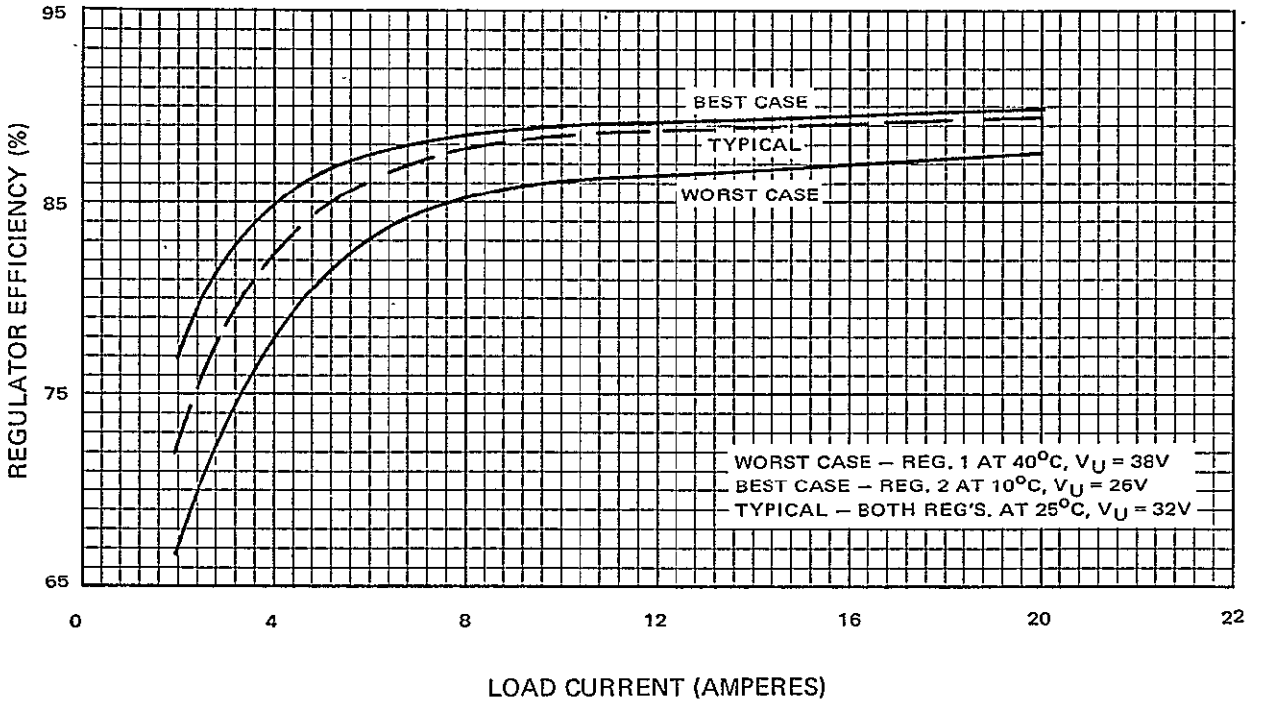

Figure VI-1. Main Regulator Efficiency

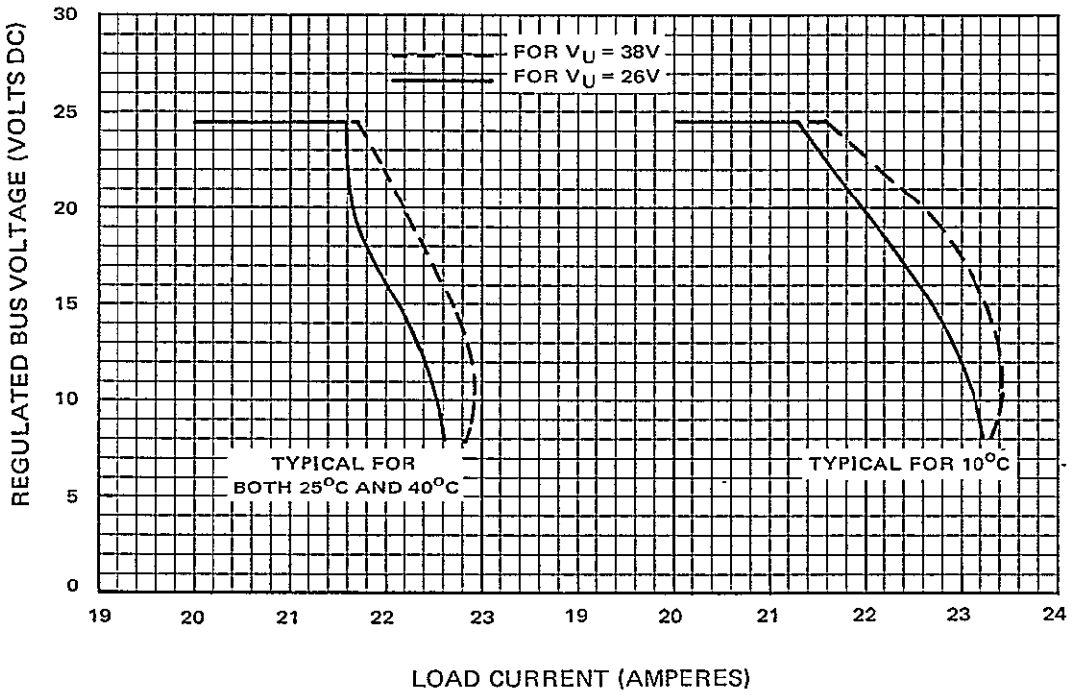

Figure VI-2. Main Regulator Current Limiting

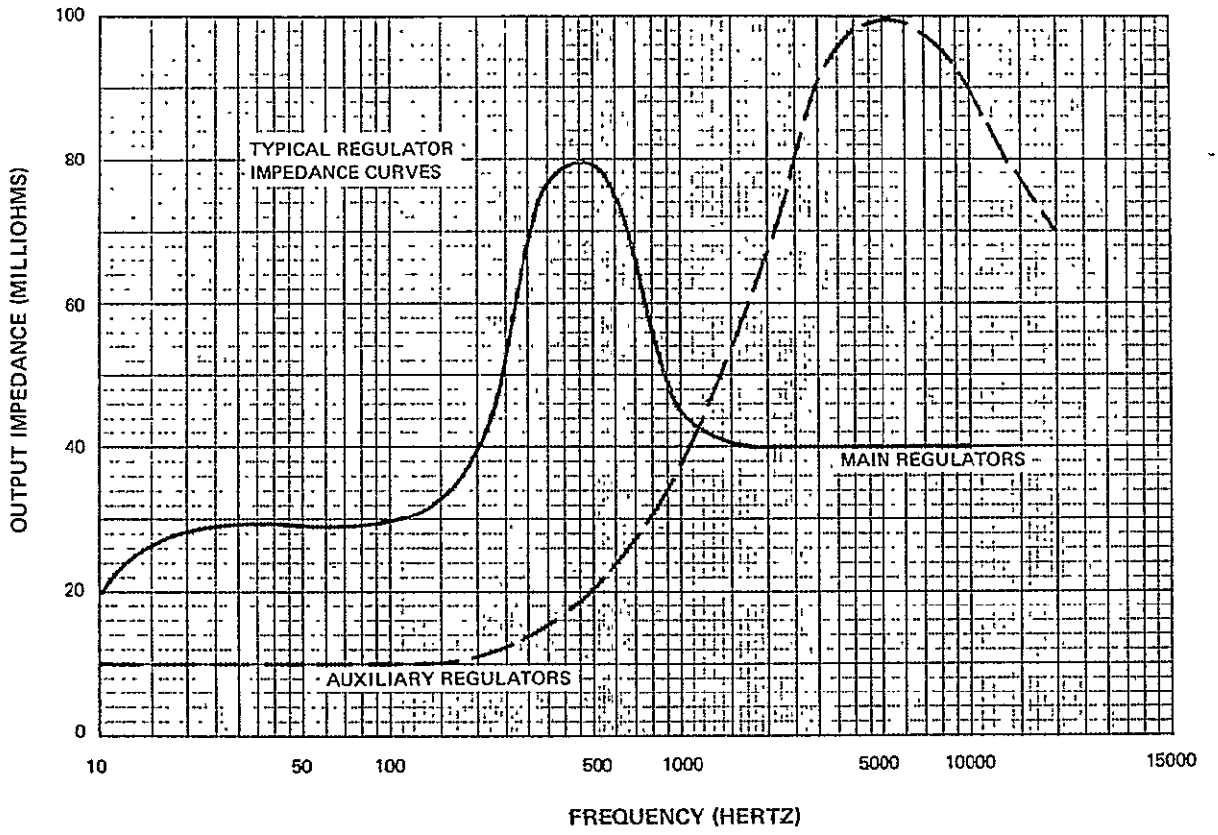

Figure VI-3. Typical Regulator Output Impedance

TABLE VI-3. CONTROL MODULE CURRENT TELEMETRY

SOLAR ARRAY CURRENT (AMPERES)	TELEMETRY VOLTAGE (VOLTS)	SOLAR ARRAY CURRENT (AMPERES)	TELEMETRY VOLTAGE (VOLTS)	SOLAR ARRAY CURRENT (AMPERES)	TELEMETRY VOLTAGE (VOLTS)	SOLAR ARRAY CURRENT (AMPERES)	TELEMETRY VOLTAGE (VOLTS)	SOLAR ARRAY CURRENT (AMPERES)	TELEMETRY VOLTAGE (VOLTS)
2.00	0.530	4.70	1.263	7.40	2.067	10.10	2.899	12.80	3.722
2.05	0.543	4.75	1.277	7.45	2.082	10.15	2.915	12.85	3.738
2.10	0.556	4.80	1.292	7.50	2.097	10.20	2.930	12.90	3.753
2.15	0.570	4.85	1.306	7.55	2.113	10.25	2.945	12.95	3.768
2.20	0.583	4.90	1.321	7.60	2.128	10.30	2.960	13.00	3.783
2.25	0.596	4.95	1.335	7.65	2.143	10.35	2.976	13.05	3.799
2.30	0.609	5.00	1.350	7.70	2.158	10.40	2.991	13.10	3.814
2.35	0.623	5.05	1.364	7.75	2.174	10.45	3.006	13.15	3.829
2.40	0.636	5.10	1.379	7.80	2.189	10.50	3.021	13.20	3.845
2.45	0.649	5.15	1.393	7.85	2.204	10.55	3.036	13.25	3.860
2.50	0.662	5.20	1.408	7.90	2.219	10.60	3.052	13.30	3.875
2.55	0.676	5.25	1.422	7.95	2.235	10.65	3.067	13.35	3.890
2.60	0.689	5.30	1.437	8.00	2.250	10.70	3.082	13.40	3.906
2.65	0.702	5.35	1.451	8.05	2.265	10.75	3.097	13.45	3.921
2.70	0.715	5.40	1.466	8.10	2.281	10.80	3.113	13.50	3.936
2.75	0.729	5.45	1.480	8.15	2.296	10.85	3.128	13.55	3.951
2.80	0.742	5.50	1.495	8.20	2.312	10.90	3.143	13.60	3.967
2.85	0.755	5.55	1.509	8.25	2.327	10.95	3.158	13.65	3.982
2.90	0.768	5.60	1.524	8.30	2.343	11.00	3.173	13.70	3.997
2.95	0.782	5.65	1.538	8.35	2.358	11.05	3.189	13.75	4.013
3.00	0.795	5.70	1.553	8.40	2.374	11.10	3.204	13.80	4.028
3.05	0.808	5.75	1.567	8.45	2.389	11.15	3.219	13.85	4.043
3.10	0.821	5.80	1.582	8.50	2.405	11.20	3.234	13.90	4.058
3.15	0.835	5.85	1.596	8.55	2.420	11.25	3.250	13.95	4.074
3.20	0.848	5.90	1.611	8.60	2.436	11.30	3.265	14.00	4.089
3.25	0.861	5.95	1.625	8.65	2.451	11.35	3.280	14.05	4.104
3.30	0.874	6.00	1.640	8.70	2.467	11.40	3.295	14.10	4.119
3.35	0.888	6.05	1.655	8.75	2.482	11.45	3.310	14.15	4.134
3.40	0.901	6.10	1.670	8.80	2.498	11.50	3.326	14.20	4.149
3.45	0.914	6.15	1.686	8.85	2.513	11.55	3.341	14.25	4.164
3.50	0.927	6.20	1.701	8.90	2.529	11.60	3.356	14.30	4.179
3.55	0.941	6.25	1.716	8.95	2.544	11.65	3.371	14.35	4.194
3.60	0.954	6.30	1.731	9.00	2.559	11.70	3.387	14.40	4.209
3.65	0.967	6.35	1.747	9.05	2.575	11.75	3.402	14.45	4.224
3.70	0.980	6.40	1.762	9.10	2.590	11.80	3.417	14.50	4.239
3.75	0.994	6.45	1.777	9.15	2.606	11.85	3.432	14.55	4.254
3.80	1.007	6.50	1.792	9.20	2.621	11.90	3.448	14.60	4.270
3.85	1.020	6.55	1.808	9.25	2.637	11.95	3.463	14.65	4.285
3.90	1.033	6.60	1.823	9.30	2.652	12.00	3.478	14.70	4.300
3.95	1.047	6.65	1.838	9.35	2.668	12.05	3.493	14.75	4.315
4.00	1.060	6.70	1.853	9.40	2.683	12.10	3.509	14.80	4.330
4.05	1.074	6.75	1.869	9.45	2.699	12.15	3.524	14.85	4.345
4.10	1.089	6.80	1.884	9.50	2.714	12.20	3.539	14.90	4.360
4.15	1.103	6.85	1.899	9.55	2.730	12.25	3.554	14.95	4.375
4.20	1.118	6.90	1.914	9.60	2.745	12.30	3.570	15.00	4.390
4.25	1.132	6.95	1.930	9.65	2.761	12.35	3.585	15.05	4.405
4.30	1.147	7.00	1.945	9.70	2.776	12.40	3.600	15.10	4.420
4.35	1.161	7.05	1.960	9.75	2.792	12.45	3.615	15.15	4.435
4.40	1.176	7.10	1.975	9.80	2.807	12.50	3.631	15.20	4.450
4.45	1.190	7.15	1.991	9.85	2.823	12.55	3.646	15.25	4.465
4.50	1.205	7.20	2.006	9.90	2.838	12.60	3.661	15.30	4.480
4.55	1.219	7.25	2.021	9.95	2.853	12.65	3.677	15.35	4.495
4.60	1.234	7.30	2.036	10.00	2.869	12.70	3.692	15.40	4.510
4.65	1.248	7.35	2.052	10.05	2.884	12.75	3.707	15.45	4.525

TABLE VI-4. CONTROL MODULE REGULATED BUS CURRENT
(CURRENT RANGE 1.50 to 14.95 AMPS)

REGULATED BUS CURRENT (AMPERES)	TELEMETRY VOLTAGE (VOLTS)	REGULATED BUS CURRENT (AMPERES)	TELEMETRY VOLTAGE (VOLTS)	REGULATED BUS CURRENT (AMPERES)	TELEMETRY VOLTAGE (VOLTS)	REGULATED BUS CURRENT (AMPERES)	TELEMETRY VOLTAGE (VOLTS)	REGULATED BUS CURRENT (AMPERES)	TELEMETRY VOLTAGE (VOLTS)
1.50	0.405	4.20	1.151	6.90	1.989	9.60	2.848	12.30	3.701
1.55	0.418	4.25	1.166	6.95	2.005	9.65	2.864	12.35	3.717
1.60	0.432	4.30	1.182	7.00	2.021	9.70	2.880	12.40	3.732
1.65	0.445	4.35	1.197	7.05	2.037	9.75	2.896	12.45	3.747
1.70	0.459	4.40	1.212	7.10	2.053	9.80	2.911	12.50	3.762
1.75	0.472	4.45	1.228	7.15	2.069	9.85	2.927	12.55	3.778
1.80	0.486	4.50	1.243	7.20	2.085	9.90	2.943	12.60	3.793
1.85	0.499	4.55	1.258	7.25	2.101	9.95	2.959	12.65	3.808
1.90	0.513	4.60	1.274	7.30	2.117	10.00	2.975	12.70	3.823
1.95	0.526	4.65	1.289	7.35	2.133	10.05	2.991	12.75	3.839
2.00	0.540	4.70	1.304	7.40	2.149	10.10	3.007	12.80	3.854
2.05	0.554	4.75	1.319	7.45	2.165	10.15	3.023	12.85	3.869
2.10	0.567	4.80	1.335	7.50	2.180	10.20	3.038	12.90	3.884
2.15	0.581	4.85	1.350	7.55	2.196	10.25	3.054	12.95	3.900
2.20	0.595	4.90	1.365	7.60	2.212	10.30	3.070	13.00	3.915
2.25	0.609	4.95	1.381	7.65	2.228	10.35	3.086	13.05	3.930
2.30	0.622	5.00	1.396	7.70	2.244	10.40	3.102	13.10	3.945
2.35	0.636	5.05	1.411	7.75	2.260	10.45	3.118	13.15	3.961
2.40	0.650	5.10	1.427	7.80	2.276	10.50	3.134	13.20	3.976
2.45	0.664	5.15	1.442	7.85	2.292	10.55	3.150	13.25	3.991
2.50	0.677	5.20	1.457	7.90	2.308	10.60	3.165	13.30	4.006
2.55	0.691	5.25	1.472	7.95	2.324	10.65	3.181	13.35	4.022
2.60	0.705	5.30	1.488	8.00	2.340	10.70	3.197	13.40	4.037
2.65	0.719	5.35	1.503	8.05	2.356	10.75	3.213	13.45	4.052
2.70	0.732	5.40	1.518	8.10	2.372	10.80	3.229	13.50	4.067
2.75	0.746	5.45	1.534	8.15	2.388	10.85	3.245	13.55	4.083
2.80	0.760	5.50	1.549	8.20	2.403	10.90	3.261	13.60	4.098
2.85	0.774	5.55	1.564	8.25	2.419	10.95	3.277	13.65	4.113
2.90	0.787	5.60	1.580	8.30	2.435	11.00	3.292	13.70	4.128
2.95	0.801	5.65	1.595	8.35	2.451	11.05	3.308	13.75	4.144
3.00	0.815	5.70	1.610	8.40	2.467	11.10	3.324	13.80	4.159
3.05	0.829	5.75	1.625	8.45	2.483	11.15	3.340	13.85	4.174
3.10	0.842	5.80	1.641	8.50	2.499	11.20	3.356	13.90	4.189
3.15	0.856	5.85	1.656	8.55	2.515	11.25	3.372	13.95	4.205
3.20	0.870	5.90	1.671	8.60	2.530	11.30	3.388	14.00	4.220
3.25	0.884	5.95	1.687	8.65	2.546	11.35	3.404	14.05	4.235
3.30	0.897	6.00	1.702	8.70	2.562	11.40	3.419	14.10	4.250
3.35	0.911	6.05	1.718	8.75	2.578	11.45	3.435	14.15	4.266
3.40	0.925	6.10	1.734	8.80	2.594	11.50	3.451	14.20	4.281
3.45	0.939	6.15	1.750	8.85	2.610	11.55	3.467	14.25	4.296
3.50	0.952	6.20	1.766	8.90	2.626	11.60	3.483	14.30	4.311
3.55	0.966	6.25	1.782	8.95	2.642	11.65	3.499	14.35	4.327
3.60	0.980	6.30	1.798	9.00	2.657	11.70	3.515	14.40	4.342
3.65	0.994	6.35	1.814	9.05	2.673	11.75	3.531	14.45	4.357
3.70	1.007	6.40	1.830	9.10	2.689	11.80	3.546	14.50	4.372
3.75	1.021	6.45	1.846	9.15	2.705	11.85	3.562	14.55	4.388
3.80	1.035	6.50	1.861	9.20	2.721	11.90	3.578	14.60	4.403
3.85	1.049	6.55	1.877	9.25	2.737	11.95	3.594	14.65	4.418
3.90	1.062	6.60	1.893	9.30	2.753	12.00	3.610	14.70	4.433
3.95	1.076	6.65	1.909	9.35	2.769	12.05	3.625	14.75	4.449
4.00	1.090	6.70	1.925	9.40	2.784	12.10	3.640	14.80	4.464
4.05	1.105	6.75	1.941	9.45	2.800	12.15	3.656	14.85	4.479
4.10	1.121	6.80	1.957	9.50	2.816	12.20	3.671	14.90	4.494
4.15	1.136	6.85	1.973	9.55	2.832	12.25	3.686	14.95	4.510

TABLE VI-5. CONTROL MODULE REGULATED BUS CURRENT
(CURRENT RANGE 7.0 to 20.45 AMPS)

REGULATED BUS CURRENT (AMPERES)	TELEMETRY VOLTAGE (VOLTS)	REGULATED BUS CURRENT (AMPERES)	TELEMETRY VOLTAGE (VOLTS)	REGULATED BUS CURRENT (AMPERES)	TELEMETRY VOLTAGE (VOLTS)	REGULATED BUS CURRENT (AMPERES)	TELEMETRY VOLTAGE (VOLTS)	REGULATED BUS CURRENT (AMPERES)	TELEMETRY VOLTAGE (VOLTS)
7.00	2.021	9.70	2.880	12.40	3.732	15.10	4.555	17.80	5.361
7.05	2.037	9.75	2.896	12.45	3.747	15.15	4.571	17.85	5.376
7.10	2.053	9.80	2.911	12.50	3.762	15.20	4.586	17.90	5.390
7.15	2.069	9.85	2.927	12.55	3.778	15.25	4.601	17.95	5.405
7.20	2.085	9.90	2.943	12.60	3.793	15.30	4.616	18.00	5.420
7.25	2.101	9.95	2.959	12.65	3.808	15.35	4.632	18.05	5.434
7.30	2.117	10.00	2.975	12.70	3.823	15.40	4.647	18.10	5.449
7.35	2.133	10.05	2.991	12.75	3.839	15.45	4.662	18.15	5.463
7.40	2.149	10.10	3.007	12.80	3.854	15.50	4.677	18.20	5.478
7.45	2.165	10.15	3.023	12.85	3.869	15.55	4.693	18.25	5.492
7.50	2.180	10.20	3.038	12.90	3.884	15.60	4.708	18.30	5.507
7.55	2.196	10.25	3.054	12.95	3.900	15.65	4.723	18.35	5.521
7.60	2.212	10.30	3.070	13.00	3.915	15.70	4.738	18.40	5.536
7.65	2.228	10.35	3.086	13.05	3.930	15.75	4.754	18.45	5.550
7.70	2.244	10.40	3.102	13.10	3.945	15.80	4.769	18.50	5.565
7.75	2.260	10.45	3.118	13.15	3.961	15.85	4.784	18.55	5.579
7.80	2.276	10.50	3.134	13.20	3.976	15.90	4.799	18.60	5.594
7.85	2.292	10.55	3.150	13.25	3.991	15.95	4.815	18.65	5.608
7.90	2.308	10.60	3.165	13.30	4.006	16.00	4.830	18.70	5.623
7.95	2.324	10.65	3.181	13.35	4.022	16.05	4.845	18.75	5.637
8.00	2.340	10.70	3.197	13.40	4.037	16.10	4.859	18.80	5.652
8.05	2.356	10.75	3.213	13.45	4.052	16.15	4.874	18.85	5.666
8.10	2.372	10.80	3.229	13.50	4.067	16.20	4.889	18.90	5.681
8.15	2.388	10.85	3.245	13.55	4.083	16.25	4.904	18.95	5.695
8.20	2.403	10.90	3.261	13.60	4.098	16.30	4.918	19.00	5.710
8.25	2.419	10.95	3.277	13.65	4.113	16.35	4.933	19.05	5.724
8.30	2.435	11.00	3.292	13.70	4.128	16.40	4.948	19.10	5.739
8.35	2.451	11.05	3.308	13.75	4.144	16.45	4.963	19.15	5.753
8.40	2.467	11.10	3.324	13.80	4.159	16.50	4.977	19.20	5.768
8.45	2.483	11.15	3.340	13.85	4.174	16.55	4.992	19.25	5.782
8.50	2.499	11.20	3.356	13.90	4.189	16.60	5.007	19.30	5.797
8.55	2.515	11.25	3.372	13.95	4.205	16.65	5.022	19.35	5.811
8.60	2.530	11.30	3.388	14.00	4.220	16.70	5.036	19.40	5.826
8.65	2.546	11.35	3.404	14.05	4.235	16.75	5.051	19.45	5.840
8.70	2.562	11.40	3.419	14.10	4.250	16.80	5.066	19.50	5.855
8.75	2.578	11.45	3.435	14.15	4.266	16.85	5.081	19.55	5.869
8.80	2.594	11.50	3.451	14.20	4.281	16.90	5.095	19.60	5.884
8.85	2.610	11.55	3.467	14.25	4.296	16.95	5.110	19.65	5.898
8.90	2.626	11.60	3.483	14.30	4.311	17.00	5.125	19.70	5.913
8.95	2.642	11.65	3.499	14.35	4.327	17.05	5.140	19.75	5.927
9.00	2.657	11.70	3.515	14.40	4.342	17.10	5.154	19.80	5.942
9.05	2.673	11.75	3.531	14.45	4.357	17.15	5.169	19.85	5.956
9.10	2.689	11.80	3.546	14.50	4.372	17.20	5.184	19.90	5.971
9.15	2.705	11.85	3.562	14.55	4.388	17.25	5.199	19.95	5.985
9.20	2.721	11.90	3.578	14.60	4.403	17.30	5.213	20.00	6.000
9.25	2.737	11.95	3.594	14.65	4.418	17.35	5.228	20.05	6.014
9.30	2.753	12.00	3.610	14.70	4.433	17.40	5.243	20.10	6.029
9.35	2.769	12.05	3.625	14.75	4.449	17.45	5.258	20.15	6.043
9.40	2.784	12.10	3.640	14.80	4.464	17.50	5.272	20.20	6.058
9.45	2.800	12.15	3.656	14.85	4.479	17.55	5.287	20.25	6.072
9.50	2.816	12.20	3.671	14.90	4.494	17.60	5.302	20.30	6.087
9.55	2.832	12.25	3.686	14.95	4.510	17.65	5.317	20.35	6.101
9.60	2.848	12.30	3.701	15.00	4.525	17.70	5.331	20.40	6.116
9.65	2.864	12.35	3.717	15.05	4.540	17.75	5.346	20.45	6.130

TABLE VI-6. CONTROL MODULE UNREGULATED BUS VOLTAGE TELEMETRY

UNREGULATED BUS VOLTAGE (VOLTS)	TELEMETRY VOLTAGE (VOLTS)	UNREGULATED BUS VOLTAGE (VOLTS)	TELEMETRY VOLTAGE (VOLTS)	UNREGULATED BUS VOLTAGE (VOLTS)	TELEMETRY VOLTAGE (VOLTS)	UNREGULATED BUS VOLTAGE (VOLTS)	TELEMETRY VOLTAGE (VOLTS)	UNREGULATED BUS VOLTAGE (VOLTS)	TELEMETRY VOLTAGE (VOLTS)
25.50	1.458	28.20	2.094	30.90	2.735	33.60	3.376	36.30	4.015
25.55	1.470	28.25	2.106	30.95	2.747	33.65	3.388	36.35	4.027
25.60	1.482	28.30	2.118	31.00	2.759	33.70	3.399	36.40	4.039
25.65	1.494	28.35	2.130	31.05	2.771	33.75	3.411	36.45	4.051
25.70	1.505	28.40	2.142	31.10	2.783	33.80	3.423	36.50	4.063
25.75	1.517	28.45	2.154	31.15	2.795	33.85	3.435	36.55	4.074
25.80	1.529	28.50	2.166	31.20	2.807	33.90	3.447	36.60	4.086
25.85	1.541	28.55	2.177	31.25	2.819	33.95	3.459	36.65	4.098
25.90	1.552	28.60	2.189	31.30	2.830	34.00	3.471	36.70	4.110
25.95	1.564	28.65	2.201	31.35	2.842	34.05	3.482	36.75	4.122
26.00	1.576	28.70	2.213	31.40	2.854	34.10	3.494	36.80	4.134
26.05	1.588	28.75	2.225	31.45	2.866	34.15	3.506	36.85	4.145
26.10	1.600	28.80	2.237	31.50	2.878	34.20	3.518	36.90	4.157
26.15	1.611	28.85	2.249	31.55	2.890	34.25	3.530	36.95	4.169
26.20	1.623	28.90	2.261	31.60	2.902	34.30	3.542	37.00	4.181
26.25	1.635	28.95	2.272	31.65	2.914	34.35	3.553	37.05	4.193
26.30	1.647	29.00	2.284	31.70	2.925	34.40	3.565	37.10	4.204
26.35	1.658	29.05	2.296	31.75	2.937	34.45	3.577	37.15	4.216
26.40	1.670	29.10	2.308	31.80	2.949	34.50	3.589	37.20	4.228
26.45	1.682	29.15	2.320	31.85	2.961	34.55	3.601	37.25	4.240
26.50	1.694	29.20	2.332	31.90	2.973	34.60	3.613	37.30	4.252
26.55	1.705	29.25	2.344	31.95	2.985	34.65	3.625	37.35	4.264
26.60	1.717	29.30	2.356	32.00	2.997	34.70	3.636	37.40	4.275
26.65	1.729	29.35	2.367	32.05	3.008	34.75	3.648	37.45	4.287
26.70	1.741	29.40	2.379	32.10	3.020	34.80	3.660	37.50	4.299
26.75	1.753	29.45	2.391	32.15	3.032	34.85	3.672	37.55	4.311
26.80	1.764	29.50	2.403	32.20	3.044	34.90	3.684	37.60	4.323
26.85	1.776	29.55	2.415	32.25	3.056	34.95	3.696	37.65	4.335
26.90	1.788	29.60	2.427	32.30	3.068	35.00	3.707	37.70	4.346
26.95	1.800	29.65	2.439	32.35	3.080	35.05	3.719	37.75	4.358
27.00	1.811	29.70	2.451	32.40	3.091	35.10	3.731	37.80	4.370
27.05	1.823	29.75	2.462	32.45	3.103	35.15	3.743	37.85	4.382
27.10	1.835	29.80	2.474	32.50	3.115	35.20	3.755	37.90	4.394
27.15	1.847	29.85	2.486	32.55	3.127	35.25	3.767	37.95	4.405
27.20	1.858	29.90	2.498	32.60	3.139	35.30	3.779	38.00	4.417
27.25	1.870	29.95	2.510	32.65	3.151	35.35	3.790	38.05	4.429
27.30	1.882	30.00	2.522	32.70	3.162	35.40	3.802	38.10	4.441
27.35	1.894	30.05	2.534	32.75	3.174	35.45	3.814	38.15	4.453
27.40	1.906	30.10	2.545	32.80	3.186	35.50	3.826	38.20	4.465
27.45	1.917	30.15	2.557	32.85	3.198	35.55	3.838	38.25	4.476
27.50	1.929	30.20	2.569	32.90	3.210	35.60	3.850	38.30	4.488
27.55	1.941	30.25	2.581	32.95	3.222	35.65	3.861	38.35	4.500
27.60	1.953	30.30	2.593	33.00	3.234	35.70	3.873	38.40	4.512
27.65	1.964	30.35	2.605	33.05	3.245	35.75	3.885	38.45	4.524
27.70	1.976	30.40	2.617	33.10	3.257	35.80	3.897	38.50	4.535
27.75	1.988	30.45	2.629	33.15	3.269	35.85	3.909	38.55	4.547
27.80	2.000	30.50	2.640	33.20	3.281	35.90	3.921	38.60	4.559
27.85	2.012	30.55	2.652	33.25	3.293	35.95	3.933	38.65	4.571
27.90	2.023	30.60	2.664	33.30	3.305	36.00	3.944	38.70	4.583
27.95	2.035	30.65	2.676	33.35	3.316	36.05	3.956	38.75	4.595
28.00	2.047	30.70	2.688	33.40	3.328	36.10	3.968	38.80	4.606
28.05	2.059	30.75	2.700	33.45	3.340	36.15	3.980	38.85	4.618
28.10	2.071	30.80	2.712	33.50	3.352	36.20	3.992	38.90	4.630
28.15	2.082	30.85	2.724	33.55	3.364	36.25	4.003	38.95	4.642

TABLE VI-7. CONTROL MODULE REGULATED AND AUXILIARY BUS VOLTAGE TELEMETRY

REGULATED BUS VOLTAGE (VOLTS)	TELEMETRY VOLTAGE (VOLTS)	REGULATED BUS VOLTAGE (VOLTS)	TELEMETRY VOLTAGE (VOLTS)	REGULATED BUS VOLTAGE (VOLTS)	TELEMETRY VOLTAGE (VOLTS)	AUXILIARY BUS VOLTAGE (VOLTS)	TELEMETRY VOLTAGE (VOLTS)
22.98	2.079	24.00	2.660	25.02	3.241	23.00	5.830
23.00	2.090	24.02	2.671	25.04	3.252	23.02	5.835
23.02	2.101	24.04	2.682	25.06	3.264	23.04	5.840
23.04	2.113	24.06	2.694	25.08	3.275	23.06	5.846
23.06	2.124	24.08	2.705	25.10	3.286	23.08	5.851
23.08	2.136	24.10	2.717	25.12	3.298	23.10	5.856
23.10	2.147	24.12	2.728	25.14	3.309	23.12	5.861
23.12	2.158	24.14	2.739	25.16	3.321	23.14	5.866
23.14	2.170	24.16	2.751	25.18	3.332	23.16	5.872
23.16	2.181	24.18	2.762	25.20	3.343	23.18	5.877
23.18	2.193	24.20	2.774	25.22	3.355	23.20	5.882
23.20	2.204	24.22	2.785	25.24	3.366	23.22	5.887
23.22	2.215	24.24	2.796	25.26	3.377	23.24	5.892
23.24	2.227	24.26	2.808	25.28	3.389	23.26	5.898
23.26	2.238	24.28	2.819	25.30	3.400	23.28	5.903
23.28	2.250	24.30	2.831	25.32	3.412	23.30	5.908
23.30	2.261	24.32	2.842	25.34	3.423	23.32	5.913
23.32	2.272	24.34	2.853	25.36	3.434	23.34	5.918
23.34	2.284	24.36	2.865	25.38	3.446	23.36	5.924
23.36	2.295	24.38	2.876	25.40	3.457	23.38	5.929
23.38	2.306	24.40	2.888	25.42	3.469	23.40	5.934
23.40	2.318	24.42	2.899	25.44	3.480	23.42	5.939
23.42	2.329	24.44	2.910	25.46	3.491	23.44	5.944
23.44	2.341	24.46	2.922	25.48	3.503	23.46	5.950
23.46	2.352	24.48	2.933	25.50	3.514	23.48	5.955
23.48	2.363	24.50	2.945	25.52	3.526	23.50	5.960
23.50	2.375	24.52	2.956	25.54	3.537	23.52	5.965
23.52	2.386	24.54	2.967	25.56	3.548	23.54	5.970
23.54	2.398	24.56	2.979	25.58	3.560	23.56	5.976
23.56	2.409	24.58	2.990	25.60	3.571	23.58	5.981
23.58	2.420	24.60	3.001	25.62	3.583	23.60	5.986
23.60	2.432	24.62	3.013	25.64	3.594	23.62	5.991
23.62	2.443	24.64	3.024	25.66	3.605	23.64	5.996
23.64	2.455	24.66	3.036	25.68	3.617	23.66	6.002
23.66	2.466	24.68	3.047	25.70	3.628	23.68	6.007
23.68	2.477	24.70	3.058	25.72	3.640	23.70	6.012
23.70	2.489	24.72	3.070	25.74	3.651	23.72	6.017
23.72	2.500	24.74	3.081	25.76	3.662	23.74	6.022
23.74	2.512	24.76	3.093	25.78	3.674	23.76	6.027
23.76	2.523	24.78	3.104	25.80	3.685	23.78	6.033
23.78	2.534	24.80	3.115	25.82	3.697	23.80	6.038
23.80	2.546	24.82	3.127	25.84	3.708	23.82	6.043
23.82	2.557	24.84	3.138	25.86	3.719	23.84	6.048
23.84	2.569	24.86	3.150	25.88	3.731	23.86	6.053
23.86	2.580	24.88	3.161	25.90	3.742	23.88	6.059
23.88	2.591	24.90	3.172	25.92	3.753	23.90	6.064
23.90	2.603	24.92	3.184	25.94	3.765	23.92	6.069
23.92	2.614	24.94	3.195	25.96	3.776	23.94	6.074
23.94	2.625	24.96	3.207	25.98	3.788	23.96	6.079
23.96	2.637	24.98	3.218	26.00	3.799	23.98	6.085
23.98	2.648	25.00	3.229	26.02	3.810	24.00	6.090

TABLE VI-8. WORST CASE TELEMETRY PARAMETERS

Telemetry Parameter	Test Limits	Worst-Case Deviation
Solar Array Current	±0.18a	0.05a
Regulated Bus Current	±0.18a	0.13a
Regulated Bus Voltage	±0.20v	0.03v
Unregulated Bus Voltage	±0.25v	0.02v
Auxiliary Reg. A Voltage	±0.25v	0.02v
Auxiliary Reg. B Voltage	±0.25v	0.01v

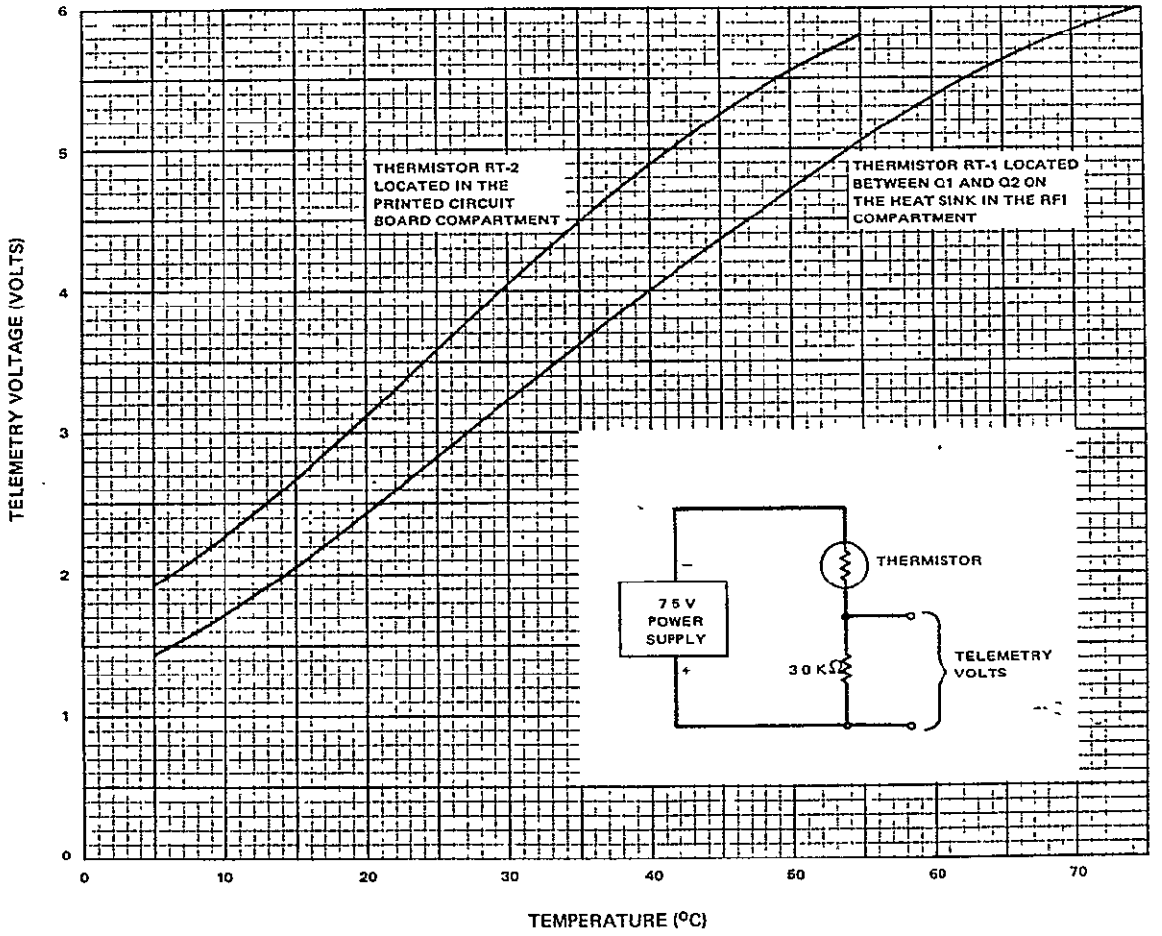

Figure VI-4. Temperature Telemetry Test Circuit, and Characteristics

APPENDIX VII

NIMBUS-B2 SOLAR ARRAY

THERMAL VACUUM TEST REPORT

A. INTRODUCTION

1. Purpose

The purpose of this report is to describe the thermal vacuum acceptance level tests of the Nimbus-B2 solar array (2 platforms - serial Nos. 15 and 16).

2. Scope

The thermal vacuum tests were performed with the platforms mounted in the NASA 10-foot Clamshell Chamber. An environmental test log, maintained by the test director, is on file at the environmental facility at the Astro-Electronics Division of RCA.

3. Summary

Thermal vacuum tests of the Nimbus-B2 platforms was conducted between September 30, 1968 and October22, 1968. The tests were completed successfully except for two equipment failures, neither of which was attributed to the solar platforms. Heater power was cycled throughout the test to duplicate the actual orbit times and regulated to simulate solar and albedo heat flux input during the daylight and eclipse portion of the orbit. Platform temperatures were allowed to seek their own levels but were monitored to prevent possible over exposure. Electrical test conducted during thermal vacuum exposure (225 cycles) were satisfactory and thermal vacuum tests were concluded pending completion of post-thermal vacuum tests. (Reference Appendix I).

B. CALIBRATION TEST

Prior to exposing the Nimbus-B2 platforms, calibration of the test chamber was completed to determine the electrical power input required to provide the specified incident thermal flux during test. The calibration test, performed on the NASA 10-foot clamshell chamber, was performed with two specially prepared calibration panels (RCA Dwgs. SK 12727436 and modification SK 1760894). The modification incorporated extension pieces to each side of the panel that increased the total width to approximately 64 inches. The temperature of the calibration panels required to provide the specified incident heat flux (0.857 watts per square

inch night) were calculated as +65°C and -85°C, respectively and the electrical power inputs required to obtain these temperatures was determined. This power input was then used to test the Nimbus-B2 solar platforms.

C. THERMAL VACUUM TEST

1. Test Setup

Prior to installation of the platforms into the test chamber, 33 fast response thermocouples (RCA 1725395) are mounted on each platform as shown on Figure VII-1. Twenty-six of the thermocouples are mounted on the sun-side; the remainder are mounted on the earth-side. The thermocouples, monitored during test with a Honeywell-Brown multi-point recorder, are used to monitor temperature extremes during test.

Thermocouple locations for the shrouds are shown on Figure VII-2. These thermocouples are used to monitor possible temperature gradient of the shrouds.

The platforms, shrouds and heaters are mounted into the chamber as shown on Figures VII-3 through VII-5.

2. Test Chronology and Results

Installation of the platforms and electrical checkout of the electrical harness was completed on September 30, 1968 and pumpdown of the chamber was initiated. When pumpdown was completed, an electrical confidence test was conducted and the shrouds were cooled to -180°C; the platform temperature was stabilized at approximately -50°C. Cycling to simulate the specified orbital conditions was started at 12:39 AM on October 1, 1968.

During the daytime portion of orbit number 1, platform number 15 displayed a temperature differential of approximately 20°C. Input power was reduced and cycling was continued until 9:30 AM. The test was then terminated and the chamber was opened to determine the cause of the temperature gradient. Inspection revealed a broken fiberglass support at the bottom of platform number 15. Both platforms were then removed and inspected; no damage was found. The thermocouples were then inspected; no anomalies were found. Any thermocouples damaged during the inspection were replaced. After installation of the thermocouples, the tape covering the thermocouples was trimmed to cover only one cell and contact of the electrical bus bars and the tape was eliminated. The fiberglass support bars were replaced with stainless steel support bars and nylon insulating blocks were manufactured to isolate the support bar from the platform support frame. The new support mechanism provided rigid support to carry the weight of the platforms and the handling frame. The fiberglass guide rods at the top of the platforms were retained to allow for thermal expansion and contraction.

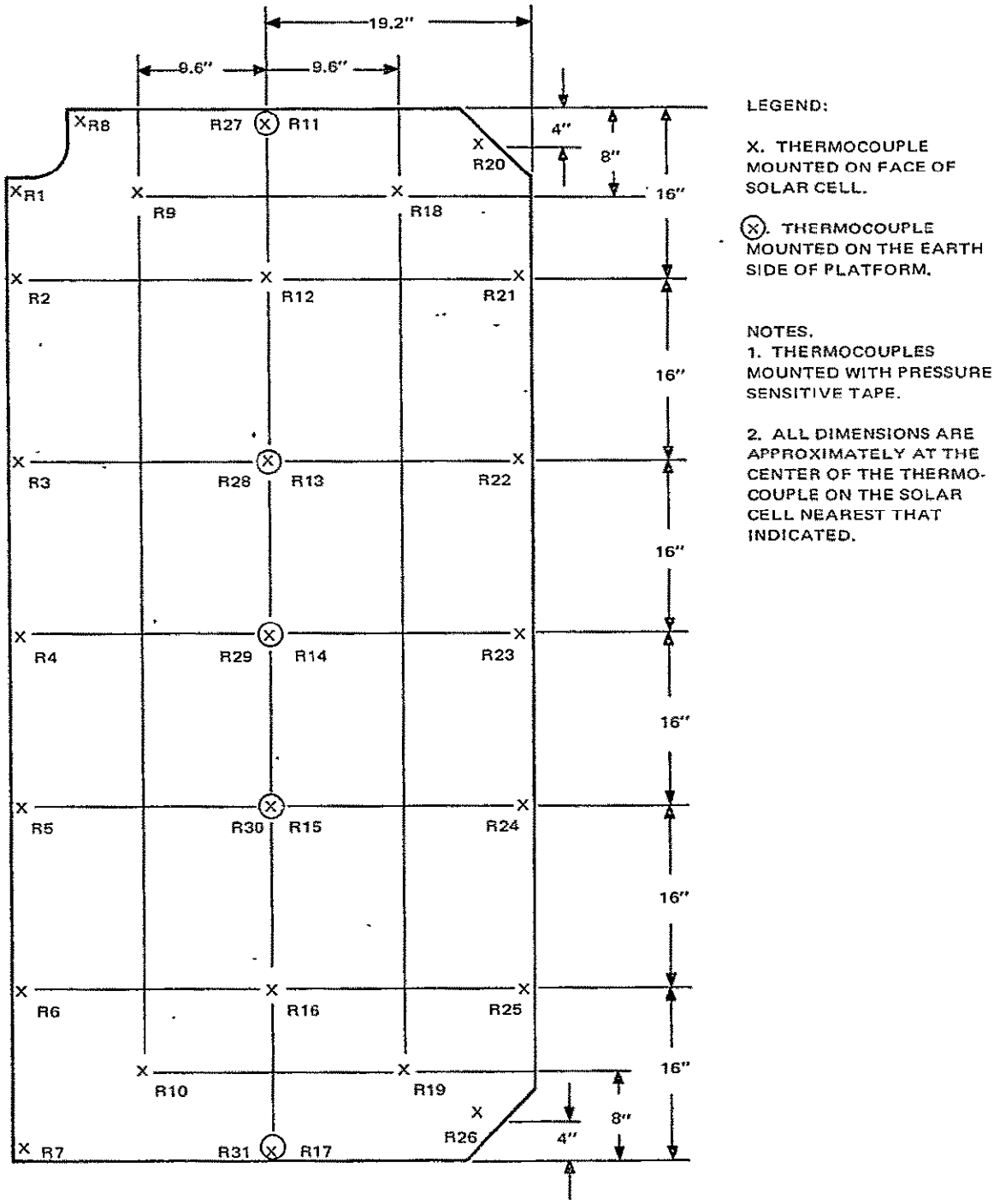

Figure VII-1. Solar Platform Thermocouple Locations

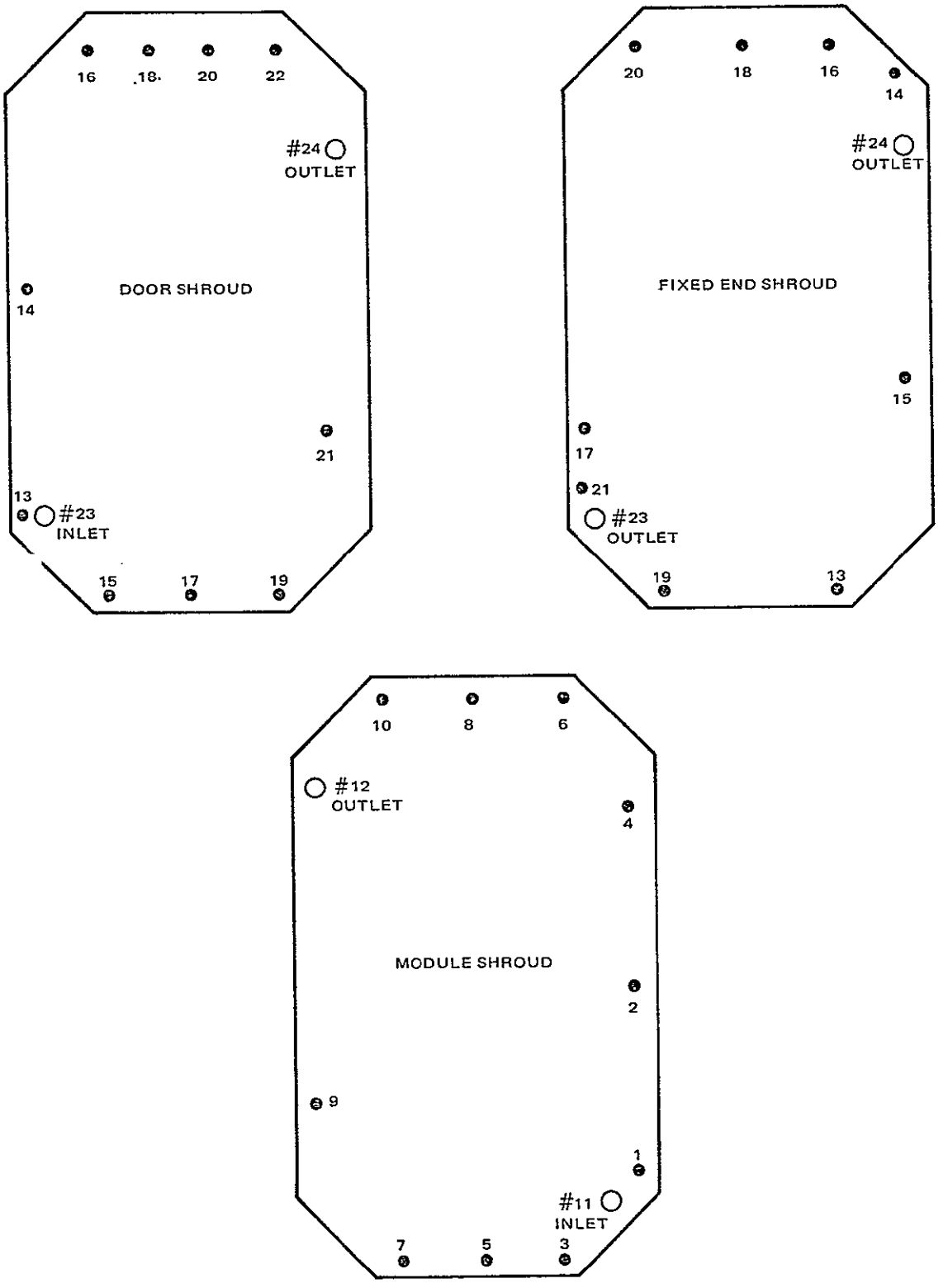

Figure VII-2. Shroud Thermocouple Locations

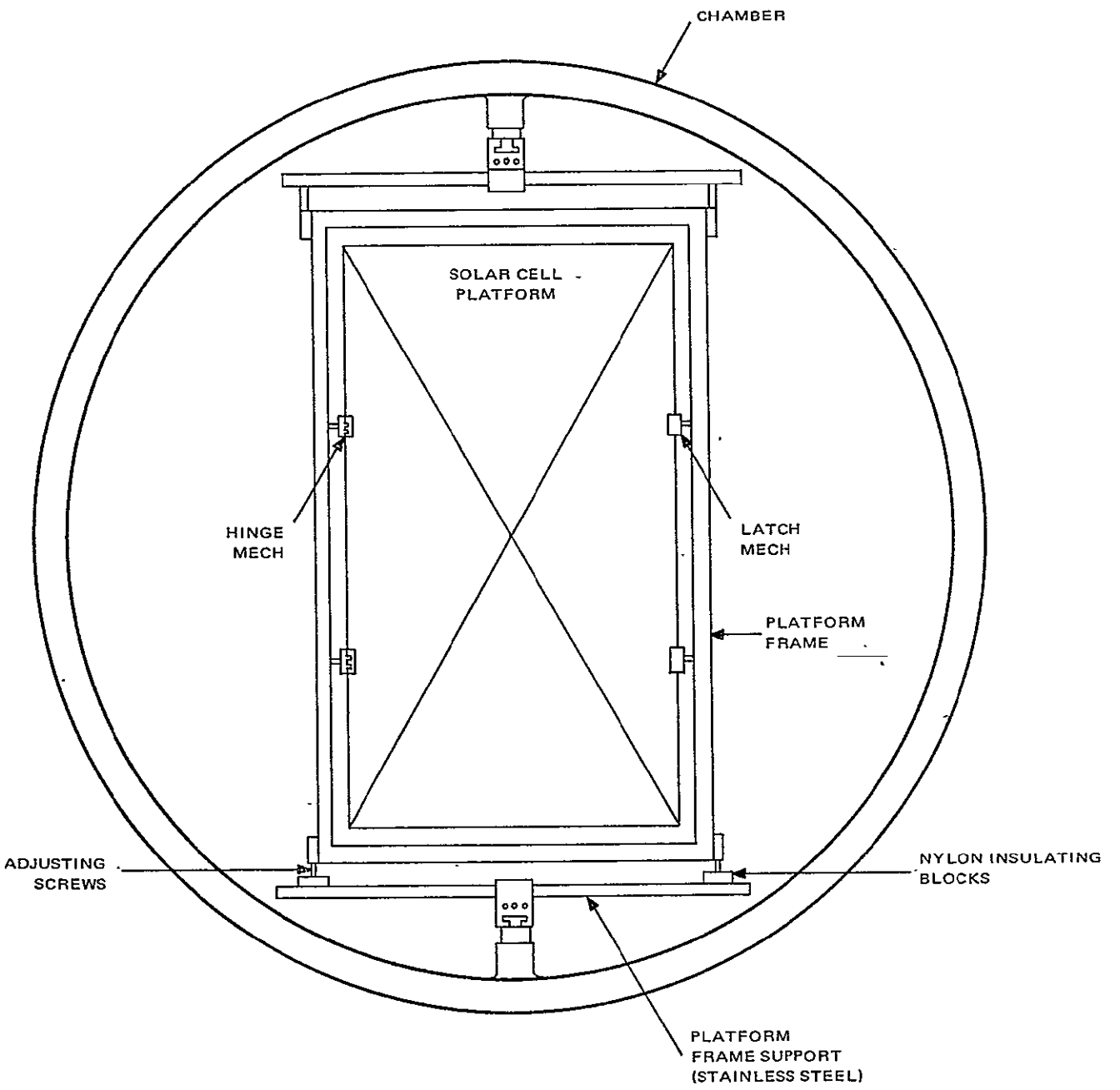

Figure VII-3. Solar Platform Installation

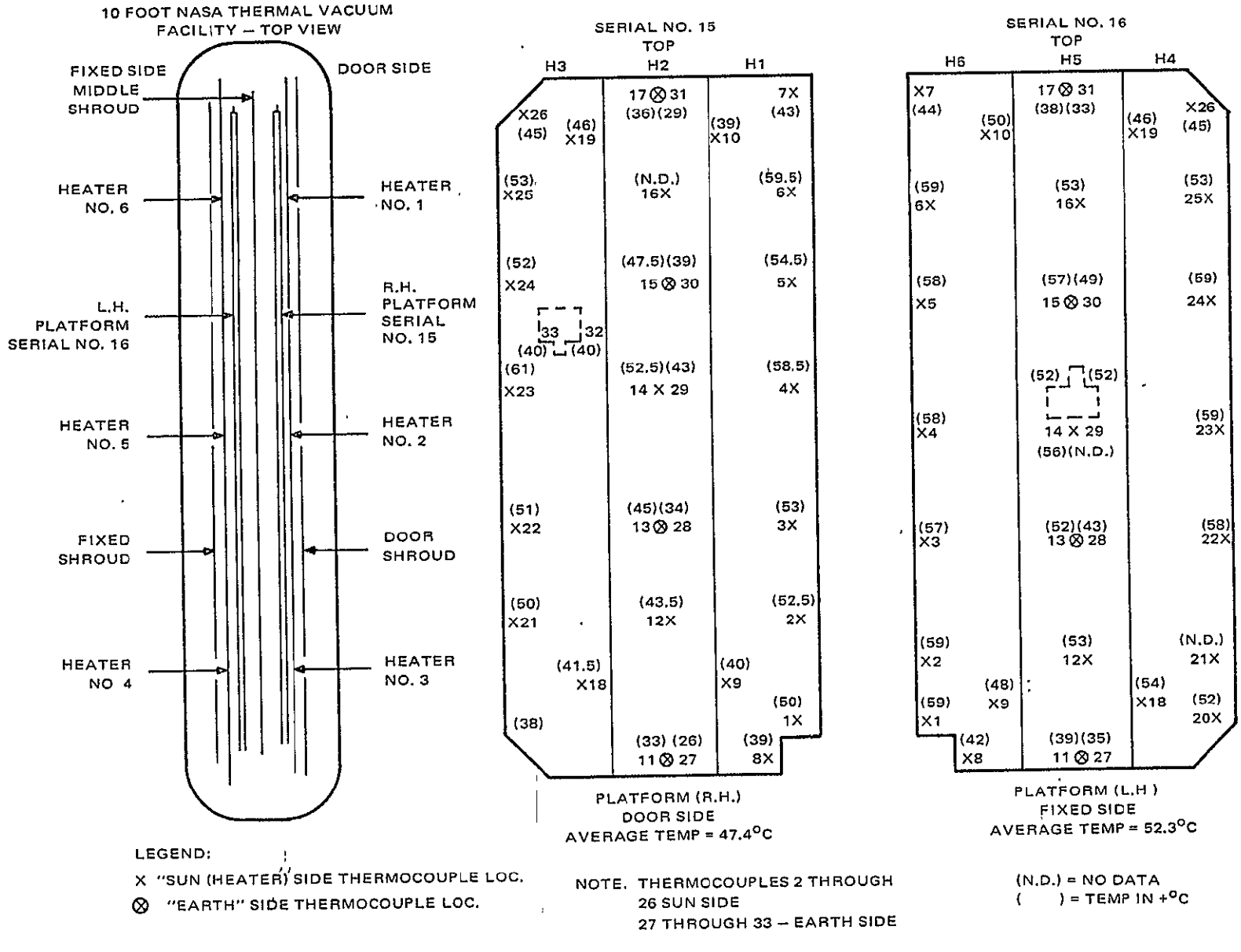

Figure VII-4. Typical Day-Time Orbit Temperature Map

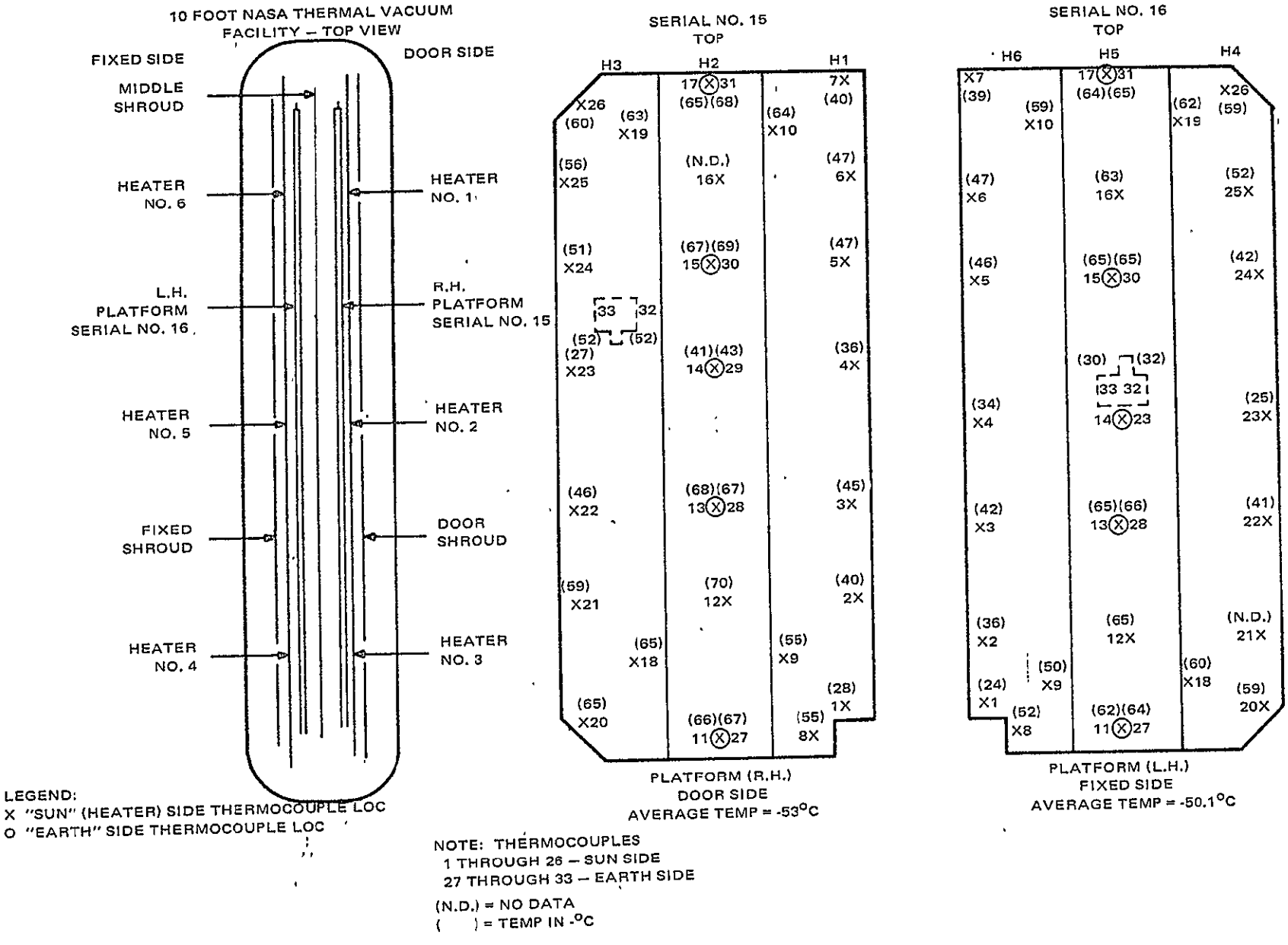

Figure VII-5. Typical Night-Time Orbit Temperature Map

Both platforms were re-installed in the chamber with particular attention directed to the alignment of the platforms with respect to the shrouds. In addition, the relative position of platform numbers 15 and 16 was reversed to determine if the thermal gradient problem would follow the platform or remain in the particular chamber position where it had occurred. Platform number 15 was placed in the chamber door side; platform number 16 was placed in the fixed side of the chamber.

Pumpdown was completed and orbital cycling was started at 8:40 AM on October 3, 1968. On October 13, 1968 orbital cycling was interrupted when the heater array control console malfunctioned. The malfunction was traced to a faulty power switching relay and thermal tests were stopped while all the power switching relays were replaced. Orbital cycling was continued on the morning of October 15 1968 and was completed on October 21, 1969 when 225 orbital cycles were completed. The platforms were removed from the chamber on October 22, 1968 and visually inspected. No anomalies were noted and the platforms were released for post-thermal vacuum electrical tests. Refer to Appendix I for post-thermal vacuum electrical test data.

Typical temperature maps for daytime and nighttime orbital test conditions are shown on Figures VII-4 and VII-5, respectively. These numbers shown in parenthesis were taken during orbit number 167.